Landscape and biodiversity change in the Willmore Wilderness Park through repeat photography

by

Julie Fortin
B.Sc. (Honours), McGill University, 2015

A Thesis Submitted in Partial Fulfillment
of the Requirements for the Degree of

MASTER OF SCIENCE

in the School of Environmental Studies

Supervisory Committee

Landscape and biodiversity change in the Willmore Wilderness Park through repeat photography

by

Julie Fortin
B.Sc. (Honours), McGill University, 2015

Supervisory Committee

Dr. Eric Higgs (School of Environmental Studies)
Supervisor

Dr. Jason Fisher (School of Environmental Studies)
Departmental Member

Abstract

Supervisory Committee
Dr. Eric Higgs (School of Environmental Studies)
Supervisor
Dr. Jason Fisher (School of Environmental Studies)
Departmental Member

Repeat photography, the process of retaking an existing photograph from the same vantage point, can give insight into long-term land cover dynamics. I advance the use of repeat photography to quantify landscape change in two ways: first, I demonstrate that rigorous field and post-processing methods can lead to highly accurate co-registration of images; second, I show that oblique photographs can provide land cover composition information similar to conventional satellite (Landsat) imagery for dominant land cover types, and that oblique photographs are better at resolving narrow or steep landscape features. I then present a novel approach to evaluate long-term biodiversity change using repeat photography: I measure land cover composition in 46 historical and modern photograph pairs in the Willmore Wilderness Park, Alberta, Canada, and use that land cover information as input into species-habitat models to predict the probability of occurrence of 15 songbird species. I show that coniferous forest cover increased over the past century, leading to a homogenization of the landscape which increased the probability of occurrence of forest-adapted species but negatively impacted non-forest-adapted species.

Table of Contents

List of Tables

List of Figures

Acknowledgments

I got so much more out of this Master's than just a degree, and there are many, many people I have to thank for that.

Eric Higgs, you are an inspiring supervisor. I appreciated the ability to have open and honest conversations with you, how you encouraged me to look at the big picture and how you offered me countless opportunities for self-development. Jason Fisher, your guidance as a committee member helped shape this thesis. Thank you for your enthusiasm, your stats wisdom, and for making me think critically about my analyses. Jeanine Rhemtulla, thank you for your insightful questions and constructive comments which helped improve this thesis post-defence.

Sandra Frey, thank you for making me laugh without fail, sharing a few "near-death" experiences, and reminding me that the most important thing to get through a Master's is to always have a healthy stash of chocolate. Navi Smith, you are quite possibly the most genuine and inspiring and contagiously happy person on Earth. I could not have asked for a better team; there is nobody with whom I would rather spend weeks in the mountains. Mary Sanseverino, you are the backbone of the Mountain Legacy Project. I am grateful for your MLP and photography-related teachings. Michael Whitney, thank you for the always intellectually stimulating conversations, for putting up with my rambles about what I would love IAT to do, and then delivering on them. To my labmates Jemma Green, Quirin Hohendorf, Julia Amerongen Maddison, Kristen Walsh, Tanya Taggart-Hodge, Hyeone Park and Heike Lettrari: thanks for the meetings, motivation, accountability, insightful comments and mindless banter.

Rick Arthur, thank you for pushing me out of my comfort zone and opening my eyes to new perspectives. Rob Watt, I am grateful I had the opportunity to work with you in the field and hear your stories. Jill Delaney and the folks at Library and Archives Canada, your work in preserving the historical photo collections is priceless. Christy James, thank you a million times for your hard work on the species-habitat models and your help deciphering how to interpret them. Thank you to Matthew Wheatley and Joyce Gould, Alberta Parks and InnoTech Alberta for bird occurrence data, and to the Earth Observation for Sustainable Development of Forests project and the Alberta Ground Cover Characterization project for the Landsat-based land cover map. Karson Sudlow, thank you for doing all the nitty-gritty work of the MLP, and for helping with the alignment accuracy assessment. I am also grateful for Alberta Agriculture and Forestry's invaluable support of the Mountain Legacy Project, to all duty officers, camp staff and firefighters who made the field work so special and all the helicopter pilots who made sure we got home safely. I would also like to acknowledge every person who has ever been involved with the MLP, from data management to field work and anything in between.

Thank you to the "Pistachio" cohort of Environmental Studies graduate students, for the shared food and ideas. To the School of Environmental Studies in general (and especially University House 4) for the great atmosphere, camaraderie, social events and snacking. To the Graduate Students' Society, and the Events Committee. To Lauren Eckert and Jillian Noel for putting up with my roommate antics. To Marion Luiz for his unwavering encouragement and support. And to my west coast friends for weekends away from this thesis, allowing me to get back into it feeling refreshed.

Last but most certainly not least, I would like to acknowledge the financial support that I received through an NSERC CGS-M scholarship, a University of Victoria fellowship and an entrance scholarship, two Mitacs Accelerate internships, Dr. Eric Higgs' SSHRC grant, three teaching assistantships at the University of Victoria, and summer field work support from Alberta Agriculture and Forestry.

Dedication

I dedicate this thesis to Paola, Gilles and Eric.

It was with you that I first saw and fell in love with mountains.

And it is because of your support that I have learned to turn my dreams (i.e. of flying on helicopters and taking pictures of mountains) into reality.

Chapter 1
Introduction

1.1 Background

Repeat photography is the process of returning to the location from which an existing photograph was taken and taking a new photograph of the same subject matter (Klett, 2011; Webb, 2010). Resulting image pairs can be compared to visualize and quantify change that occurred in the elapsed time.

Repeat photography takes advantage of collections of historical photographs, which can give valuable insight into the past conditions of a landscape. Those studying ecology will find particular interest in these historical data to compare past conditions to the present or future state of the landscape. Comparing views of the landscape at multiple points in time can help in the analysis of trends and mechanisms of land cover change (Griffiths & Mather, 2010; Hastings & Turner, 1965; Luckman, 1998).

To visualize and quantify change in a photograph pair, it is critical that the original photographic and geographic conditions are well replicated such that the landscape represented by the repeat image corresponds closely to the landscape in the historical image (Goin, Raymond, & Blesse, 1992; Webb, 2010). Most importantly, the position and orientation of the camera capturing the repeat photograph should match the position and orientation of the camera that captured the historical photograph. As the exact vantage point of the original photograph is rarely known, repeat photographers have refined methods to deduce the historical vantage point based on the relative position of foreground and background features in an image (Harrison, 1974; Klett, Manchester, Verburg, Bushaw, & Dingus, 1984; Malde, 1973; Rogers, Malde, &

Turner, 1984; Strausz, 2001). Thus, image alignment is achieved through trial and error while relocating the camera in the field and is improved during post-acquisition data processing by applying appropriate transformations to digitally co-register images (i.e. align images with one another). The level of accuracy of this alignment of photograph pairs has implications on ensuing analyses; images with poor alignment can only be compared qualitatively, while images with high alignment accuracy permit quantitative change detection, for example through cross-tabulation (Goin et al., 1992; Townshend, Justice, Gurney, & McManus, 1992; Verbyla & Hammond, 1995).

Another oft-cited challenge of repeat photography is the fact that land-based repeat photographs – henceforth referred to as “oblique” photographs due to their oblique angle of incidence – represent the landscape with a spatially variable scale (Pickard, 2002; Roush, Munroe, & Fagre, 2007). Compared to conventional overhead (orthogonal) land cover data, oblique photographs are more challenging to analyze because the basal unit (pixel) does not represent a constant area within an image, so spatially accurate measurements cannot be inferred directly from pixel counts.

Despite these challenges, repeat oblique photographs have numerous advantages as sources of land cover data. (1) Historical land-based photographs typically reach farther back in time than aerial or satellite imagery – as early as the mid 19^{th} century, decades before reliable aerial survey data became available (MacLaren, Higgs, & Zezulka-Mailloux, 2005). This can be beneficial in extending temporal comparisons to early industrial times, to the era of colonization and significant land cover change in western North America (Kull, 2005; Roush et al., 2007; Stockdale, 2017; Stockdale, Bozzini, Macdonald, & Higgs, 2015). (2) Some historical large format cameras produced remarkably high-quality photographs with very high spatial resolution (pixels ranging from a few decimetres to 1-2 metres) compared to standard remote sensing products (e.g. the 30 m pixels of Landsat imagery). This can allow fine-scale analysis due to the amount of detail captured within an image (Chandler, Ashmore, Paola, Gooch, & Varkaris, 2002). (3) Oblique photographs present the landscape in an intuitive way, as if from a "human's eye view", which aids both in image interpretation and in activities of public education and outreach (Grenzdorffer, Guretzki, & Friedlander, 2008). (4) Because of their oblique angle of incidence, terrestrial photographs tend to sample high topography landscapes in a more appropriate way than orthogonal imagery (Delaney, 2008; Sanseverino, Higgs, & Whitney, 2016). Orthogonal imagery is assumed to be perpendicular to the surface of the Earth, but in mountainous landscapes where slopes are significant, this assumption is violated (e.g. if the slope is 45°, a 30 m-wide pixel represents approximately 42 m on the ground; Figure 1-1). Thus, repeat photography can be of particular value in mountain environments, where "orthogonal" imagery from satellite and aerial sensors effectively becomes "oblique" imagery, and misses important land cover information on steep slopes and cliffs. (5) Land-based photographs are extremely common as amateur and professional photographers alike enjoy taking pictures of scenic vistas (Kaim, 2017). As such, there is enormous potential in tapping into citizen science data, especially as a source of historical photographs, for repeat photography.

1.2 Research objectives

Despite the large number of studies using repeat photography to describe or quantify changes in land cover (e.g. Butler and DeChano, 2001; Byers, 2008; Frankl et al., 2011; Hastings and Turner, 1965; Kaim, 2017; Pickard, 2002; Roush et al., 2007; Taggart-Hodge, 2016), the impacts of camera relocation errors on alignment accuracy have been largely unexplored.

Certainly, the physics behind and the importance of accurate repeat camera placement have been described (Klett, 2011; Klett et al., 1984; Malde, 1973; Rogers et al., 1984; Webb, 2010). For example, Hall (2001) presented experiments on the effects of camera displacement on the relative position of objects in sequential photographs (albeit for objects at distances on the order of 10 m from the camera rather than hundreds or even thousands of metres away, as is often the case in landscape photographs). In parallel, many studies have reported co-registration accuracy of repeat photographs (e.g. Kaim, 2017; Kolecka et al., 2015a; Rhemtulla et al., 2002); however, they did not estimate the distance between their repeat photograph's camera placement and the original vantage point. Thus, to my knowledge, no direct link has yet been established between camera relocation error and co-registration error. Chapter 2 of this thesis addresses this knowledge gap by conducting an experiment evaluating in-field alignment and co-registration accuracy.

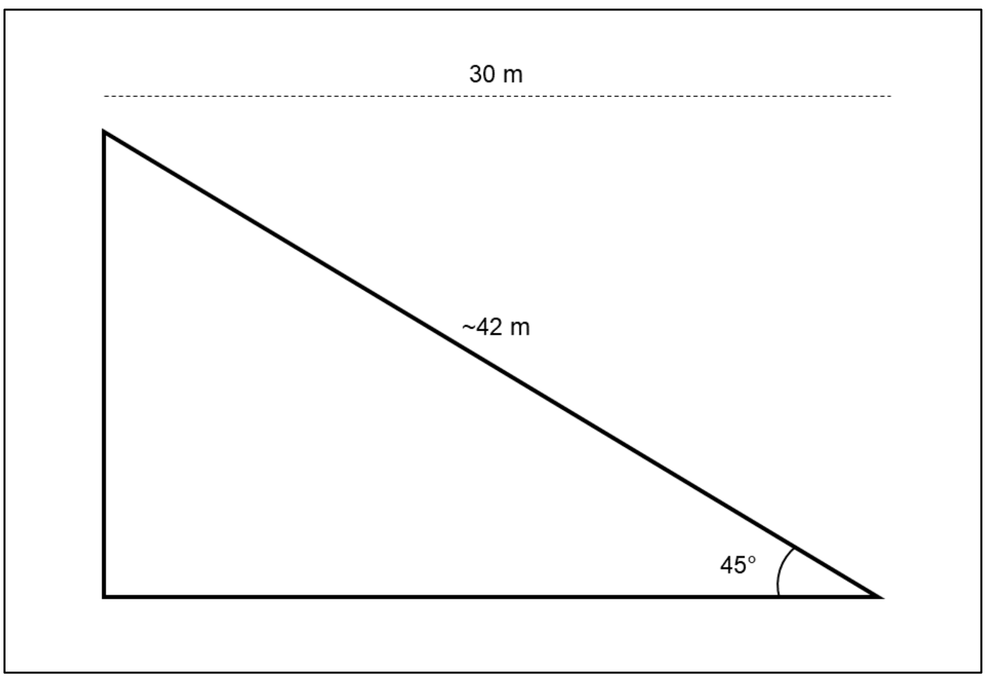

Figure 1-1. Impact of slope on area captured by an "orthogonal" view.
An orthogonal view assumes a view perpendicular to the surface. In environments with high topography, this assumption is violated. An inclination of the surface will result in a fixed-width pixel capturing a larger area than specified. For example, if the slope is 45°, a presumed 30 m-wide pixel will actually cover a width of approximately 42 m.

In contrast, the issue of variable scale and non-georeferenced data in oblique landscape photographs is the subject of numerous studies (Aschenwald, Leichter, Tasser, & Tappeiner, 2001; Bozzini, Conedara, & Krebs, 2012; Rhemtulla, 1999; Stockdale et al., 2015), most of which attempt to convert oblique photographs to a spatially accurate format for land cover interpretation. Chapter 3 explores an alternative: interpreting land cover composition in oblique photographs without orthorectification or georeferencing, simply by estimating the percent cover of each category as a function of pixel counts. This has been done by many repeat photography studies (e.g. Falk, 2014; Kaim, 2017; Taggart-Hodge, 2016), but to date the land cover products generated by this method have not been directly compared to more widely-used orthogonal imagery-generated products, as in this chapter.

Chapter 4 of this thesis demonstrates one of myriad potential applications of repeat photography (without orthorectification) to gain insight into long-term ecological trends. I developed a novel method using land cover information derived from historical and repeat oblique photographs as input into species distribution models to evaluate past and current biotic conditions. I demonstrated this method in a Rocky Mountain ecosystem by estimating the probability of occurrence of breeding songbird species in the Willmore Wilderness Park, a vast remote mountain park in west-central Alberta.

1.3 The Mountain Legacy Project

This thesis fits within the broader scope of the Mountain Legacy Project (MLP), an ongoing repeat photography research project spanning the mountains of western Canada (Trant, Starzomski, & Higgs, 2015). The historical photographs repeated by the MLP were taken by surveyors in the late 19th and early 20th centuries to create the first topographic maps of Canadian mountains using distinctive Canadian photo-topographic survey methods (Bridgland, 1916, 1924; MacLaren et al., 2005). These images have been preserved on glass plates as negatives and housed and managed mainly by Library and Archives Canada/Bibliothèque et Archives Canada and the British Columbia Archives. The combined collections of more than 120,000 historical photographs provide a comprehensive view of the Canadian mountain west. To date, MLP researchers have repeated nearly 7000 images.

This staggering number of images puts the MLP among the largest systematic repeat photography projects in the world. Since its inception in 1997, the MLP has made thousands of attempts at aligning cameras with historical photos and has developed custom methods and analysis tools to visualize, process and quantify the landscape in repeat photograph pairs (Gat, 2011; Jean et al., 2015b; Sanseverino et al., 2016). The experience that comes with thousands of attempts at rephotographing historical images, the custom-built analysis tools, and the copious amount of available data make the MLP's dataset ideally suited to addressing the aforementioned challenges of repeat photography (alignment and land cover interpretation) and to test innovative ecological applications of repeat photography.

Chapter 2
How close is close enough? Alignment accuracy in repeat photography

Chapter 2 of this thesis is in preparation to be submitted as a manuscript with co-authors Michael Whitney, Karson Sudlow, Mary Sanseverino and Eric Higgs.

2.1 Abstract

Repeat photography can be used to study landscape change quantitatively if the photographs are well aligned. This involves taking the photographs from the same vantage point and digitally applying transformations to the images to ensure adequate co-registration (i.e. alignment). We present an experiment exploring the effects of misplacement of the camera (i.e. failing to find the exact original vantage point) on co-registration accuracy. We took a variety of repeat photographs with known relocation errors and aligned them with "historical" photographs via six user-defined control point pairs in a custom-built software program, the Image Analysis Toolkit. For each photograph pair, the alignment algorithm iterated through combinations of three control point pairs and calculated the root mean square error (RMSE) on the remaining points. We compared the minimum RMSE values of all photograph pairs to evaluate the differences in co-registration accuracy arising from errors in camera position or orientation. We found that errors in orientation had large impacts on RMSE, misplacements of 1 m had small impacts on RMSE, but RMSE increased with increasing distance from the original location. We further found that relocation error had an overall greater impact on RMSE in photographs that contained no foreground features than in photographs that did. These findings suggest that rigorous field methods for repeat photography that result in a camera set-up within 1 m of the original location could be corrected by digital alignment to yield high co-registration accuracy.

This has implications for cost and time resources of field crews as well as for quantitative analyses that use repeat photography products.

2.2 Introduction

Repeat photography is the process of retaking an existing photograph from the same vantage point after some time has elapsed. This allows an observer to detect similarities and differences in the pair of photographs, which enables them to visualize and potentially measure changes that occurred in the time between captures (Klett, 2011). The technique – as it pertains to landscape photography – is credited to Sebastien Finsterwalder who first took repeat photographs of the Tyrolean Alps in 1887 and 1888 to observe glacier flows (Webb, 2010).

Repeat photography can have scientific value, notably to study long-term landscape change (Hall, 2001; Klett, 2011; Webb, 2010). In many parts of the world, there are well-preserved, high-resolution historical landscape photographs that lend themselves well to repeat photography studies (e.g. Butler and DeChano, 2001; Byers, 2008; Chandler et al., 2002; Delaney, 2008; Falk, 2014; Frankl et al., 2011; Jean et al., 2015b; Kaim, 2017; Pickard, 2002; Roush et al., 2007; Strausz, 2001; Taggart-Hodge, 2016). These land-based photographs, typically referred to as “oblique photographs” due to their oblique angle of incidence, present the landscape in a “human’s eye view”, as opposed to a bird’s eye view like aerial or satellite remotely sensed imagery (Figure 2-1; Chandler et al., 2002; Gat, 2011; Grenzdorffer et al., 2008). In addition, terrestrial oblique photographs often have higher spatial resolution and greater temporal reach – they can provide detailed information on the state of the landscape decades before the first aerial or satellite photographs were taken over the same area (Kull, 2005;

Rogers et al., 1984). As such, repeating terrestrial oblique photographs can bring to light landscape-scale changes that span a century or longer.

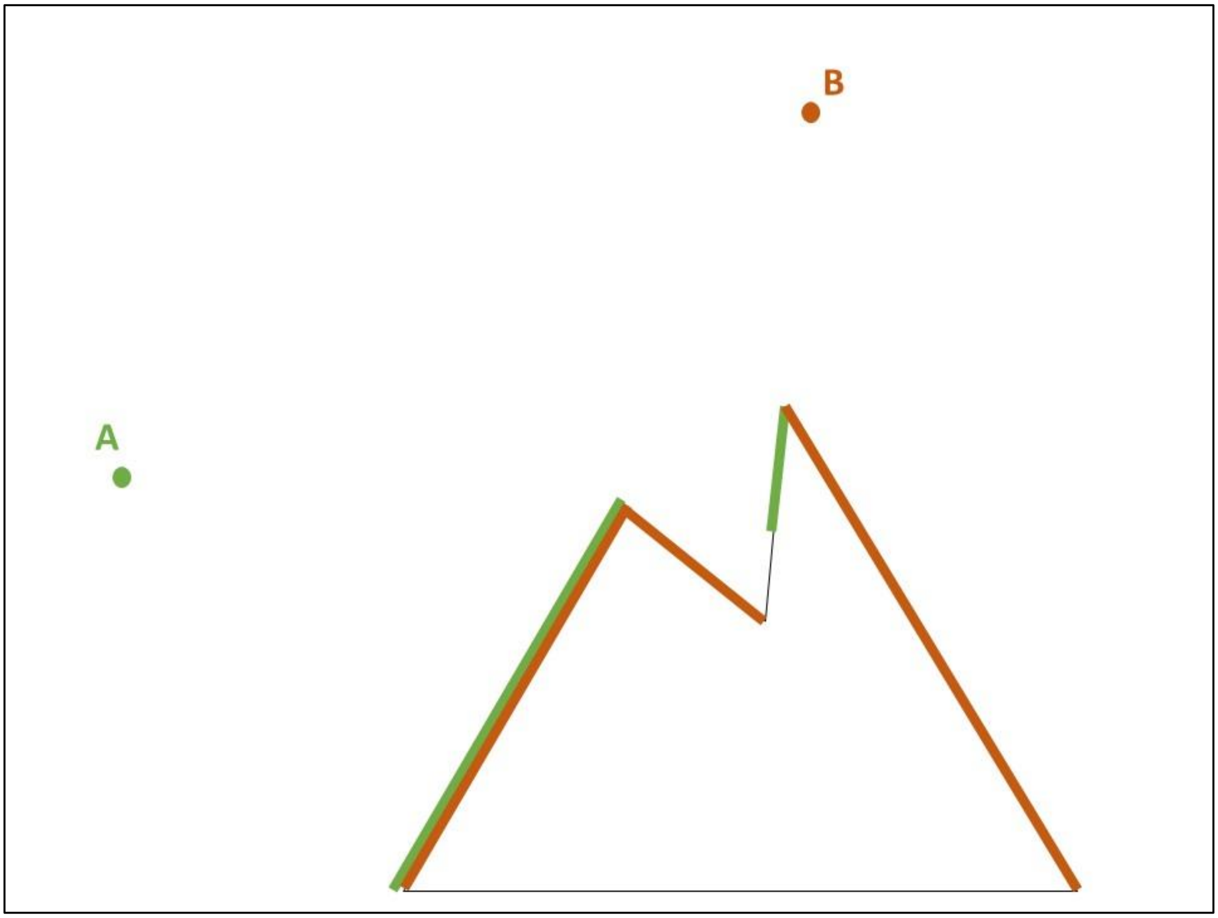

Figure 2-1. Oblique and orthogonal views of a high topography landscape.
Point A represents a land-based camera, with green lines indicating the landscape that is captured in an oblique photograph taken from point A. Point B represents a satellite or aircraft, with orange lines indicating the landscape that is captured in an orthogonal image taken from point B. Note that there are parts of the landscape that are captured from one viewpoint but not the other.

In an ideal scenario, repeat photographs would be taken from the same location (camera position), facing the same direction (camera orientation), using the same camera system. This way, photographs would line up perfectly to represent the same landscape. This perfect scenario is unattainable in reality; photographers rarely use the same cameras as a century ago, opting instead for more convenient modern cameras that can produce photographs of similar or superior quality, and the exact vantage point of historical photographs is usually unknown. Many methods exist to relocate a historical vantage point (e.g. Harrison, 1974; Malde, 1973; Strausz, 2001), with varying degrees of precision, though the most common is a trial-and-error process based on the principles of parallax (Figure 2-2; Rogers et al., 1984). The general vicinity of the original camera location is typically identified through photograph metadata such as field notes or by visually comparing the view in the photograph to that of known landforms in programs such as Google Earth (*Google Earth*, 2017; Webb, 2010). Crews travel to that location in the field and, from there, make minor adjustments to the camera's position and orientation based on how features in the foreground (on the order of 10 m from the camera), midground (~100 m) and background (~1000 m) line up.

Camera relocation using this method is not always perfect (Klett, 2011; Webb, 2010). Given the high costs of field work, there is a trade-off between accuracy and time. As relocating the original vantage point can take up to several hours (United States Department of Agriculture, 1993), sometimes the repeat photograph is taken from a point that is deemed "close enough" to save time at the expense of perfect alignment. On other occasions, it is simply impossible to replicate the original vantage point due to shifts in the landform atop which the historical photograph was taken (e.g. movement of boulders, melting of glacier, erosion, growth of vegetation, site disturbance, etc.; Webb, 2010).

To account for differences in camera position and orientation, it is commonplace to digitally align historical and repeat photographs with one another (i.e. to "co-register" the images) as part of post-acquisition processing (Gat, 2011; Gilvear & Bryant, 2003). Either automated or manually-defined points identifying corresponding features in the photographs are used to compute an appropriate transformation (typically involving translation, rotation, scaling and cropping) that is then applied on one image to match its counterpart.

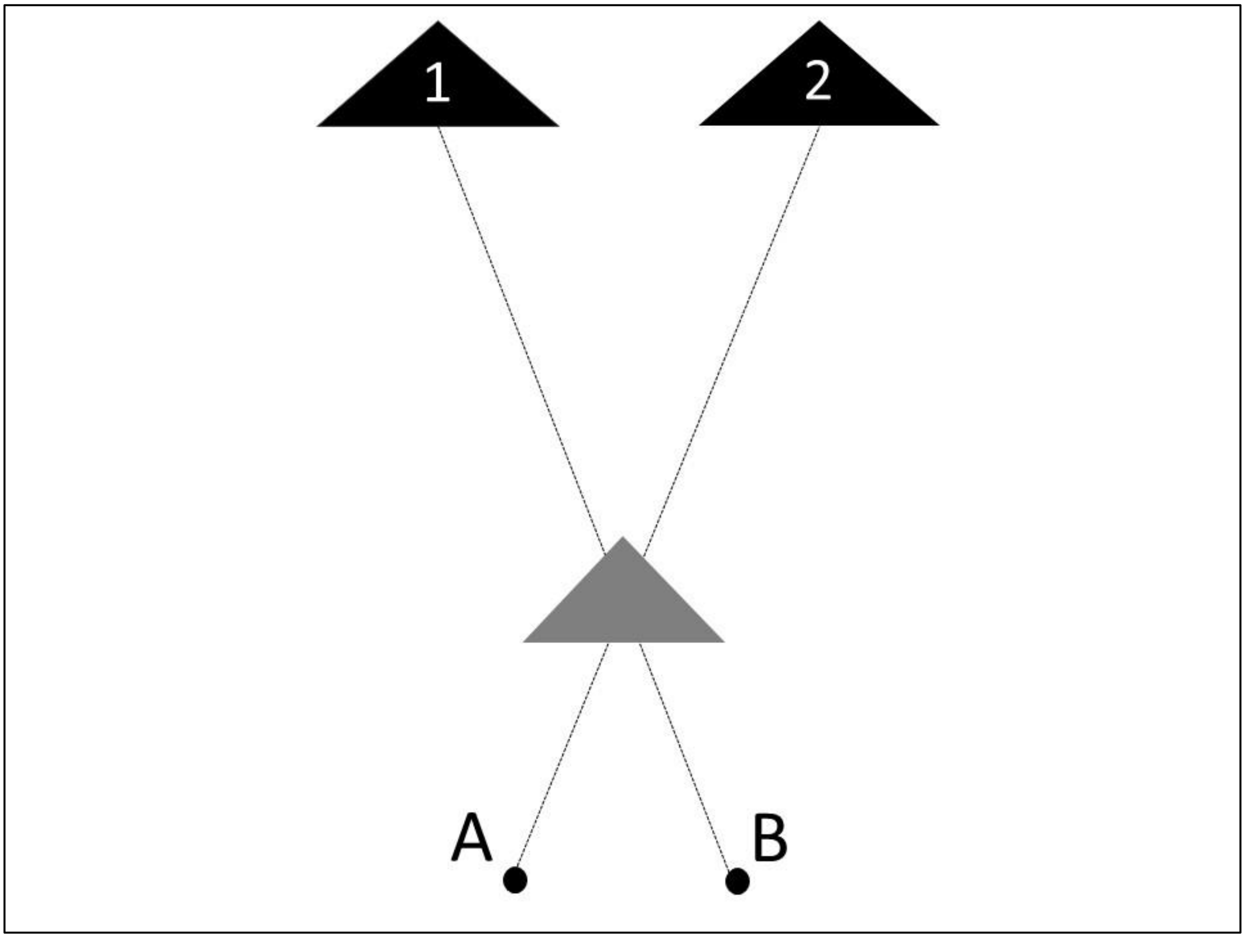

Figure 2-2. Parallax.
Diagram illustrating parallax. From vantage point A, the midground feature (gray) obscures background feature number 2. From vantage point B, the midground feature appears to have moved to the left relative to the background; it now obscures background feature number 1.

Even after co-registration, it is possible to have imperfect alignment. Alignment errors can get carried over into change detection analyses, resulting in type I or type II errors (Foody, 2002; Goin et al., 1992; Roy, 2000; Townshend et al., 1992). Therefore, it is important to evaluate the co-registration accuracy of repeat photographs to identify and correct alignment issues to ensure that the landscape change signal eclipses any alignment errors. Current approaches to assessing co-registration accuracy of repeat photography products are mostly qualitative; alignment is often verified by visual inspection using an image overlay, fade or slider tool (Frankl et al., 2011; Gat, 2011). Concurrently, approaches to assessing co-registration accuracy of orthogonal – satellite or aerial – imagery are more developed: often root mean square error (RMSE; a measure of the difference between observed and predicted values) is reported as a metric of alignment accuracy in conventional remote sensing products (Dai & Khorram, 1997, 1998; Foody, 2002; Townshend et al., 1992). Some terrestrial oblique repeat photography studies have followed suit and have likewise reported RMSE to illustrate the alignment accuracy of their photograph pairs (Kaim, 2017; Rhemtulla et al., 2002).

One project that has ample experience with the co-registration process is the Mountain Legacy Project (MLP), a 20-year ongoing repeat photography research project (mountainlegacy.ca). The MLP is built upon a collection of over 120,000 systematically captured historical photographs that provide a comprehensive view of the mountains of western Canada. MLP field crews have repeated nearly 7000 of those photographs to date. Over the years, the MLP has developed and refined rigorous field methods (Falk, 2014; Rhemtulla et al., 2002; Roush, 2009; Taggart-Hodge, 2016) and software tools (Gat, 2011; Gat, Albu, German, & Higgs, 2011; Jean et al., 2015b; Sanseverino et al., 2016) to optimize the alignment of repeat photographs. Co-registration in particular is a challenge that was recognized early on and has been tackled multiple times through iterations of different methodologies: from acetate overlays (Rhemtulla, 1999) to Adobe Photoshop (Gat, 2011) to a first customized alignment tool in the Mountain Legacy Editing and Administering Tool (Taggart-Hodge, 2016) to the current Image Analysis Toolkit (Sanseverino et al., 2016). However, besides anecdotal evidence from the MLP and other sources (Webb, 2010), to our knowledge, no empirical evaluation of the effects of camera relocation errors on co-registration accuracy has been accomplished.

As it is not possible to collect such empirical evidence on “true” repeats of historical photographs (because the exact vantage point of the historical photographs is unknown and thus the proximity of the camera location cannot be measured definitively), we instead present a controlled experiment simulating a typical repeat photography scenario, based on years of experience conducting repeat photography with the MLP. We sought to describe the link between errors in replicating the vantage point of a historical photograph and co-registration accuracy. We hypothesized that errors in camera orientation would have substantial impacts on alignment as the landscape pictured in the photographs would not correspond exactly. We further hypothesized that errors in camera position would entrain varying levels of co-registration error, with greater distance from the original vantage point leading to greater RMSE, according to the principles of parallax. We hypothesized that photographs with foreground features would present a greater challenge in accurate co-registration than photographs consisting solely of mid-to-background features, because others have noted the difficulty of properly aligning foreground features when conducting repeat photography (Harrison, 1974; Malde, 1973). In sum, we evaluated the impacts on co-registration that can be brought on by different kinds of error in camera position and orientation during repeat photography.

2.3 Methods

2.3.1 Repeat photography

To assess the effects of camera misplacement on co-registration accuracy, we conducted a controlled experiment to simulate typical errors in camera position and orientation that can occur in repeat photography.

We took photographs from an elevated viewpoint 125 m.a.s.l. at the top of Mount Tolmie in Victoria, British Columbia, Canada (48°27.406'N, 123°19.536'W). We captured two series of photographs: first of a view without any foreground features, then of a view containing foreground features (Appendix A). In both instances, we took a reference “historical” photograph, followed by a series of “repeat” photographs entrained with known camera position and orientation errors (Figure 2-3). Due to time constraints of this Master’s limiting the scope of the analysis, we completed each series of repeat photographs only once; although increasing sample size (i.e. gathering multiple iterations of series of historical and repeat photographs) would allow for statistically robust conclusions about the influence of relocation error on RMSE, this experiment still tested our hypotheses and aided in the description of a relationship between relocation error and co-registration accuracy. Specifically, this experimental design allowed us to identify the types of relocation errors likely to have large impacts on alignment.

We chose camera position and orientation modifications to reflect errors that could realistically occur during repeat photography (Table 2-1). We increased the tripod height by 23 cm; this height increment could simulate a shift at the site preventing the tripod from being positioned at the right height (e.g. growth of vegetation). We modified the azimuth by 15° to simulate a situation in which the repeat photographer focused the vertical line of the camera on the wrong feature, and modified the elevation angle by 10° to indicate differences in leveling that can arise between historical and repeat photographs. We chose to test both lateral and forward misplacement of the camera at 1 m, to compare directional error. Lastly, we took repeat photographs from lateral increments of 1, 3 and 5 m from the original location to examine the effects of increasing distance from the original vantage point (Figure 2-3).

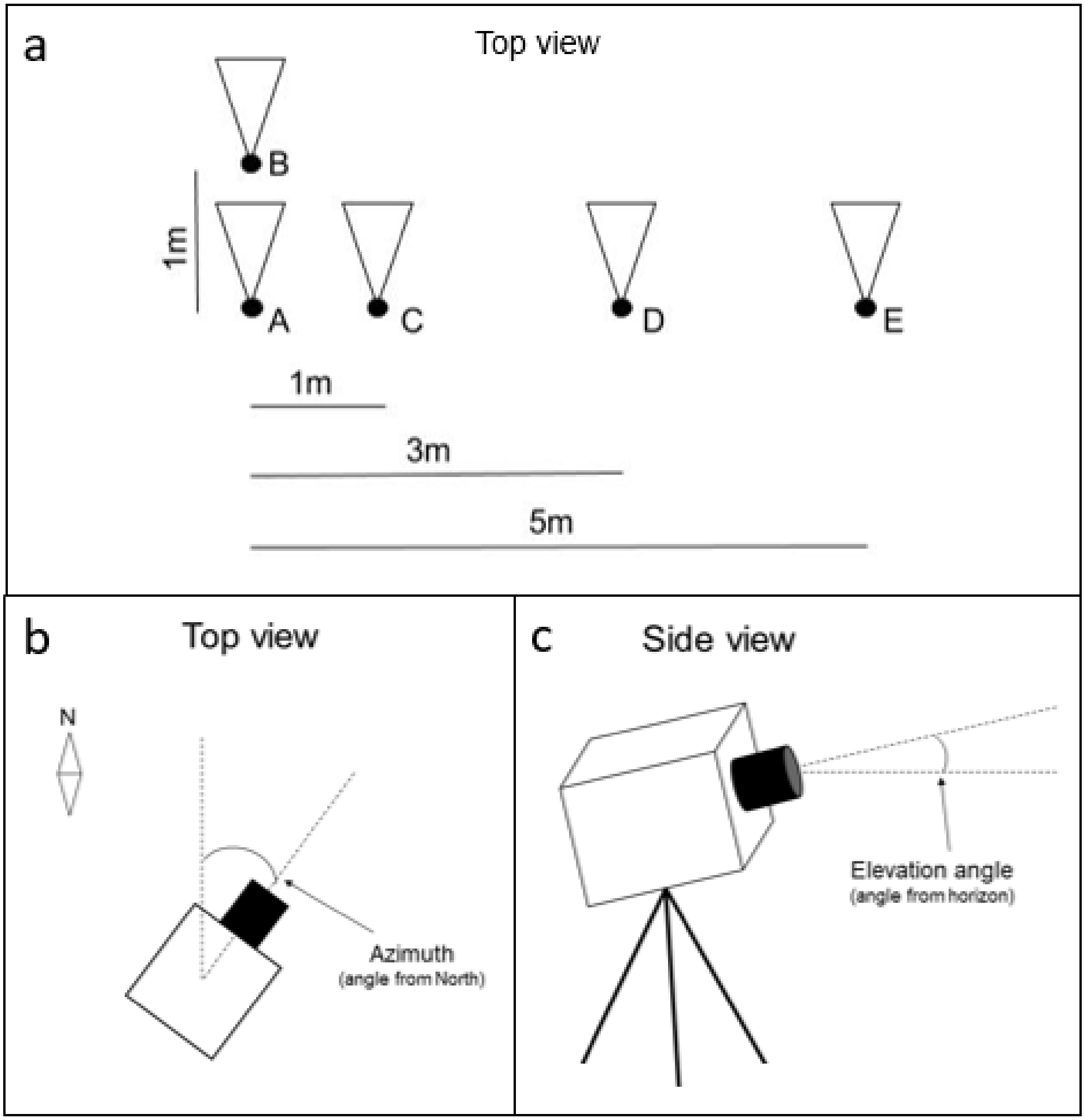

Figure 2-3. Camera position and orientation.
(a) Illustrates camera positions as measured in this experiment. The historical photograph and the first four repeat photographs (no modifications, modified tripod height, modified azimuth and modified elevation angle) were all taken from point A. The repeat photographs taken from 1 m ahead of the original location was taken from point B. The subsequent repeat photographs listed in Table 2-1 were taken from points C, D and E, in order. (b) and (c) Demonstrate azimuth and elevation angle: azimuth is the angle that the camera has been rotated from North (0°), whereas elevation angle is the angle of the viewer of the camera above the horizon.

We captured “historical” photographs with a mirrorless digital Fuji X-T2 with an 18-55 mm lens, shot at a focal length of 30.2 mm. The camera was mounted on a Manfrotto 3-way tripod head set up on a Gitzo GT2932 tripod with the camera sensor 125 cm above the ground. We immediately loaded these original photographs onto an iPad using the FUJIFILM Camera Application. We then gridded the photographs with vertical and horizontal crosshairs on-site using the Affinity Photo application. The gridded images served as references for aligning the subsequent photographs in their respective series (with and without foreground).

We opted for a different camera for all “repeat” photographs – a Nikon D800 with a 35-mm lens – to reflect the fact that repeat photographs are rarely taken with the same camera as the originals (Gat et al., 2011). In addition, the combination of Nikon D800 and 35-mm lens provided a wider horizontal field of view than the Fuji X-T2 with a focal length of 30.2 mm (54.4° versus 40.2°, respectively); this allowed more room for adjustments and cropping during the co-registration process such that no information was lost relative to the historical photographs. For all repeat photographs, we moved the tripod as necessary (Table 2-1), levelled the camera and adjusted the azimuth and elevation angle as necessary to match the centre point of the field of view of the camera with the centre point of the gridded historical photograph on the iPad. To account for optical distortion resulting from the way light reaches the sensor through the camera lens, we applied appropriate lens corrections (specific to the lenses we used) to all photographs in Adobe Lightroom.

2.3.2 Co-registration

We co-registered each repeat photograph with its corresponding historical counterpart. Notably, the first repeat photographs both with and without foreground were taken without entrained errors; that is, from the exact same camera position and orientation as their respective historical photographs, but with a different camera (Nikon D800 versus Fuji X-T2). These repeat photographs served as controls for the rest of the assessment, accounting for differences in camera sensors/lenses while assuming zero error in camera relocation.

We manually co-registered the photograph pairs in a custom-built software program, the Image Analysis Toolkit (Sanseverino et al., 2016). We carefully selected six points that represented unmistakeable features in the landscape (e.g. corners of buildings) in one photograph, then selected the six exact corresponding features in the second photograph (Figure 2-4). For consistency, the same six point-pairs were used for all photograph pairs in a given series. We selected points for their spread across the image, thus avoiding issues with collinearity and accounting for the fact that error is not uniformly distributed across an image (De Leeuw, Veugen, & Van Stokkom, 1988; Gat, 2011). We avoided selecting points in the foreground, as the landscape of interest typically forms the midground and background of photographs. It was more important to train and evaluate alignment in the midground and background of the images.

We opted to use six point-pairs as this number provided sufficient points to train the transformation and evaluate the resulting co-registration accuracy. Other studies have used similar numbers of points for co-registration training and evaluation: Aschenwald et al. (2001) used ten, Kaim (2017) used “at least” five, Rhemtulla et al. (2002) used eight to twelve and Roush et al. (2007) used five control points.

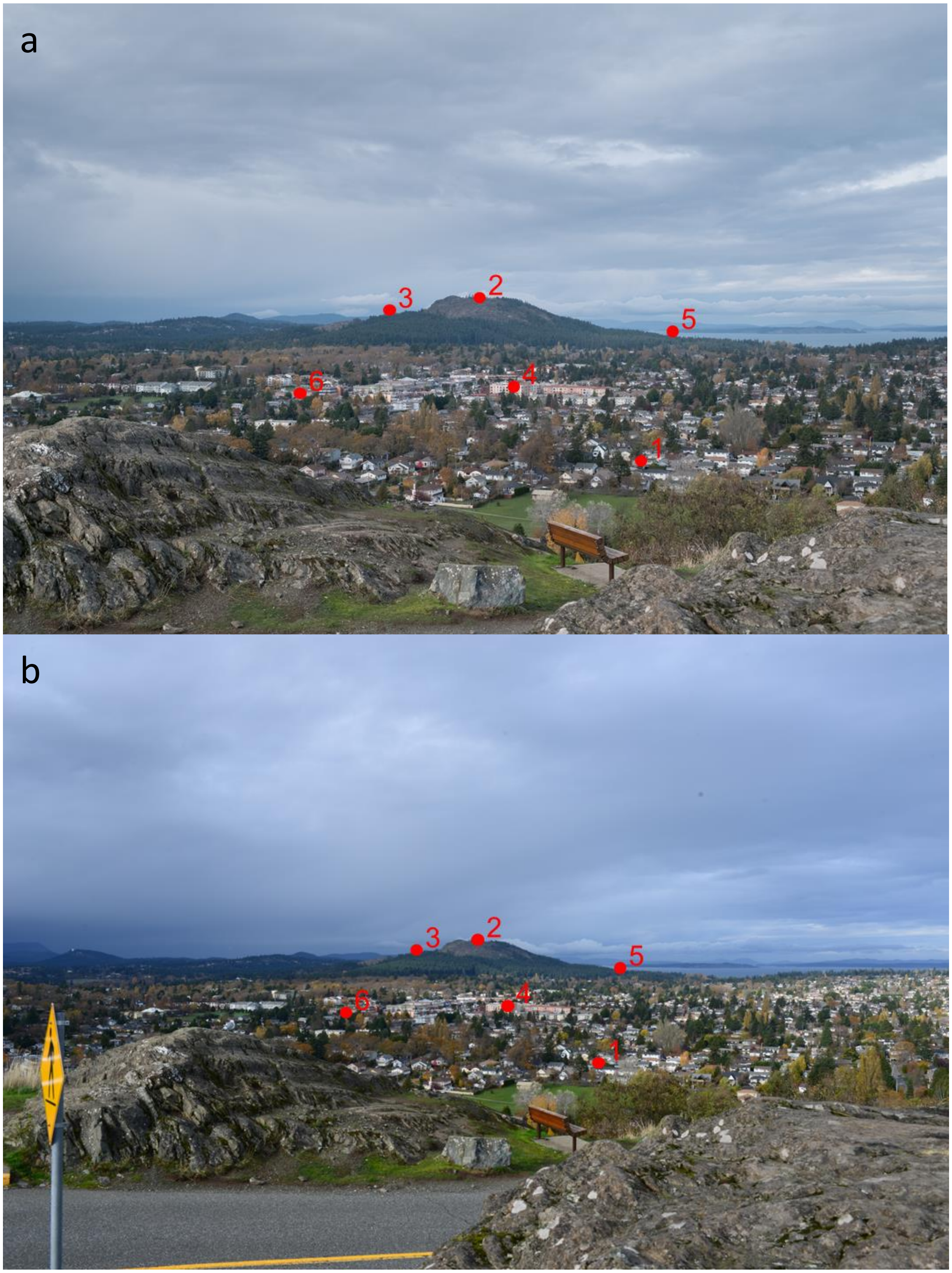

Figure 2-4. Sample image pair with control points.
(a) Historical photograph with foreground. (b) Repeat photograph (no modifications in camera position or orientation). Points that correspond have matching numbers in both photographs. There are noticeably no points along the outer margins of the image because we opted to use the same control points for all image pairs in a series, but in some repeat photographs the margins were cut off, so we could not use points in the margins.

2.3.3 Accuracy

The alignment tool in IAT works by computing an affine transformation (a linear mapping method involving translation, rotation, scaling and cropping while preserving straight lines) based on three user-defined control point pairs. The algorithm performs the transformation on any additional point-pairs, then calculates the root mean square error (RMSE) on the transformed points to give an estimate of the accuracy of the alignment. The RMSE is measured according to the distance between two points belonging to the same pair, in units of pixels, as described by the equation:

$$RMSE = \sqrt{\frac{\sum_{i,j=1}^{n}(R_i - H_i)^2 + (R_j - H_j)^2}{n}}$$

where R_i and R_j are the x- and y-coordinates of a given point in the repeat image, H_i and H_j are the x- and y-coordinates of the corresponding point in the historical image, and n is the total number of point-pairs.

For the six point-pairs defined in each part of this study, IAT iteratively tested combinations of three point-pairs, outputting the RMSE on the remaining three point-pairs. We assumed the model with the lowest RMSE to be the best model (Appendix B). Thus, to assess accuracy, we compared the minimum RMSE value of each photograph pair.

2.4 Results

2.4.1 Without foreground

The RMSE values for all photograph pairs without foreground varied markedly, up to an order of magnitude (Table 2-1). The RMSE for the control pair without foreground was 2.74 pixels. Modifying the tripod height led to a slightly larger RMSE than the control. Lateral movements of the camera sensor to 1 m, 3 m and 5 m from the original location increased RMSE progressively to approximately 2.5 times the control RMSE. Displacement of the camera sensor 1 m forward from the original location resulted in a slightly lower RMSE. Maintaining the camera in the same position but introducing error in the orientation increased RMSE substantially (i.e. tripled to quadrupled) relative to the control for both azimuth and elevation angle modifications.

Table 2-1. Results of co-registration accuracy assessment.
Root mean square error (in units of pixels) measured on three control points between the historical image and each of the listed repeat images, both with and without foreground. Rows denoted with a star (*) indicate that the azimuth and elevation angle of the camera were adjusted to match the centre point of the viewfinder with the centre point of the historical image; rows without a star indicate that the centre point of the camera was "wrong" by the specified increment.

Difference from original camera position and orientation	RMSE for images without foreground	RMSE for images with foreground
No modifications*	2.74	2.02
Tripod height increased by 23 cm*	3.39	0.96
Azimuth increased by 15°	10.77	22.59
Elevation angle decreased by 10°	8.45	7.45
Tripod moved 1 m forward*	2.54	1.89
Tripod moved 1 m to the right*	3.72	1.44
Tripod moved 3 m to the right*	4.64	2.67
Tripod moved 5 m to the right*	7.00	4.77

2.4.2 With foreground

The RMSE values for all photograph pairs with foreground also exhibited marked variation (Table 2-1). The control pair containing foreground had a lower RMSE than its counterpart without foreground, at 2.02 pixels. Modifying the height of the tripod resulted in a slightly smaller RMSE than the control. Similarly, camera position errors of 1 m (both forward and to the right of the original location) resulted in lower RMSE values (1.89 and 1.44 pixels respectively). Nevertheless, the RMSE values increased with increasing distance from the original vantage point, with the RMSE at 5 m nearly twice as high as the RMSE of the control.

Differences in camera orientation (i.e. azimuth and elevation angle) led to even higher RMSE compared to the control, with modified azimuth increasing the RMSE by a factor of greater than 10.

2.4.3 Overall co-registration accuracy

In general, errors in the orientation of the camera led to lower co-registration accuracy (higher RMSE) than errors in the position of the camera. Furthermore, errors in camera position and orientation had a greater impact on RMSE in photographs that did not contain foreground than in photographs that did. RMSE increased with increasing distance from the original camera location, and that difference was greater for photographs containing foreground.

Modifying tripod height did not have a large impact on RMSE, but affected what was captured in the field of view. Nevertheless, the wider field of view of the repeat camera resulted in minimal loss of information from this scenario. Conversely, modifying the azimuth and elevation angle by magnitudes of 15° and 10° respectively did result in margins being cut off, because the difference in field of view between the two camera systems only gave approximately 7° of additional width.

When the repeat photograph was taken from the same location with the same orientation, but with the sensor at a different height above the ground, co-registration was relatively unaffected. What was captured in the camera’s field of view, particularly along the lower margin of the photograph, was affected only slightly. Similarly, errors in azimuth and elevation angle could affect what was captured, but the wider field of view of the repeat camera resulted in minimal loss of information compared to the field of view in the historical photograph.

2.5 Discussion

2.5.1 Effects of camera position and orientation on co-registration accuracy

Our results suggest that, in order to achieve highly accurate co-registration (RMSE < ~5 pixels), repeat photographs must be centred on the correct feature and must be taken from within approximately 1 m of the original vantage point. Anecdotally, when taking those repeat photographs in this experiment with position errors of 3-5 m and orientation errors of 10-15°, it became immediately evident to experienced repeat photographers that the alignment would be poor. As such, we expect that experienced repeat photographers regularly achieve relocation errors of approximately 1 m and centre the repeat photographs on the correct feature to within less than 10° error. This suggests that rigorous field repeat photography methods such as those employed by the MLP can indeed result in highly accurate co-registration of images.

In photographs both with and without foreground features, errors in camera orientation (azimuth and elevation angle) had a larger impact on co-registration than errors in camera position. This is logical; if the centre of the field of view is not fixed on the same point in the landscape, the landscape pictured in the photographs will not be the same, which will lead to low co-registration accuracy. Our findings suggest that errors in orientation should be much less than 15° to achieve high co-registration accuracy.

Supporting our hypothesis, the greater the distance from the original camera location, the greater the impact on co-registration accuracy. This is consistent with the principles of parallax (Rogers et al., 1984). The RMSE at 1 m to the right was not noticeably different from the RMSE at 1 m forward from the original location, but was approximately half the RMSE at 5 m to the right of the original location, for photographs with and without foreground. This means that efforts to repeat a photograph from a location as close as possible to the original vantage point are warranted. However, our results suggest that returns are marginal within 1 m of the original vantage point (RMSE at 1 m in either direction was less than 50% higher than the RMSE of the control pair). As such, trade-offs between accuracy and time spent identifying the correct location to within a few centimetres should be considered in the field (Webb, 2010).

2.5.2 Effects of foreground on co-registration accuracy

The RMSE values for images with foreground were consistently lower than those without foreground, contrary to our hypothesis. One possible explanation is that, seeing as the relocation errors were fixed in this experiment, we did not present repeat photographers with the challenge of lining up foreground features, which was the greatest difficulty described by Malde (1973) and Harrison (1974). In addition, according to parallax, the alignment of midground and background features is much less affected by errors in position of the camera than the alignment of foreground features. Since no control points were selected in the foreground for this analysis, any amplified misalignment was not captured in the RMSE value of photograph pairs with foreground.

2.5.3 Implications

In general, our findings show that RMSE was on the order of 1 to 10 pixels for most photograph pairs. These results are fairly consistent with other repeat photography studies that have reported co-registration accuracy with errors spanning 3 to 30 pixels (Kaim, 2017; Kolecka et al., 2015a; Rhemtulla, 1999). For terrestrial oblique photographs, this magnitude of error is difficult to interpret spatially; the variable scale of pixels in an oblique photograph means that an error of one pixel could represent a fraction of a centimetre in the foreground but several metres in the background. Still, in an image of 6000 by 4000 pixels (approximately the scale of the images presented in this study), an error of 10 pixels represents less than 0.2% the width of the image, and it is virtually unnoticeable by visual inspection at 100% image scale. Photograph pairs with this magnitude of co-registration accuracy can be said to sample the same landscape.

For cross-tabulation or pixel-to-pixel change detection, the remote sensing literature cites sub-pixel accuracy as desirable (Townshend et al., 1992). Imperfect co-registration by one pixel has been found to lead to errors exceeding 10%, both false positives ("commission error") and false negatives ("omission error"), in detecting change in land cover classifications (Figure 2-5; Dai and Khorram, 1998; Verbyla and Hammond, 1995). While such analyses have not, to our knowledge, been conducted on cross-tabulations of masks generated from terrestrial oblique photographs, the concepts are analogous as oblique masks and orthogonal masks are both raster grids. As such, researchers comparing repeat photographs with co-registration errors of 1 to 10 pixels, as demonstrated in this study, through pixel-to-pixel change detection should discuss co-registration error as a potential source of bias in change detection. In particular, the heterogeneity of the landscape assessed should be considered, as patchy land cover is more affected by misregistration than homogeneous land cover (Verbyla & Hammond, 1995). Alternatively, researchers analyzing repeat photographs by pixel-to-pixel methods could seek co-registration algorithms that allow for highly precise point selection and sub-pixel co-registration accuracy, to minimize change detection bias.

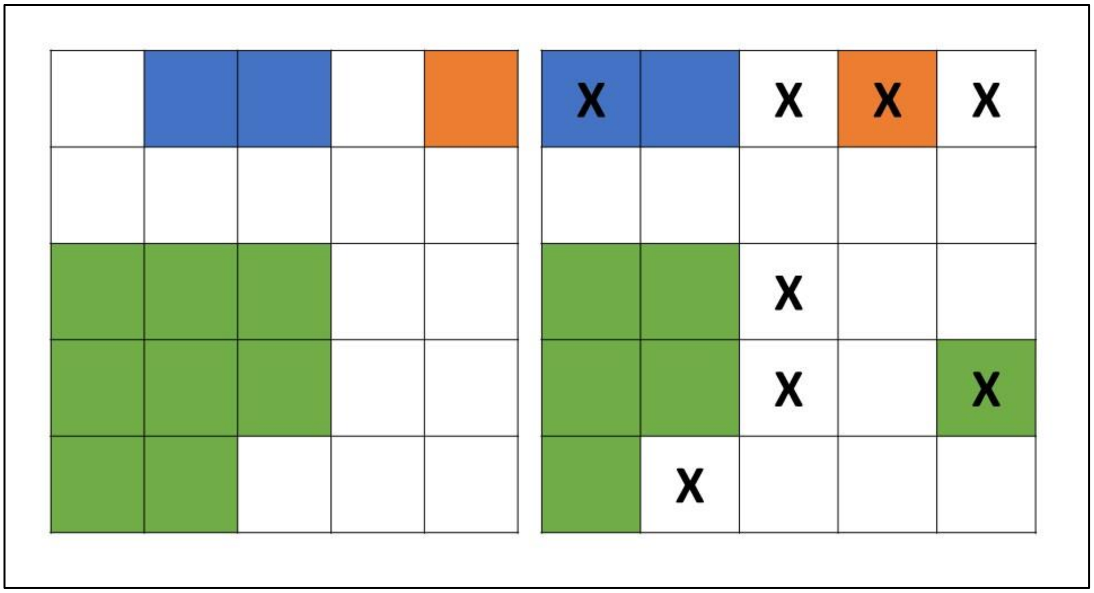

Figure 2-5. Errors in change detection that can be induced by imperfect co-registration. Here, each box represents a pixel. White, blue, orange and green all represent different land cover types. In this example, assume the grid on the left represents a "historical" classified image and the grid on the right represents a "repeat" classified image. Note that the land cover in the two grids has not changed, but the repeat image in this scenario has a co-registration error of 1 pixel (to the left). If comparing these two images pixel-by-pixel, grid cells marked with the letter X in the right panel denote pixels which would have erroneously detected land cover change, even though there is no difference in the land cover depicted by these grids (type I error).

Land cover change can also be evaluated quantitatively from oblique photographs using methods other than cross-tabulation. As noted above, if a photograph pair has a magnitude of co-registration error of 1-10 pixels, it can be said that the same landscape is sampled by the two photographs. Thus, quantification of land cover composition in historical and repeat photographs can allow analyses of change in terms of the proportion of pixels occupied by each class (see Chapter 3). In this type of change detection, the impact of misregistration is much less and is not exacerbated by the heterogeneity of the landscape.

2.5.4 Sources of error

Even when the camera used to take a repeat photograph was in the exact same position and orientation as the camera used to take the historical photograph, alignment was not perfect.

This was at least partly due to differences in cameras and lenses: light reached the sensors differently, and image scale was different for each camera system. Correcting this imperfect alignment through co-registration was possible, yet it resulted in an RMSE greater than 0 pixels (2.02 and 2.74 pixels for photographs with and without foreground, respectively). This reflects inherent challenges of manual co-registration: human error, image scale and image resolution may result in the selection of points that do not correspond to the exact same position in reality. Furthermore, it was assumed that the centre point of the repeat photographs was perfectly positioned in the same location as the historical photographs, but undoubtedly a small margin of error existed. Because the tripod and tripod head used were designed for photographic, not surveying purposes, the orientation of the camera was not prone to high precision adjustments. This magnitude of error (2.02 and 2.74 pixels) is thus a baseline error expected to occur for all repeat photographs in this analysis; hence the importance of comparing RMSE values for each of the photograph pairs to the "control" pair with no alterations in camera position or orientation. In some instances, however, photograph pairs had lower RMSE values than their corresponding control pairs. This could be explained by the above factors (challenges of manual co-registration, imperfect alignment of the centre point). Additional replications of this experiment would likely average out such anomalies.

2.6 Conclusion

In this experiment, we tested to what extent errors in relocation of the camera affected the co-registration accuracy of repeat photograph pairs. We found that co-registration accuracy was most affected by errors in camera orientation (i.e. when the camera was not centred on the right feature) and, to a lesser extent, by errors in camera position beyond 1 m from the original vantage point. We found that these observations were consistent for both images with and without foreground features.

The implications of these findings are twofold. First, when conducting repeat landscape photography, researchers should aim to locate the original vantage point to within 1 m; from there, it is more important to verify that the centre point of the photograph is correct than to spend hours fretting over a few centimetres around the camera location. Second, our results suggest that cumulative errors in camera set-up (i.e. ways in which the camera position or orientation differ from the set-up of the historical camera) could be corrected to a reasonable degree by a digital alignment tool with careful selection of control points. Such careful alignment of repeat photographs helps ensure that sampling error remains lower than the ecological signal being analyzed thus minimizing type I and type II errors.

This study has provided a reference for achievable co-registration accuracy, as well as an indication of which factors to take into account when weighing trade-offs between accuracy and time for field repeat photographers. Furthermore, our findings suggest that experienced repeat photographers are likely able to find the original camera location to within 1 m by trial-and-error using the principles of parallax, enabling them to achieve high co-registration accuracy with the help of digital alignment algorithms in post-processing. This reinforces the use of repeat photography for quantitative analyses of landscape change. Future studies could replicate this experiment to examine broadly applicable trends in co-registration accuracy expected in repeat landscape photographs, considering variability introduced by the cameras used, the distance of the landscape of interest from the camera, the clarity of the features pictured, and the user-defined control points selected in the alignment algorithm.

Chapter 3
Terrestrial oblique photographs as measures of landscape composition and change

Chapter 3 of this thesis is in preparation to be submitted as a manuscript with co-authors Jason Fisher and Eric Higgs.

3.1 Abstract

While orthogonal (i.e. aerial or satellite) imagery has become the more conventional source of land cover data because it can yield spatially accurate land cover maps, terrestrial oblique photographs present a valuable, relatively untapped source of raw optical data for studies of land cover change. To contrast how these two types of imagery sample landscape composition, we quantified land cover in the Willmore Wilderness Park, a remote mountain park in Alberta, Canada, with both data sources and empirically compared the two using linear models. We classified 46 oblique photographs and regressed the land cover proportions of each against those extracted from a Landsat-based classified map of the same area. There was a strong positive relationship for most land cover types, especially dominant ones (coniferous forest, herbaceous cover, and rock). Oblique images detected narrow categories (wetland, water and snow/ice) more frequently than orthogonal images due to the higher spatial resolution of the former. Oblique images also did a better job of sampling steep slopes and cliffs in high topography landscapes, owing to their angle of incidence. These advantages, paired with the fact that the record of land-based oblique photographs goes back decades before the first aerial or satellite imagery, suggest that oblique photographs have great potential as a source of land cover data for quantitative studies of long-term landscape dynamics.

3.2 Introduction

Many types of land cover change, especially degradation and practically irreversible conversion, pose a global environmental challenge with numerous causes and far-reaching effects (Brunsden & Thornes, 1979; Foley et al., 2005; Lambin, Geist, & Lepers, 2003; Turner, 2005; United Nations, 2017; Vitousek, Mooney, Lubchenco, & Melillo, 1997). To monitor such changes, it is important to establish reference conditions for historical landscape composition. While the predominant source of contemporary land cover data is remotely sensed orthogonal imagery – i.e. imagery approximately perpendicular to the land surface – this imagery only became widely available in the 1970s for satellites and in the 1930s for aerial photography (Belward & Skøien, 2015; Browning, Archer, & Byrne, 2009; Kaim, 2017; Shao & Wu, 2008; Stockdale et al., 2015). Conversely, the first terrestrial landscape photographs were taken as early as the 1860s, predating even the earliest orthogonal imagery by several decades (MacLaren et al., 2005; Roush et al., 2007; Stockdale et al., 2015; Webb, 2010). Thus, land-based photographs can offer greater temporal depth than their aerial counterparts, a significant opportunity for long-term landscape change monitoring.

Many studies have taken advantage of historical land-based photographs to examine long-term land cover change through the process of repeat photography (e.g. Butler and DeChano, 2001; Byers, 2008; Frankl et al., 2011; Hastings and Turner, 1965; Kaim, 2017; Pickard, 2002; Roush et al., 2007; Taggart-Hodge, 2016). These images, also referred to as "terrestrial oblique photographs" (henceforth "oblique photographs") because of the oblique angle of incidence from which they are taken, have numerous advantages over standard orthogonal images. First, as noted above, oblique photographs can offer greater temporal depth.

Second, oblique photographs present the landscape in a way that people (and terrestrial animals) are accustomed to seeing it – a human's eye view, as opposed to an overhead or bird's eye view, which is less intuitive (Grenzdorffer et al., 2008). Third, in areas where there is significant topography, such as mountainous landscapes with steep cliffs, oblique photographs capture a significant amount of detail on slopes which aerial photographs miss due to the latter's angle of incidence (Delaney, 2008; Sanseverino et al., 2016). Fourth, oblique photographs often provide much greater spatial resolution than typical satellite products covering the same area (Chandler et al., 2002). Fifth and finally, photographs taken from the ground are numerous (and hence a potentially voluminous source of citizen science data), because people like to take pictures of remarkable landscapes. As such, oblique photographs present a useful but relatively untapped data source for studies of landscape change, particularly around mountains (Kaim, 2017).

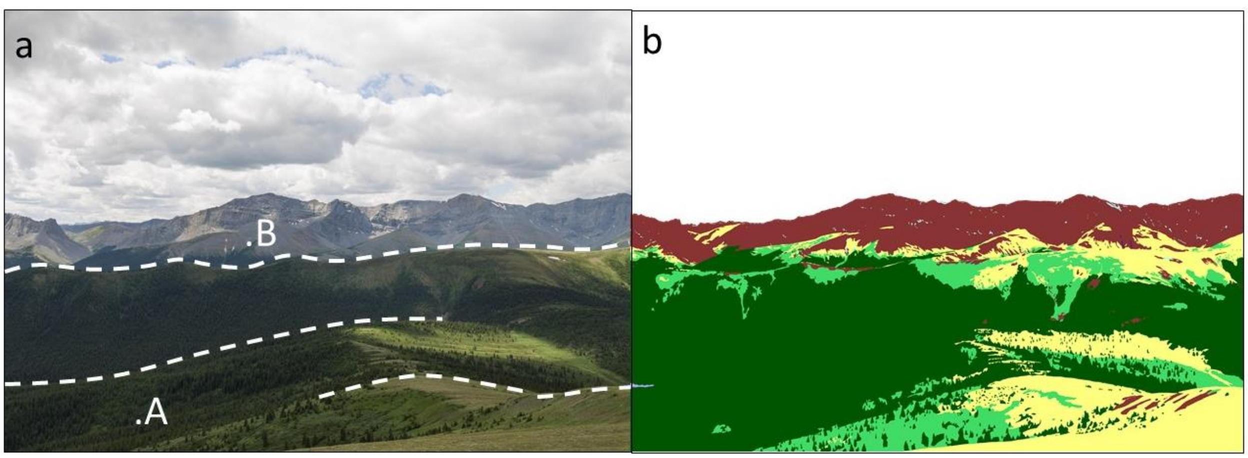

Figure 3-1. Sample image and associated land cover mask.
(a) An example of an oblique photograph, taken in 2014. A pixel at point A would represent a smaller area in the landscape than a pixel at point B, because point B is farther away from the camera. The dotted lines show horizon lines beyond which there are parts of the landscape that are obscured from view from this oblique viewpoint. (b) The classified mask associated with this photograph.

Despite these advantages, oblique images are not used as frequently as orthogonal images for studies of land cover. Orthogonal photographs are typically favoured because their basal unit (i.e. the pixel) represents a constant area, making it easy to use orthogonal photographs as the basis of spatially consistent land cover maps of large areas (Campbell & Wynne, 2011). In contrast, oblique photographs are not spatially consistent; pixel size varies within an image and viewsheds include obscured areas (Figure 3-1).

Techniques exist to orthorectify oblique images to yield spatially accurate land cover data (e.g. Bozzini et al., 2012; Stockdale et al., 2015). However, this process is non-trivial and time-consuming, particularly for large sample sizes, and entrains its own sources of error (Kolecka et al., 2015b; Stockdale et al., 2015). Another option is to create land cover masks by segmenting and classifying oblique images without orthorectification (Figure 3-1). Land cover proportions can be estimated from these oblique masks by computing pixel counts of various classes (Jean et al., 2015a). If, despite the variable pixel size in oblique photographs, these estimates of land cover proportions are found to be similar to those derived from spatially accurate satellite imagery, many research questions could be answered using oblique photographs without requiring the orthorectification process and its associated error propagation. The data-rich world of oblique imagery, including citizen science data, could be leveraged to ask questions that span longer temporal periods and at greater spatial resolutions than possible with typical satellite products. A model of such oblique imagery is the data collected by the Mountain Legacy Project in the mountains of western Canada.

The Mountain Legacy Project (MLP) is an ongoing repeat photography project based on over 120,000 historical terrestrial oblique photographs (Sanseverino et al., 2016). The original photographs were taken systematically by surveyors from the mid 19th to the early 20th centuries to create comprehensive topographic maps of the Canadian mountain west. The photographs were preserved on glass plates at Library and Archives Canada/Bibliothèque et Archives Canada and the British Columbia Archives using such fine photographic emulsions that the image quality requires at minimum a 35-megapixel modern digital camera to replicate. Over the years, the MLP has repeated nearly 7000 of the historic images, and has built a suite of custom tools for categorization and analysis of oblique images (Gat et al., 2011; Jean et al., 2015b; Sanseverino et al., 2016).

In this study, we took advantage of the MLP's vast collection and custom software tools to test whether the land cover proportions predicted by masks of oblique photographs are similar to those predicted by thematic maps based on satellite imagery. Given that both types of imagery are optical representations of the same landscape, we hypothesized that land cover composition would be fairly consistent between the two, with discrepancies reflecting inherent differences – but not necessarily biases – in the way the data sources sample the landscape. We predicted that: (1) land cover types characteristic of highly topographically variable areas (i.e. steep slopes) would represent a higher proportion of the landscape in oblique masks than in satellite-based maps (Sanseverino et al., 2016), and (2) oblique images would capture a greater amount of detail in the landscape due to their higher spatial resolution (Chandler et al., 2002). By testing these predictions, we examined the validity of two frequently-cited arguments in favour of oblique imagery, as well as the feasibility of quantifying landscape features directly from oblique photographs without orthorectification.

3.3 Method

3.3.1 Acquisition of oblique photographs

The photographs we used are contemporary (< 12 years old) repeats of historical photographs in the MLP collection. The photographs were taken in the summer months during field seasons between 2007 and 2016 inclusively. Images were captured with high resolution camera systems (Hasselblad H3 with a 35-mm lens, Nikon D800 with a 28-mm lens or Nikon D810 with a 28-60-mm zoom lens) on a levelled tripod.

3.3.2 Study area

The 46 oblique photographs in this analysis (Appendix C) were selected from a total of nearly 500 in or within one kilometer of the Willmore Wilderness Park, in Alberta, Canada. The Willmore is a 4,568 km^2 mountainous wildland park immediately north of Jasper National Park (Figure 3-2). Topography in the park is rugged, with high peaks and steep ridge slopes (Fisher, Anholt, & Volpe, 2011). Vegetation is dominated by Engelmann spruce (*Picea engelmannii*) and subalpine fir (*Abies lasiocarpa)*, although alpine meadows of herb and shrub are common, and the eastern edge of the park supports more deciduous tree species (Fisher, Anholt, et al., 2011; Hall, Walsworth, Gartrell, Wang, & Klita, 2000; Mucha, 2013). This study area was chosen for its relatively low human footprint (Fisher, Wheatley, & Mackenzie, 2014; Stewart et al., 2016); given that the oblique photographs were taken in some cases years apart from when the satellite imagery was acquired (see section 3.3.5), it was important to opt for a landscape that would not exhibit substantial changes between the time of acquisition of both sources of imagery. This way, differences observed between the two data sources more likely represented differences in the way they sampled the landscape rather than actual changes that occurred in the landscape in the time between image captures.

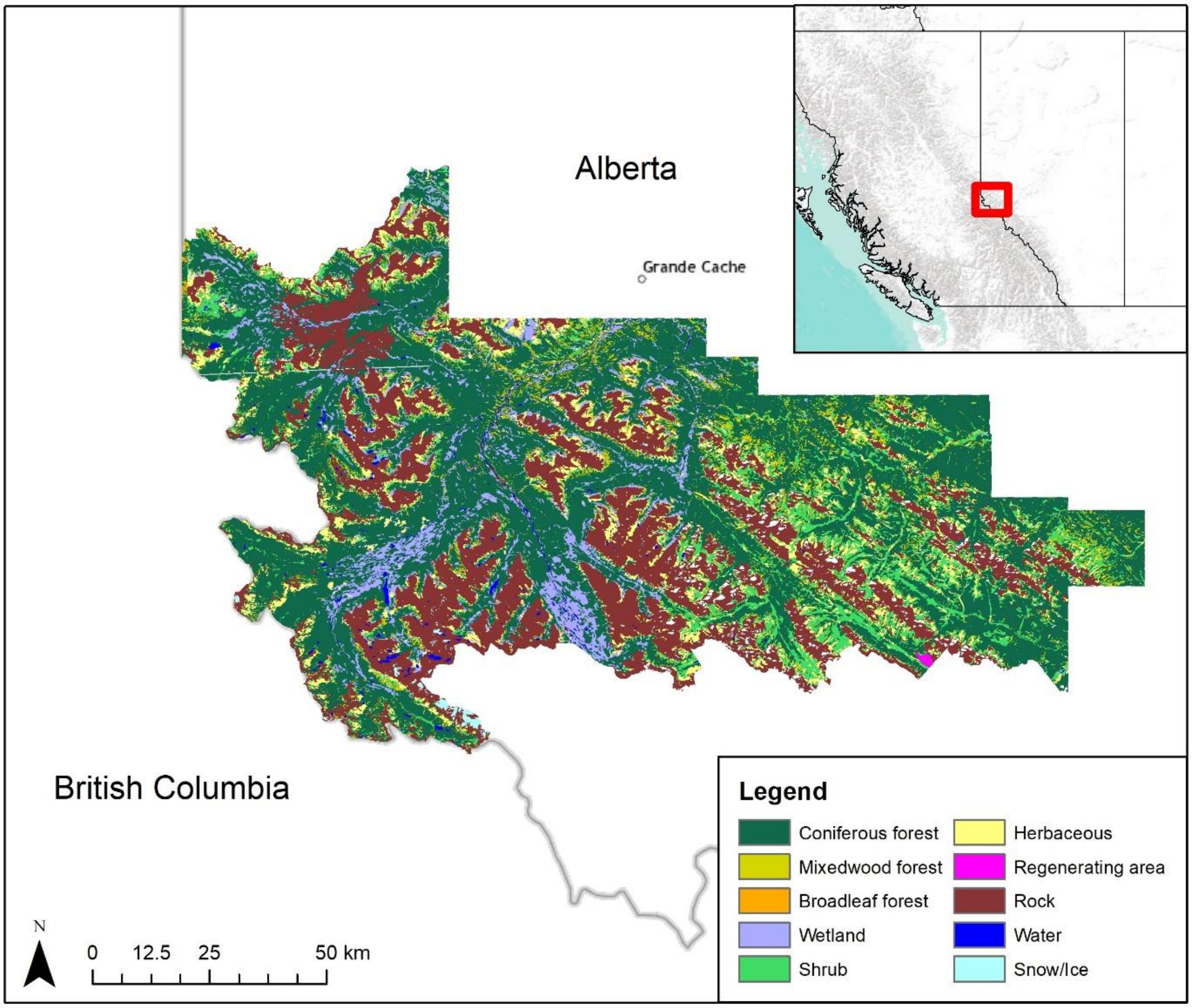

Figure 3-2. Study area map.
Landsat-based classified map, dated 2010, of the Willmore Wilderness Park in west-central Alberta, Canada.

3.3.3 Sample selection

We selected the 46 photographs (Appendix D) according to the following criteria:

- Images were clear and sharp, with no exposure or focus issues, to facilitate classification.
- Images consisted of 20% or less foreground, to maximize usable pixels. (Foreground pixels were omitted from analysis as recommended by Rhemtulla et al. (2002), as

pixels in the foreground of an image represent a much smaller area than pixels in the background. By omitting disproportionately small pixels, the land cover proportions of an image are less affected by variable pixel size.)

- Images captured the view from valley to peak, to show the full range of possible land cover types.
- Images were geographically dispersed across the study area, to capture east-west and north-south climatic and topographic gradients.

Beyond this, we selected images to minimize overlap and to ensure no bias in any compass direction (e.g. not sampling only north-facing slopes). In some cases, overlap between the viewsheds of multiple images occurred; this was regarded as sampling with replacement and did not affect our analysis or conclusions. Each image remained an independent sample as the land cover proportions calculated from one image did not affect the land cover proportions of a slightly overlapping image (and thus did not inflate degrees of freedom in analysis). Lastly, in cases where there were multiple retakes of the same photograph a few years apart, the clearer one was favoured.

3.3.4 Segmentation and classification of oblique images

Typical methodologies to segment and classify orthogonal imagery (i.e. automated or semi-automated classification algorithms) are less successful when applied to oblique photographs, primarily due to the limited spectral resolution of single lens reflex cameras compared to Earth observation satellites (Jean et al., 2015a). This technical challenge required a different approach for the segmentation and classification of oblique images: manual classification. An expert familiar with the study area used a custom-built MLP software program called Image Labeler to manually classify the oblique images (Jean et al., 2015a; Taggart-Hodge, 2016) . The program works by displaying a photograph and allowing a user to draw over it, creating a “mask” with customizable categories. The expert used a Wacom Intuos PTZ-930 pen tablet to delineate the masks with great precision; the width of features drawn by the pen in Image Labeler was 5 pixels, meaning that the minimum mapping unit of these masks is a 5 pixel by 5 pixel square.

The 10-category classification scheme used on the oblique photographs was adapted from the classification scheme of the Landsat-based dataset to which the oblique photographs were compared (Table 3-1; McDermid, 2009). Vegetation categories were not identified based on crown closure, but rather, based on the type of vegetation as visible from an oblique angle. Foreground pixels were omitted from classification due to issues with pixel distortion (Rhemtulla et al., 2002). In some photographs, smoke and fog made classification of the background questionable; such areas with high uncertainty were omitted from analysis.

By means of this process, we created 46 oblique photograph-based land cover masks (Appendix D) according to the categories outlined in the second column of Table 3-1, and estimated land cover proportions of each category by calculating pixel counts with respect to the total number of classified pixels.

3.3.5 Extraction of Landsat polygons

A 16-category thematic map of the province of Alberta generated by incorporating Landsat imagery and digital elevation models was the orthogonal mask used for this analysis (Figure 3-2; Fisher, Wheatley, & Gould, 2011; McDermid et al., 2009). We digitally delineated polygons corresponding to the viewshed of the oblique images in Google Earth Pro using the

Ruler tool by comparing the view iteratively with the photographs (*Google Earth*, 2017). We then extracted land cover proportions in terms of pixel counts from the Landsat-generated map within these polygons using the Extract By Mask tool in ArcMap 10.4.1 (*ESRI*, 2015).

Table 3-1. Land cover categories.
Corresponding categories in the Landsat masks and oblique masks, with their associated interpretations for the oblique masks.

Category in Landsat masks	Equivalent category for oblique masks	Definition of category used in oblique masks
Dense conifer forest	Coniferous forest	Conifer trees
Moderate conifer forest		
Open conifer forest		
Treed wetland		
Mixedwood forest	Mixedwood forest	Patches with 30-70% cover by broadleaf trees and the rest by coniferous trees
Broadleaf forest	Broadleaf forest	Broadleaf trees
Open wetland	Wetland	Vegetation with a wet or aquatic moisture regime
Upland shrub	Shrub	Shrubby vegetation
Upland herbaceous	Herbaceous	Grasses and herbaceous vegetation
Regenerating area	Regenerating area	Visibly recently burned forest (charred trees)
Barren land	Rock	Bedrock, rubble, rocky outcrops
Water	Water	Lakes, rivers, ponds
Snow/Ice	Snow/Ice	Patches of snow/ice, glaciers
Agriculture	N/A	N/A
Cloud/No data		
Shadow/No data		

3.3.6 Regression analysis

We conducted data exploration in the statistical software program R (R Core Team, 2015) to ensure that the assumptions of linear regression were upheld, as recommended by Zuur et al. (2010) to avoid type I or type II errors in our statistical analysis. Minor issues with nonlinearity, nonnormality and heteroskedasticity in some land cover categories prompted further investigation into data transformations. We found that transformations did not improve the measures of normality for most categories. Moreover, probability distributions for generalized linear models (Poisson, etc.) did not fit the data. Given that the purpose was not to find the best fit model for each category, but rather to test whether there exists a linear relationship between the two data sources, despite the few breaches in assumptions (nonlinearity, nonnormality and heteroskedasticity), we computed simple linear regression in R on the untransformed data, for all categories, using the *lm* function in the STATS package (R Core Team, 2015).

3.4 Results

3.4.1 Image scale

At the image level, the most dominant categories – coniferous forest, herbaceous cover and rock, which together form over 86% of the total number of pixels in the oblique masks – exhibited relatively strong (coniferous forest $r^2 = 0.319$; herbaceous cover $r^2 = 0.391$; rock $r^2 = 0.589$; all $p < 0.0001$) positive linear relationships (Figure 3-3). The slopes of the best fit lines for these land cover categories were all less than 1 (slopes of 0.497, 0.347 and 0.777 respectively), suggesting that within individual images, oblique masks tend to assign more pixels to these categories than Landsat masks do.

Mixedwood forest was a less frequent category, but despite the lack of observations, still showed evidence of a strong positive linear relationship (slope = 0.165, $r^2 = 0.589$, $p < 0.0001$; Figure 3-3). Similarly, regenerating areas showed a relatively strong ($r^2 = 0.187$, $p = 0.00272$; Figure 3-3) but nearly null (slope = 0.0256) linear relationship.

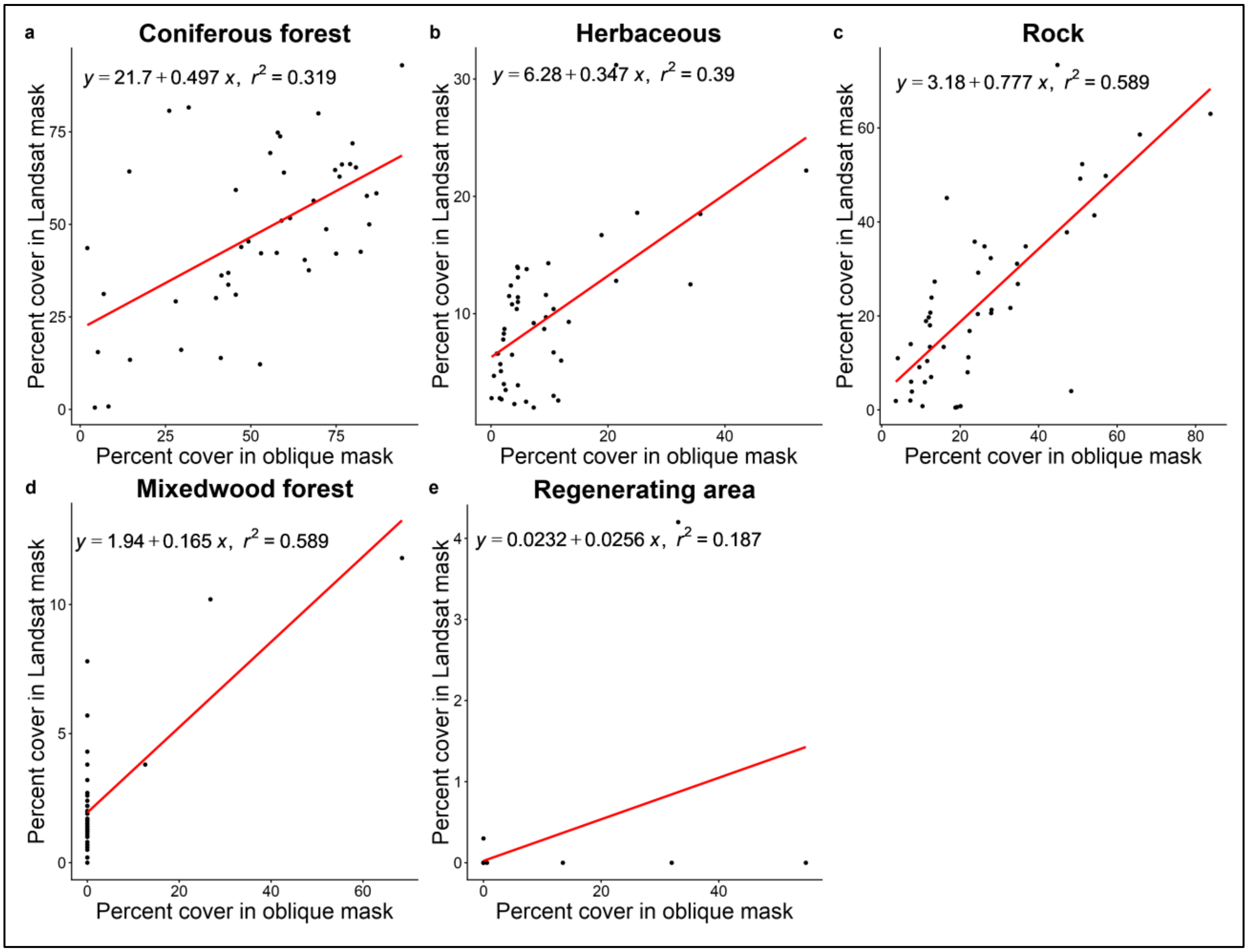

Figure 3-3. Correlation between oblique and Landsat masks.
Percent cover of (a) coniferous forest, (b) herbaceous cover, (c) rock cover, (d) mixedwood forest, and (e) regenerating area, in both the oblique mask and Landsat mask for each of the 46 sites.

The remaining categories (broadleaf forest, wetland, shrub, water and snow/ice) each consisted of less than 5% of the total number of pixels in the oblique images. Many of these categories were entirely unrepresented in the majority of samples (Figure 3-4), and did not exhibit evidence of a linear relationship between land cover proportions predicted by oblique and Landsat imagery at $p < 0.05$.

3.4.2 Landscape scale

Across the entire study area, oblique and Landsat masks predicted similar proportions for most land cover types (Figure 3-5). Most categories were within 1% of one another, with the exception of coniferous forest (within 5%), shrub (within 9%), rock and regenerating area (both within 3%). All categories had high standard deviations (nearly 50% of the mean or higher, and in many cases exceeding the value of the mean), in both oblique and Landsat masks.

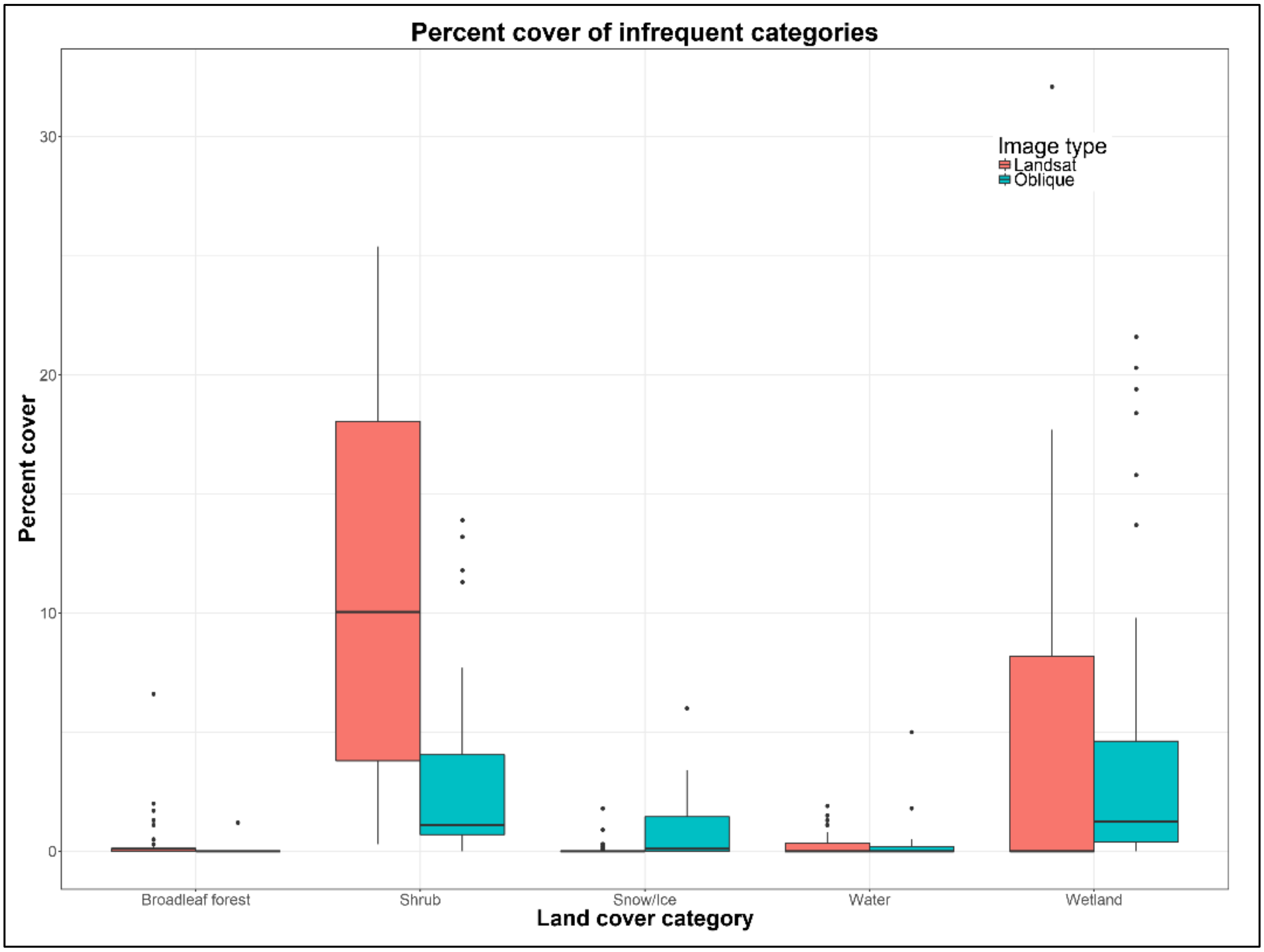

Figure 3-4. Percent cover of infrequent categories in oblique and Landsat masks. Boxplots representing the percent cover of the more infrequent categories for both the oblique and Landsat masks for all 46 sites.

3.4.3 Resolution

On average, oblique masks contained over 10,344,024 pixels (s.d. = 4,352,621) while the corresponding Landsat polygons counted 18,023 pixels (s.d. = 13,082). Assuming the minimum mapping unit of 5x5 pixels for the oblique images, and of single pixels for the Landsat imagery, this means that oblique masks have, on average, approximately two orders of magnitude more mapping units covering the same area. The mean areal sample of an oblique image was approximately 17 km^2, with a total area of nearly 423 km^2 sampled by the aggregate collection of images.

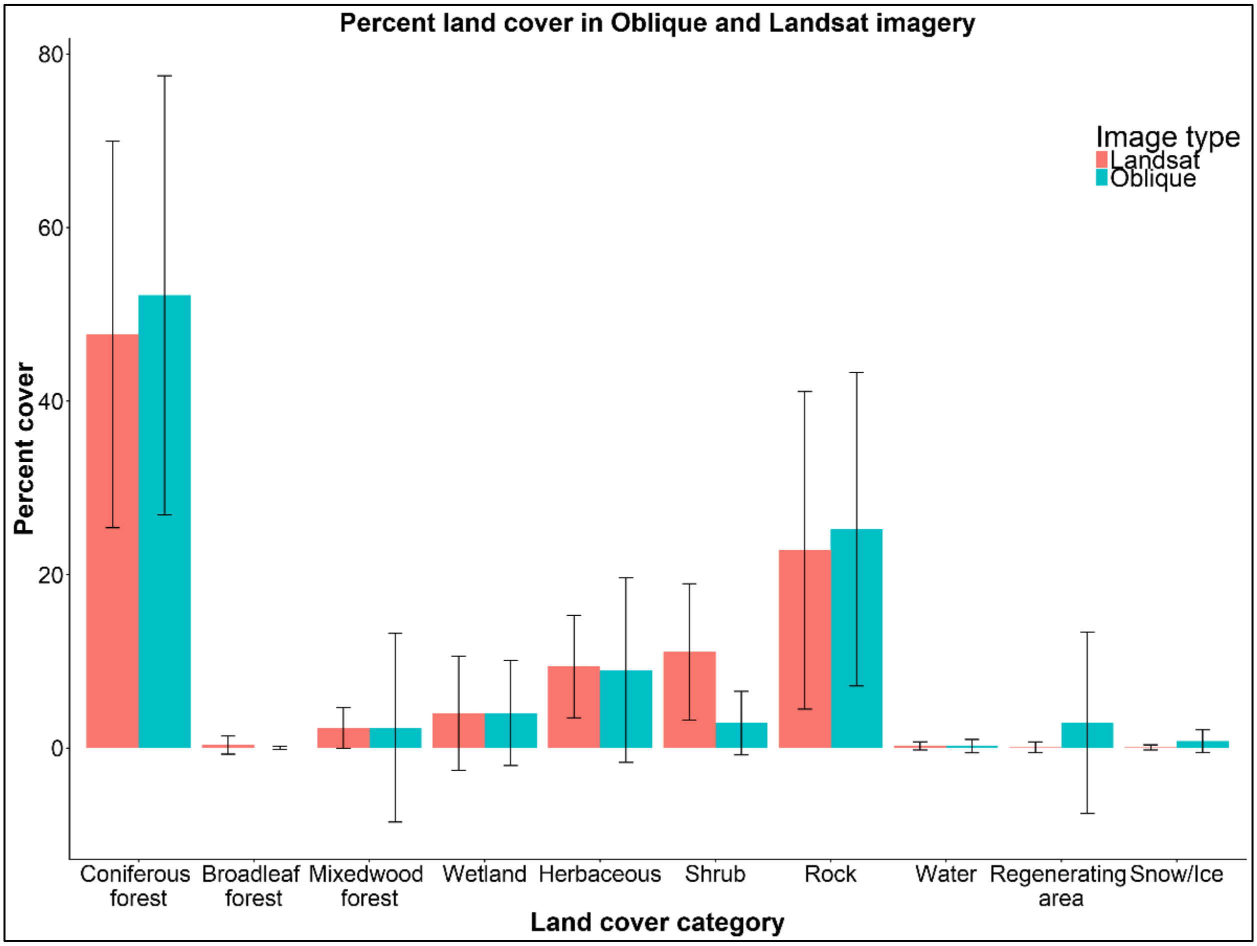

Figure 3-5. Comparison of landscape-scale land cover proportions.
The mean percent cover of each land cover category in both the Landsat and oblique masks, with error bars (1 standard deviation).

3.5 Discussion

3.5.1 Landscape-scale agreement

At the landscape scale (i.e. when averaged across all samples), oblique and orthogonal masks show reasonable agreement with respect to land cover proportions, similar to Rhemtulla et al. (2002). The high standard deviations in each category (Figure 3-5) suggest that there is high variability in both data sources, as expected in this diverse, heterogeneous landscape. Nevertheless, across the study area, the difference in the percentage of the landscape covered by each category predicted by the two data sources is no greater than 3%, except for coniferous forest and shrub cover.

Coniferous forest dominates the landscape, with both oblique and orthogonal imagery predicting that it makes up approximately half (~50%) of the landscape. However, oblique masks tend to assign a greater proportion of pixels to coniferous forest than Landsat masks, by a small (<5%) margin. This tendency might be a consequence of misclassification of either image (i.e. commission error in oblique masks or omission error in Landsat masks), or of pixel distortion in the oblique image: 1 m^2 of landscape in the midground of an image will be represented by a greater number of pixels than 1 m^2 in the background. Because forest pixels most often make up the midground rather than background of oblique images, the proportion of forest cover of oblique photographs will be larger than that of its corresponding orthogonal image (greater proportion of pixels covering the same area).

Conversely, Landsat masks predicted a greater proportion of shrub cover than did oblique masks – 11.1% versus 2.9% – making shrub the category with the largest disagreement between the two sources. Possibly, shrubs were consistently over-represented in the Landsat map product because of the definition of the category: “>25% shrub cover; <6% tree cover” (McDermid et al., 2009). By this definition, a 30 m by 30 m Landsat pixel could have as low as 225 m^2 (25%) of shrub cover and still be classified as shrubland, meaning the remaining 75% cover within that pixel, which actually consists of different land cover types, would be misclassified as shrub. It is possible that the oblique photographs avoid this kind of misclassification given their finer resolution (oblique masks contained two orders of magnitude more mapping units than their corresponding Landsat polygons). Thus, oblique photographs would measure a smaller proportion of pixels in the shrub category compared to the Landsat masks. This suggest that the oblique images might provide a more accurate sample of the landscape due to their higher spatial resolution and thus greater ability to resolve small features (Lausch & Herzog, 2002).

3.5.2 Image-scale agreement

At the image scale (i.e. for each of the 46 sample sites), agreement was strong for dominant land cover categories and weak for rare categories. Thus, both types of imagery did a similar job of capturing the majority of the landscape. The oblique masks, however, owing to their higher spatial resolution, better predicted land cover types that appeared as narrow or small patches (wetland, water and snow/ice).

Coniferous forest, herbaceous cover, rock

Oblique and Landsat masks generally predicted the same trends for coniferous forest, herbaceous cover and rock (i.e. when oblique masks predicted a high proportion of coniferous forest in the landscape, so did Landsat masks). However, there was a systematic tendency for oblique images to sample more of these land covers compared to the Landsat images (slopes all < 1; Figure 3-3). A number of factors may have contributed to this tendency. First, these categories may have been better sampled by the oblique images due to their angle of incidence, particularly rock as it makes up the majority of steep terrain such as cliff faces. This implies that oblique photographs can be advantageous in that they provide information about the landscape that satellite images fail to capture, especially in mountainous landscapes with high topography. Second, the higher spatial resolution of oblique images means that they will have fewer issues with mixed pixels (i.e. pixels that contain multiple different land cover types). This is relevant because some areas that might have included coniferous forest, herbaceous cover or rock might have been classified otherwise in the Landsat product based on the category definitions described in McDermid et al. (2009), decreasing the percent cover of those land cover types. Third, it may be an artefact of pixel distortion in the oblique photographs: the same area in reality will contain more pixels in an oblique image if it is in the midground rather than the background.

Mixedwood forest

Although Landsat and oblique masks exhibited a relatively strong relationship for mixedwood forest, the near-null slope suggests that Landsat masks predict this category regardless of what is predicted by oblique masks. Indeed, mixedwood forest was observed at 45 of the 46 sites in the Landsat polygons, but at only 3 of the 46 sites in the oblique photographs. The discrepancy in detection of mixedwood forest between the two may be attributable to the angled view in oblique photographs. Coniferous trees such as Engelmann spruce and subalpine fir seen in this park can reach heights of 30 – 40 m, whereas broadleaf species in the area do not often reach maturity and are thus smaller (Alexander, 1987; Arsenault, 2003). As such, it is possible that the broadleaf trees were obscured by taller coniferous trees in the oblique images, but were observed from atop in the orthogonal images – this is supported by the fact that 22

Landsat masks contained broadleaf pixels but only a single oblique mask did. Alternatively, confusion might have arisen between coniferous and broadleaf/mixedwood forest patches in the Landsat classifications due to their spectral similarity (Foody & Atkinson, 2003).

Regenerating area

Regenerating area, on the other hand, was detected in only 5 oblique masks and 2 Landsat masks. The relationship between the two data sources was once again strong but nearly null, indicating that the proportion of regenerating area in oblique images did not predict the proportion of said class in orthogonal images. Regenerating area is a short-lived land cover type – burned forest is distinguishable for a few years post-fire, after which point it would be classified as herbaceous or shrub cover as it enters secondary succession. Given that the two data sources compared in this study did not always acquire images at the same time, it is likely that there would be disagreement on this land cover type.

Broadleaf forest, wetland, shrub, water, snow/ice

There was found to be no relationship between oblique and Landsat masks for the remaining categories, suggesting that the two data sources sample broadleaf forest, wetland, shrub, water and snow/ice cover in different ways. These categories either consistently represented small proportions of the landscape, or were unrepresented at a large number of sites (Figure 3-4).

For instance, broadleaf forest was observed in only one oblique photo. Similar to mixedwood forest, possible explanations include obstruction of broadleaf trees by coniferous trees in an oblique view, or misclassification of broadleaf forest.

Shrub cover, conversely, was well represented across the samples, but there was no relationship between the proportions of shrub predicted by Landsat and oblique masks. This means that the two data sources do not sample the shrub category the same way, or that shrub is interpreted differently in both types of imagery. Once again, obstruction of this class from taller coniferous trees could affect oblique photographs' ability to capture shrubs. Alternatively, "shrub" is a broad term that could include many different species or types of vegetation that have various structures, textures and spectral signatures, and can often be confused with young forest in Landsat classification algorithms (Castilla, Hird, Hall, Schiek, & McDermind, 2014).

Wetland was detected at twice as many sites in oblique photographs (42) compared to Landsat (21). Water was also included more frequently in oblique masks than in Landsat masks (20 and 16, respectively), as was snow/ice (26 oblique masks and 9 Landsat masks). Wetlands, rivers (water) and snow patches have the common characteristic of appearing as narrow features on the landscape. As such, it is possible that Landsat polygons failed to resolve these categories due to the large (30 m) grain size of Landsat imagery, but that they were captured in oblique masks due to the higher spatial resolution of oblique photographs. Indeed, the oblique masks contained three orders of magnitude more pixels than their corresponding Landsat polygons.

3.5.3 Challenges of classification

Classification of the oblique masks was optimized to minimize interpretation error. Manual segmentation and classification of the oblique photographs was done by a trained expert, with comprehensive, mutually exclusive and well-defined land cover classes, using a graphics tablet for high precision. The photographs analyzed were all clear and sharp, due to the high-quality camera equipment (Hasselblad H3, Nikon D800 and Nikon D810) and careful methodology applied in the field as well as the sampling design of this study. Most categories were easy to differentiate based on colour and texture, especially due to the high spatial resolution of the oblique photographs. Nevertheless, it is possible that boundary effects (i.e. transitions that are difficult to define) made interpretation ambiguous in some areas.

As with the oblique images, there are challenges in classifying the Landsat images. McDermid et al. (2009) noted an overall accuracy of 64.5% in their product, with low confidence in the wetland and shrub categories and confusion between shrub and forest classes, and between shrub and herbaceous cover. Thus, disagreement between oblique and Landsat masks is not necessarily indicative of errors in the oblique masks; it may stem from misclassification of the Landsat imagery. Furthermore, Landsat masks are more likely to have mixed pixels (pixels that contain more than one land cover type) due to their larger grain size.

Another difference between the two data sources is the date of image acquisition. The Landsat-based map used imagery from Landsat 5 EMT+ from 1999-2002 (McDermid et al., 2009), whereas the oblique photographs were taken between 2007 and 2016. Disagreements between the two sources may have arisen because the landscape had changed between captures. However, we chose the Willmore Wilderness Park as our study area due to the low direct human impact on the landscape, aiming to minimize this error.

3.6 Conclusion

In this study, we analyzed classified masks generated from two different sources (oblique and Landsat imagery), using two different classification methods (manual and semi-automated, respectively). Satellite-based thematic maps are often used in studies of land cover change despite their uncertainties and errors; we sought to answer whether the same could be done with oblique masks. Without ground-truthed knowledge of land cover in the area sampled, we did not judge each approach for thematic accuracy (i.e. whether the mask reflects the true land cover of its viewshed). Instead, we compared land cover composition generated from oblique and Landsat masks. Disagreements observed do not necessarily reflect errors in the oblique masks; disagreements could also be a result of misclassification of the Landsat imagery, or of inherent differences in the way the two data sources sample the landscape.

Our findings suggest the two data sources yield similar land cover information for dominant land cover types (coniferous forest, herbaceous cover and rock). For less common categories (i.e. those covering less than 5% of the masks), comparison is more challenging due to the lack of observations. Nevertheless, our work has highlighted several advantages of using oblique imagery in landscape composition analysis. First, on average, the pixel density in our oblique photographs was three orders of magnitude higher than that of the corresponding Landsat polygons. This higher spatial resolution allows oblique photographs to capture narrow or small features (e.g. rivers or snow patches) that are likely not to be resolved by Landsat's 30 m pixels, and to distinguish features at a finer scale than allowed by Landsat class definitions. Second, greater pixel density also allows for more precise classification, reducing the effects of mixed pixels often observed in satellite-based maps. Third, landscapes with high topography are more likely to be adequately sampled by oblique images than by orthogonal images due to their optimal angle of incidence.

Our results suggest that land cover proportions can be estimated from oblique photographs within the same scope of error as conventional satellite imagery. Thus, oblique masks could be used in quantitative studies of land cover composition, even without orthorectification or georeferencing. This offers a much less resource-intensive approach to analyzing land cover data from oblique images, opening the door to numerous land-based photography data sets, such as citizen science data and collections of historic oblique photographs. This has implications for studies of temporal land cover shifts as a consequence of climate, ecological and land use change; delving into such data sets could lead to large-scale quantitative analyses of long-term (i.e. century scale) landscape change through repeat oblique photography.

Chapter 4
Climate change and fire regime-driven landscape homogenization and changes in songbird diversity in a Rocky Mountain ecosystem

Chapter 4 of this thesis is in preparation to be submitted as a manuscript with co-authors Jason Fisher, Christy James and Eric Higgs.

4.1 Abstract

Biodiversity and land cover data often extend no more than a few decades, which means there are remarkably few longitudinal studies on the effects of climate and land cover change on biodiversity. Mountain systems are of particular interest for such studies due to their heterogeneity, unique biodiversity and susceptibility to external stressors. We assessed long-term biotic change in a Rocky Mountain ecosystem using repeat photography. We quantified land cover composition in 46 historical and contemporary photograph pairs to evaluate changes in land cover, and applied species distribution models to examine associated changes in songbird diversity in the Willmore Wilderness Park in Alberta, Canada. We found that forest cover increased over the past century at the expense of other land cover types, leading to decreased landscape diversity. This homogenization correlated with a decline in alpine meadow-adapted songbirds, while forest-adapted species were positively impacted. These century-scale changes describe the impacts of climate change and fire regime shifts on a mountain avian community and provide historical context for projected changes: continued warming without changes in land management practices will likely lead to an even greater loss of landscape and songbird diversity. This approach can improve ecological change monitoring efforts in mountain ecosystems, using historical landscape photographs to provide context about changes in land

cover and biodiversity. This has implications for conservation and landscape management in remote mountain environments, some of the most challenging places to monitor.

4.2 Introduction

Climate change and land cover change are two of the dominant ecological challenges of our time (Foley et al., 2005; Lambin et al., 2003; Parmesan & Yohe, 2003; Vitousek et al., 1997), and are the main drivers of biodiversity loss globally (Bellard, Bertelsmeier, Leadley, Thuiller, & Courchamp, 2012; Sala et al., 2000). Most evaluations of the staggering rates of said biodiversity loss (Baillie, Hilton-Taylor, Stuart, & Commission, 2004) use relatively recent data (dating back a few decades at most). While longitudinal studies providing scientifically robust estimates of near-past rates of biodiversity change are key to understanding the context of current rates (Krebs, 1991; Rittenhouse et al., 2010; Yoccoz, Nichols, & Boulinier, 2001), longer-term assessments are often not possible; there have been remarkably few longitudinal ecological datasets collected over the last century (Magurran et al., 2010; Willis & Birks, 2006; Willis, Gillson, Brncic, & Figueroa-Rangel, 2005). Thus, it is a critical endeavour to tap into existing historical datasets in innovative ways to “backcast” historical biotic conditions. The ability to infer past biodiversity is important for conservation biologists seeking to manage climate, landscape and biodiversity change, as well as for ecologists seeking to understand the mechanisms of contemporary and future biotic change.

Mountain systems are of particular interest to ecologists and conservationists alike; mountains are unique in the diversity of life that they support (Körner, 2004; Molau, 2004), while simultaneously being regarded as “indicators of environmental health” due to their climatically sensitive nature (Luckman, 1998). The strong altitudinal gradients and microclimates found in mountain ranges produce heterogeneous land cover, and the resulting diverse habitat types sustain a high diversity of both generalist and mountain-adapted species (Dufour, Gadallah, Wagner, Guisan, & Buttler, 2006; Ruggiero & Hawkins, 2008; Whiteman, 2000). Because of the heterogeneity of the landscape, mountains and the species that inhabit them are especially susceptible to pressures such as climate change, land use change and anthropogenic disturbance (Beniston, 2003; Hansen-Bristow, Ives, & Wilson, 1988). As a result, substantial changes in vegetation and species distributions have been documented in the world's mountain ranges, including in the North American western Cordillera (Inouye, Barr, Armitage, & Inouye, 2000; Maestas, Knight, & Gilgert, 2001; Roush, 2009).

Bird species are especially diverse in alpine and montane ecosystems (McCain, 2009; Ruggiero & Hawkins, 2008), leading to the avian community having varied responses to landscape heterogeneity and change (Rotenberry & Wiens, 1980; Stralberg et al., 2009). Montane birds especially can exhibit high variability in population size (Lehikoinen, Green, Husby, Kålås, & Lindström, 2014). Still, bird taxa make up an important part of the species and population declines observed in mountain systems worldwide because of their sensitivity to stressors such as habitat loss, forest encroachment and wetland drying (Jetz, Wilcove, & Dobson, 2007; Lehikoinen et al., 2014; Rittenhouse et al., 2012; Zamora & Barea-Azcón, 2015). Thus, it is all the more critical to study long-term trends in mountain bird communities to understand the historical context of observed rates of change of this taxonomic group that is being impacted by climate and land cover change.

In the Rocky Mountains, data on bird diversity and abundance only exist a few decades into the past (e.g. the North American Breeding Bird Survey launched in 1966; Sauer et al., 2013). These data do not predate periods of significant landscape change induced by climate change and shifts in land management practices (e.g. fire exclusion; Keane et al., 2002). As such, to fully understand the historical context of avian communities before they were subjected to all contemporary stressors, estimates of earlier species occurrence or abundance must be inferred via other forms of data. For instance, models linking species and habitat can use historical land cover data (which, depending on the source, can reach farther back in time than species presence data) as input to predict species occurrence in past landscapes (Griffiths & Mather, 2010).

Species distribution models (SDMs) are a key tool used in conservation and management for estimating population sizes and predicting future biotic conditions (Elith & Leathwick, 2009; Guisan & Thuiller, 2005). Habitat selection is a critical ecological principle underlying SDMs, as fine-grain decisions accumulate into coarse-grain patterns that help us study and understand species-habitat relationships (Fretwell & Lucas, 1969). For breeding birds, central place foraging strategies offer a strong pattern of species-habitat use, because they remain within a limited range of the nest during natal care periods (Rosenberg & McKelvey, 1999). As such, SDMs are well suited to relate land cover information to occurrence of breeding bird species to establish change over a long timeframe.

To backcast bird diversity beyond existing empirical data (i.e. earlier than 1966, the start of the North American Breeding Bird Survey), SDMs can be informed with earlier land cover data. One of the only sources of such land cover information is terrestrial oblique photographs, the earliest of which were taken in the second half of the nineteenth century (Frankl et al., 2011; Kaim, 2017). We propose harnessing these historical data to estimate past rates of change in bird diversity by a process we call “repeat photography distribution modelling”. First, historical photographs are repeated through the photogrammetric method of repeat photography (Webb, 2010). Next, both historical and repeat photographs are analyzed for land cover composition, and are compared to estimate land cover change. Then, land cover information from both historical and repeat photographs is used in SDMs to estimate past and current bird diversity, and biodiversity change is inferred (Figure 4-1).

An example of a repeat photography project that holds historical and repeat photographs is the Mountain Legacy Project (MLP). The MLP is a 20-year ongoing research project and host of one of the world's largest databases of historical landscape photographs: over 120,000 photographs taken systematically by surveyors to provide a comprehensive view of the mountains of western Canada. To date, MLP field crews have repeated nearly 7000 of those photographs. The MLP has a suite of customized tools to visualize and quantify landscape composition in the images so as to measure land cover change (Gat et al., 2011; Jean et al., 2015b; Sanseverino et al., 2016; Trant et al., 2015).

In this study, we apply our proposed "repeat photography distribution modelling" approach on MLP photograph pairs to evaluate long-term bird diversity change in a mountainous ecosystem. We use historical and contemporary MLP photographs from the Willmore Wilderness Park in Alberta, Canada, to quantify land cover composition and estimate land cover change. We then use that information in conjunction with species distribution models to backcast bird diversity in the early 20th century. Given that other studies have noted mountain system sensitivity and changes such as forest encroachment (Keane et al., 2002; Rhemtulla et al., 2002; Roush, 2009), we hypothesize that coniferous forest cover in our study area has increased over the past century and that concomitant changes in avian community structure have occurred. We expect to observe increases in forest-adapted songbird species (e.g. gray jay, *Perisoreus canadensis*) but declines in species better adapted to habitats that have decreased in coverage, like alpine meadows (e.g. Savannah sparrow, *Passerculus sandwichensis*).

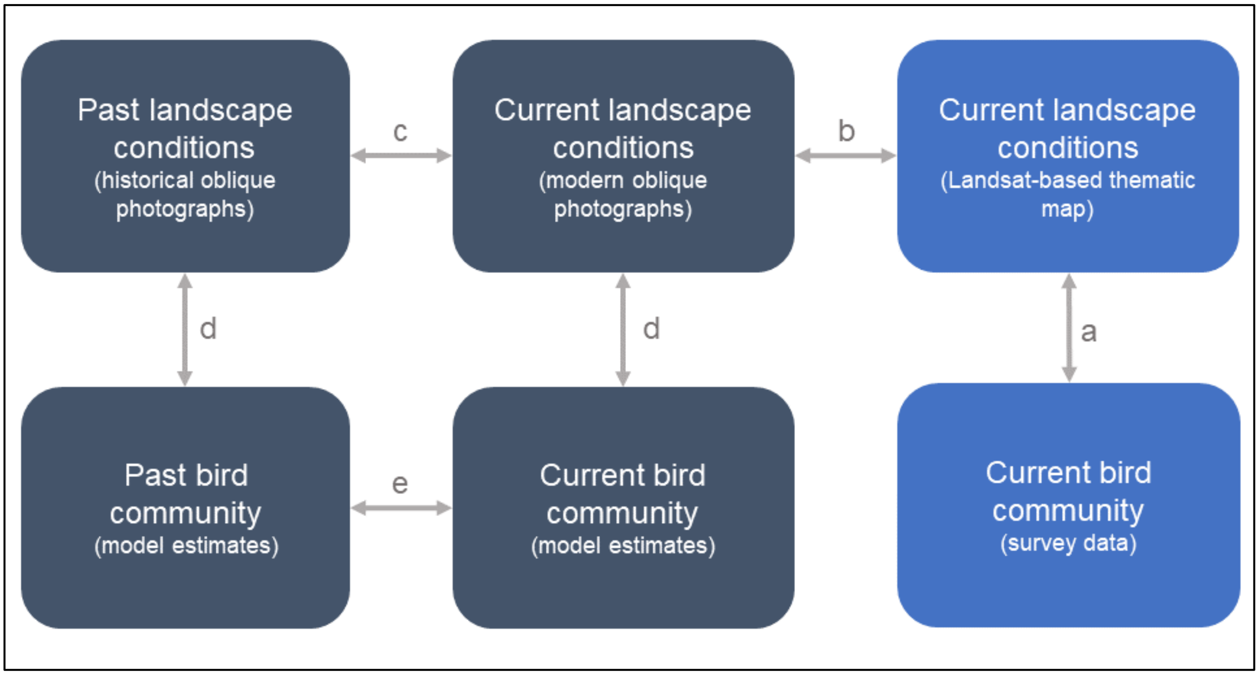

Figure 4-1. Conceptual model for repeat photography distribution modelling.
Diagram illustrating a conceptual model for our proposed method.
(a) Bird survey data will be linked with current landscape conditions to create species distribution models. (b) It was shown in Chapter 3 that land cover estimates derived from modern oblique photographs are similar to those from Landsat-based thematic maps. (c) Past and current landscape conditions will be estimated from classifications of historical and modern oblique photographs, respectively. Land cover change will be assessed by comparison of past and current conditions. (d) Species distribution models generated in (a) will be applied on past and current land cover composition estimated in (c) to estimate past and current probability of occurrence of birds. (e) Bird community change will be assessed by comparison of past and current estimates of bird occurrence probability.

4.3 Methods

4.3.1 Study area

Our sampling frame is the western Cordillera in North America, specifically the northern Rocky Mountains; our sampling area is the Willmore Wilderness Park (WWP) in west-central Alberta, Canada (Figure 4-2). The WWP was selected because of limited direct anthropogenic change over the last century compared with surrounding areas (Fisher, Bradbury, et al., 2013;

Fisher, Anholt, et al., 2011; Mucha, 2013). This makes it possible to infer that any observed land cover changes are a consequence of indirect stressors – namely climate change and shifts in wildfire regime (Keane et al., 2002; Magurran et al., 2010).

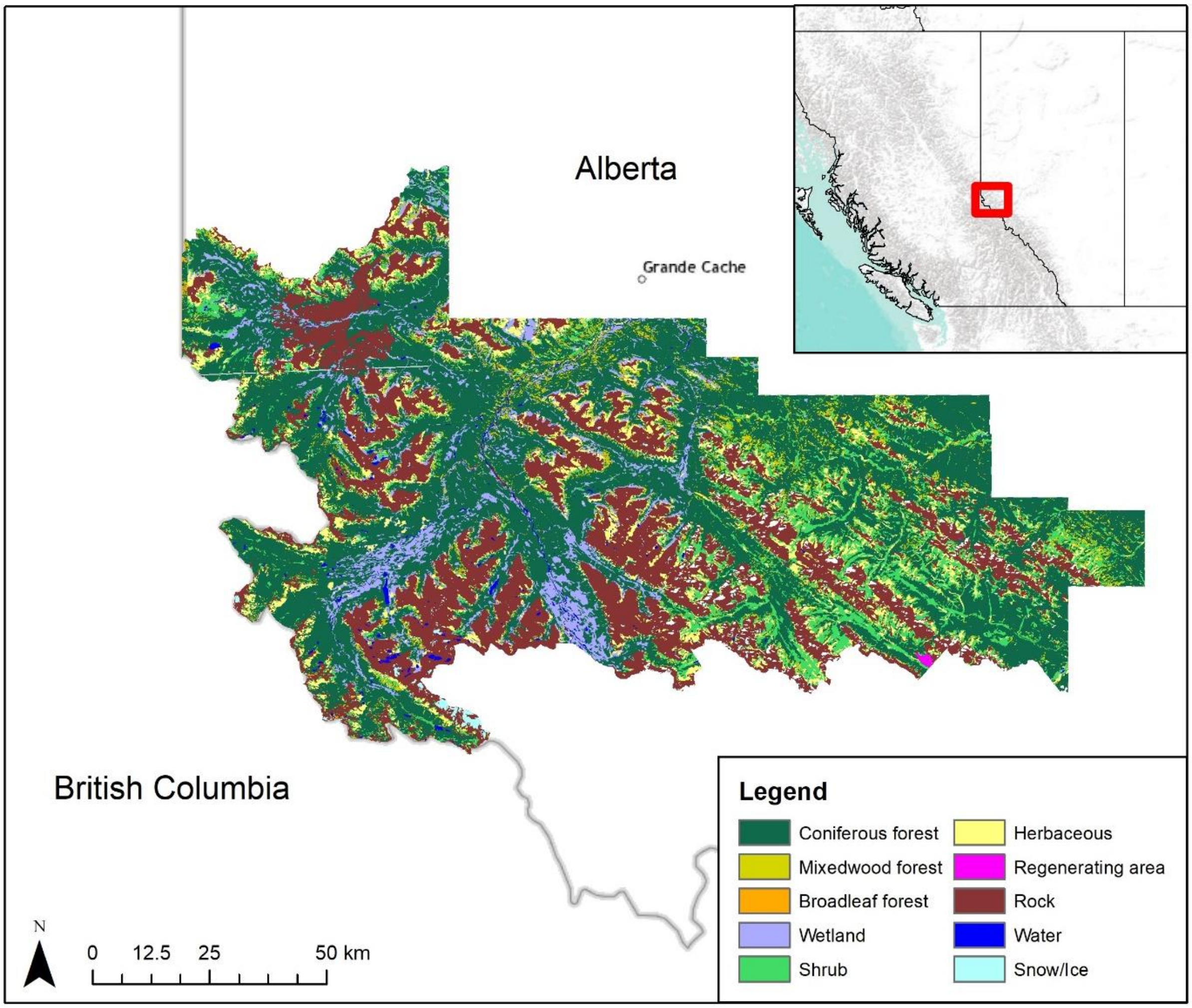

Figure 4-2. Study area map.
Landsat-based classified map, dated 2010, of the Willmore Wilderness Park in west-central Alberta, Canada.

The WWP is a 4568 km^2 provincial park that was designated through the Willmore Wilderness Park Act in 1959 to protect the area from oil and gas exploration (Province of Alberta, 2002). To this day, resource extraction and motorized transport are prohibited, although trails exist in the park for recreation and fur trapping, and signs of resource exploration prior to the park's inception can still be detected on the landscape (Fisher, Bradbury, et al., 2013; Fisher, Anholt, et al., 2011; Mucha, 2013). Still, only 0.0005% ± 0.0001% of the land area within the park is considered “human settlement” (Stewart et al., 2016).

Fire had been used as a tool to manage the landscape for centuries, if not millennia, by the Indigenous peoples that inhabited this area, namely the Metis and the Aseniwuche Winewak, Secwépemc, Stoney and Tsuu T’ina Nations. However, in the last century, since European colonization, low-intensity frequent fire that characterized Indigenous burning has been largely excluded from the landscape. Wildfire in general is suppressed in much of the park (Edgecombe, 1982; Keane et al., 2002).

The topography of the park is rugged, with steep mountain slopes providing habitat ranging from jagged peaks to alpine meadows and shrubs to forests dominated by Engelmann spruce (*Picea engelmanni*) and subalpine fir (*Abies lasiocarpa*) to moist valley bottoms filled with black spruce (*Picea mariana*). The climate, topography and vegetation shift from the West of the park toward the foothills of the East, with a greater diversity of deciduous trees in the East (Hall et al., 2000). The diversity of habitats in this area support a diverse avian community: upwards of 60 songbird species have been detected in the park, including several species listed as “sensitive” according to Alberta’s provincial ranking (Fisher, Wheatley, et al., 2011).

4.3.2 Historical photographs

The historical photographs we analyzed are part of the MLP’s much larger collection originally captured to create maps using photo-topographic survey methods, providing a comprehensive view of the mountains of western Canada (Bridgland, 1916, 1924; MacLaren et al., 2005; Trant et al., 2015). Photographs were taken with a large format camera, with fine emulsion 4” by 6” glass plates, on a levelled tripod. This generated remarkably high-quality and durable images that were preserved in national and provincial archives, mainly at Library and Archives Canada/ Bibliothèque et Archives Canada (Delaney, 2008). The glass plate negatives were digitized via scanning at 1800 pixels per inch and at 16-bit grayscale using an Epson 10000XL Flatbed Scanner. This resolution was necessary to recover as much information as possible from the fine emulsion.

4.3.3 Repeat photographs

Mountain Legacy Project field crews returned to the vantage points from which the historical photographs were taken and, using prints of the historical photographs as a reference, positioned their tripods by verifying the alignment of foreground and background features in the camera's viewfinder (Klett, 2011; Rogers et al., 1984; Webb, 2010). Repeat photographs were shot with high resolution digital camera systems: a Hasselblad H3 with a 35-mm lens, a Nikon D800 with a 28-mm lens or a Nikon D810 with a 28-60-mm zoom lens. The combinations of lenses and sensors used for the repeat photographs were selected to give a wider field of view than the historical images, which allows for cropping during the digital alignment process. Appropriate software lens corrections were applied to adjust for optical distortion.

Historical and repeat photographs were digitally aligned with one another (i.e. co-registered) using a custom-built feature in the Mountain Legacy Editing and Administering Tool (Taggart-Hodge, 2016). A user defined four point-pairs representing corresponding features in the photographs, and the alignment tool applied an affine transformation to crop, rotate, translate and scale the repeat image to match the historical one.

4.3.4 Sample selection

The 46 photograph pairs analyzed (Appendix C) were selected from a total of approximately 500 within the study area based on several criteria: (i) no exposure or focus issues; (ii) < 20% foreground (as foreground pixels were omitted from analysis); (iii) captured the full elevational habitat gradient (from valley bottom to mountain peak). The samples spanned the east-west and north-south climatic and topographic gradients of the park.

The historical photographs were taken between 1923 and 1953 while the repeat photographs were taken between 2007 and 2016, all in summer months (Appendix D). The mean time elapsed between images in a pair was 81.3 years, with a standard deviation of 7.7 years.

4.3.5 Segmentation and classification of oblique images

We segmented and classified all 92 photographs (46 historical and 46 modern) into 10 land cover categories (Table 4-1). A digital delineation expert used a custom-built software program called Image Labeler for segmentation, which works by displaying the photograph of interest and overlaying the mask on top as it is being drawn. The expert used a Wacom Intuos PTZ-930 pen tablet for pixel-level precision.

This produced 92 digital land cover "masks" (Appendix D). We calculated percent cover (in terms of the number of pixels) of each category for each mask. Although oblique images do not yield spatially exact measurements due to variable pixel size (Rhemtulla et al., 2002), previous tests have shown that land cover proportions extracted from oblique images are comparable to those extracted from conventional orthogonal imagery, with some distinct advantages (including better representation of high topography landscapes and finer spatial resolution; see Chapter 3).

Table 4-1. Land cover category definitions.
Definitions of land cover categories used in the oblique classifications.

Category	**Definition**
Coniferous forest (CF)	Conifer trees
Mixedwood forest (MF)	Patches with 30-70% cover by broadleaf trees and the rest by coniferous trees
Broadleaf forest (BF)	Broadleaf trees
Wetland (WE)	Vegetation with a wet or aquatic moisture regime
Shrub (SH)	Shrubby vegetation
Herbaceous (HE)	Grasses and herbaceous vegetation
Regenerating area (RG)	Visibly recently burned forest (charred trees)
Rock (RO)	Bedrock, rubble, rocky outcrops
Water (WA)	Lakes, rivers, ponds
Snow/Ice (SN)	Patches of snow/ice, glaciers

4.3.6 Models

We generated species distribution models using avian data from the Willmore Biodiversity Research Project, a multi-agency project monitoring wildlife populations in the WWP, and land cover data extracted from satellite imagery.

The Willmore Biodiversity Research Project collected breeding songbird species occurrence data in May and June 2010, at n=43 sites established using a combined systematic and stratified sampling design to ensure adequate representation of rare habitat types such as wetlands and alpine meadows (Figure 4-3). Songbird relative abundance in the WWP was measured using point count methods via three-minute auditory recordings at nine points around a given site (Fisher, Wheatley, et al., 2011). Species were identified by professional bird transcribers experienced in auditory identification of North American birds.

Land cover data was acquired by combining a province-wide Landsat-based thematic map with a digital elevation model to extract 16 potential habitat types (Fisher, Wheatley, et al., 2011; McDermid et al., 2009). From there, we combined categories distinguishing vegetation density by thresholds of crown cover to establish simplified categories better suited for comparison with oblique images (Table 4-1).

We used generalized linear models (proportional binomial – or quasibinomial in instances where overdispersion > 1.5) in R version 3.4.3 to link probability of occurrence of breeding songbirds to percent cover of the various land cover types (R Core Team, 2015; Zuur, Ieno, Walker, Saveliev, & Smith, 2009). The response variable was probability of occurrence at a given site, for each species. We created candidate models with percent cover of all land cover categories, for spatial scales ranging from a 250 m-radius around the site to 4500 m in increments of 250 m to test for scale dependency. We ran model selection to narrow down the land cover categories and scale that best explained species occurrence using stepwise Akaike Information Criterion methods via the *step-AIC* function in the MASS package for R software. We selected the model with the lowest Akaike Information Criterion score for each species as the best-supported model (Burnham & Anderson, 2002). Only species that had sufficient observations to yield significant models were retained in analysis (Table 4-2).

4.3.7 Quantification of landscape change

We calculated Shannon's diversity index and Pielou's evenness index as metrics of landscape diversity for each of the 92 masks. We chose Shannon's index over other diversity indices for its sensitivity to rare land cover types (Nagendra, 2002), which are of particular interest here. We ran paired t-tests using the *t test* function in the STATS package in R version 3.4.3 on historical and modern land cover composition for each land cover category as well as on Shannon and Pielou indices to determine whether changes in landscape composition or diversity were significant (R Core Team, 2015).

4.3.8 Quantification of bird diversity change

We back-transformed models from parameter estimates to a standard response scale according to a logit-link to estimate probability of occurrence of each species given land cover composition estimates extracted from both historical and modern masks for each of the 46 oblique photograph sites. For example, the top model for Gray Jays (*Perisoreus canadensis*) on the standard response scale was

$$P = \frac{1}{(1 + e^{-(-4.41+0.04*CF+0.06*SH)})}$$

where P is the probability of occurrence, CF is the percentage of coniferous forest in the landscape and SH is the percentage of shrub in the landscape, at a scale of 1250 m. Thus, the percentage of coniferous forest and of shrub cover predicted by each of the 92 land cover masks was inputted into the above equation to estimate the probability of occurrence of the gray jay historically and contemporarily at each of the 46 sites. This process was repeated for each bird species studied. We then ran paired t-tests to test for changes in the probability of occurrence of each species over the last century.

4.3.9 Influence of landscape diversity on probability of occurrence

To test whether landscape diversity influenced changes in the avian community, we ran a multivariate analysis. We examined the data in R according to standard data exploration protocols (R Core Team, 2015; Zuur et al., 2010). We then ran multiple linear regression with changes in probability of occurrence as the response variable and changes in Shannon and Pielou indices of landscape diversity as explanatory variables:

$$\Delta P_o \sim \Delta S + \Delta Pi$$

where ΔP_o is the difference between contemporary and historical probability of occurrence of a given species, ΔS is the change in the value of the Shannon diversity index in the landscape over the last century and ΔPi is the change in the value of the Pielou evenness index in the landscape over the last century.

4.4 Results

4.4.1 Land cover changes over the last century

Overall the Rocky Mountain landscape became more homogenous and less diverse via increased forest cover (Figure 4-4). Coniferous forest cover increased significantly between the historical and modern photographs ($p < 0.05$), from 40.07% (s.d. 21.32%) to 52.50% (s.d. 25.37%). Proportion of wetland decreased from 4.81% (s.d. 7.29%) to 4.14% (s.d. 6.17%), herbaceous land from 15.50% (s.d. 14.61%) to 9.02% (s.d. 10.39%), and water from 0.30% (s.d. 0.78%) to 0.20% (s.d. 0.75%) (all $p < 0.05$). All other categories except mixedwood forest showed non-significant trends decreasing over time; mixedwood forest showed non-significant increase. There were high standard deviations (often 50% of the mean or higher) for all categories. The Shannon diversity index of landcover decreased significantly in the study area, from 1.20 (s.d. 0.27) to 1.00 (s.d. 0.30) on average, as did Pielou's evenness index, from a mean of 0.64 (s.d. 0.13) to a mean of 0.55 (s.d. 0.16; both $p < 0.05$).

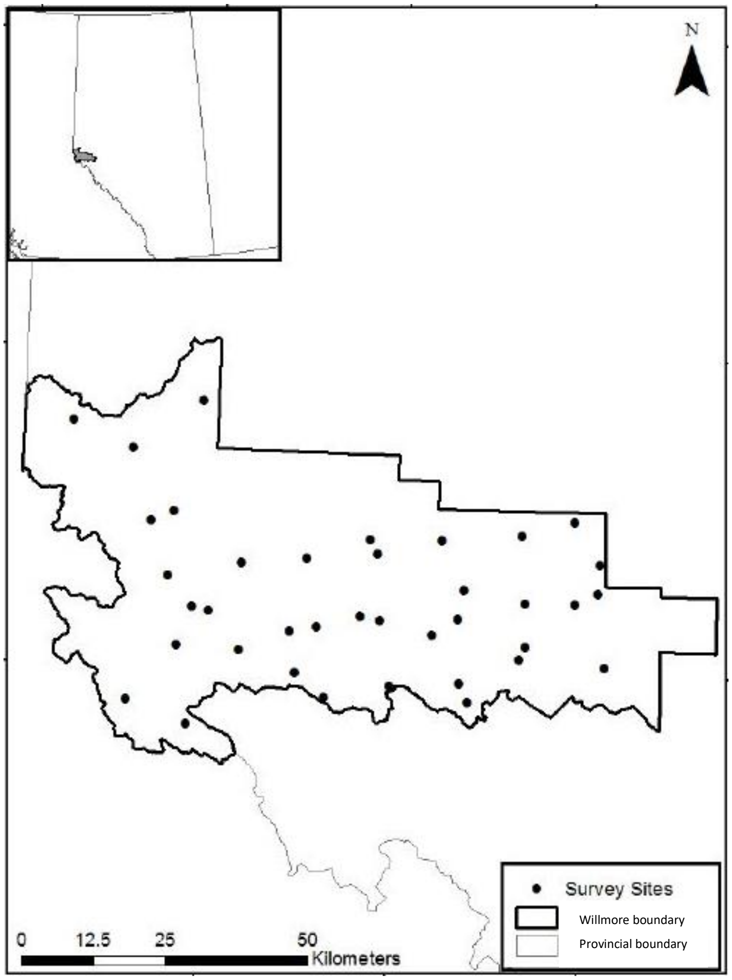

Figure 4-3. Bird survey sites.
Sites at which auditory bird surveys were conducted. Courtesy of Christy James.

4.4.2 Probability of occurrence according to land cover

Each bird species had a unique set of parameters and scale that best explained occurrence (Table 4-2). Each of the 15 species was either likely to occur in (positively correlated with) or avoided (negatively correlated with) coniferous forest, broadleaf forest, shrub cover, herbaceous cover and wetland; other land cover types (mixedwood forest, rock, regenerating area, water, snow/ice) did not have a strong influence on bird occurrence. For example, probability of occurrence of the hermit thrush (*Catharus guttatus*) was found to be positively correlated with coniferous and broadleaf forest, but negatively correlated with wetland, suggesting that this species prefers to occupy forested areas than wetlands.

Table 4-2. Top model parameter estimates.
Parameter estimates, with supporting evidence, for the variables included in the top model for each species. Two-letter codes correspond to land cover categories as described in Table 4-1.

Species	Scale (m)	Parameter	Estimate	Standard error	t-value	Pr(>|t|)
Gray Jay (*Perisoreus canadensis*)	1250	Intercept	-4.41432	0.83430	-5.291	7.19e-06
		CF	0.04345	0.01026	4.233	0.000165
		SH	0.06422	0.02529	2.540	0.015837
Wilson's Warbler (*Cardellina pusilla*)	1250	Intercept	-2.04493	0.37147	-5.505	3.79e-06
		HE	-0.05813	0.03198	-1.818	0.0779
		SH	0.07854	0.02332	3.367	0.0019
Savannah Sparrow (*Passerculus sandwichensis*)	4250	Intercept	-5.26319	0.80942	-6.502	7.9e-11
		HE	0.23697	0.06716	3.529	0.000418
Golden-Crowned Kinglet (*Regulus satrapa*)	250	Intercept	-6.22088	1.39384	-4.463	8.08e-06
		CF	0.04872	0.01441	3.382	0.000721
		WE	0.04949	0.01494	3.312	0.000926
		SH	0.04056	0.01909	2.125	0.033586
Ruby-Crowned Kinglet (*Regulus calendula*)	1500	Intercept	-4.84614	1.22028	-3.971	0.000365
		CF	0.03008	0.01287	2.337	0.025638
		BF	0.73270	0.35501	2.034	0.046962
		WE	0.03927	0.02034	1.931	0.062072
		SH	0.04634	0.02560	1.810	0.079422
Dark-Eyed Junco (*Junco hyemalis*)	1250	Intercept	-1.56105	0.27146	-5.751	1.65e-06
		HE	-0.14222	0.04567	-3.114	0.00367
		SH	0.04149	0.01661	2.498	0.01732
American Robin (*Turdus migratorius*)	1500	Intercept	-0.802771	0.371008	-2.164	0.03739
		CF	-0.025303	0.008502	-2.976	0.00526
		BF	0.485604	0.255258	1.902	0.06537
Hermit Thrush (*Catharus guttatus*)	500	Intercept	-2.360104	0.529999	-4.453	8.69e-05
		CF	0.014709	0.007358	1.999	0.05367
		BF	0.938919	0.331041	2.836	0.00764
		WE	-0.018119	0.019003	-0.953	0.34709
Pine Siskin (*Spinus pinus*)	4500	Intercept	-1.022244	0.395315	-2.586	0.01403
		CF	0.015959	0.007274	2.194	0.03495
		BF	-2.130380	0.655748	-3.249	0.00256
American Pipit (*Anthus rubescens*)	250	Intercept	0.21381	0.19584	1.092	0.28261
		CF	-0.08054	0.01531	-5.259	7.92e-06
		WE	-0.03271	0.01274	-2.568	0.01479
		BF	0.72939	0.23281	3.133	0.00355
Golden-Crowned Sparrow (*Zonotrichia atricapilla*)	250	Intercept	-0.11314	0.21668	-0.522	0.604968
		CF	-0.08410	0.01982	-4.243	0.000161
		WE	-0.02521	0.01239	-2.035	0.049747

		BF	1.28239	0.38444	3.336	0.002067
Swainson's Thrush (*Catharus ustulatus*)	4000	Intercept	-9.52346	1.99620	-4.771	3.62e-05
		CF	0.07140	0.01844	3.872	0.000483
		WE	0.11318	0.03814	2.968	0.005550
		SH	0.14192	0.04857	2.922	0.006232
		BF	1.47314	0.66464	2.216	0.033666
Yellow-Rumped Warbler (*Setophaga coronate*)	4500	Intercept	-1.00599	0.92673	-1.086	0.2851
		CF	0.03107	0.01232	2.522	0.0164
		HE	-0.12507	0.06328	-1.976	0.0560
Chipping Sparrow (*Spizella passerina*)	250	Intercept	1.049734	0.468174	2.242	0.03158
		CF	-0.018323	0.006169	-2.970	0.00543
		WE	-0.023371	0.008305	-2.814	0.00807
		HE	-0.012844	0.007985	-1.609	0.11695
Varied Thrush (*Ixoreus naevius*)	3750	Intercept	-3.79240	0.89230	-4.250	0.000157
		BF	1.94461	0.65889	2.951	0.005697
		WE	-0.10873	0.09755	-1.115	0.272864
		SH	0.04748	0.03787	1.254	0.218436

4.4.3 Bird community changes over the last century

Models showed that most forest-adapted bird species increased significantly in probability of occurrence, and non-forest-adapted species showed significant declines (Figure 4-5). Gray jay (*Perisoreus canadensis*), golden-crowned kinglet (*Regulus satrapa*), ruby-crowned kinglet (*Regulus calendula*), hermit thrush (*Catharus guttatus*), pine siskin (*Spinus pinus*) and yellow-rumped warbler (*Setophaga coronata*) were all positively correlated with coniferous forest cover, and all exhibited statistically significant ($p < 0.05$) increases in probability of occurrence (Figure 4-5). Swainson's thrush (*Catharus ustulatus*) was also positively correlated with coniferous forest cover and also increased, but the increase was not statistically significant ($p = 0.64$). Conversely, the American robin (*Turdus migratorius*) and chipping sparrow (*Spizella passerina*) were negatively correlated with coniferous forest, and declined significantly ($p < 0.05$), as did the Savannah sparrow (*Passerculus sandwichensis*), an alpine meadow-adapted (i.e. positively correlated with herbaceous cover) species. In fact, all species that decreased across the landscape were either negatively correlated with coniferous forest or positively correlated with upland herbaceous or shrub categories.

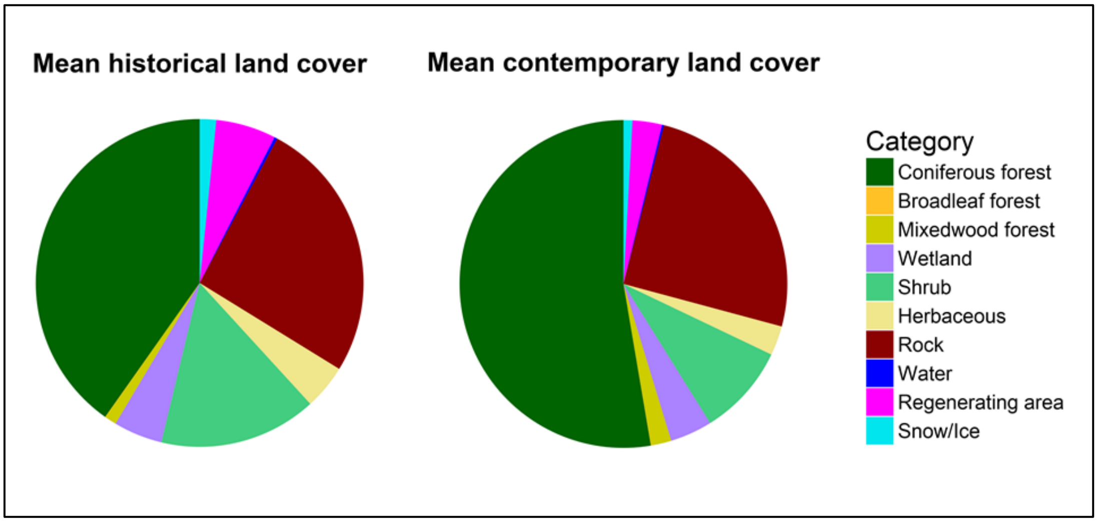

Figure 4-4. Homogenization of land cover.
Pie charts illustrating the mean relative proportion of each land cover category in the historical and modern photographs.

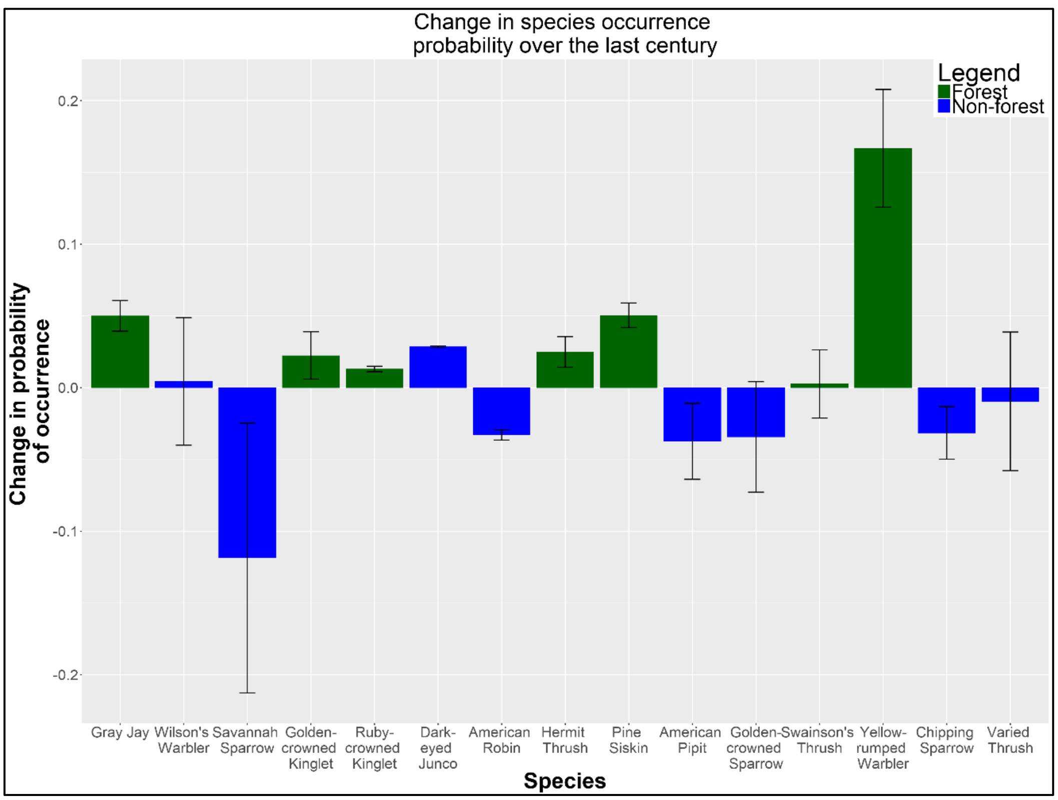

Figure 4-5. Change in probability of occurrence of bird species.
Difference between contemporary and historical probability of occurrence, with error bars (1 standard deviation). Species that were positively correlated with coniferous forest cover in the models are shown in green, while species that were negatively or not correlated with coniferous forest are shown in blue.

Based on the multivariate analysis, bird species occurrence was affected by changes in landscape diversity and evenness (as measured by Shannon and Pielou indices). Difference in Shannon index values was a significant ($p < 0.05$) predictor of change in probability of occurrence for 11 out of 15 species, while difference in Pielou index values was a significant predictor of change in probability of occurrence for just over half (8 out of 15 species). Forest-adapted species were generally negatively correlated with landscape diversity, i.e. at sites where Shannon's index decreased, coniferous forest-dwelling species increased in probability of occurrence. Alternatively, the probability of occurrence of most forest-adapted species was positively correlated with landscape evenness; increased Pielou indices led to increased probability of occurrence.

4.5 Discussion

4.5.1 Trends and mechanisms of change

Coniferous forest cover increased in the Rocky Mountains over the last century, leading to a homogenization of the landscape and a reduction in the diversity of available habitat types (Figure 4-4). This resulted in marked changes in the relative abundance of songbird species, namely increased occurrence of forest-adapted species and decreased occurrence of non-forest-adapted species.

Increases we observed in coniferous forest cover in the WWP are consistent with climate- and fire regime-induced changes reported in other studies on Rocky Mountain forests (e.g. Brown et al., 1999; Rhemtulla et al., 2002; Stockdale, 2017). Increases in coniferous forest cover take place by way of forest infilling and forest encroachment (i.e. trees growing where they did not previously). Fuel accumulation resulting from a modified fire regime and lack of disturbance leads to densification of forests (Butler & DeChano, 2001; Keane et al., 2002; Ryan, Knapp, & Varner, 2013). Furthermore, many studies have documented forest encroachment via a phenomenon known as "treeline creep" in which the uppermost range of the treeline ecotone has increased in altitude due to broad-scale climatic warming or local-scale biotic and abiotic factors (Coop & Givnish, 2007; Lloyd & Fastie, 2003; Roush, 2009; Walther, Beißner, & Burga, 2005; Westbrook, 2014; Widenmaier & Strong, 2010). Many such factors, including changes in temperature and precipitation patterns, duration of growing season, and fire regime, are expected to be at play in the WWP, and could explain our observed increase in coniferous forest cover (Falk, 2014; O'Neill, 2011).

Forest densification and encroachment simultaneously increase the proportion of forest in a given area and decrease the proportion of other categories via land cover conversion. In Rocky Mountain systems where forest cover already dominates the landscape, this results in increased dominance of coniferous forest while rare categories become rarer. Indeed, we observed declines in every land cover category other than forest, particularly in wetland and herbaceous cover, which were both important habitat types for many of the species studied. Hence, the overarching trend in land cover change that occurred in the WWP over the past century is landscape homogenization, which we quantified through the declines in landscape diversity and evenness indices. Not only does the homogenization of the landscape affect biotic community structure because of the shifts in available habitat, it also decreases ecosystem stability and facilitates spread of disturbance (Oliver et al., 2015; Risser, 1984).

Part of the distinctiveness of mountain systems that explains why mountains support such a wide variety of species lies in the diverse habitats available in a heterogeneous landscape over a relatively small area (Dufour et al., 2006; Ruggiero & Hawkins, 2008). As such, homogenization of land cover directly diminishes the value of mountains as hotspots of biodiversity, and can have serious impacts on alpine and montane biotic communities. This was reflected in our estimates of probability of occurrence of songbirds in the WWP. The relative abundance of conifer-adapted species is significantly higher in contemporary avian communities in Rocky Mountain systems than was historically the case. Thus, shifts in the songbird community reflect the homogenization of the Rocky Mountain landscape, which was once much more diverse.

Our results are fairly consistent with other studies on bird populations in mountainous protected areas in Alberta – notably, we measured increases in golden-crowned kinglets, Swainson's thrushes and yellow-rumped warblers, and decreases in chipping sparrows and American pipits (Downes, Collins, & Damus, 2004; Dunn, Downes, & Collins, 2000; Romme & Turner, 1991; St. Laurent, 2007). Most other species were considered to have "stable" populations in the literature, but exhibited small differences in probability of occurrence between historical and modern images in our analysis, which could be indicative of the importance of longer-term assessments as presented in this study. While all species assessed were labeled "secure" in recent provincial rankings (Fisher, Wheatley, et al., 2011), the long-term population declines inferred in this analysis are projected to continue with continued loss of rare habitat types such as alpine meadows and shrublands, which will have further impacts on these populations.

4.5.2 Considerations

Notably, there was high variability in the land cover composition predicted by the oblique photographs. Nevertheless, we were interested in changes in land cover visible in corresponding historical and repeat photograph pairs. As such, spatial variability was less of a concern for this analysis than temporal variability. Given that forest cover increase (and, more generally, shifts in vegetation) is a slow process operating on decadal timescales, and given that the mean time elapsed between repeat photographs was over 80 years, we can safely assume that the changes we captured reflected long-term trends rather than short-term stochasticity at a landscape scale.

Another consideration is that several factors that may affect species occurrence probability were not included in these models, such as landscape configuration and interspecific interactions (Fisher, Anholt, Bradbury, Wheatley, & Volpe, 2013). Missing terms could explain some of the variation observed in the relationship between land cover and probability of occurrence. In addition, the 15 species included in this study do not represent the entire avian community of the Rocky Mountains; only breeding songbird species that had sufficiently frequent observations in the auditory surveys to form significant models were retained. Although sampling methods were stratified to ensure representation of rare habitat types, this step in our analysis may have skewed the sample toward forest-adapted species. This could explain why most bird species studied increased in probability of occurrence. The relative paucity of observations means that we might be failing to detect loss of diversity of rare species. This does not detract from our overall findings, but rather provides further incentive to understand the historical context of rare and at-risk species.

4.6 Conclusion

At a time when biological systems are changing at staggering rates, being able to frame current changes in the context of historical conditions is critical for ecologists and land managers. Given the paucity of biodiversity data dating back more than a few decades, it is helpful to analyze existing historical data in new ways to examine historical ecological conditions. Historical land-based oblique photographs are one such example that can act as a “Hubble”, allowing us to peer farther into the past than possible with any other remotely sensed data. We proposed a novel method combining repeat photography and species distribution modelling to compare current species occurrence to that of a century ago through inference from historical oblique photographs. We demonstrated this method on breeding songbirds in the Willmore Wilderness Park. We recorded forest densification and encroachment in our study area that is representative of a broadly observed trend across the Rocky Mountains. It can be inferred, based on the landscape mechanisms known to be at play in the WWP, that this increase in forest cover has been brought on by climate change and human land use change (i.e. changes in use and management of wildfire). This homogenization has led to significant increases in forest-adapted songbird species at the detriment of alpine meadow-adapted species, negatively impacting community-level diversity. Communities are shifting from diverse species adapted to diverse habitat types to a conifer-dominated landscape filled with conifer-adapted species.

Our conclusions could have implications on the management practices of the Willmore Wilderness Park and of remote mountain parklands in general. As our findings suggest negative impacts on community-level bird diversity stemming from increased forest cover and landscape homogenization, land managers seeking to conserve bird diversity might consider practices that counter these trends and encourage habitat diversity (e.g. prescribed burning). More generally, remote mountain parklands, which can be some of the most challenging places to monitor biodiversity, could employ repeat photography distribution modelling to establish historical conditions and understand the historical context of current shifts in biodiversity.

We argue that terrestrial oblique photographs are a powerful tool for reconstructing a longer history of biotic changes than possible through other sources of data given the temporal reach of oblique photographs in comparison with remotely sensed and aerial images. While we demonstrated this method with breeding songbirds in the Willmore Wilderness Park, it could be applied with other taxa for which species distribution models are available and in any area where historical photographs exist. For instance, the MLP alone has nearly 7000 repeat photograph pairs that could establish shifting species population estimates across the Canadian Rocky Mountains. There are many other repeat photography datasets globally that could be tapped to answer questions regarding biodiversity change at large spatial scales and fine spatial resolution.

"Backcasting" these century-scale changes provides context to interpret forecasted trends: continued (and accelerating) warming and wildfire suppression will exacerbate the patterns observed here. Next steps of this work would coincidentally involve forecasting changes in avian community structure based on expected land cover shifts.

Chapter 5
Conclusion

5.1 Summary

Repeat photography is already a well-developed field, with accepted methodologies and widespread applications. In an ever-changing world, it is becoming increasingly important to understand the patterns and drivers of landscape change, and researchers are turning to sources of data that give us a window into the past to study longer-term trends. The ability of terrestrial oblique photographs to provide such a data source is one of its main advantages and the reason behind the growing interest in the field of repeat photography.

In this thesis, I demonstrated the potential robustness of the repeat photographic method. Chapter 2 showed that the types of errors researchers are most likely to make when locating the historical vantage point in-field (for example, being in the wrong location by approximately 1 m, or setting the camera too high/too low on the tripod) do not have large impacts on the alignment of the images. Furthermore, careful co-registration can correct for small errors in placement of the camera and differences in camera sensors and lenses. Camera relocation errors of greater magnitude (e.g. 5 m from the original vantage point or 15° from the original azimuth) cannot be adequately corrected by means of co-registration, but such errors are unlikely to be committed by experienced repeat photographers. These findings should allow repeat photographers to make better informed decisions on trade-offs between accuracy and time spent trying to pinpoint the exact vantage point in the field.

In Chapter 3, I directly addressed claims that oblique imagery, because of its spatially variable scale, is unable to provide landscape scale land cover composition estimates. I compared land cover masks generated from oblique photographs to Landsat-based masks. My findings showed that the two data sources provide similar information on composition of dominant land cover types, that oblique images are better at capturing small or narrow features due to their higher spatial resolution, and that steep high-topography landscapes are better represented from land-based views than from overhead views. This suggests that oblique masks provide a different, but not necessarily less useful or less accurate, view of the landscape than Landsat-generated masks at a landscape scale. The main implication of this experiment is strengthened confidence in the suitability of oblique-generated masks for describing land cover composition and change, as in the example discussed in Chapter 4.

Chapter 4 described a new approach using historical and repeat oblique photographs in conjunction with species distribution models to answer questions about land cover change and related ecological patterns. I first evaluated land cover change by comparing land cover composition estimated from historical and modern land-based photographs, and then modelled the probability of occurrence of 15 songbird species at both time periods. I found a homogenization of land cover by means of an increase in coniferous forest cover at the expense of non-forest land cover types such as herbaceous and shrub cover. These shifts in habitat availability positively impacted forest-adapted songbird species but negatively impacted non-forest-adapted species, pointing to land cover homogenization as an important factor driving change in bird diversity in the montane forests of western Canada.

5.2 Implications

The implications of this research are several for future work by ongoing repeat photography studies such as the Mountain Legacy Project. First, repeat photography field work can now point to empirical evidence when considering trade-offs between alignment accuracy and time. Second, I provided a reference for achievable levels of co-registration accuracy in repeat photography. Third, I solidified arguments in favour of using oblique images to study land cover composition – namely, their higher spatial resolution and better ability to resolve high topography landscapes compared to conventional orthogonal imagery – while showing that the two data sources in fact sample the landscape in a similar way. Future repeat photography work can point to these findings to confirm that their data is a reliable source of land cover composition information for quantitative analyses of landscape change. Fourth, I showed that repeat photography can provide information on long-term land cover trends; thus, we can extend the temporal reach of existing data in areas where historical photograph collections exist. Finally, I showed that historical and repeat oblique photographs can be used to estimate species occurrence through species-habitat models; my findings suggest that songbird diversity in a Rocky Mountain ecosystem is closely tied to the homogenization of the landscape via coniferous forest encroachment. These results have implications for land managers responsible for maintaining habitat heterogeneity and biodiversity in the Willmore Wilderness Park.

5.3 Future directions

Future directions of this work could take many paths. The relationship between camera relocation error and co-registration accuracy of historical and repeat photographs could be examined in a more statistically robust manner through additional replications of the experiment presented in Chapter 2. Further analyses could consider whether the distance between the camera and the landscape being aligned has an effect on co-registration accuracy at given relocation errors, whether using the same camera system throughout would produce similar results, or to what extent control point selection impacts RMSE. Another avenue to be explored would be applying different kinds of transformations in the alignment algorithm; in this study, I used affine transformations, but oblique photographs may also fare well with higher-order projective transformations, for example.

While the ability of oblique photographs to sample land cover proportions was confirmed in Chapter 3, the validity of measuring metrics of landscape spatial heterogeneity could be an interesting next step. The relative size and spatial distribution of patches of land cover are as important as land cover composition to understand patterns and processes contributing to landscape change, and are components of many species distribution models.

As for the pairing of repeat photography and species distribution models to backcast biotic community structure: the approach I presented in Chapter 4 has broad geographical applicability anywhere historical photographs exist (though I argue it is particularly effective around mountainous landscapes), and it could be applied on other taxa for which species distribution models exist in the same area. In fact, in the Willmore Wilderness Park, there are datasets on vegetation and mammal species distributions; as such, “repeat photography distribution modelling” could be applied to estimate long-term changes in both mammal and vegetation communities in the WWP just as I did with songbirds.

While there remains much to be done in the way of accuracy analysis in repeat photography, here I presented findings that will hopefully benefit future repeat photography studies. I also proposed a novel application of repeat photography to answer ecological questions about biodiversity in a landscape increasingly affected by climate change. I hope this work encourages land managers, conservationists and ecologists alike to tap into promising datasets of oblique photography to study and understand long-term land cover dynamics, and the mechanisms and consequences of such changes.

Bibliography

Alexander, R. R. (1987). *Ecology, Silviculture, and Management of the Engelmann Spruce - Subalpine Fir Type in the Central and Southern Rocky Mountains*. USDA Forest Service. Retrieved from https://digitalcommons.usu.edu/cgi/viewcontent.cgi?referer=https://scholar.google.ca/&httpsredir=1&article=1144&context=barkbeetles

Arsenault, A. (2003). A note on the ecology and management of old-growth forests in the Montane Cordillera. *The Forestry Chronicle*, *79*(3), 441–454.

Aschenwald, J., Leichter, K., Tasser, E., & Tappeiner, U. (2001). Spatio-temporal landscape analysis in mountain terrain by means of small format photography: a methodological approach. *IEEE Transactions on Geoscience and Remote Sensing*, *39*(4), 885–893.

Baillie, J., Hilton-Taylor, C., Stuart, S. N., & Commission, I. S. S. (2004). *2004 IUCN Red List of Threatened Species: A Global Species Assessment*. IUCN.

Bellard, C., Bertelsmeier, C., Leadley, P., Thuiller, W., & Courchamp, F. (2012). Impacts of climate change on the future of biodiversity. *Ecology Letters*, *15*(4), 365–377. https://doi.org/10.1111/j.1461-0248.2011.01736.x

Belward, A. S., & Skøien, J. O. (2015). Who launched what, when and why; trends in global land-cover observation capacity from civilian earth observation satellites. *ISPRS Journal of Photogrammetry and Remote Sensing*, *103*, 115–128. https://doi.org/10.1016/j.isprsjprs.2014.03.009

Beniston, M. (2003). Climatic Change in Mountain Regions: A Review of Possible Impacts. In *Climate Variability and Change in High Elevation Regions: Past, Present & Future* (pp. 5–31). Springer, Dordrecht. https://doi.org/10.1007/978-94-015-1252-7_2

Bozzini, C., Conedara, M., & Krebs, P. (2012). A New Monoplotting Tool to Extract Georeferenced Vector Data and Orthorectified Raster Data from Oblique Non-Metric Photographs. *International Journal of Heritage in the Digital Era*, *1*(3), 498–518.

Bridgland, M. P. (1916). Photographic surveying in Canada. *Geographical Review*, *2*(1), 19–26. https://doi.org/10.2307/207459

Bridgland, M. P. (1924). *Photographic Surveying*. Ottawa, Ont.: Canada Department of the Interior. Topographical surveys branch.

Brown, P. M., Kaufmann, M. R., & Shepperd, W. D. (1999). Long-term, landscape patterns of past fire events in a montane ponderosa pine forest of central Colorado. *Landscape Ecology*, *14*(6), 513–532. https://doi.org/10.1023/A:1008137005355

Browning, D. M., Archer, S. R., & Byrne, A. T. (2009). Field validation of 1930s aerial photography: What are we missing? *Journal of Arid Environments*, *73*(9), 844–853. https://doi.org/10.1016/j.jaridenv.2009.04.003

Brunsden, D., & Thornes, J. B. (1979). Landscape sensitivity and change. *Transactions of the Institute of British Geographers*, *4*(4), 463–484. https://doi.org/10.2307/622210

Burnham, K. P., & Anderson, D. R. (2002). *Model selection and multimodel inference: a practical information-theoretic approach*. New York: Springer.

Butler, D. R., & DeChano, L. M. (2001). Environmental change in Glacier National Park, Montana: An assessment through repeat photography from fire lookouts. *Physical Geography*, *22*(4), 291–304. https://doi.org/10.1080/02723646.2001.10642744

Byers, A. C. (2008). An assessment of contemporary glacier fluctuations in Nepal's Khumbu Himal using repeat photography. *Himalayan Journal of Sciences*, *4*(6). https://doi.org/10.3126/hjs.v4i6.979

Campbell, J. B., & Wynne, R. H. (2011). *Introduction to Remote Sensing* (5th ed.). Guilford Press.

Castilla, G., Hird, J., Hall, R. J., Schiek, J., & McDermind, G. J. (2014). Completion and updating of a Landsat based land cover polygon layer for Alberta. *Canadian Journal of Remote Sensing*, *40*(2).

Chandler, J., Ashmore, P., Paola, C., Gooch, M., & Varkaris, F. (2002). Monitoring river-channel change using terrestrial oblique digital imagery and automated digital photogrammetry. *Annals of the Association of American Geographers*, *92*(4), 631–644.

Coop, J. D., & Givnish, T. J. (2007). Spatial and temporal patterns of recent forest encroachment in montane grasslands of the Valles Caldera, New Mexico, USA. *Journal of Biogeography*, *34*(5), 914–927.

Dai, X., & Khorram, S. (1997). Development of a feature-based approach to automated image registration for multitemporal and multisensor remotely sensed imagery. In *Geoscience and Remote Sensing, 1997. IGARSS '97. Remote Sensing - A Scientific Vision for Sustainable Development., 1997 IEEE International* (Vol. 1, pp. 243–245 vol.1). https://doi.org/10.1109/IGARSS.1997.615851

Dai, X., & Khorram, S. (1998). The effects of image misregistration on the accuracy of remotely sensed change detection. *IEEE Transactions on Geoscience and Remote Sensing*, *36*(5), 1566–1577. https://doi.org/10.1109/36.718860

De Leeuw, A. J., Veugen, L. M. M., & Van Stokkom, H. T. C. (1988). Geometric correction of remotely-sensed imagery usiing ground control points and orthogonal polynomials. *International Journal of Remote Sensing*, *9*(10–11), 1751–1759.

Delaney, J. (2008). An inconvenient truth? Scientific photography and archival ambivalence. *Archivaria*, *65*(Spring), 75–95.

Downes, C. M., Collins, B. T., & Damus, M. (2004). *Canadian Bird Trends* (Website Version 2.1). Gatineau, QC: Canadian Wildlife Service.

Dufour, A., Gadallah, F., Wagner, H. H., Guisan, A., & Buttler, A. (2006). Plant Species Richness and Environmental Heterogeneity in a Mountain Landscape: Effects of Variability and Spatial Configuration. *Ecography*, *29*(4), 573–584.

Dunn, E. H., Downes, C. M., & Collins, B. T. (2000). *The Canadian Breeding Bird Survey* (Program Notes No. No. 2016) (p. 40). Canadian Wildlife Service.

Edgecombe, A. H. (1982). *The last patrol: Willmore Wilderness Park management report*. Edmonton, AB: Alberta Forest Service.

Elith, J., & Leathwick, J. R. (2009). Species Distribution Models: Ecological Explanation and Prediction Across Space and Time. *Annual Review of Ecology, Evolution, and Systematics*, *40*(1), 677–697. https://doi.org/10.1146/annurev.ecolsys.110308.120159

Environmental Systems Research Institute. (2015). (Version 10.4.1). Redlands, California: ESRI.

Falk, J. (2014). *Historical Landscape Change in Remote Mountainous Parks: Management Challenges Observed Through a Repeat Photographic Lens* (Thesis). Retrieved from https://dspace.library.uvic.ca//handle/1828/5305

Fisher, J. T., Anholt, B., Bradbury, S., Wheatley, M., & Volpe, J. P. (2013). Spatial segregation of sympatric marten and fishers: the influence of landscapes and species-scapes. *Ecography*, *36*(2), 240–248. https://doi.org/10.1111/j.1600-0587.2012.07556.x

Fisher, J. T., Anholt, B., & Volpe, J. P. (2011). Body mass explains characteristic scales of habitat selection in terrestrial mammals. *Ecology and Evolution*, *1*(4), 517–528. https://doi.org/10.1002/ece3.45

Fisher, J. T., Bradbury, S., Anholt, B., Nolan, L., Roy, L., Volpe, J., & Wheatley, M. (2013). Wolverines (Gulo gulo luscus) on the Rocky Mountain slopes: Natural heterogeneity and landscape alteration as predictors of distribution. *Canadian Journal of Zoology*, *91*, 706–716. https://doi.org/10.1139/cjz-2013-0022

Fisher, J. T., Wheatley, M., & Gould, J. (2011). *Rocky Mountain Biodiversity: Ecological communities and rare elusive species in heterogeneous landscapes* (Interim Report). Alberta: Government of Alberta, Alberta Innovates - Technology Futures, Alberta Biodiveristy Monitoring Institute. Retrieved from http://209.61.254.117/?attachment_id=215

Fisher, J. T., Wheatley, M., & Mackenzie, D. (2014). Spatial patterns of breeding success of grizzly bears derived from hierarchical multistate models. *Conservation Biology*, *0*(0), 1–11.

Foley, J. A., DeFries, R., Asner, G. P., Barford, C., Bonan, G., Carpenter, S. R., … Snyder, P. K. (2005). Global consequences of land use. *Science*, *309*(5734), 570–574. https://doi.org/10.1126/science.1111772

Foody, G. M. (2002). Status of land cover classification accuracy assessment. *Remote Sensing of Environment*, *80*(1), 185–201.

Foody, G. M., & Atkinson, P. M. (2003). *Uncertainty in Remote Sensing and GIS*. John Wiley & sons. Retrieved from https://s3.amazonaws.com/academia.edu.documents/42262076/Analysing_Uncertainty_Propagation_in_GIS20160206-23789-rc32nz.pdf?AWSAccessKeyId=AKIAIWOWYYGZ2Y53UL3A&Expires=1512442220&Signature=3XXTgBTvCe41%2BSy47HnaROCLaxA%3D&response-content-disposition=inline%3B%20filename%3DAnalysing_Uncertainty_Propagation_in_GIS.pdf#page=307

Frankl, A., Nyssen, J., De Dapper, M., Haile, M., Billi, P., Munro, R. N., … Poesen, J. (2011). Linking long-term gully and river channel dynamics to environmental change using repeat photography (Northern Ethiopia). *Geomorphology*, *129*(3), 238–251.

Fretwell, S. D., & Lucas, H. L. J. (1969). On territorial behavior and other factors influencing habitat distribution in birds. *Acta Biotheoretica*, *19*(1), 16–36.

Gat, C. (2011). *Feature-based matching in historic repeat photography: an evaluation and assessment of feasibility.* (Thesis). Retrieved from https://dspace.library.uvic.ca//handle/1828/3461

Gat, C., Albu, A. B., German, D., & Higgs, E. (2011). A comparative evaluation of feature detectors on historic repeat photography. In G. Bebis, R. Boyle, B. Parvin, D. Koracin, S. Wang, K. Kyungnam, … J. Ming (Eds.), *Advances in Visual Computing* (Vol. 6939, pp. 701–714). Berlin, Heidelberg: Springer Berlin Heidelberg. Retrieved from http://link.springer.com/10.1007/978-3-642-24031-7_70

Gilvear, D., & Bryant, R. (2003). Analysis of aerial photography and other remotely sensed data. In *Tools in Fluvial Geomorphology* (5.8, Vol. 600, p. 23). Red. Retrieved from http://www.robert-bryant.staff.shef.ac.uk/KP2003.pdf

Goin, P., Raymond, C. E., & Blesse, R. E. (1992). *Stopping Time: A Rephotographic Survey of Lake Tahoe*. UNM Press.

Google Earth. (2017). (Version 7.3.0). Mountain View, California: Google Inc. Retrieved from Available at: https://www.google.com/earth/desktop/

Grenzdorffer, G. J., Guretzki, M., & Friedlander, I. (2008). Photogrammetric image acquisition and image analysis of oblique imagery - a new challenge for the digital airborne system PFIFF. *The Photogrammetric Record*, *23*(124), 372–386.

Griffiths, G. H., & Mather, P. M. (2010, November 25). Remote sensing and landscape ecology: landscape patterns and landscape change. Retrieved August 30, 2016, from http://www.tandfonline.com/doi/pdf/10.1080/01431160050110151

Guisan, A., & Thuiller, W. (2005). Predicting species distribution: offering more than simple habitat models. *Ecology Letters*, *8*, 993–1009.

Hall, F. C. (2001). *Ground-based photographic monitoring*. Portland, OR : Retrieved from http://hdl.handle.net/2027/umn.31951d02977214o

Hall, R. J., Walsworth, N. A., Gartrell, M., Wang, Y., & Klita, D. L. (2000). *Project Report Willmore Wilderness Park Inventory and Map Analysis*. Edmonton, AB: Canadian Forest Service.

Hansen-Bristow, K. J., Ives, J. D., & Wilson, J. P. (1988). Climatic Variability and Tree Response within the Forest-Alpine Tundra Ecotone. *Annals of the Association of American Geographers*, *78*(3), 505–519.

Harrison, A. E. (1974). Reoccupying unmarked Camera Stations for Geological Observations. *Geology*, *2*(9), 469–471. https://doi.org/10.1130/0091-7613(1974)2<469:RUCSFG>2.0.CO;2

Hastings, J. R., & Turner, R. M. (1965). The changing mile. An ecological study of vegetation change with time in the lower mile of an arid and semiarid region. *The Changing Mile. An Ecological Study of Vegetation Change with Time in the Lower Mile of an Arid and Semiarid Region.* Retrieved from https://www.cabdirect.org/cabdirect/abstract/19670700517

Inouye, D. W., Barr, B., Armitage, K. B., & Inouye, B. D. (2000). Climate change is affecting altitudinal migrants and hibernating species. *Proceedings of the National Academy of Sciences*, *97*(4), 1630–1633. https://doi.org/10.1073/pnas.97.4.1630

Jean, F. C., Albu, A. B., Capson, D., Higgs, E., Fisher, J. T., & Starzomski, B. M. (2015a). The mountain habitats segmentation and change detection dataset. In *2015 IEEE Winter Conference on Applications of Computer Vision* (pp. 603–609). https://doi.org/10.1109/WACV.2015.86

Jean, F. C., Albu, A. B., Capson, D., Higgs, E., Fisher, J. T., & Starzomski, B. M. (2015b). Visualizing category-specific changes in oblique photographs of mountain landscapes. In *Workshop of Visualisation in Environmental Sciences (EnvirVis)*. The Eurographics Association.

Jetz, W., Wilcove, D. S., & Dobson, A. P. (2007). Projected Impacts of Climate and Land-Use Change on the Global Diversity of Birds. *PLOS Biology*, *5*(6), e157. https://doi.org/10.1371/journal.pbio.0050157

Kaim, D. (2017). Land cover changes in the polish Carpathians based on repeat photography. *Carpathian Journal of Earth and Environmental Sciences*, *12*(2), 485–498.

Keane, R. E., Ryan, K. C., Veblen, T. T., Allen, C. D., Logan, J., & Hawkes, B. (2002). *Cascading effects of fire exclusion in Rocky Mountain ecosystems: a literature review* (General Technical Report No. RMRS-GTR-91) (p. 24). USDA Forest Service.

Klett, M. (2011). Repeat photography in landscape research. In E. Margolis & L. Pauwels, *The SAGE Handbook of Visual Research Methods* (pp. 114–131). 1 Oliver's Yard, 55 City Road, London EC1Y 1SP United Kingdom: SAGE Publications Ltd. https://doi.org/10.4135/9781446268278.n6

Klett, M., Manchester, E., Verburg, J., Bushaw, G., & Dingus, R. (1984). *Second View: the Rephotographic Survey Project*. Albuquerque, NM: University of New Mexico Press.

Kolecka, N., Kozak, J., Kaim, D., Dobosz, M., Ginzler, C., & Psomas, A. (2015a). Mapping Secondary Forest Succession on Abandoned Agricultural Land with LiDAR Point Clouds and Terrestrial Photography. *Remote Sensing*, *7*(7), 8300–8322. https://doi.org/10.3390/rs70708300

Kolecka, N., Kozak, J., Kaim, D., Dobosz, M., Ginzler, C., & Psomas, A. (2015b). Mapping secondary forest succession on abandoned agricultural land with LiDAR point clouds and terrestrial photography. *Remote Sensing*, *7*(7), 8300–8322.

Körner, C. (2004). Mountain biodiversity, its causes and function. *Ambio*, *Spec No 13*, 11–17.

Krebs, C. J. (1991). The experimental paradigm and long-term population studies. *Ibis*, *133*, 3–8. https://doi.org/10.1111/j.1474-919X.1991.tb07663.x

Kull, C. A. (2005). Historical landscape repeat photography as a tool for land use change research. *Norsk Geografisk Tidsskrift - Norwegian Journal of Geography*, *59*(4), 253–268. https://doi.org/10.1080/00291950500375443

Lambin, E. F., Geist, H. J., & Lepers, E. (2003). Dynamics of land-use and land-cover change in tropical regions. *Annual Review of Environment and Resources*, *28*(1), 205–241. https://doi.org/10.1146/annurev.energy.28.050302.105459

Lausch, A., & Herzog, F. (2002). Applicability of landscape metrics for the monitoring of landscape change: issues of scale, resolution and interpretability. *Ecological Indicators*, *2*(1), 3–15. https://doi.org/10.1016/S1470-160X(02)00053-5

Lehikoinen, A., Green, M., Husby, M., Kålås, J. A., & Lindström, Å. (2014). Common montane birds are declining in northern Europe. *Journal of Avian Biology*, *45*(1), 3–14. https://doi.org/10.1111/j.1600-048X.2013.00177.x

Lloyd, A. H., & Fastie, C. L. (2003). Recent changes in treeline forest distribution and structure in interior Alaska. *Écoscience*, *10*(2), 176–185. https://doi.org/10.1080/11956860.2003.11682765

Luckman, B. H. (1998). Landscape and climate change in the central Canadian Rockies during the 20th century. *Canadian Geographer / Le Géographe Canadien*, *42*(4), 319–336. https://doi.org/10.1111/j.1541-0064.1998.tb01349.x

MacLaren, I. S., Higgs, E., & Zezulka-Mailloux, G. (2005). *Mapper of Mountains: M.P. Bridgland in the Canadian Rockies, 1902-1930*. University of Alberta.

Maestas, J. D., Knight, R. L., & Gilgert, W. C. (2001). Biodiversity and land-use change in the American mountain west. *Geographical Review*, *91*(3), 509–524.

Magurran, A. E., Baillie, S. R., Buckland, S. T., Dick, J. M., Elston, D. A., Scott, E. M., … Watt, A. D. (2010). Long-term datasets in biodiversity research and monitoring: assessing change in ecological communities through time. *Trends in Ecology & Evolution*, *25*(10), 574–582. https://doi.org/10.1016/j.tree.2010.06.016

Malde, H. E. (1973). Geologic bench marks by terrestrial photography. *US Geological Survey Journal of Research*, *1*(2), 193–206.

McCain, C. M. (2009). Global analysis of bird elevational diversity. *Global Ecology and Biogeography*, *18*(3), 346–360. https://doi.org/10.1111/j.1466-8238.2008.00443.x

McDermid, G. J., Hall, R. J., Sanchez-Azofeifa, G. A., Franklin, S. E., Stenhouse, G., Kobliuk, T., & LeDrew, E. F. (2009). Remote sensing and forest inventory for wildlife habitat assessment. *Forest Ecology and Management*, *257*.

Molau, U. (2004). Mountain biodiversity patterns at low and high latitudes. *Ambio - Journal of Human Environment Research and Management*, 24–28.

Mucha, D. (2013). *Acquiring an Improved Understanding of Willmore Wilderness Park Visitors, Alberta, Canada* (M.A.). University of Alberta, Edmonton. Retrieved from https://search.proquest.com/openview/c0112a97fd6bf6f5cd372ff25cd457b2/1?pq-origsite=gscholar&cbl=18750&diss=y

Nagendra, H. (2002). Opposite trends in response for the Shannon and Simpson indices of landscape diversity. *Applied Geography*, *22*(2), 175–186. https://doi.org/10.1016/S0143-6228(02)00002-4

Oliver, T. H., Heard, M. S., Isaac, N. J., Roy, D. B., Procter, D., Eigenbrod, F., … Proenca, V. (2015). Biodiversity and resilience of ecosystem functions. *Trends in Ecology & Evolution*, *30*(11), 673–684.

O’Neill, N. A. (2011, May 17). *Transboundary Regional Planning Collaboration for Climate Change Adaptation: A Case Study of Jasper National Park, Mount Robson Provincial Park, and Willmore Wilderness Park.* University of Waterloo. Retrieved from https://uwspace.uwaterloo.ca/handle/10012/5931

Parmesan, C., & Yohe, G. (2003). A globally coherent fingerprint of climate change impacts across natural systems. *Nature*, *421*, 37–42. https://doi.org/10.1038/nature01286

Pickard, J. (2002). Assessing vegetation change over a century using repeat photography. *Australian Journal of Botany*, *50*, 409–414.

Province of Alberta. Willmore Wilderness Park Act, § Revised Statutes of Alberta 2000 Chapter W-11 (2002).

R Core Team. (2015). R: A language and environment for statistical computing (Version 3.2.3). Vienna, Austria: The R Foundation for Statistical Computing. Retrieved from https://www.R-project.org/

Rhemtulla, J. (1999). *Eighty years of change: the montane vegetation of Jasper National Park* (M.Sc.). University of Alberta, Edmonton, AB. Retrieved from http://www.collectionscanada.gc.ca/obj/s4/f2/dsk2/ftp01/MQ40099.pdf

Rhemtulla, J., Hall, R., Higgs, E., & Macdonald, S. E. (2002). Eighty years of change - vegetation in the montane ecoregion of Jasper National Park. *Canadian Journal of Forest Research*, *32*, 2010–2021.

Risser, P. G. (1984). Landscape ecology: directions and approaches. *Illinois Natural History Survey*, *No 2*.

Rittenhouse, C. D., Pidgeon, A. M., Albright, T. P., Culbert, P. D., Clayton, M. K., Flather, C. H., … Radeloff, V. C. (2010). Conservation of Forest Birds: Evidence of a Shifting Baseline in Community Structure. *PLOS ONE*, *5*(8), e11938. https://doi.org/10.1371/journal.pone.0011938

Rittenhouse, C. D., Pidgeon, A. M., Albright, T. P., Culbert, P. D., Clayton, M. K., Flather, C. H., … Radeloff, V. C. (2012). Land-Cover Change and Avian Diversity in the Conterminous United States. *Conservation Biology*, *26*(5), 821–829.

Rogers, G. F., Malde, H. E., & Turner, R. M. (1984). *Bibliography of repeat photography for evaluating landscape change.* Retrieved from http://agris.fao.org/agris-search/search.do?recordID=US19850103458

Romme, W. H., & Turner, M. G. (1991). Implications of Global Climate Change for Biogeographic Patterns in the Greater Yellowstone Ecosystem. *Conservation Biology*, *5*(3), 373–386. https://doi.org/10.1111/j.1523-1739.1991.tb00151.x

Rosenberg, D. K., & McKelvey, K. S. (1999). Estimation of Habitat Selection for Central-Place Foraging Animals. *The Journal of Wildlife Management*, *63*(3), 1028–1038. https://doi.org/10.2307/3802818

Rotenberry, J. T., & Wiens, J. A. (1980). Habitat Structure, Patchiness, and Avian Communities in North American Steppe Vegetation: A Multivariate Analysis. *Ecology*, *61*(5), 1228–1250. https://doi.org/10.2307/1936840

Roush, W. M. (2009). *A substantial upward shift of the alpine treeline ecotone in the southern Canadian Rocky Mountains* (Thesis). Retrieved from https://dspace.library.uvic.ca//handle/1828/2031

Roush, W. M., Munroe, J. S., & Fagre, D. B. (2007). Development of a Spatial Analysis Method Using Ground-Based Repeat Photography to Detect Changes in the Alpine Treeline Ecotone, Glacier National Park, Montana, U.S.A. *Arctic, Antarctic, and Alpine Research*, *39*(2), 297–308. https://doi.org/10.1657/1523-0430(2007)39[297:DOASAM]2.0.CO;2

Roy, D. P. (2000). The impact of misregistration upon composited wide field of view satellite data and implications for change detection. *IEEE Transactions on Geoscience and Remote Sensing*, *38*(4), 2017–2032.

Ruggiero, A., & Hawkins, B. A. (2008). Why do Mountains Support so many Species of Birds? *Ecography*, *31*(3), 306–315.

Ryan, K. C., Knapp, E. E., & Varner, J. M. (2013). Prescribed fire in North American forests and woodlands: history, current practice, and challenges. *Frontiers in Ecology and the Environment*, *11*(s1), e15–e24. https://doi.org/10.1890/120329

Sala, O. E., Chapin, F. S., Iii, Armesto, J. J., Berlow, E., Bloomfield, J., … Wall, D. H. (2000). Global Biodiversity Scenarios for the Year 2100. *Science*, *287*(5459), 1770–1774. https://doi.org/10.1126/science.287.5459.1770

Sanseverino, M., Higgs, E., & Whitney, M. J. (2016). Exploring landscape change in mountain environments with the Mountain Legacy Online Image Analysis Toolkit. *Mountain Research and Development*, *36*(4), 407–416.

Shao, G., & Wu, J. (2008). On the accuracy of landscape pattern analysis using remote sensing data. *Landscape Ecology*, *23*, 505–511.

St. Laurent, K. M. (2007). *Bird Inventory for Kakwa Wildland Provincial Park* (Parks, Conservation, Recreation and Sports Division). Edmonton, AB: Alberta Tourism, Parks, Recreation and Culture. Retrieved from https://uat.albertaparks.ca/media/3193882/Bird_Inventory_kakwa_2007.pdf

Stewart, F. E. C., Heim, N. A., Clevenger, A. P., Paczkowski, J., Volpe, J. P., & Fisher, J. T. (2016). Wolverine behavior varies spatially with anthropogenic footprint: implications for conservation and inferences about declines. *Ecology and Evolution*, *6*(5), 1493–1503. https://doi.org/10.1002/ece3.1921

Stockdale, C. A. (2017). *A century of landscape change in the southern Rocky Mountains and Foothills of Alberta: Using historical photography to quantify ecological change* (PhD). Univeristy of Alberta, Edmonton, AB. Retrieved from https://era.library.ualberta.ca/files/cjq085k18x/Stockdale_Christopher_A_201701_PhD.pdf

Stockdale, C. A., Bozzini, C., Macdonald, S. E., & Higgs, E. (2015). Extracting ecological information from oblique angle terrestrial landscape photographs: Performance evaluation of the WSL Monoplotting Tool. *Applied Geography*, *63*, 315–325. https://doi.org/10.1016/j.apgeog.2015.07.012

Stralberg, D., Jongsomjit, D., Howell, C. A., Snyder, M. A., Alexander, J. D., Wiens, J. A., & Root, T. L. (2009). Re-Shuffling of Species with Climate Disruption: A No-Analog Future for California Birds? *PLOS ONE*, *4*(9), e6825. https://doi.org/10.1371/journal.pone.0006825

Strausz, D. A. J. (2001). *An application of photogrammetric techniques to the measurement of historic photographs*. Oregon State.

Taggart-Hodge, T. (2016). *A century of landscape-level changes in the Bow watershed, Alberta, Canada, and implications for flood management* (M.Sc.). University of Victoria, Victoria, BC, Canada.

Townshend, J. R. G., Justice, C. O., Gurney, C., & McManus, J. (1992). The impact of misregistration on change detection. *IEEE Transactions on Geoscience and Remote Sensing*, *30*(5), 1054–1060.

Trant, A. J., Starzomski, B. M., & Higgs, E. (2015). A publically available database for studying ecological change in mountain ecosystems. *Frontiers in Ecology and the Environment*, *13*(4), 187–187. https://doi.org/10.1890/15.WB.007

Turner, M. G. (2005). Landscape ecology - the state of the science. *Annual Review of Ecology, Evolution and Systematics*, (36), 319–344.

United Nations. (2017). *The Global Land Outlook* (First Edition). Bonn, Germany: United Nations Convention to Combat Desertification.

United States Department of Agriculture. (1993). Snapshot in Time, Repeat Photography on the Boise National Forest 1870-1992. *Forestry*. Retrieved from https://digitalcommons.usu.edu/govdocs_forest/2

Verbyla, D. L., & Hammond, T. O. (1995). Conservative bias in classification accuracy assessment due to pixel-by-pixel comparison of classified images with reference grids. *International Journal of Remote Sensing*, *16*(3), 581–587. https://doi.org/10.1080/01431169508954424

Vitousek, P. M., Mooney, H. A., Lubchenco, J., & Melillo, J. M. (1997). Human domination of Earth’s ecosystems. *Science*, *277*(5325), 494–499. https://doi.org/10.1126/science.277.5325.494

Walther, G.-R., Beißner, S., & Burga, C. A. (2005). Trends in the Upward Shift of Alpine Plants. *Journal of Vegetation Science*, *16*(5), 541–548.

Webb, R. H. (2010). *Repeat photography: methods and applications in the natural sciences*. Island Press.

Westbrook, M. R. (2014). *Local scale forest encroachment into alpine habitat: past patterns and future predictions* (M.Sc.). University of Cincinnati, Cincinnati, Ohio.

Whiteman, C. D. (2000). *Mountain Meteorology: Fundamentals and Applications*. Oxford University Press.

Widenmaier, K. J., & L Strong, W. (2010). Tree and forest encroachment into fescue grasslands on the Cypress Hills plateau, southeast Alberta, Canada. *Forest Ecology and Management*, *259*(10), 1870–1879. https://doi.org/10.1016/j.foreco.2010.01.049

Willis, K. J., & Birks, H. J. B. (2006). What Is Natural? The Need for a Long-Term Perspective in Biodiversity Conservation. *Science*, *314*(5803), 1261–1265. https://doi.org/10.1126/science.1122667

Willis, Katherine J., Gillson, L., Brncic, T. M., & Figueroa-Rangel, B. L. (2005). Providing baselines for biodiversity measurement. *Trends in Ecology & Evolution*, *20*(3), 107–108. https://doi.org/10.1016/j.tree.2004.12.003

Yoccoz, N. G., Nichols, J. D., & Boulinier, T. (2001). Monitoring of biological diversity in space and time. *Trends in Ecology & Evolution*, *16*(8), 446–453. https://doi.org/10.1016/S0169-5347(01)02205-4

Zamora, R., & Barea-Azcón, J. M. (2015). Long-Term Changes in Mountain Passerine Bird Communities in the Sierra Nevada (Southern Spain): A 30-Year Case Study. *Ardeola*, *62*(1), 3–18. https://doi.org/10.13157/arla.62.1.2015.3

Zuur, A. F., Ieno, E. N., & Elphick, C. S. (2010). A protocol for data exploration to avoid common statistical mistakes. *Methods in Ecology and Evolution*, *1*(1), 3–14.

Zuur, A. F., Ieno, E. N., Walker, N. J., Saveliev, A. A., & Smith, G. M. (2009). Zero-Truncated and Zero-Inflated Models for Count Data. In *Mixed effects models and extensions in ecology with R* (pp. 261–293). Springer, New York, NY. https://doi.org/10.1007/978-0-387-87458-6_11

Appendix A
Photographs from alignment experiment

A1: "Historical" photograph without foreground, taken with Fuji X-T2.

B1: Repeat photograph of A1 taken with Nikon D800 from the same position, with the same orientation.

C1: Repeat photograph of A1 taken with Nikon D800 from the same position and orientation but with tripod height increased by 23 cm.

D1: Repeat photograph of A1 taken with Nikon D800 from 1 m to the right of A1's tripod location.

E1: Repeat photograph of A1 taken with Nikon D800 from 3 m to the right of A1's tripod location.

F1: Repeat photograph of A1 taken with Nikon D800 from 5 m to the right of A1's tripod location.

G1: Repeat photograph of A1 taken with Nikon D800 from 1 m forward from A1's tripod location.

H1: Repeat photograph of A1 taken with Nikon D800 from same location as A1, but with azimuth modified 15° to the right.

I1: Repeat photograph of A1 taken with Nikon D800 from same location as A1, but with elevation angle modified 10° downward.

A2: "Historical" photograph with foreground, taken with Fuji X-T2.

B2: Repeat photograph of A2 taken with Nikon D800 from the same position, with the same orientation.

C2: Repeat photograph of A2 taken with Nikon D800 from the same position and orientation but with tripod height increased by 23 cm.

D2: Repeat photograph of A2 taken with Nikon D800 from 1 m to the right of A2's tripod location.

E2: Repeat photograph of A2 taken with Nikon D800 from 3 m to the right of A2's tripod location.

F2: Repeat photograph of A2 taken with Nikon D800 from 5 m to the right of A2's tripod location.

G2: Repeat photograph of A2 taken with Nikon D800 from 1 m forward from A2's tripod location.

H2: Repeat photograph of A2 taken with Nikon D800 from same location as A2, but with azimuth modified 15° to the right.

I2: Repeat photograph of A2 taken with Nikon D800 from same location as A2, but with elevation angle modified 10° downward.

Appendix B
Image Analysis Toolkit output for alignment pairs

Images	Points used in transformation	Transformation matrix determinant	Distances of points used in RMSE calculation	RMSE (pixels)
A1B1	1-2 7-8 11-12	-5.63	3-4: (3.12, -1.94) 5-6: (1.33, 0.55) 9-10: (-1.95, 1.8)	2.74
A1C1	1-2 7-8 11-12	-5.63	3-4: (3.19, -2.64) 5-6: (0.57, 1.76) 9-10: (-2.94, 2.33)	3.39
A1D1	1-2 7-8 11-12	-5.52	3-4: (5.48, -1.64) 5-6: (1.24, 0.18) 9-10: (-2.48, 1)	3.72
A1E1	1-2 7-8 11-12	-5.63	3-4: (5.67, -0.99) 5-6: (-0.55, -1.51) 9-10: (-5.3, 0.96)	4.64
A1F1	1-2 5-6 11-12	-4.51	3-4: (8.8, -1.82) 7-8: (2.05, 0.78) 9-10: (-7.43, 2.57)	7.00
A1G1	1-2 7-8 11-12	-5.63	3-4: (3.4, -0.62) 5-6: (-1.61, -0.78) 9-10: (0.16, 2.04)	2.54
A1H1	1-2 5-6 11-12	-4.51	3-4: (-14.23, 1.45) 7-8: (-0.68, 0.65) 9-10: (0.93, -11.93)	10.77
A1I1	1-2 7-8 11-12	-5.63	3-4: (4.87, -3.13) 5-6: (3.7, -4.29) 9-10: (-12.17, 0.87)	8.45
A2B2	1-2 5-6 9-10	2.22	3-4: (0.96, 1.4) 7-8: (0.68, 0.02) 11-12: (-2.95, -0.56)	2.02
A2C2	1-2 3-4 5-6	0.45	7-8: (0.01, 0.36) 9-10: (-0.61, 0.03) 11-12: (-1.44, -0.47)	0.96
A2D2	1-2 9-10 11-12	-3.29	3-4: (-0.98, 1.32) 5-6: (1.37, 1.16) 7-8: (0.45, -0.31)	1.44
A2E2	1-2 3-4 11-12	-2.99	5-6: (3.25, -1.04) 7-8: (0.82, -0.77) 9-10: (-2.73, -1.07)	2.67

A2F2	5-6 7-8 11-12	-0.42	1-2: (-5.91, 2.01) 3-4: (-4.67, -0.06) 9-10: (2.54, -1.09)	4.77
A2G2	1-2 3-4 11-12	-2.99	5-6: (-0.34, 0.32) 7-8: (0.74, -1.24) 9-10: (-2.38, -1.67)	1.89
A2H2	1-2 3-4 11-12	-2.99	5-6: (-0.16, -8.51) 7-8: (14.35, 4.58) 9-10: (-31.68, 15.12)	22.59
A2I2	3-4 7-8 11-12	-0.55	1-2: (3.03, 5.47) 5-6: (4.81, -1.14) 9-10: (-9.39, -3.89)	7.45

Note: Image codes (A1, B1, …) correspond to the images described in Appendix A.

Appendix C
List of historical and repeat photographs from the MLP

#	Label	Historical surveyor	Station #	Image #	Historical year	Repeat year
1	LAM5	H. F. J. Lambart	5	24	1927	2014
2	LAM15	H. F. J. Lambart	15	2	1927	2011
3	LAM33	H. F. J. Lambart	33	3	1927	2011
4	LAM35	H. F. J. Lambart	35	261	1927	2007
5	LAM36	H. F. J. Lambart	36	268	1927	2016
6	LAM37	H. F. J. Lambart	37	280	1927	2007
7	LAM39	H. F. J. Lambart	39	293	1927	2016
8	LAM42	H. F. J. Lambart	42	320B	1927	2007
9	LAM51	H. F. J. Lambart	51	390	1927	2007
10	MIL1	W. H. Miller	1	819	1928	2014
11	MIL2	W. H. Miller	2	821	1928	2014
12	MIL4.5	W. H. Miller	4.5	840	1928	2014
13	MIL5	W. H. Miller	5	843	1928	2014
14	MIL6	W. H. Miller	6	852	1928	2014
15	MIL7	W. H. Miller	7	859	1928	2014
16	MIL8	W. H. Miller	8	864	1928	2014
17	MIL9	W. H. Miller	9	876	1928	2014
18	MIL10	W. H. Miller	10	880	1928	2014
19	MIL12	W. H. Miller	12	901	1928	2014
20	MIL13	W. H. Miller	13	908	1928	2014
21	MIL14	W. H. Miller	14	912	1928	2014
22	MIL16	W. H. Miller	16	924	1928	2014
23	MIL18	W. H. Miller	18	949	1928	2014
24	MIL19	W. H. Miller	19	953	1928	2014
25	MIL20	W. H. Miller	20	957	1928	2014
26	NID11	M. E. Nidd	11	1	1944	2012
27	NID12	M. E. Nidd	12	2	1944	2012
28	NID15	M. E. Nidd	15	3	1944	2012
29	NID19	M. E. Nidd	19	3	1944	2012
30	NID21	M. E. Nidd	21	2	1944	2012
31	NID8	M. E. Nidd	8	77	1946	2016
32	NID12B	M. E. Nidd	12	121	1946	2016
33	NID2	M. E. Nidd	2	402	1947	2016
34	NID3	M. E. Nidd	3	500	1953	2016
35	NID5	M. E. Nidd	5	24	1953	2016
36	WHE245	A. O. Wheeler	245	183	1923	2007
37	WHE247	A. O. Wheeler	247	202	1923	2007
38	WHE248	A. O. Wheeler	248	213	1923	2007

39	WHE249	A. O. Wheeler	249	219	1923	2007
40	WHE250	A. O. Wheeler	250	222	1923	2007
41	WHE251	A. O. Wheeler	251	235	1923	2007
42	WHE254	A. O. Wheeler	254	256	1923	2007
43	WHE289	A. O. Wheeler	289	5	1924	2011
44	WHE292	A. O. Wheeler	292	30	1924	2011
45	WHE297	A. O. Wheeler	297	64	1924	2011
46	WHE309	A. O. Wheeler	309	173	1924	2011

Appendix D
Historical and repeat photographs and associated land cover masks

Images appear in the following order: historical photograph, repeat photograph, historical mask, repeat mask. Image labels are as shown in Appendix C.

Legend for all masks below:

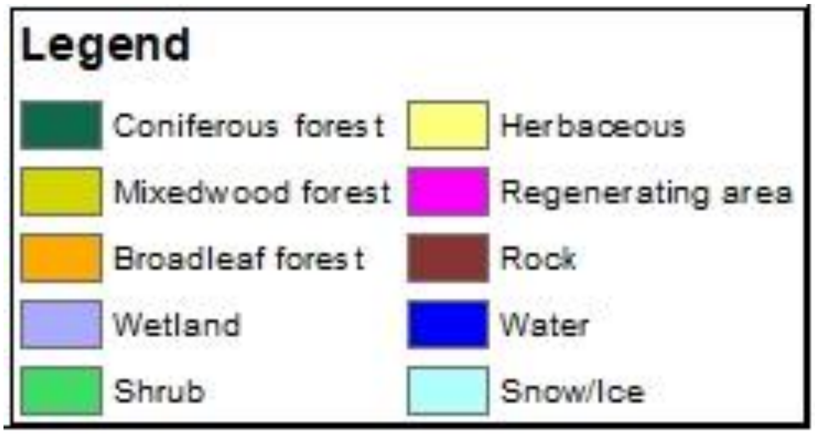

LAM5

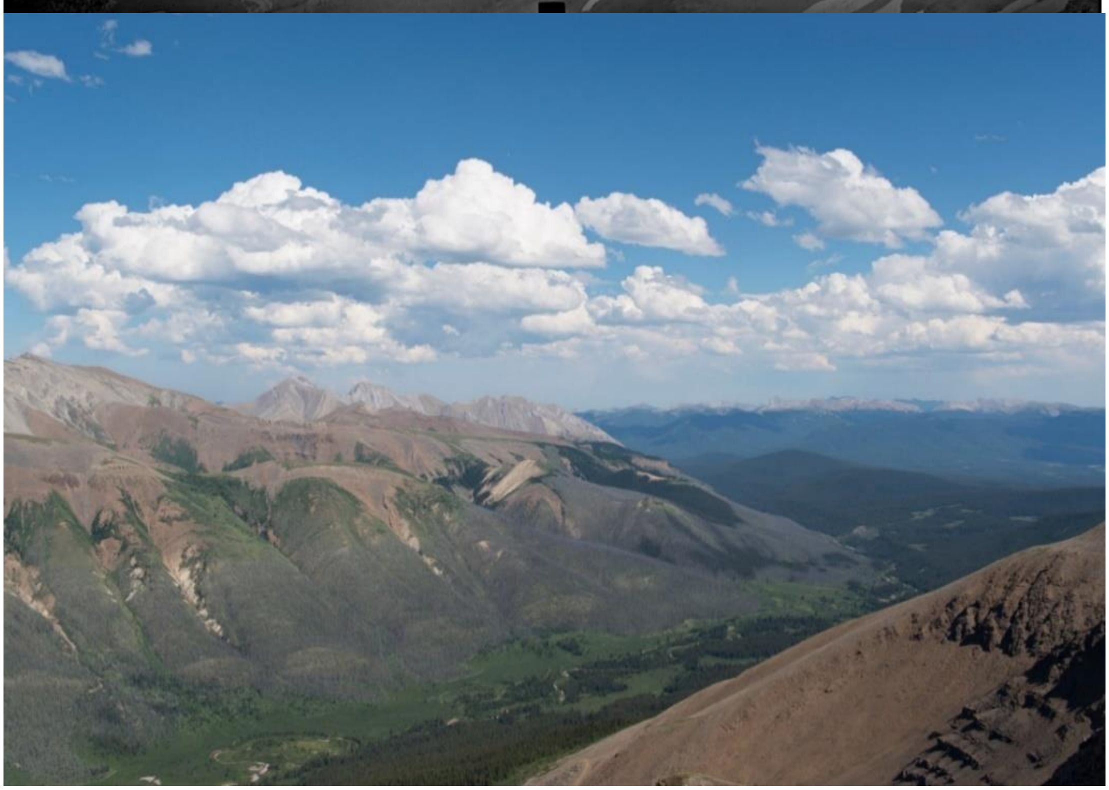

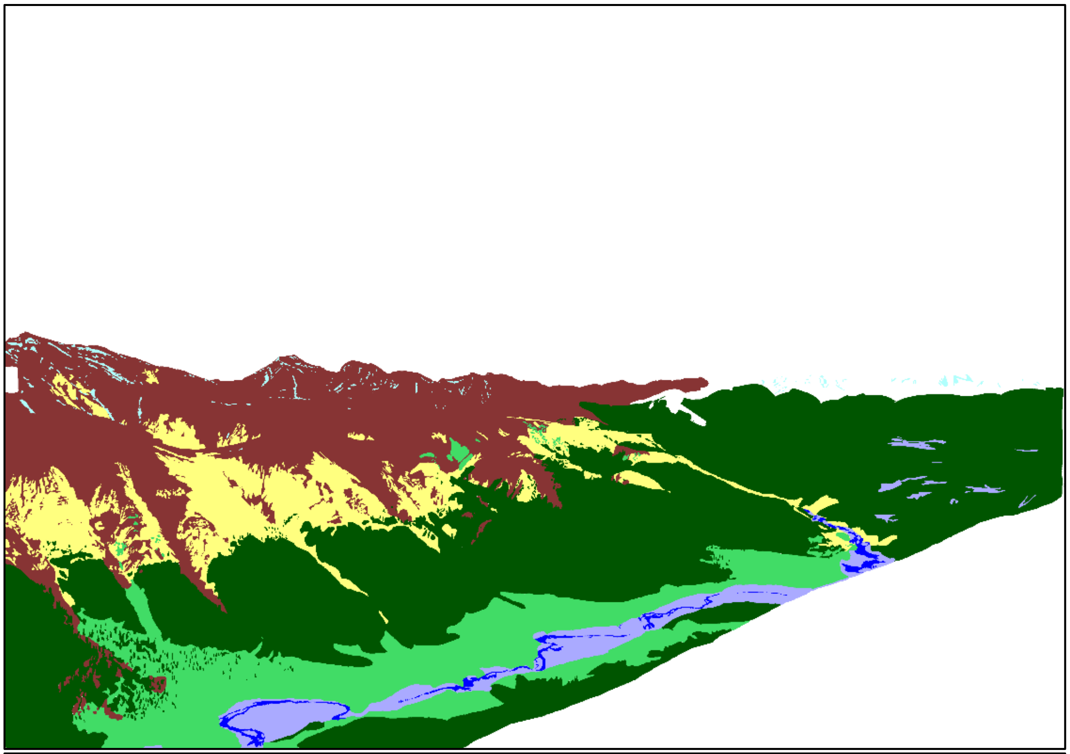

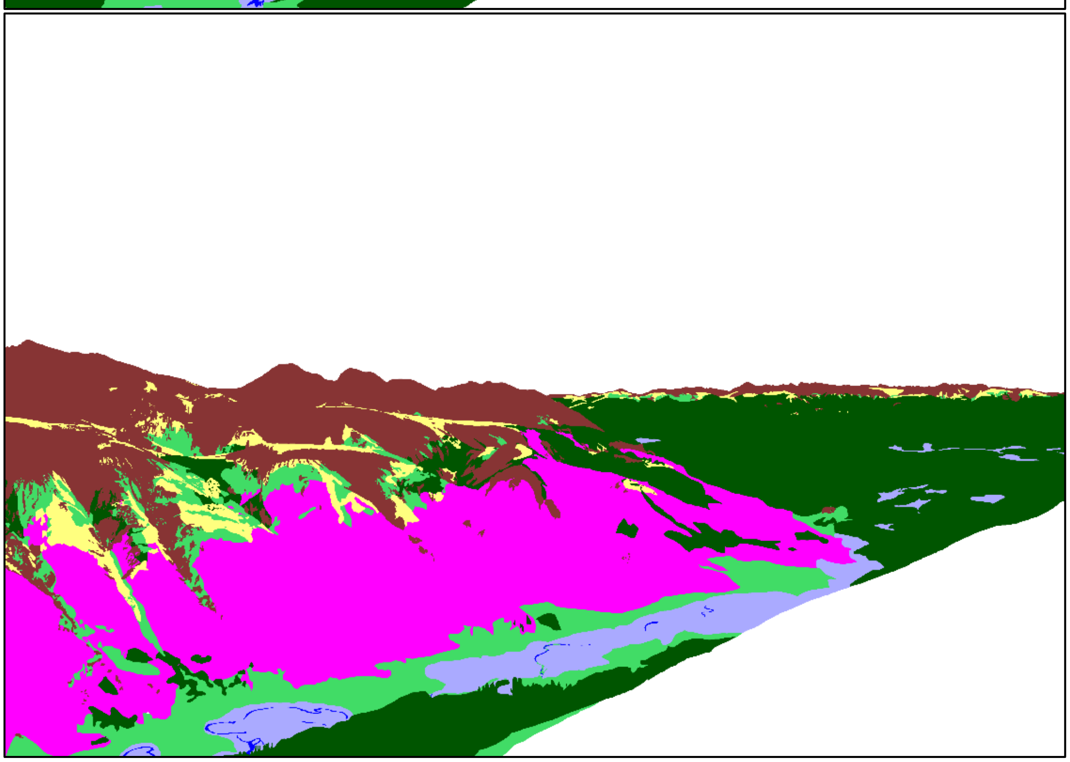

LAM15

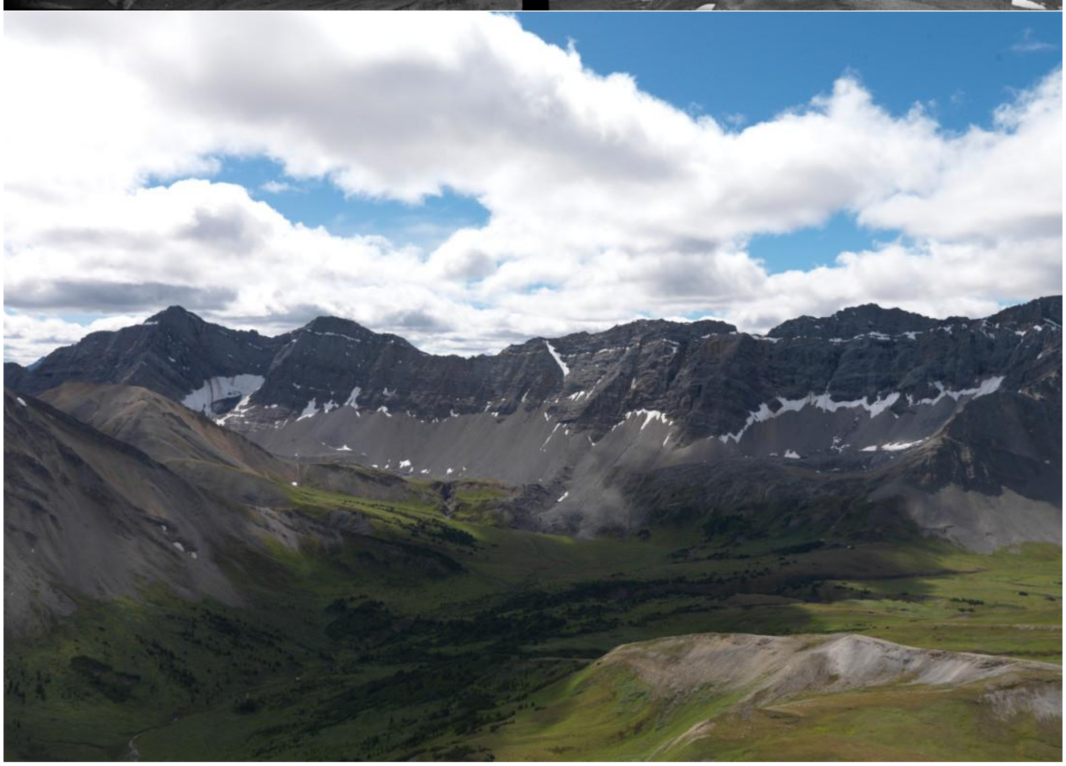

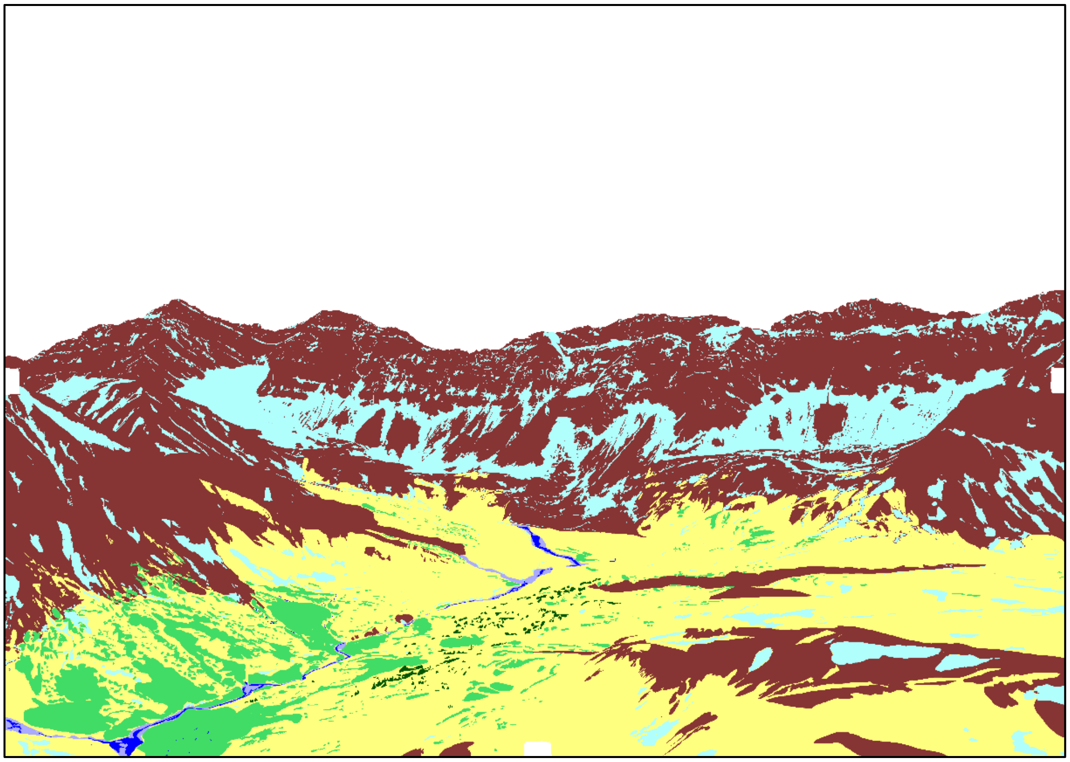

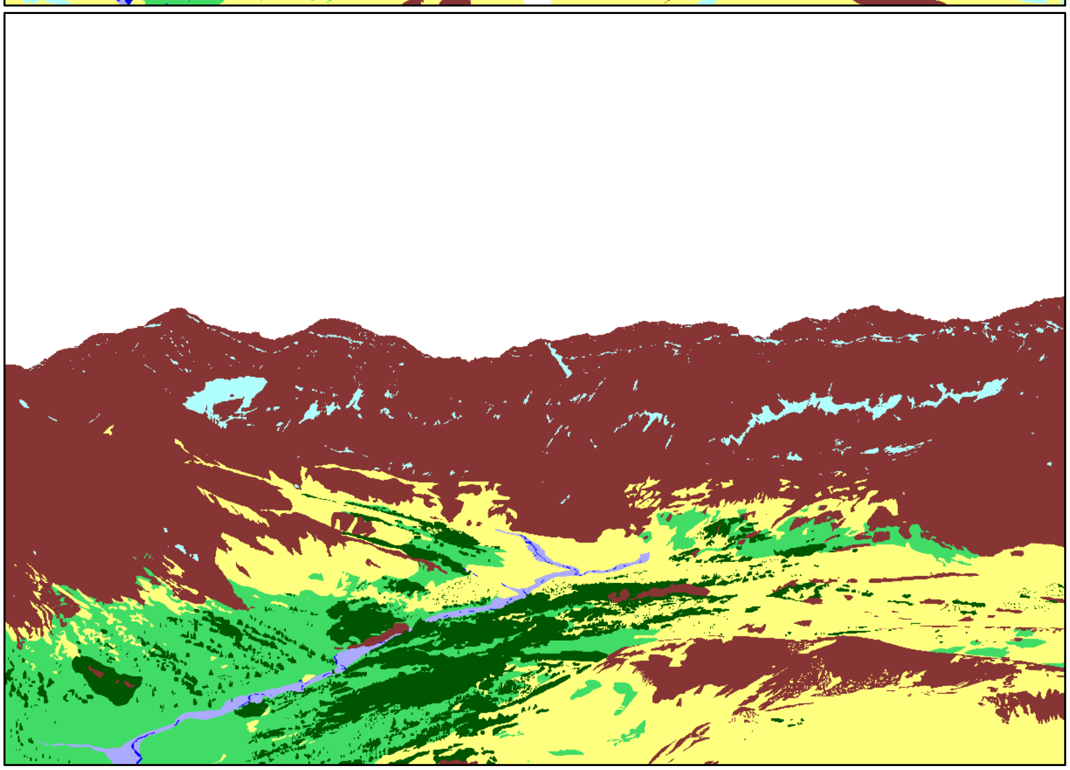

LAM33

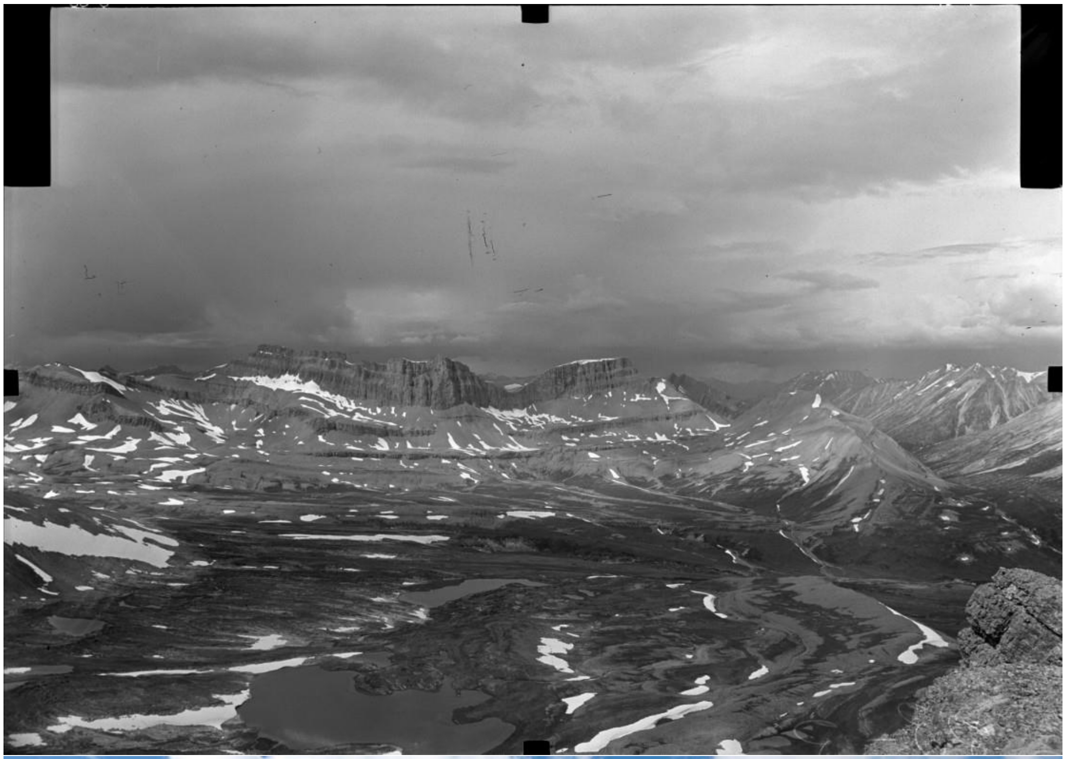

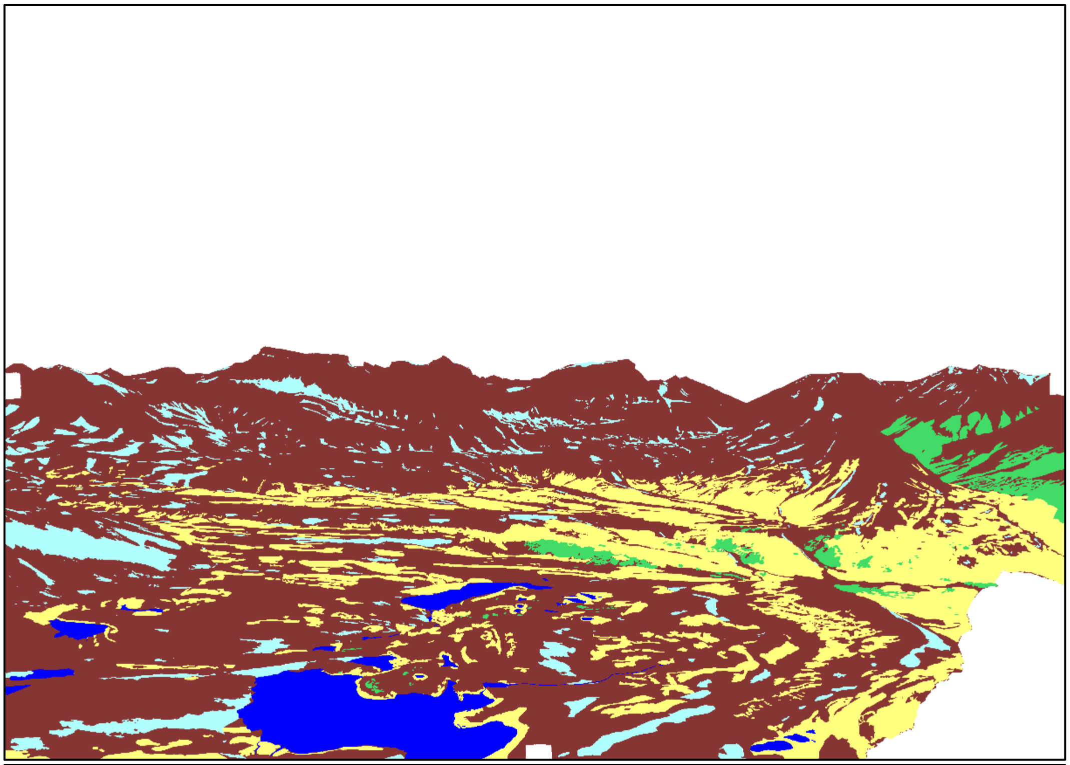

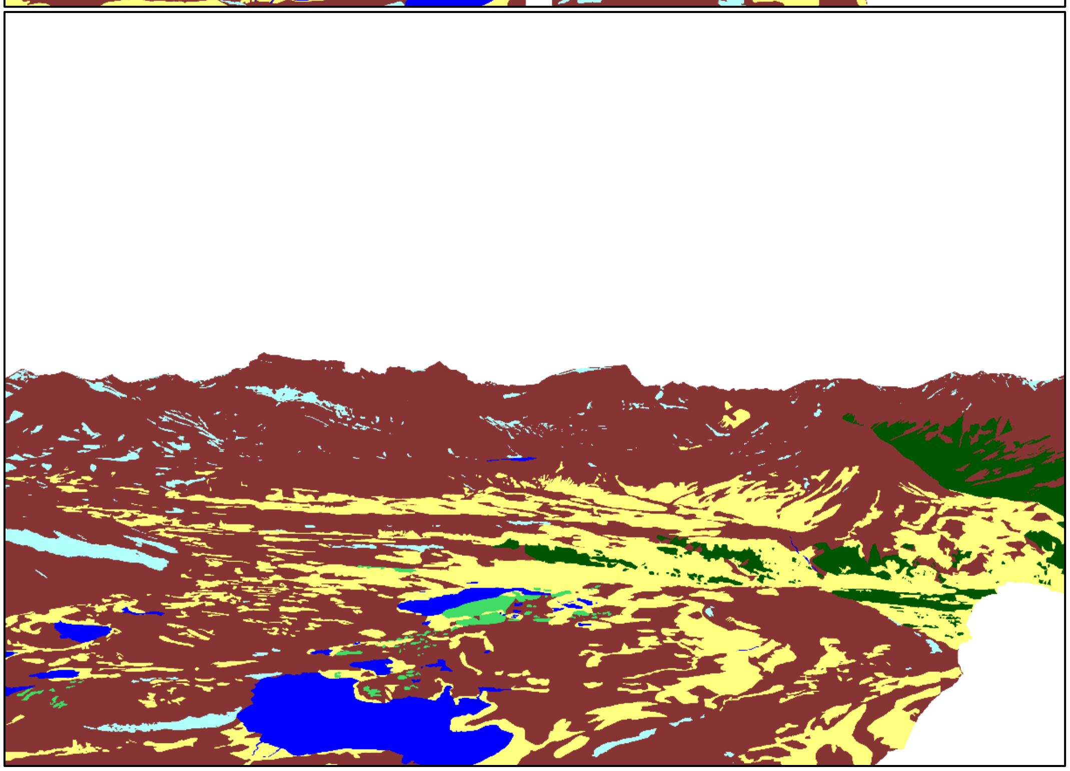

LAM35

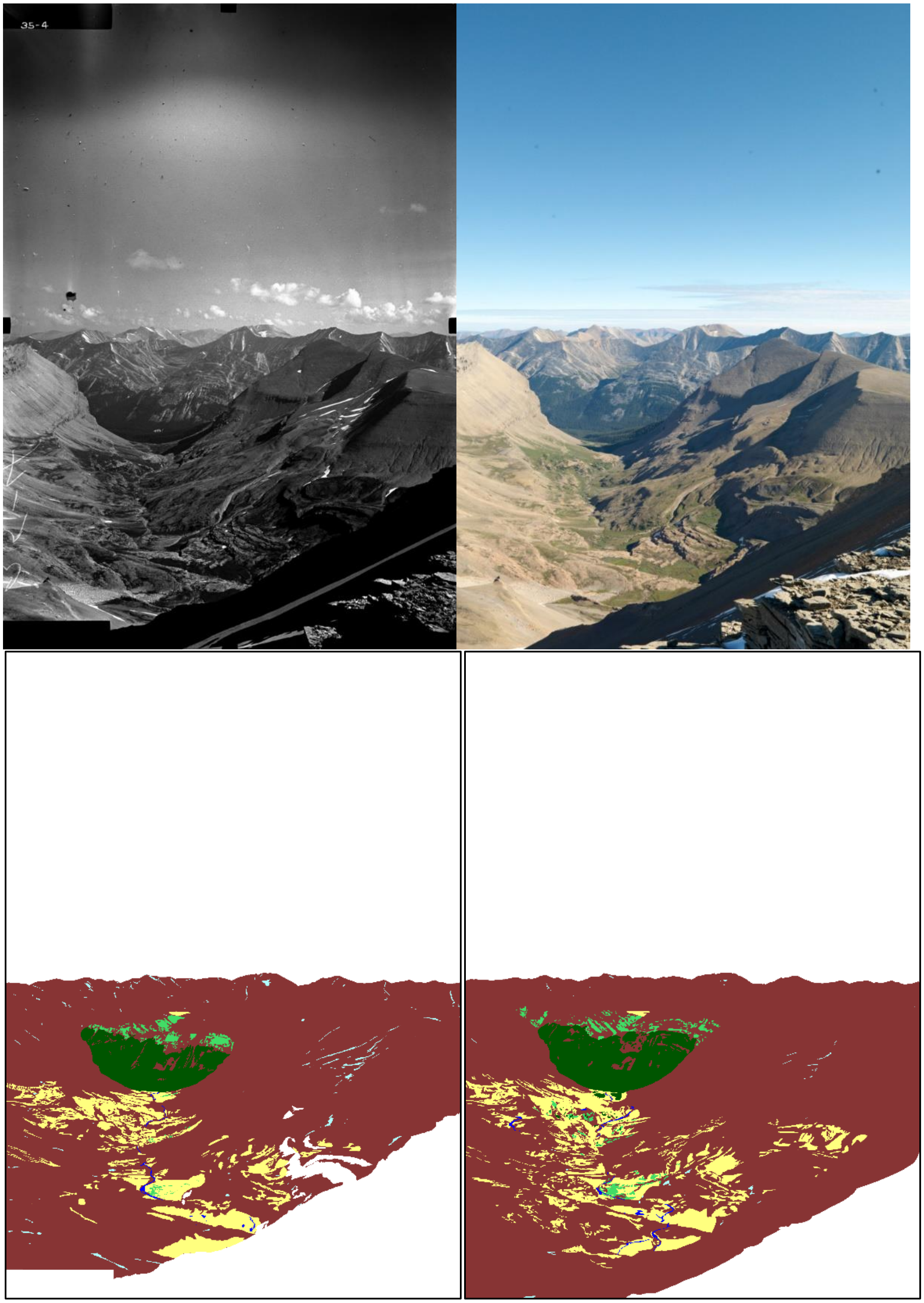

LAM36

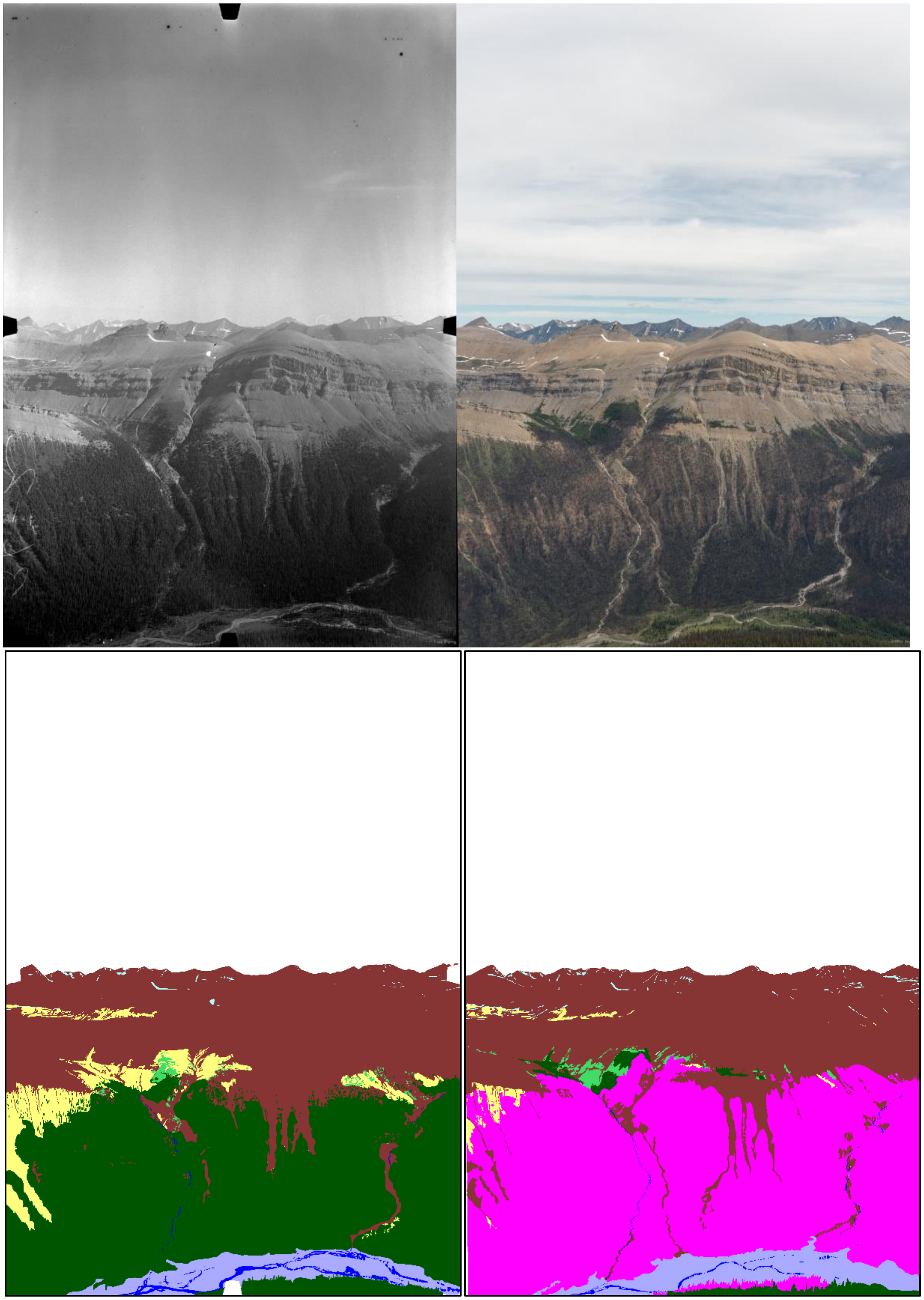

LAM37

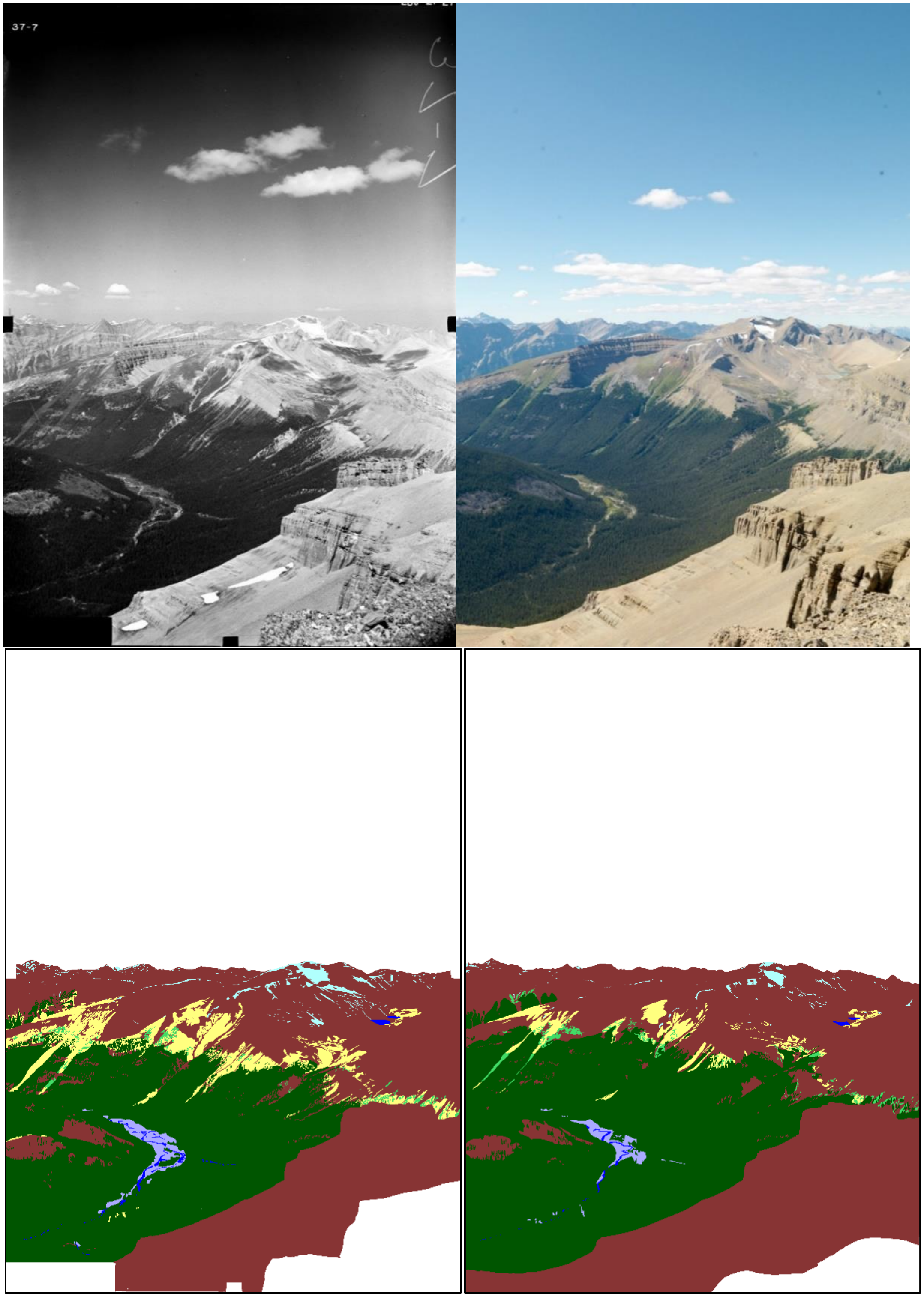

LAM39

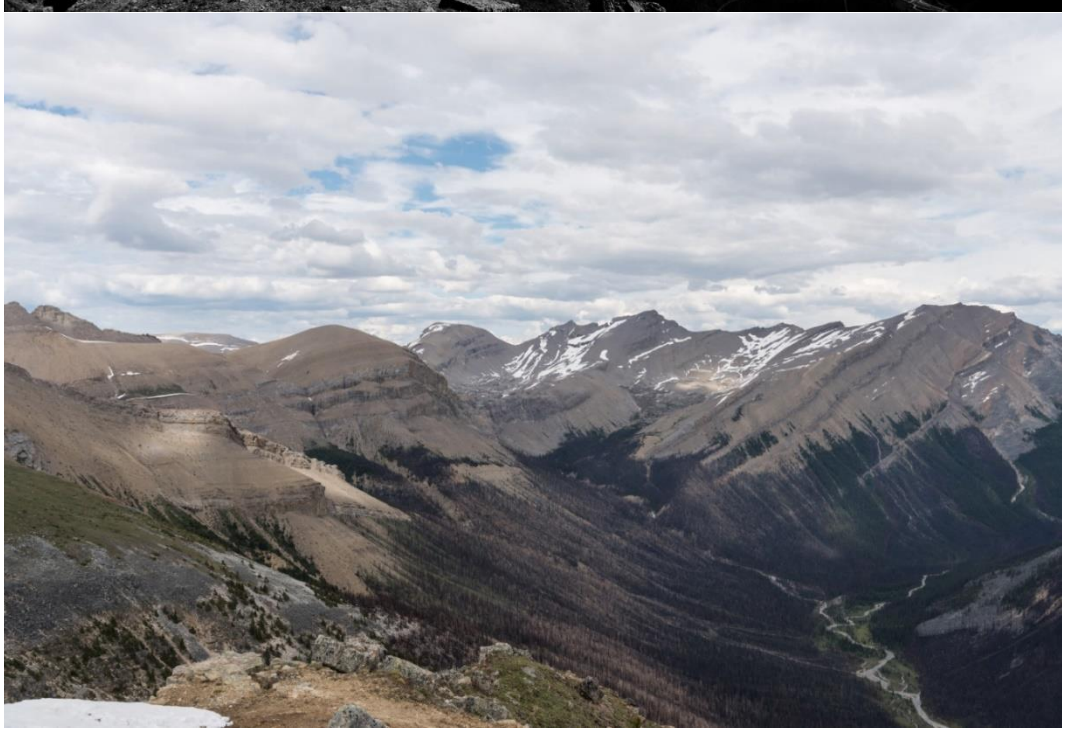

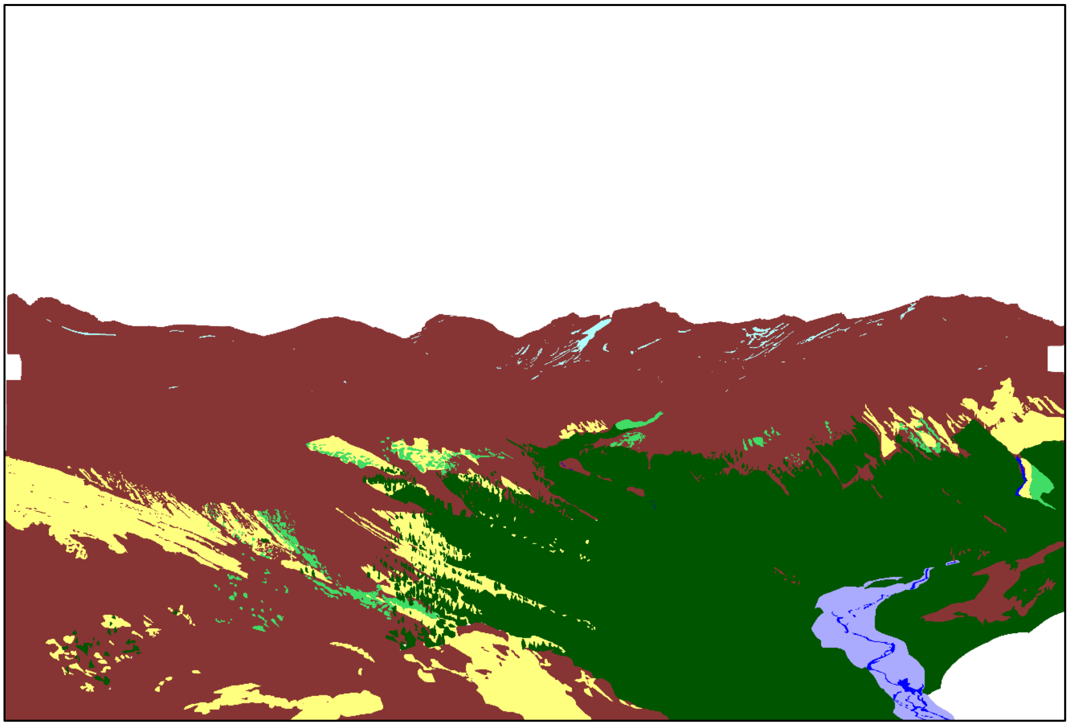

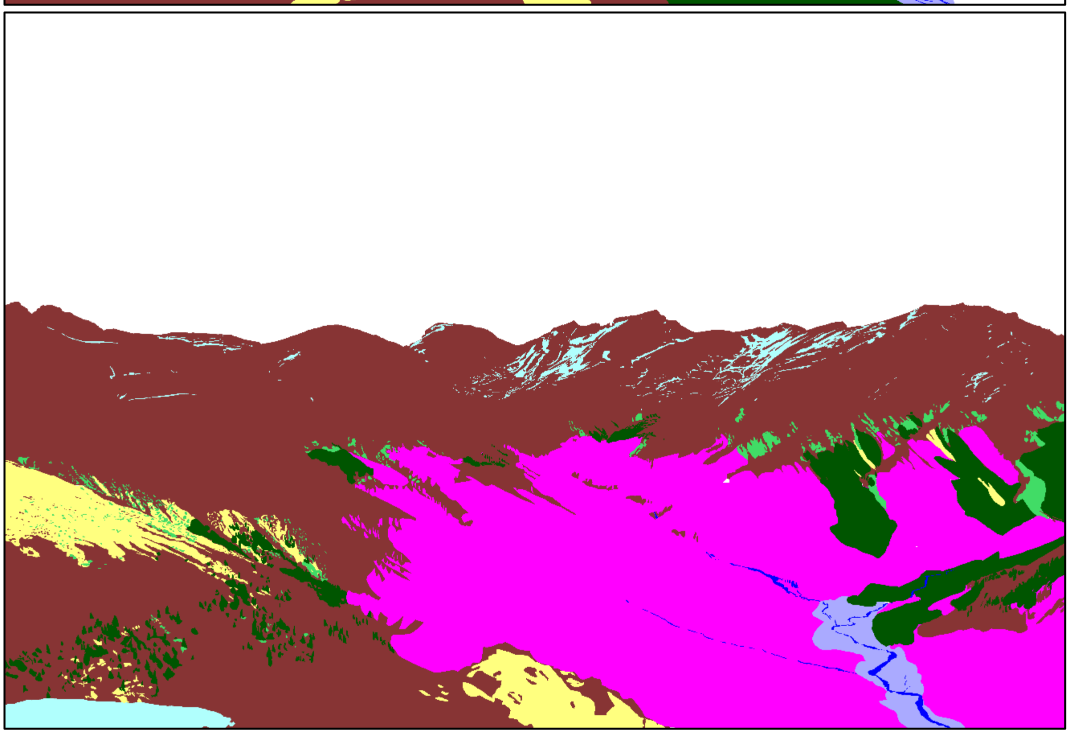

LAM42

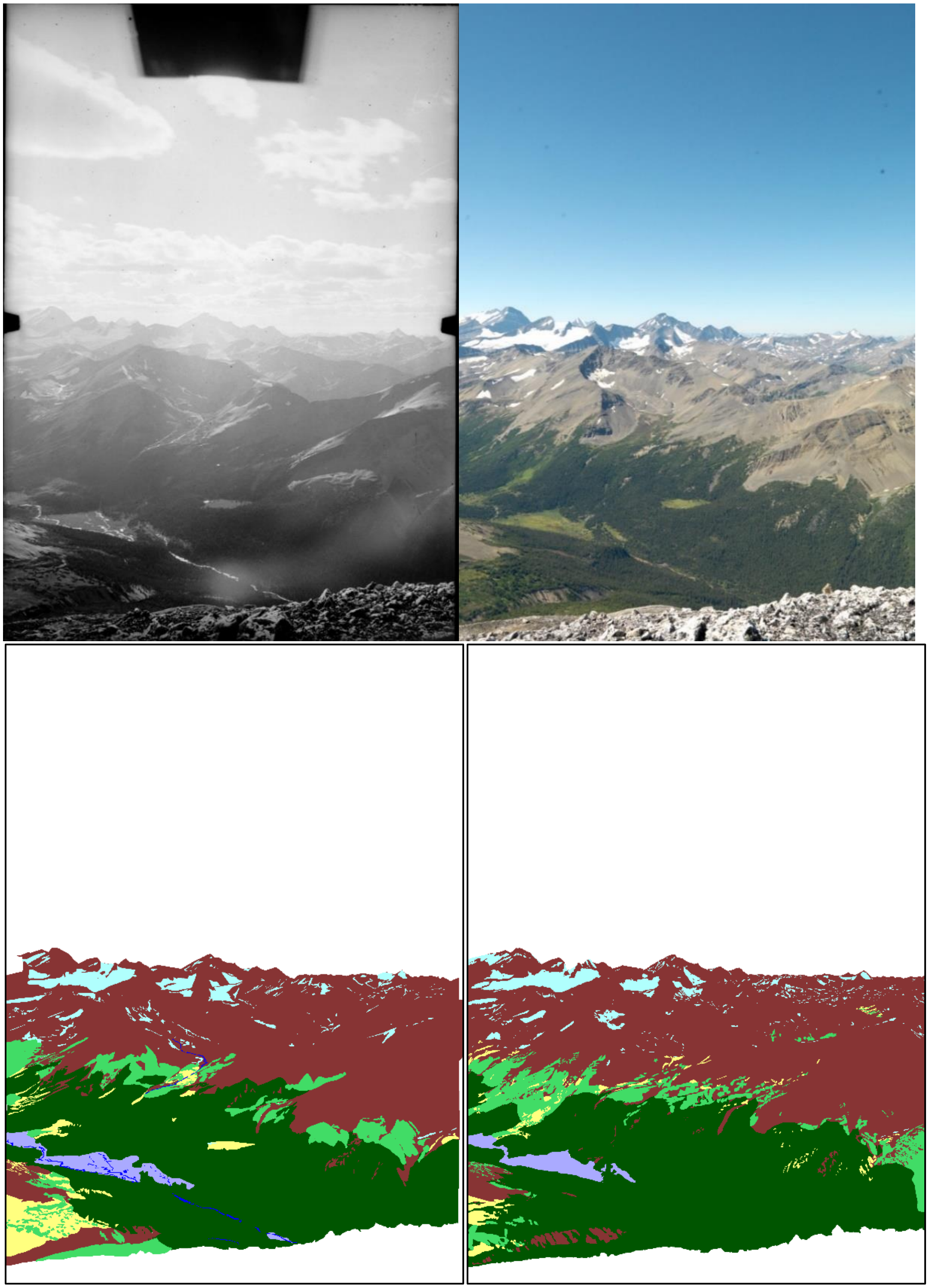

LAM51

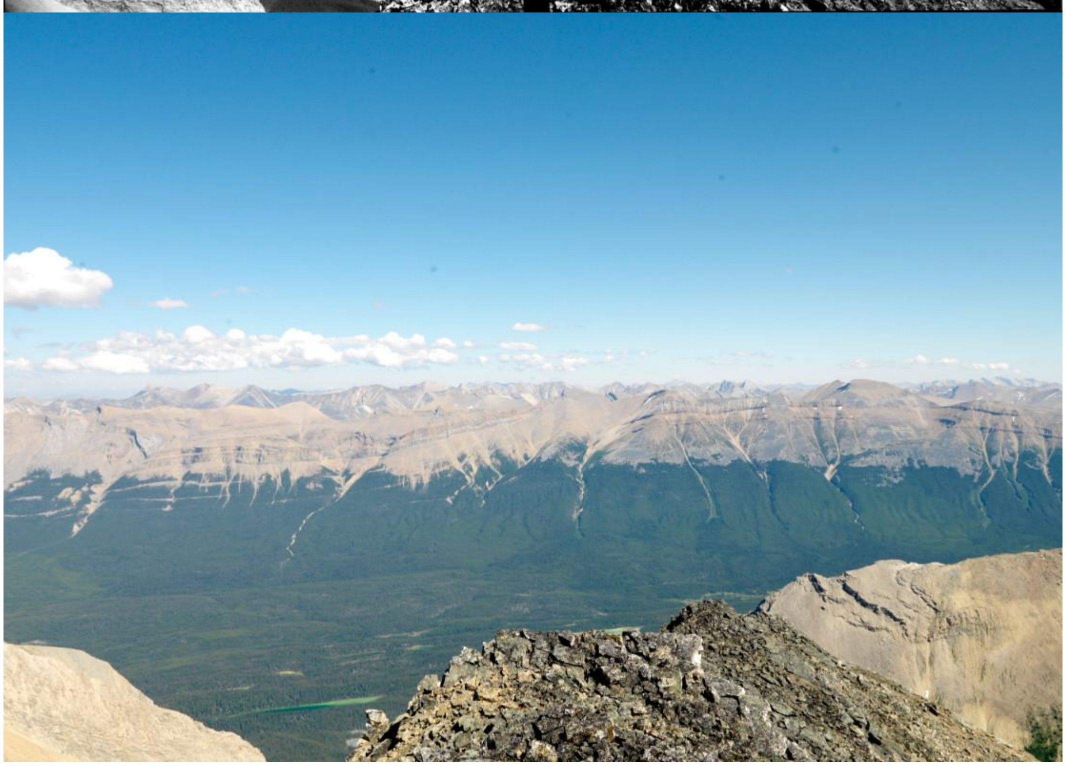

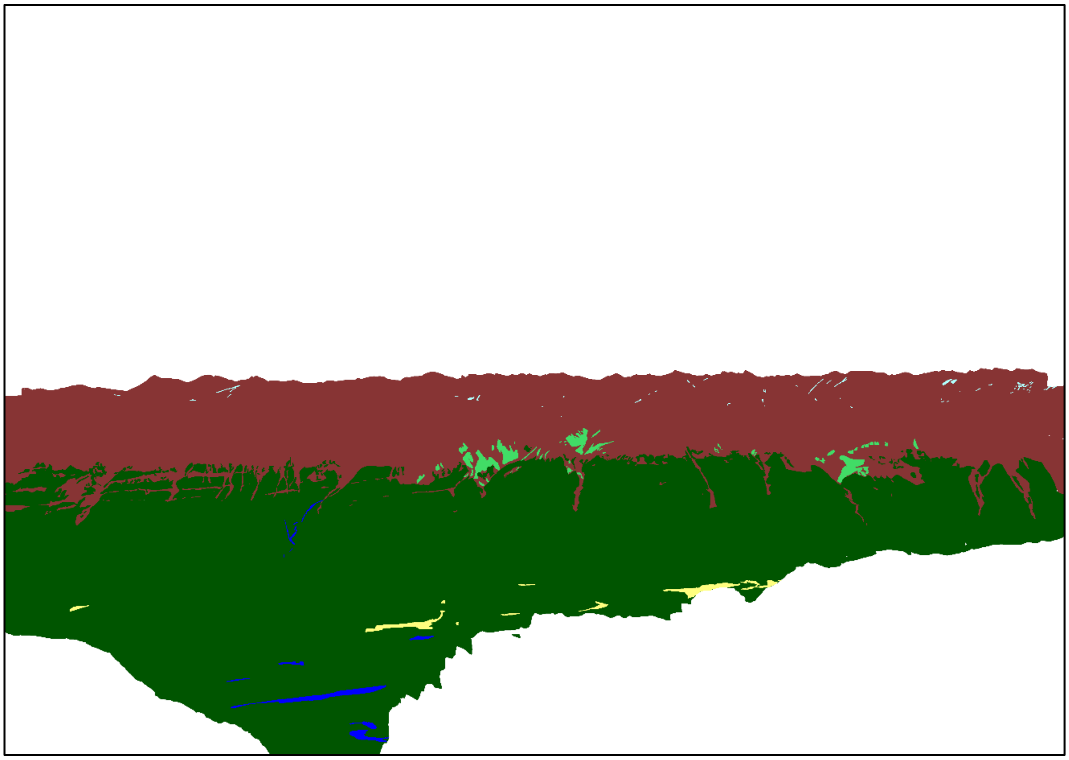

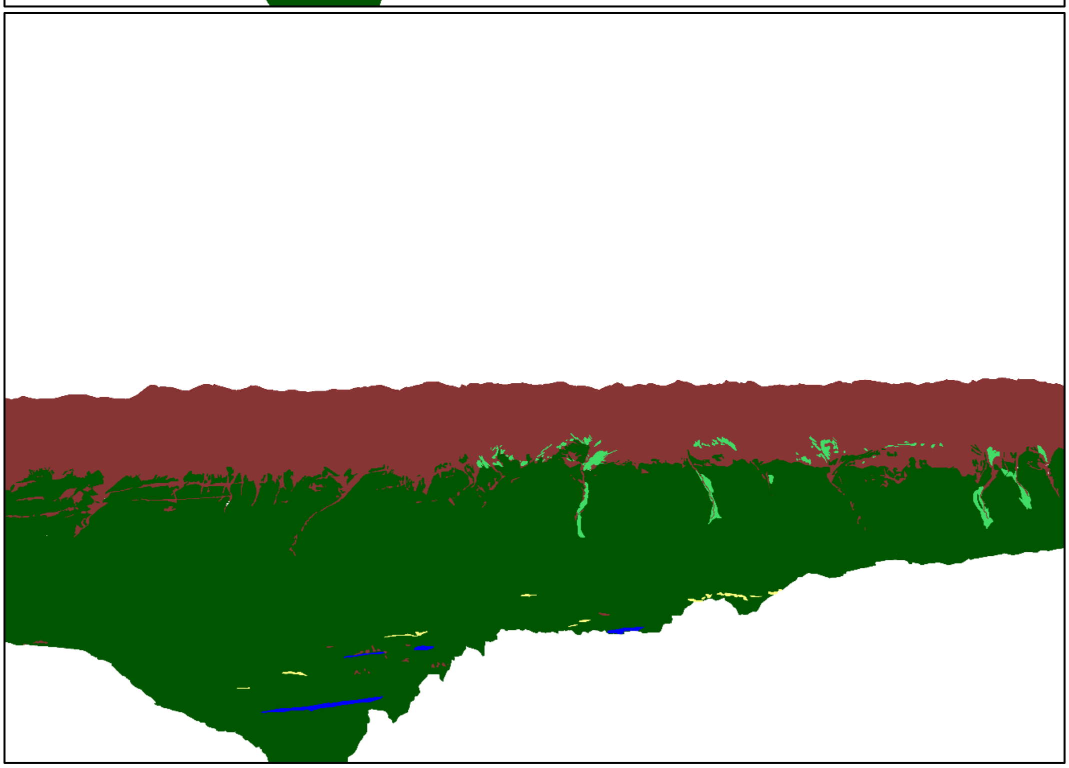

MIL1

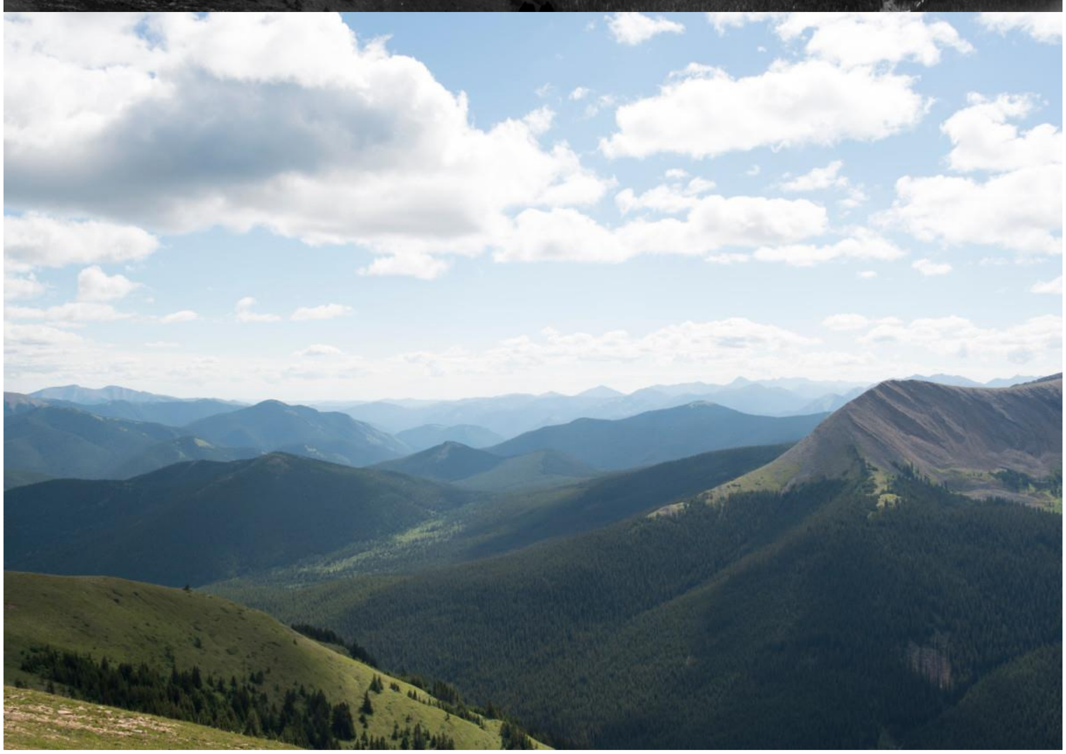

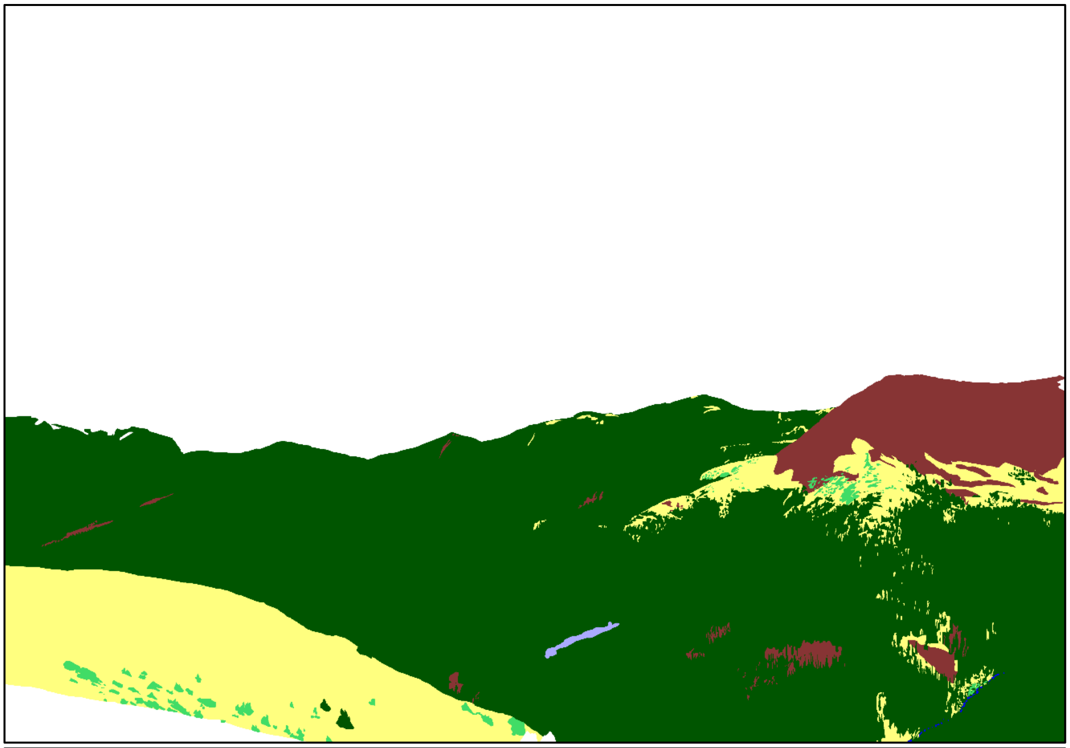

MIL2

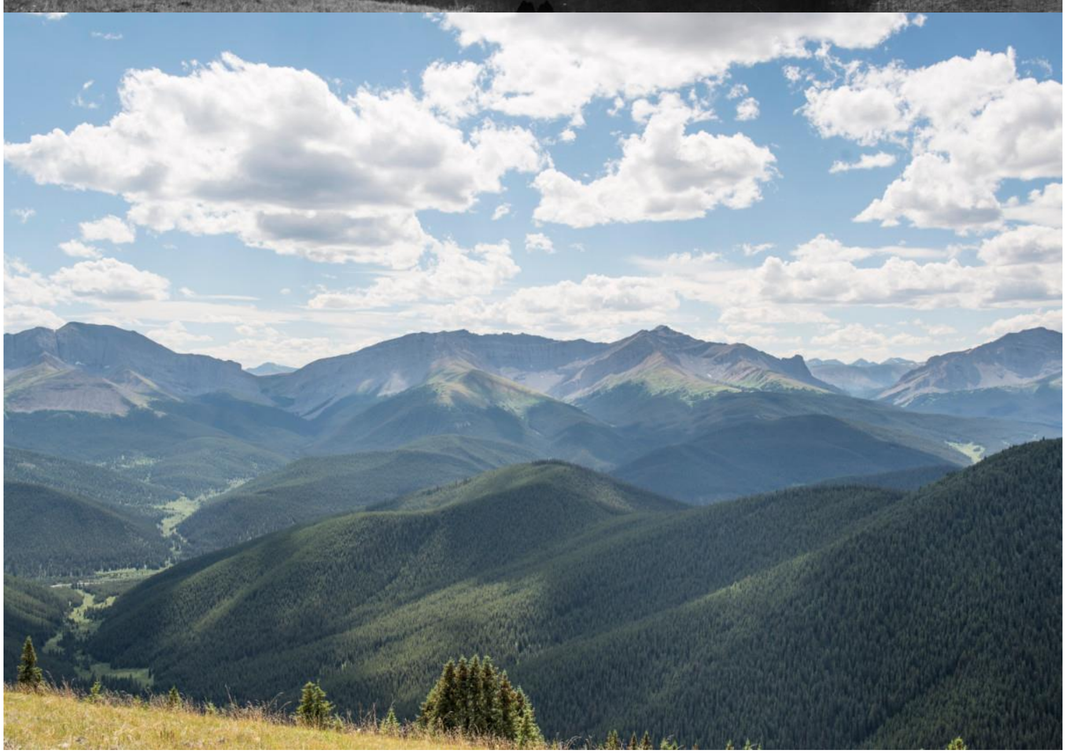

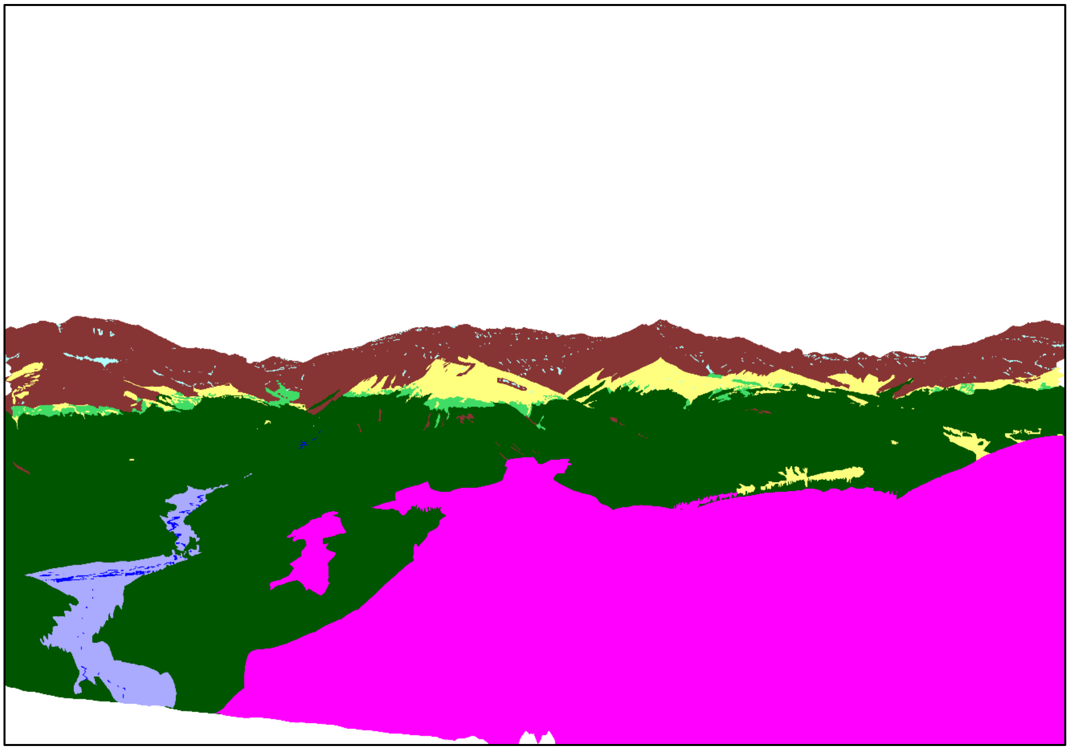

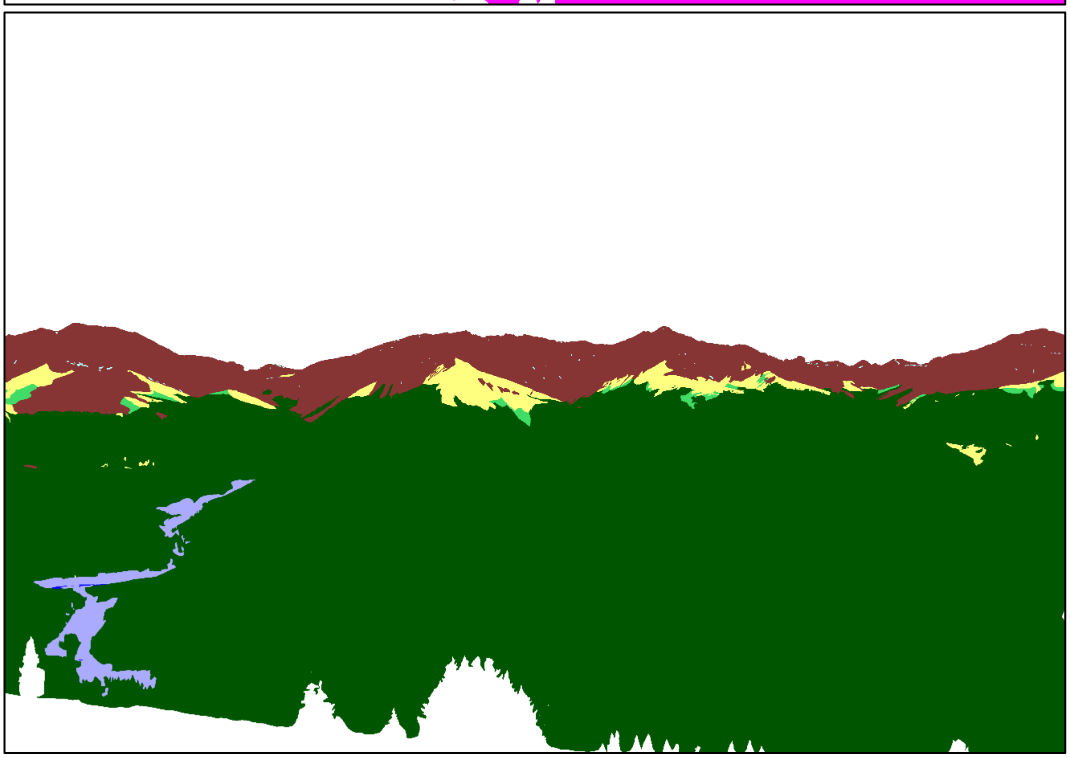

MIL4.5

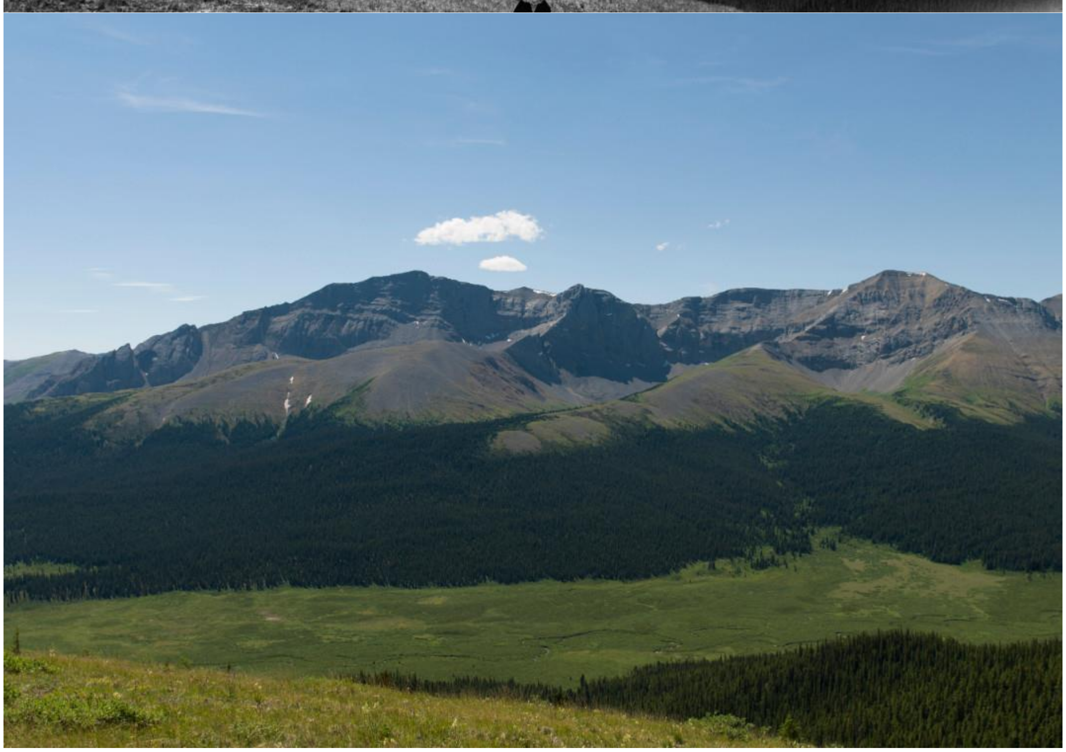

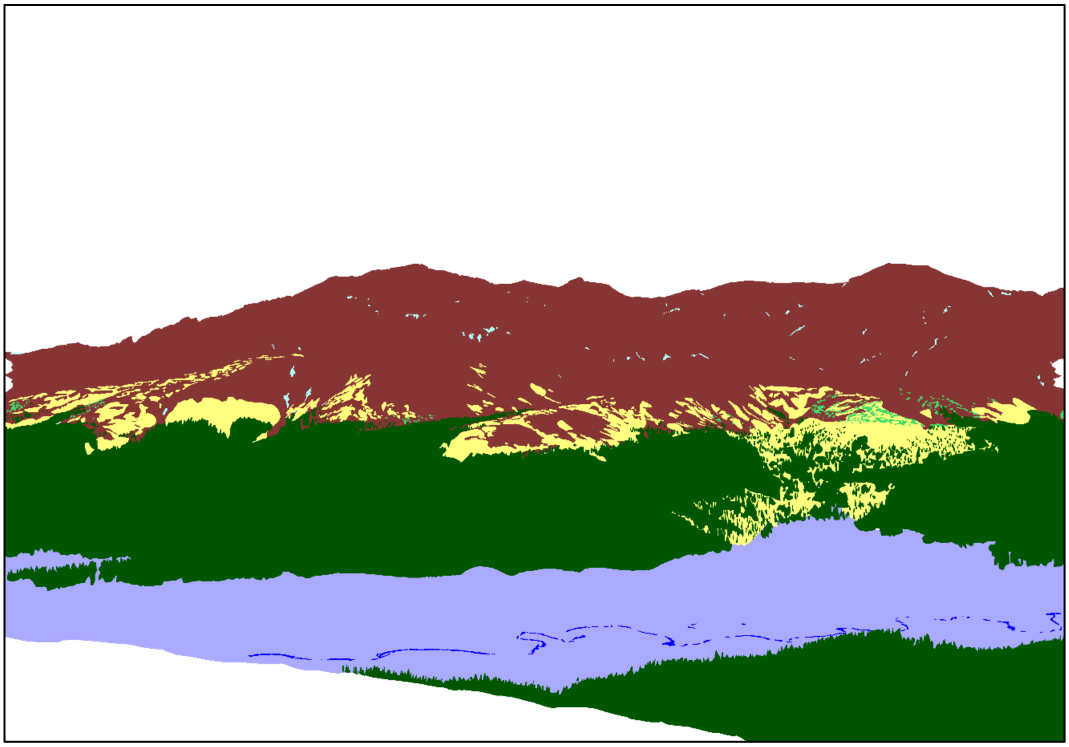

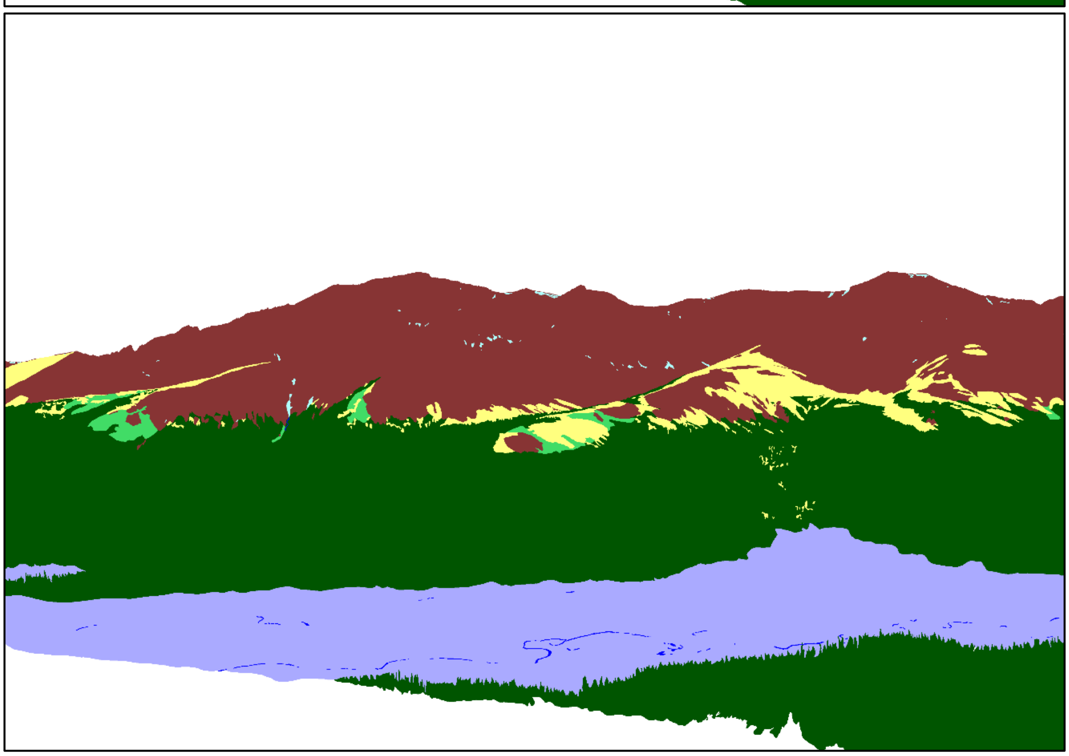

MIL5

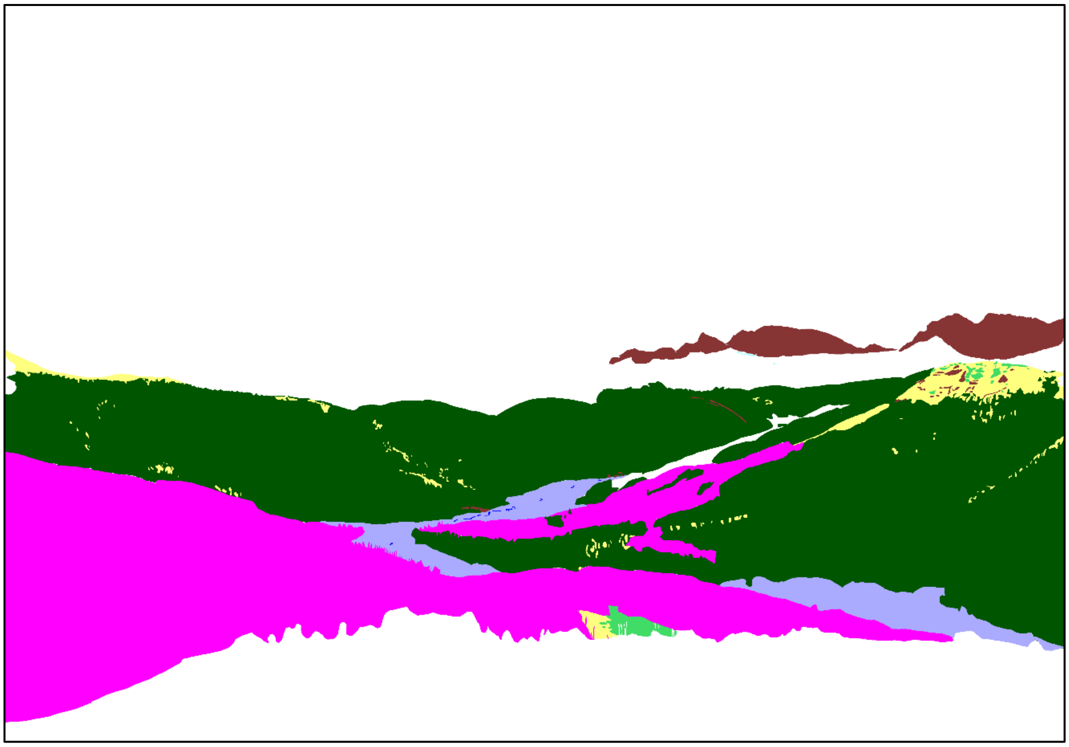

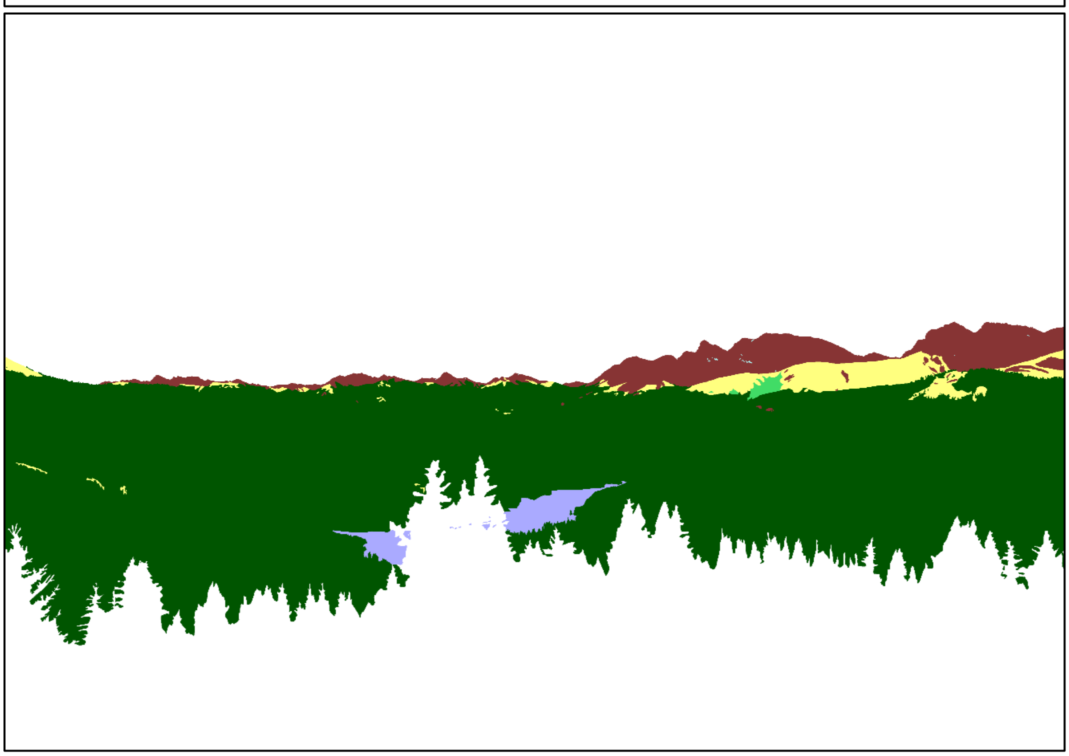

MIL6

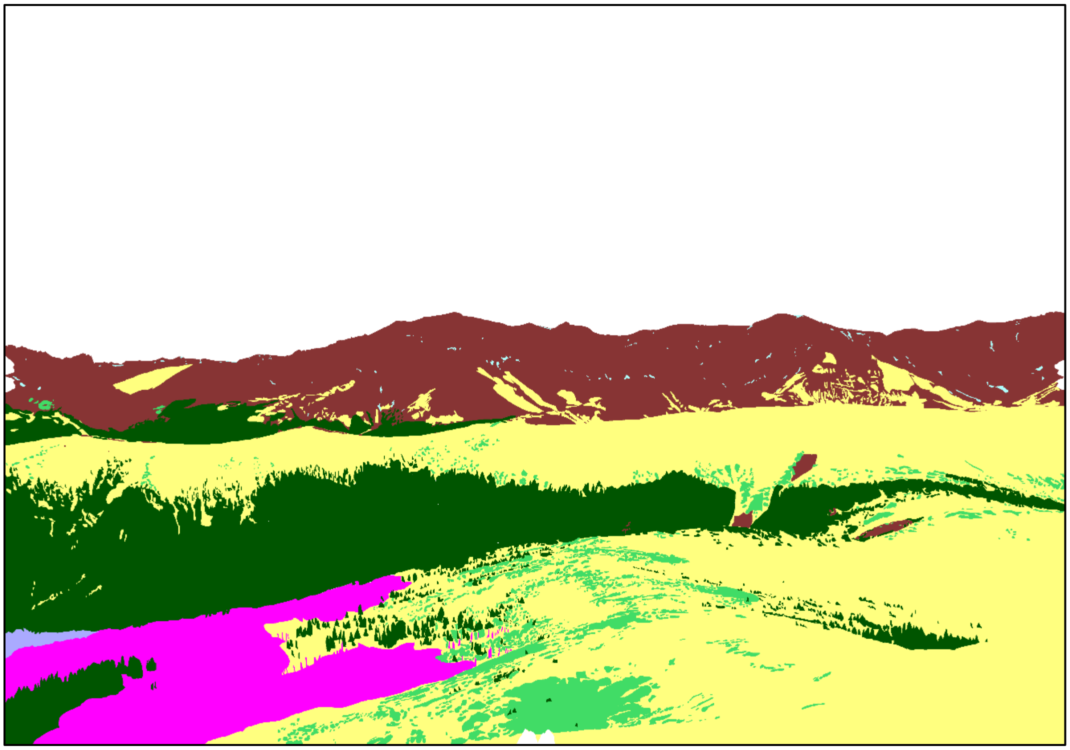

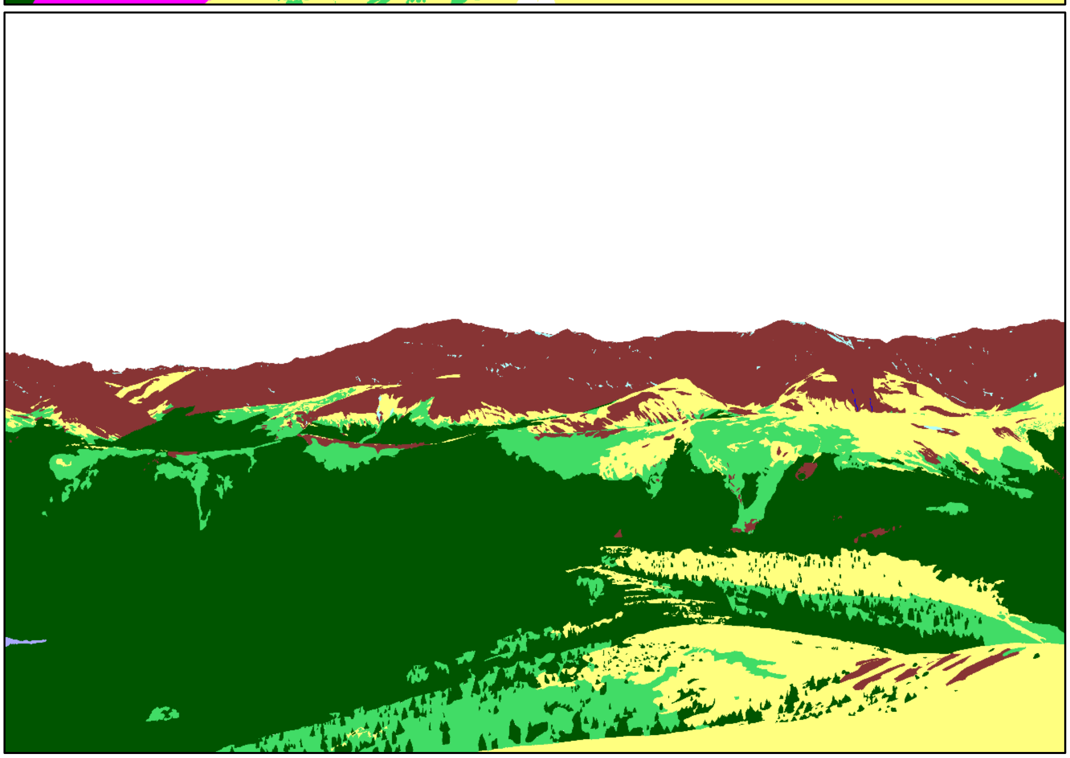

MIL7

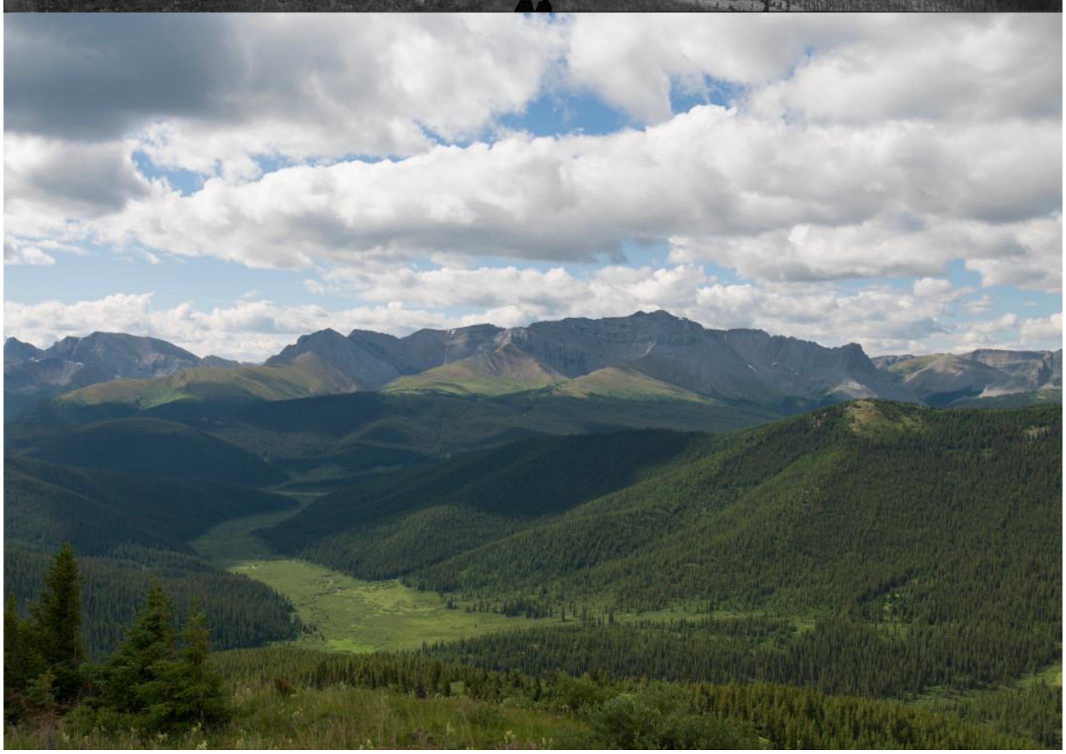

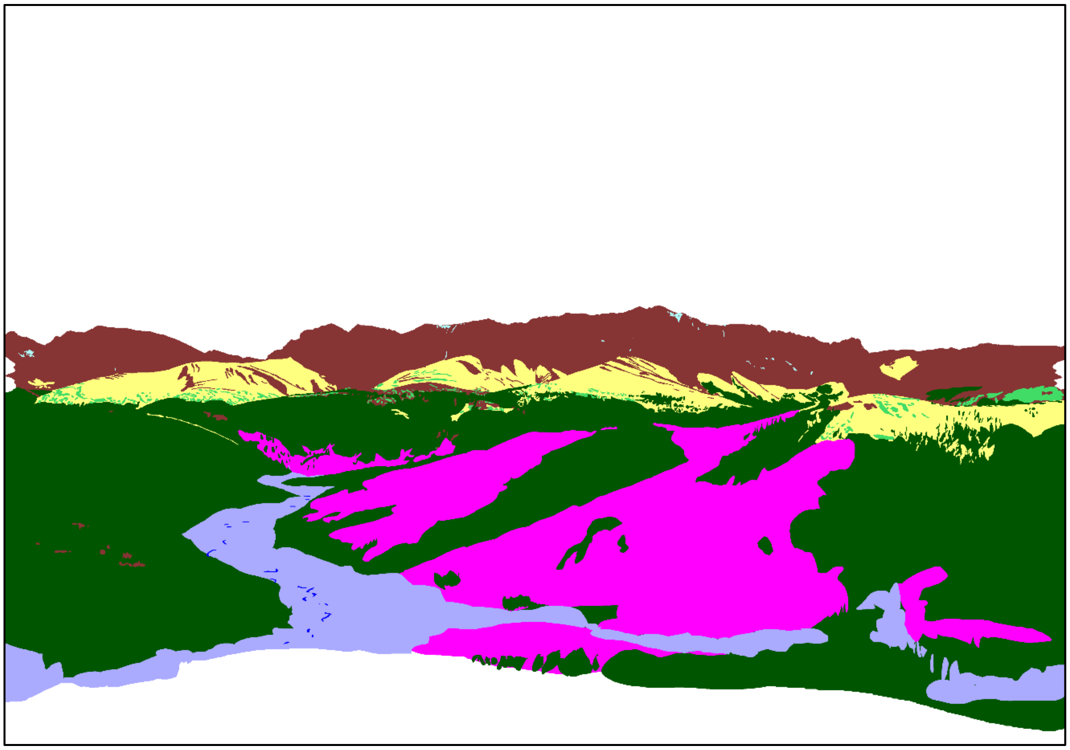

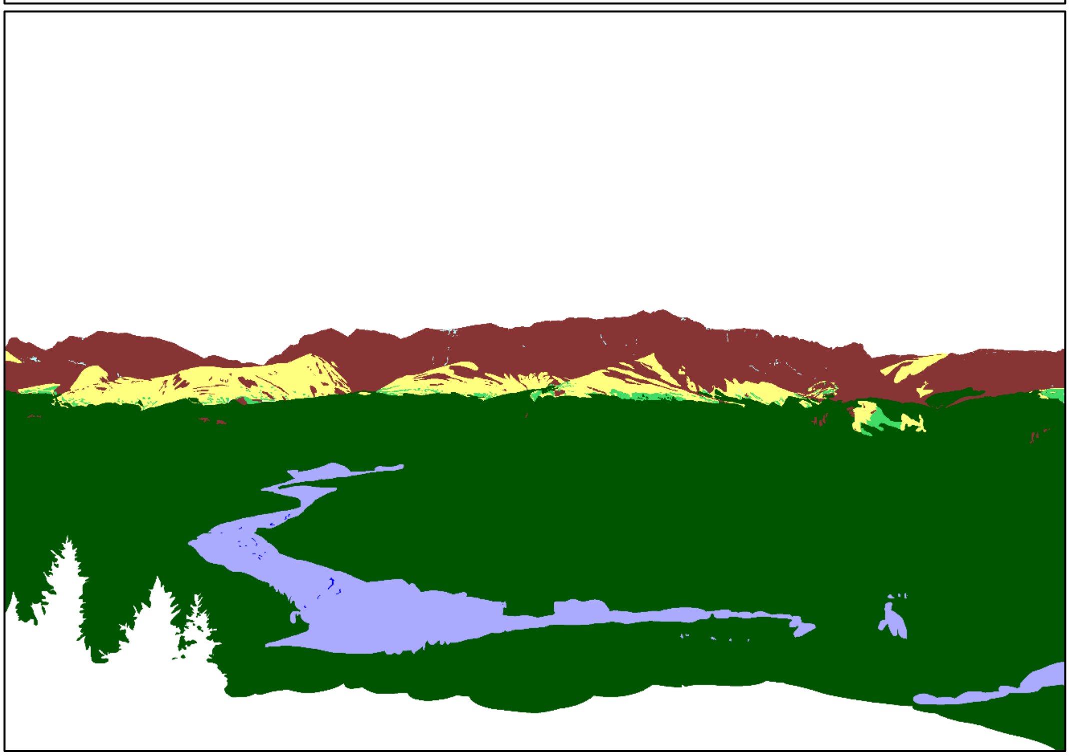

MIL8

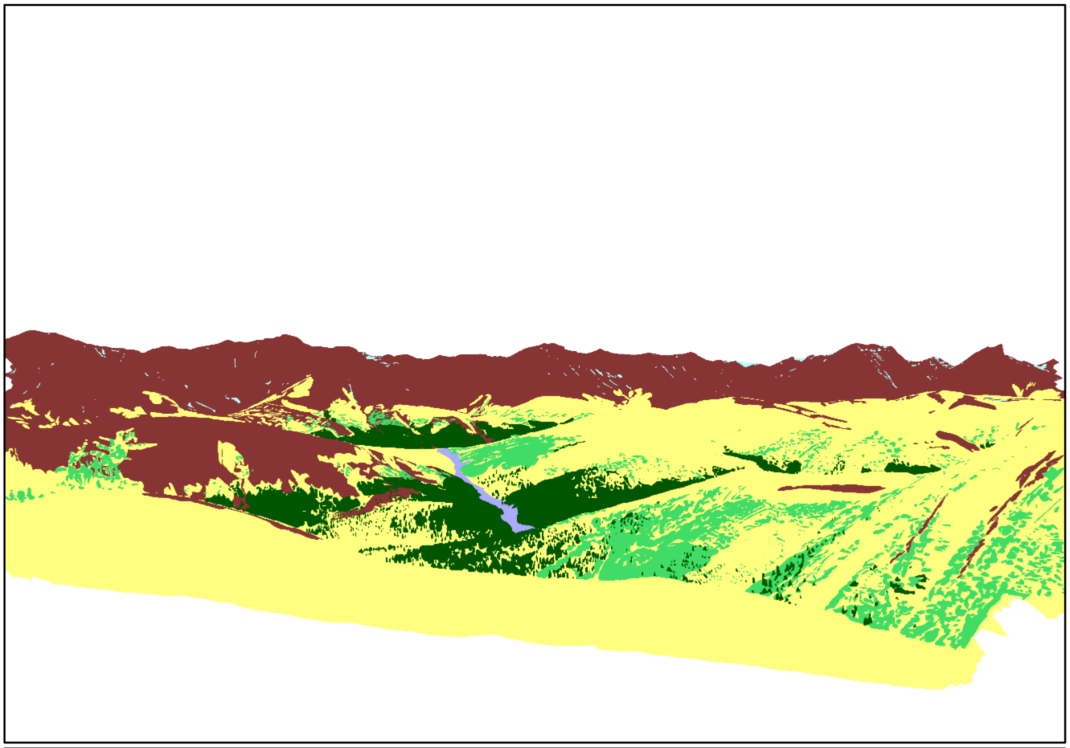

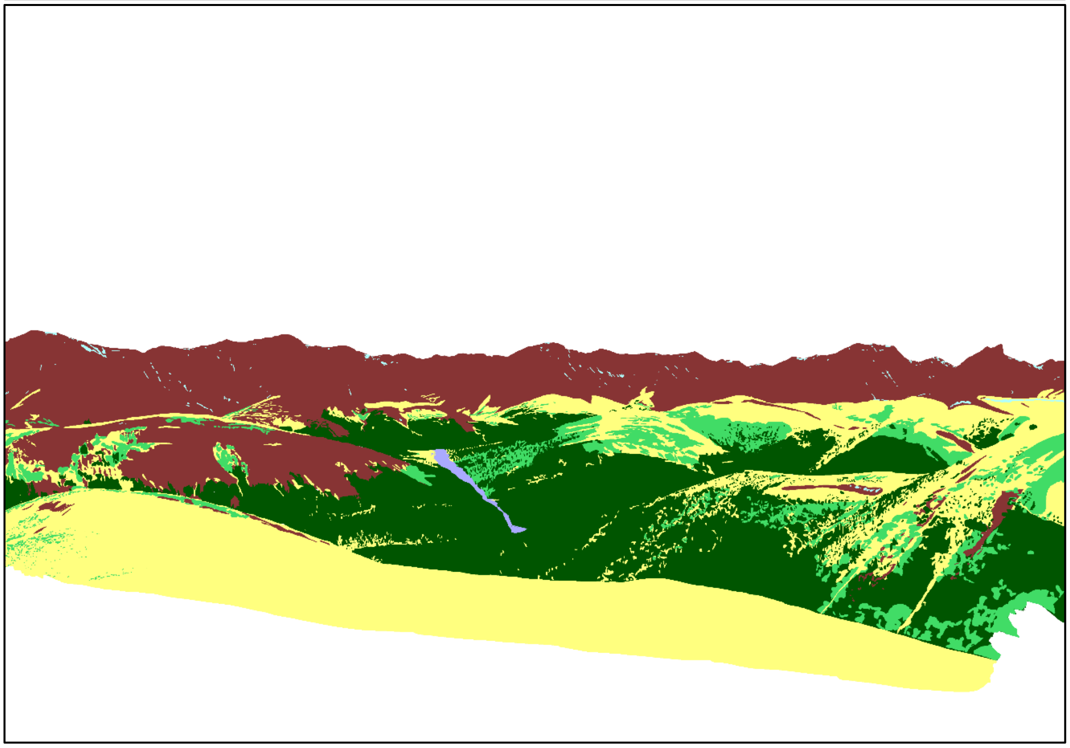

MIL9

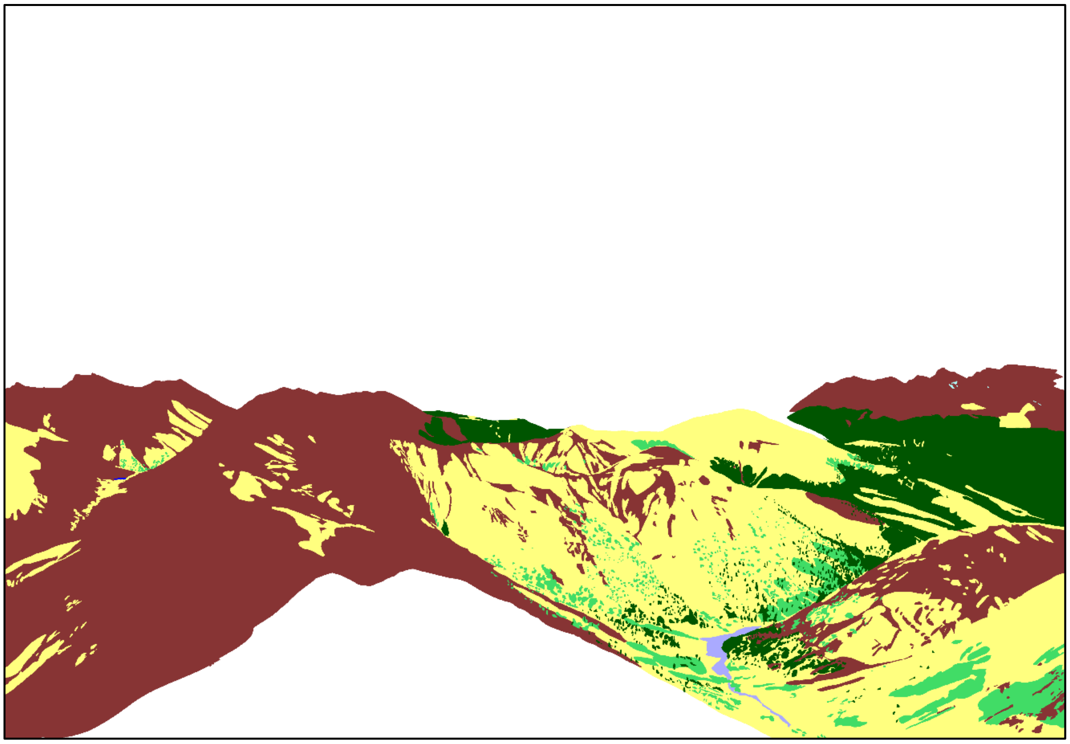

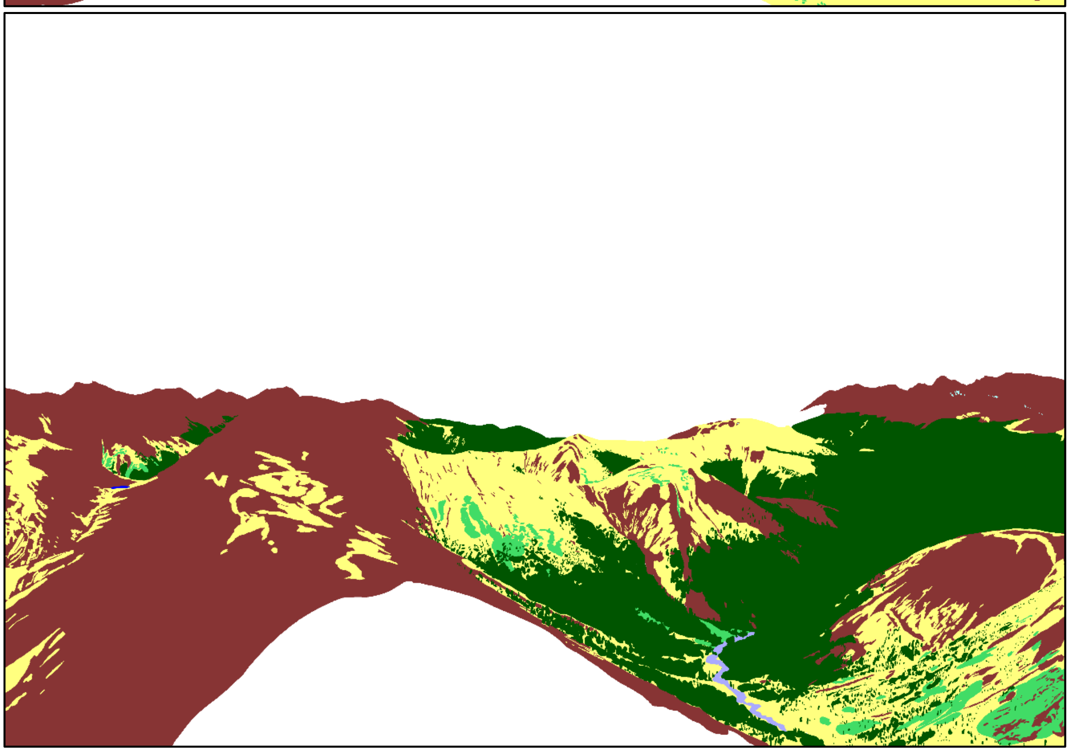

MIL10

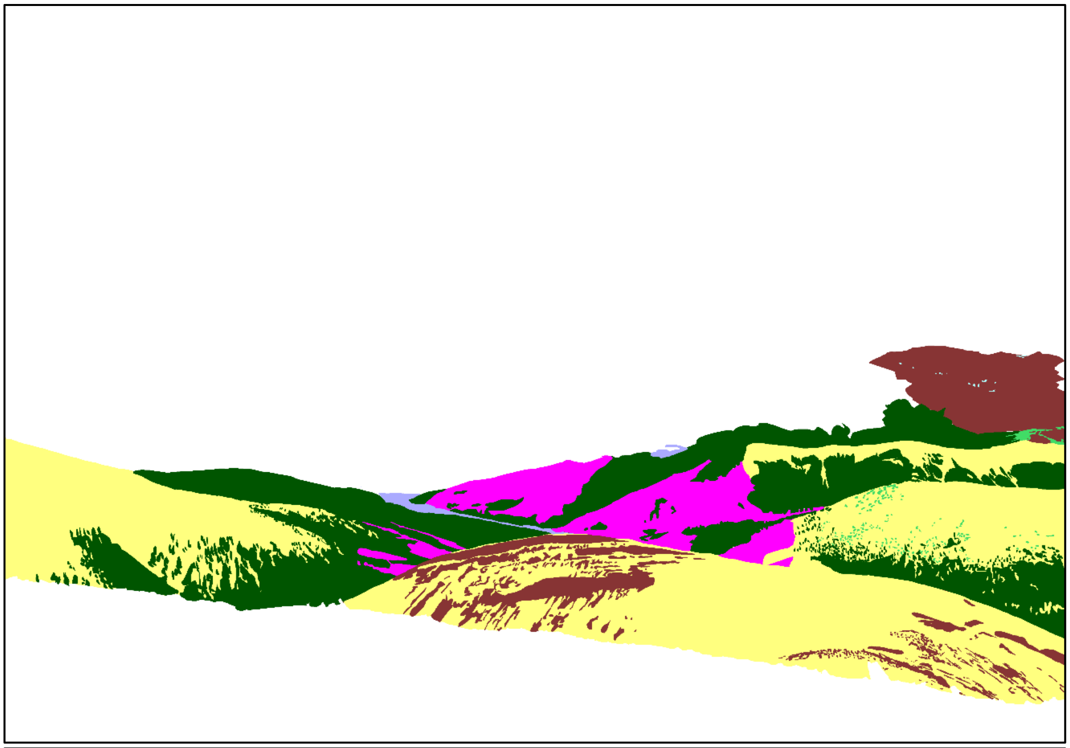

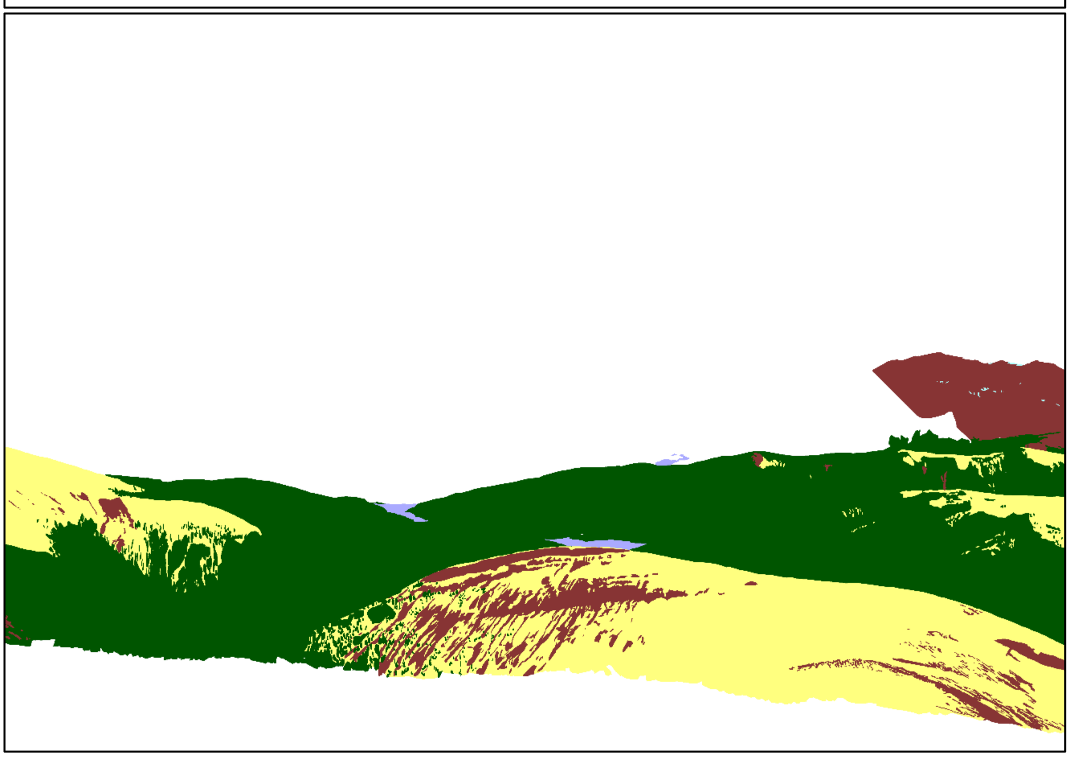

MIL11

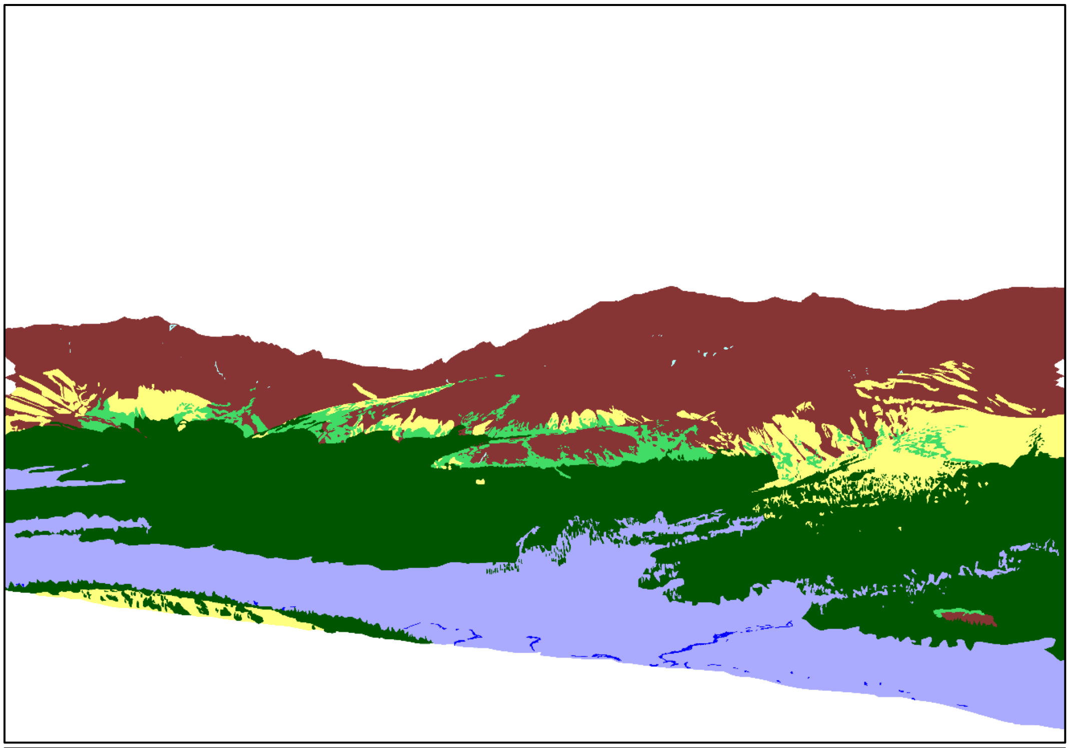

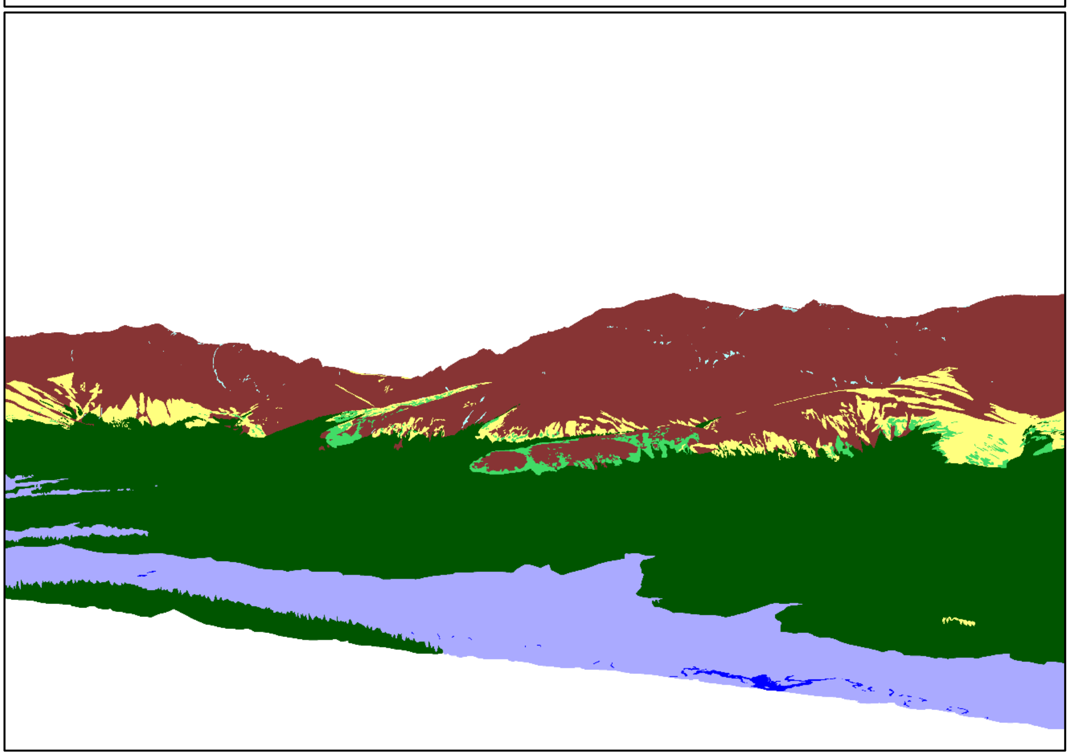

MIL13

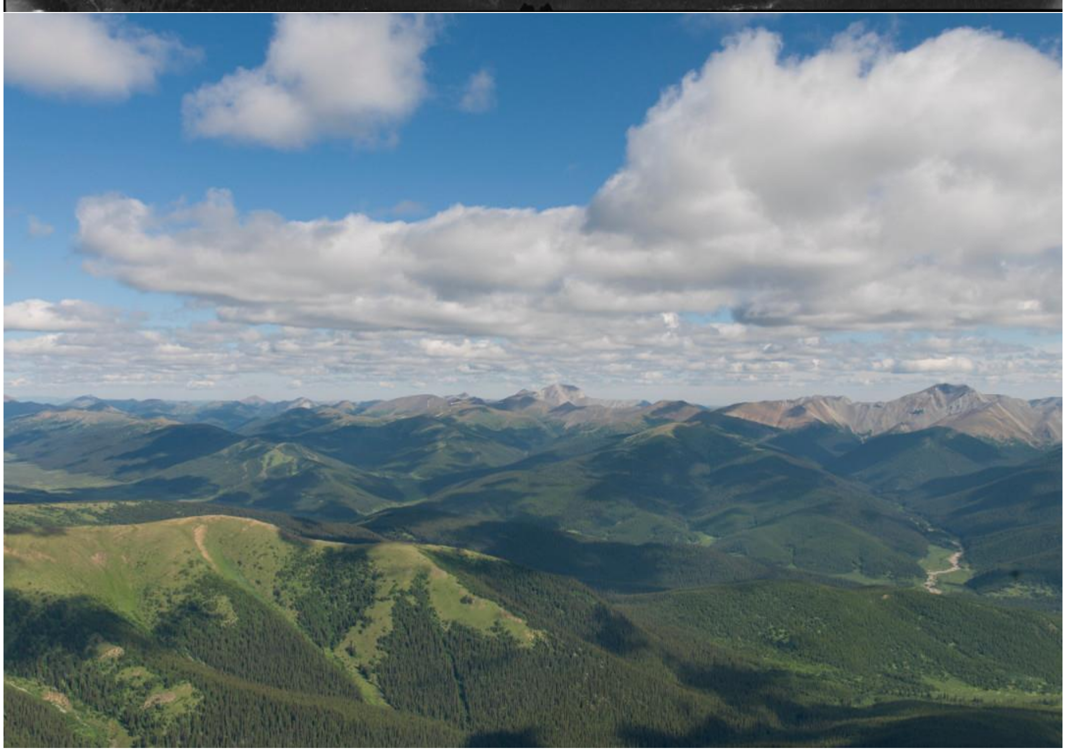

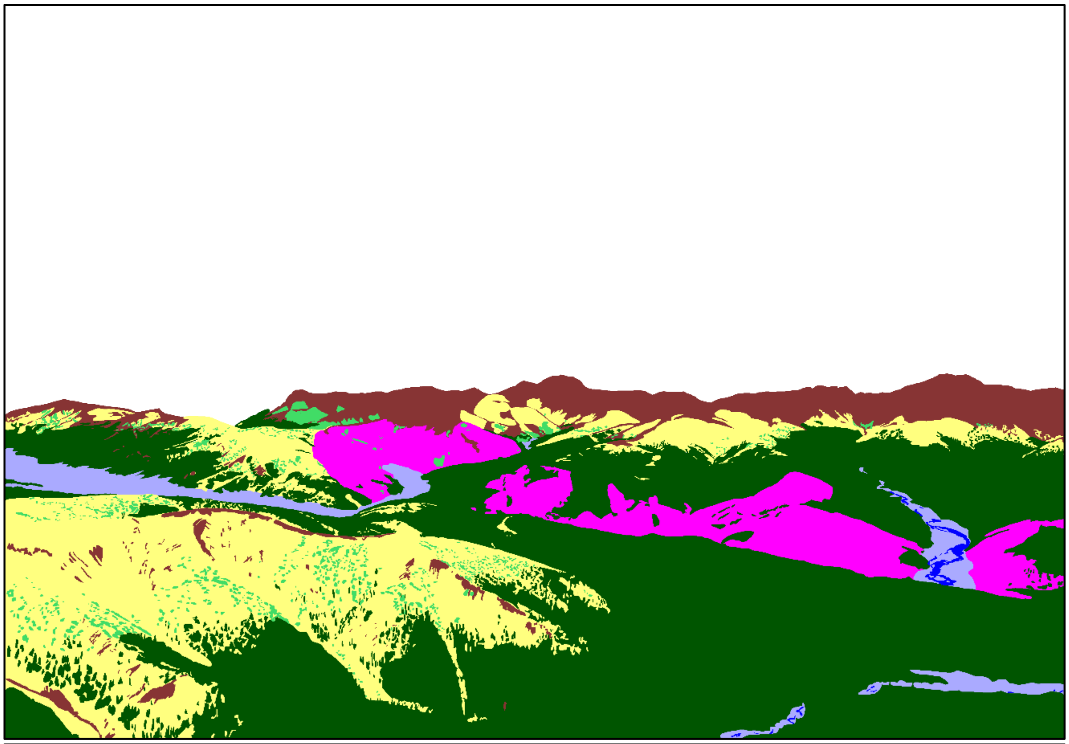

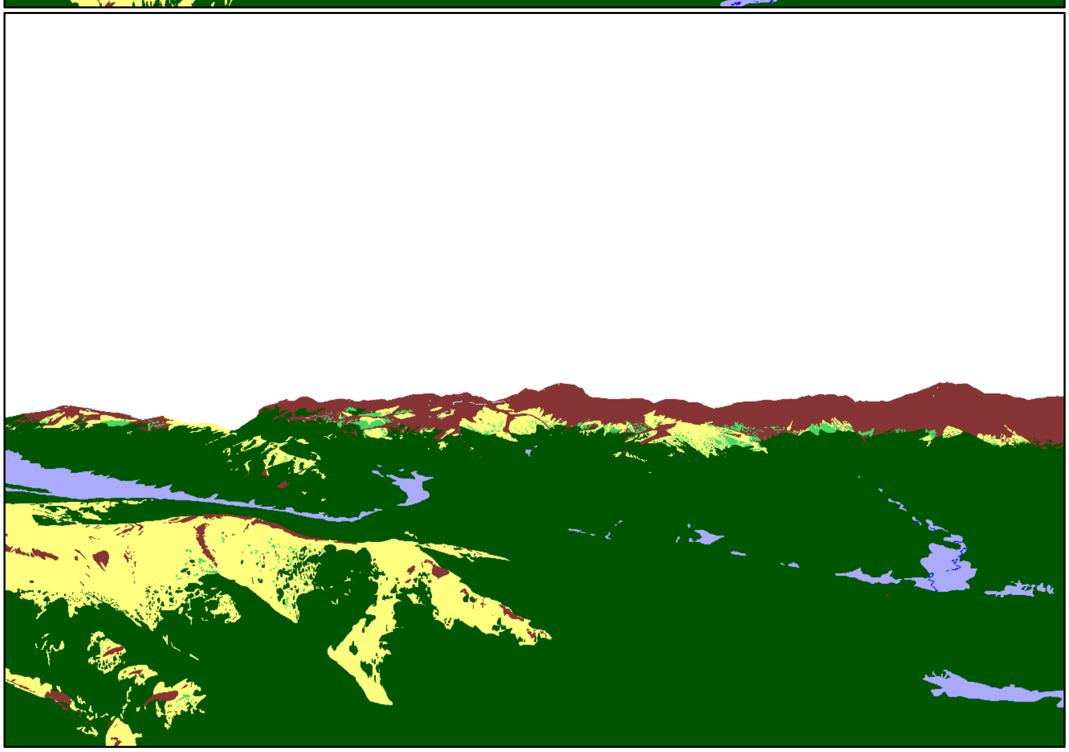

MIL14

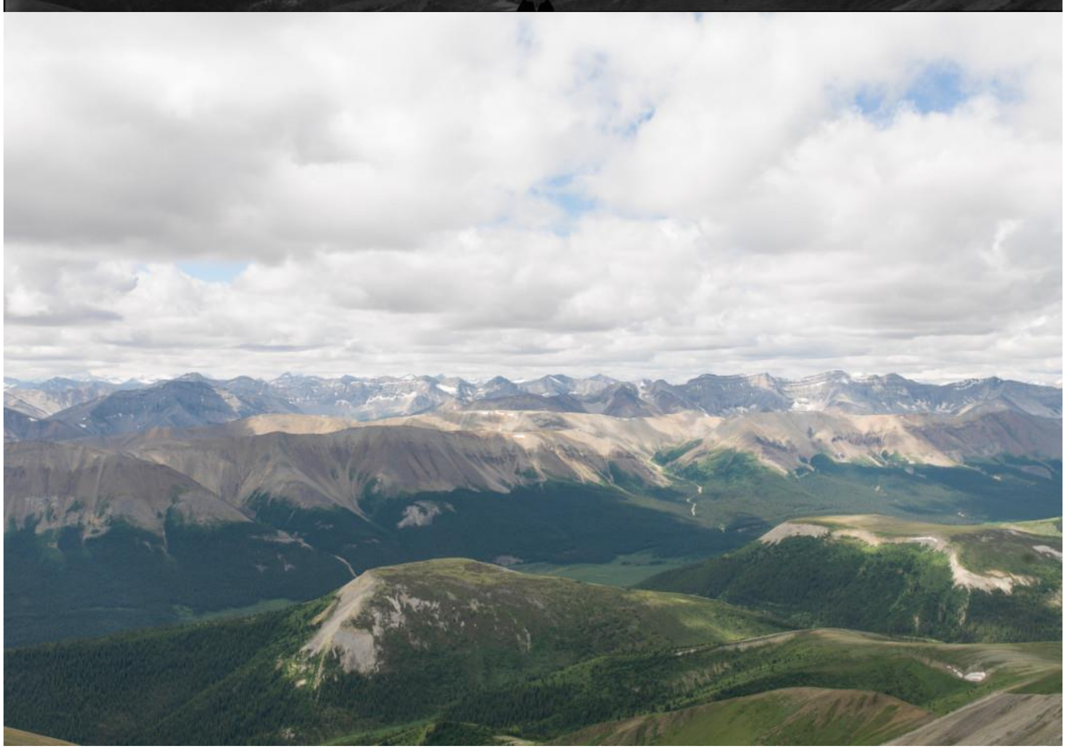

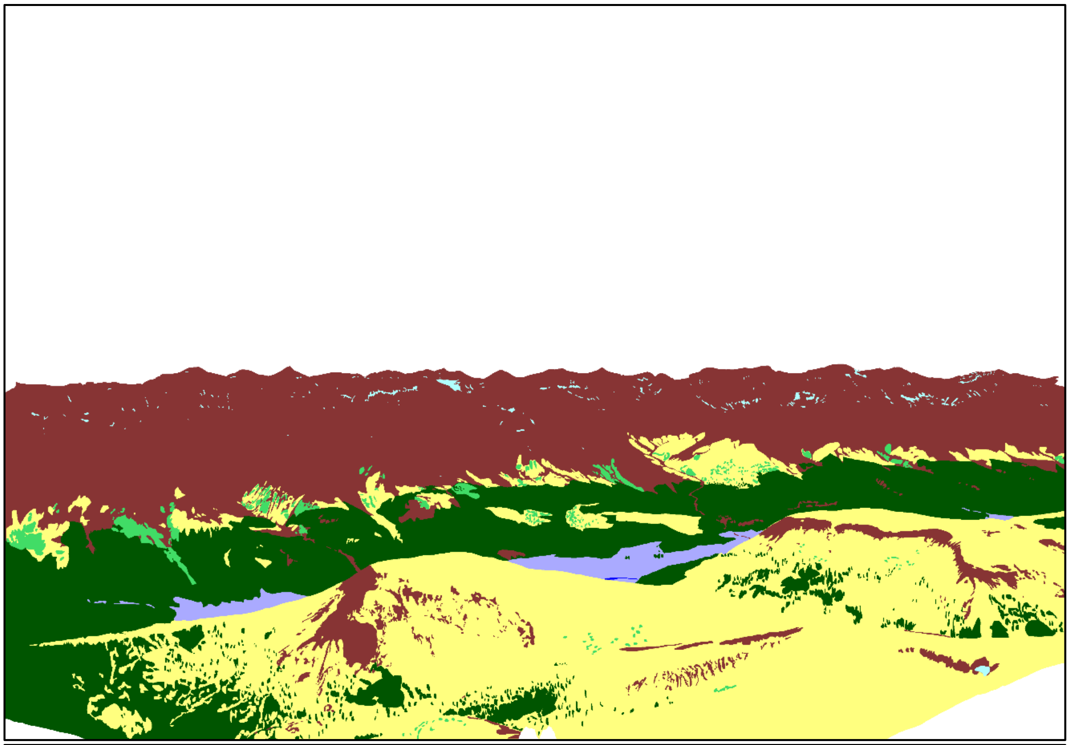

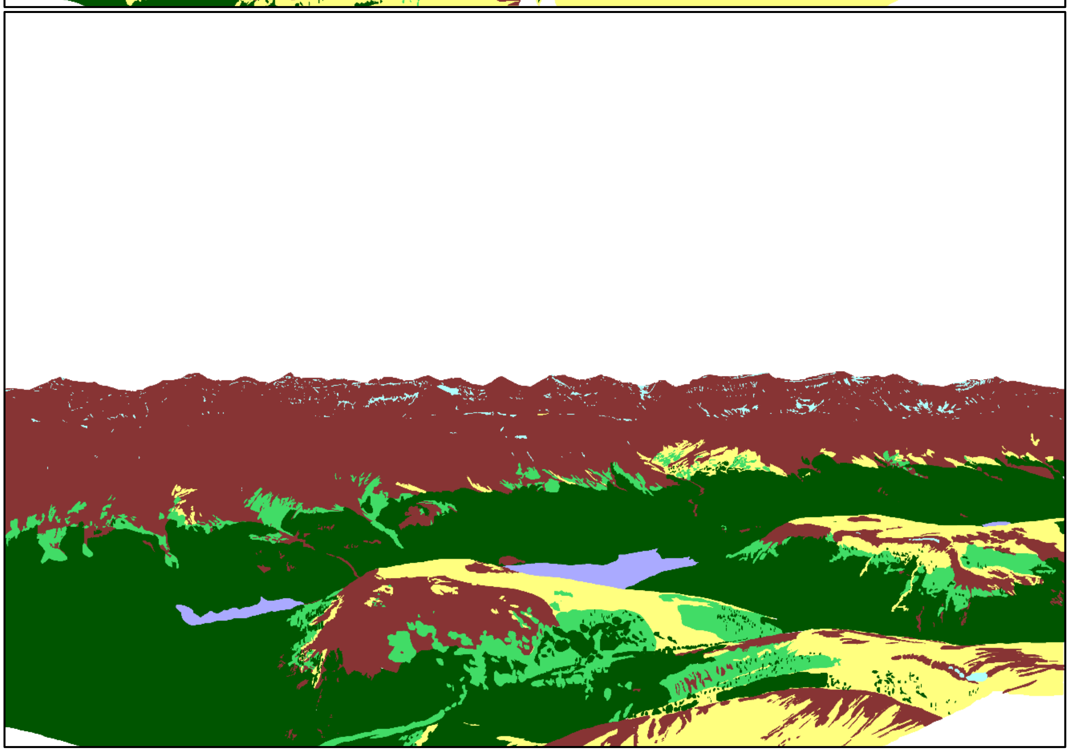

MIL16

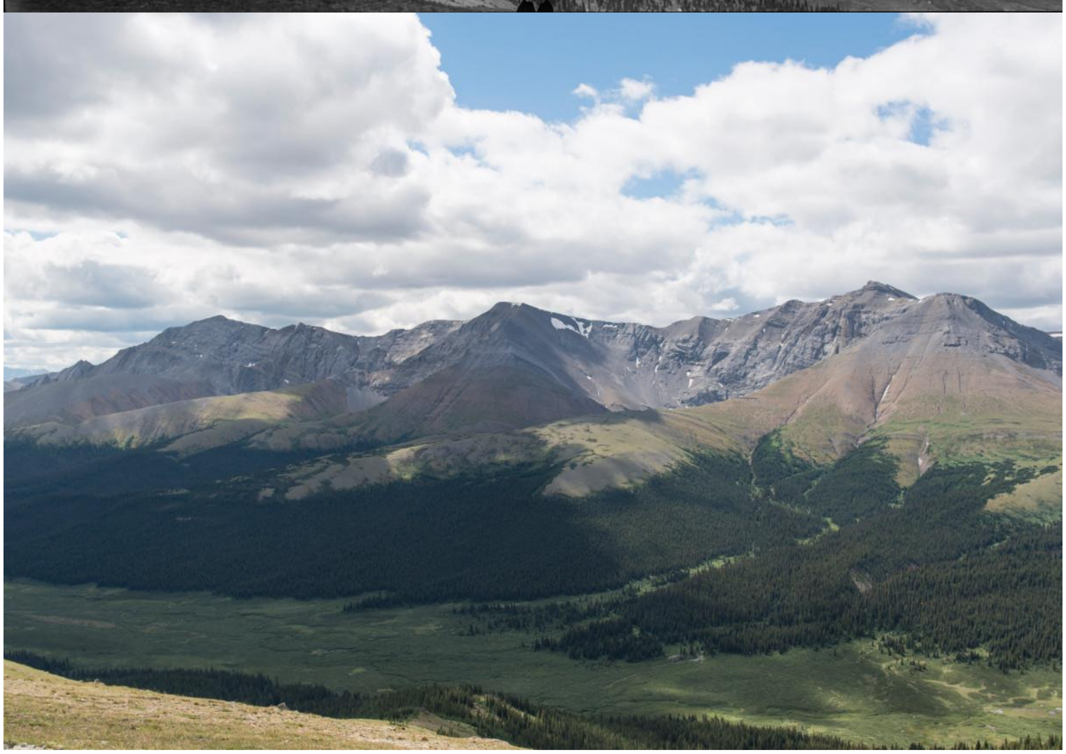

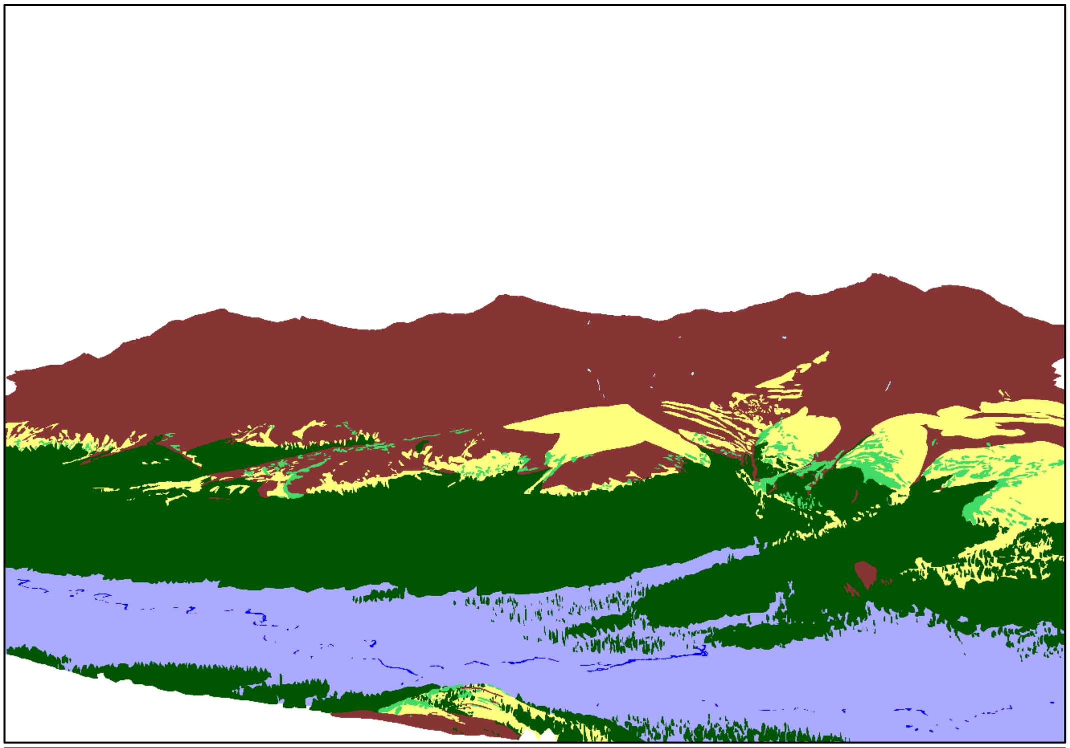

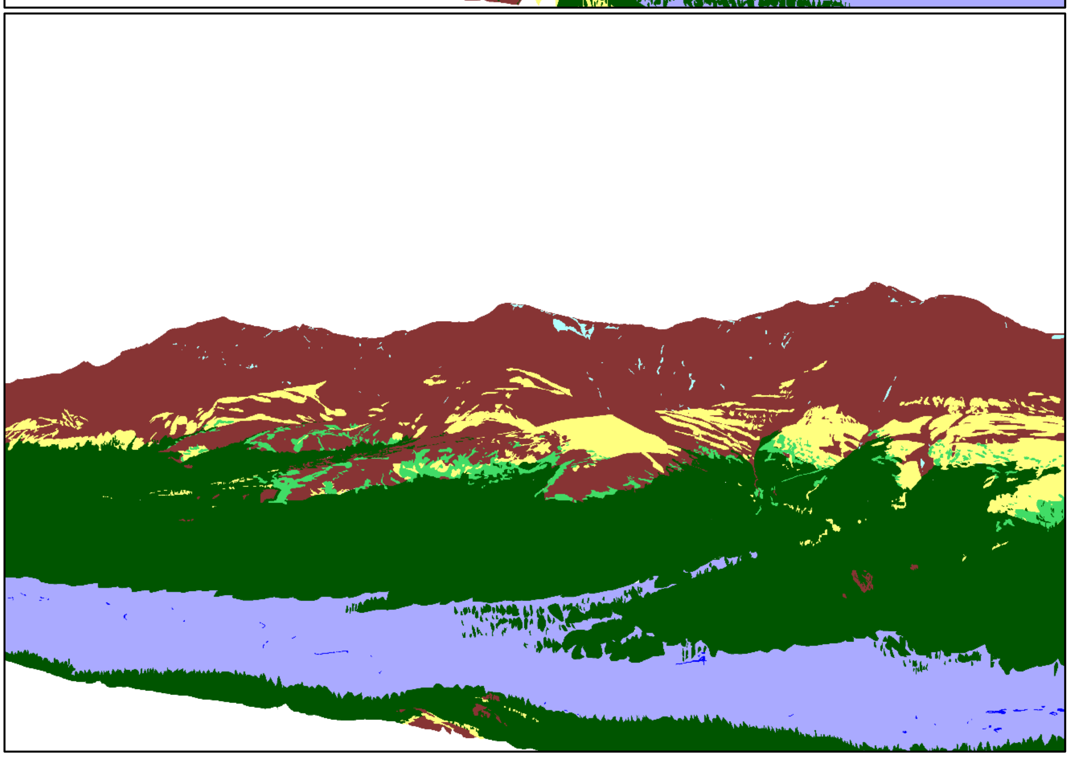

MIL18

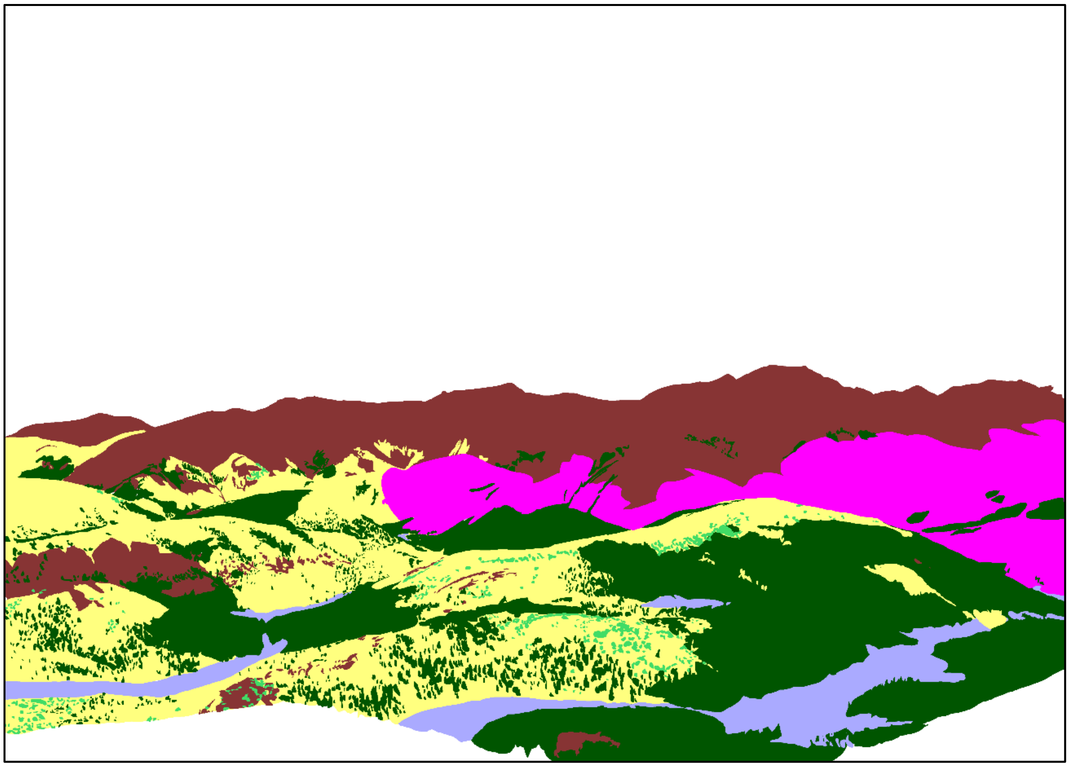

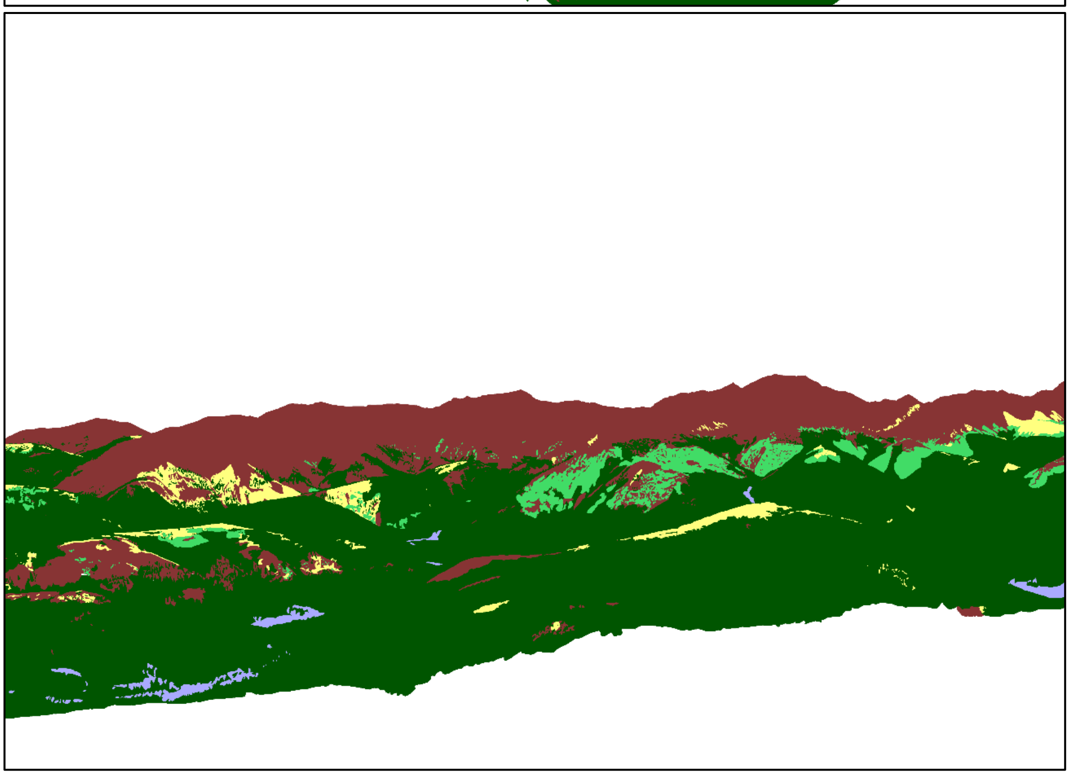

MIL19

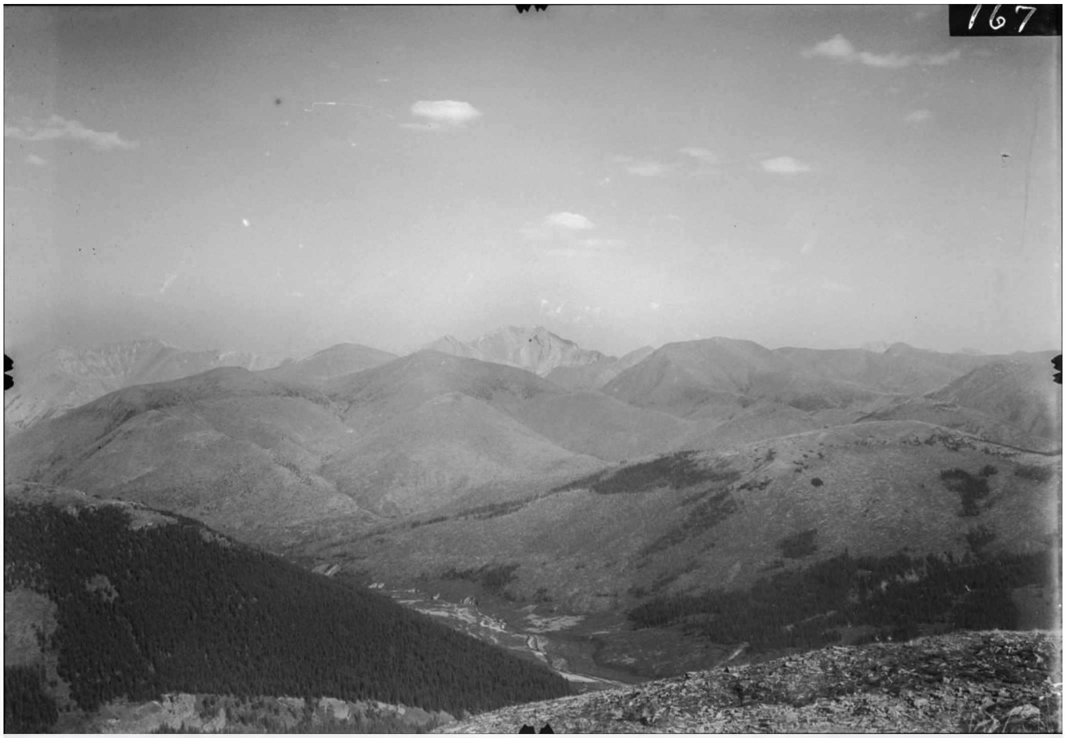

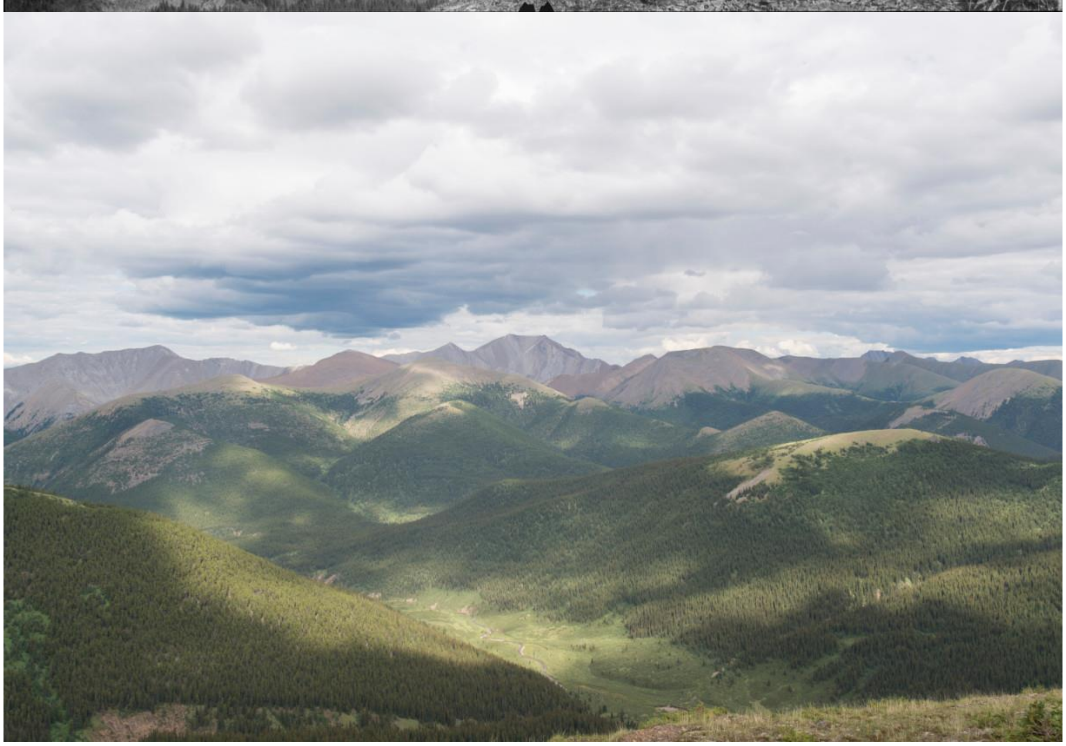

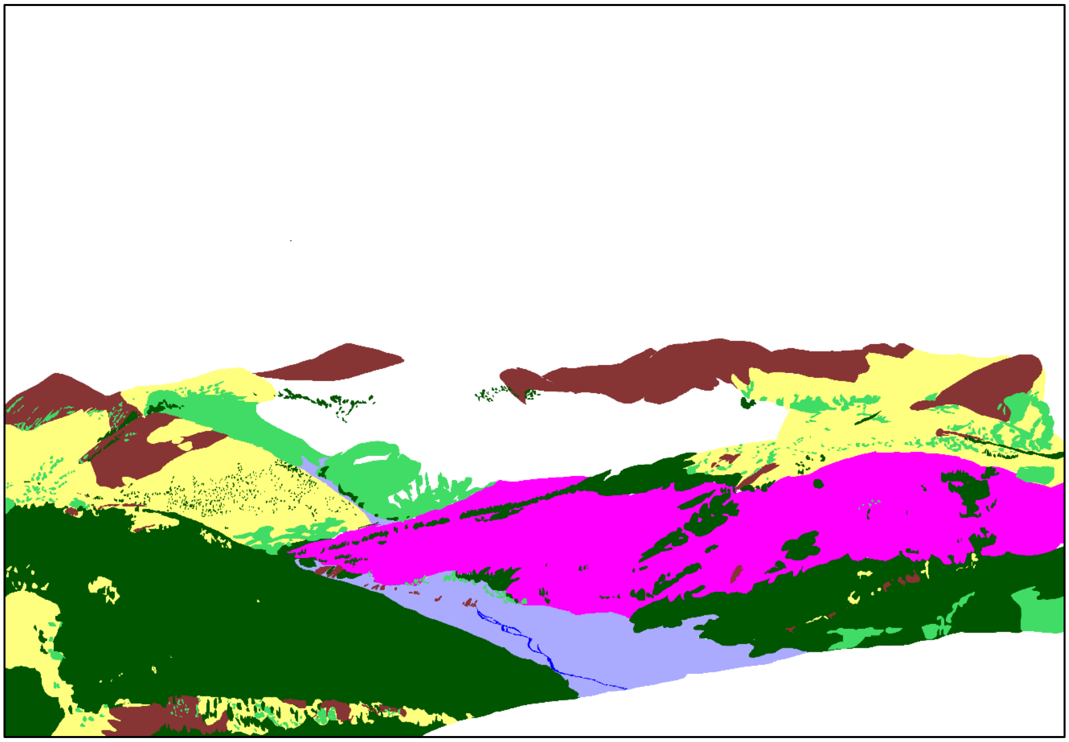

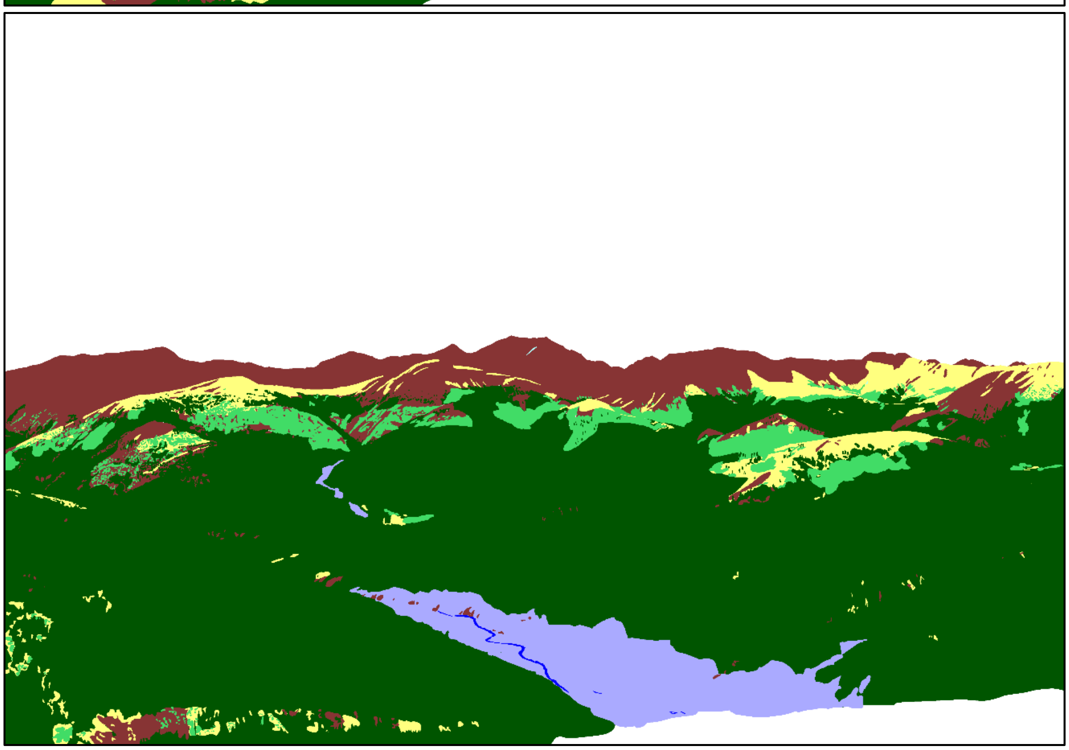

MIL20

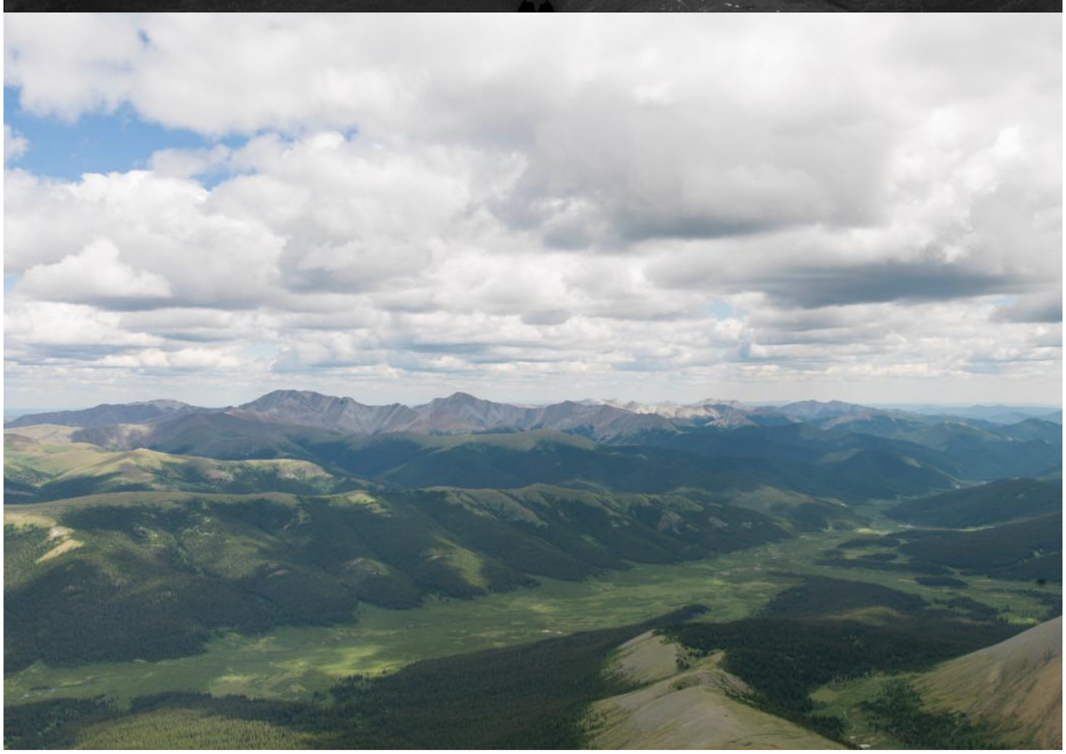

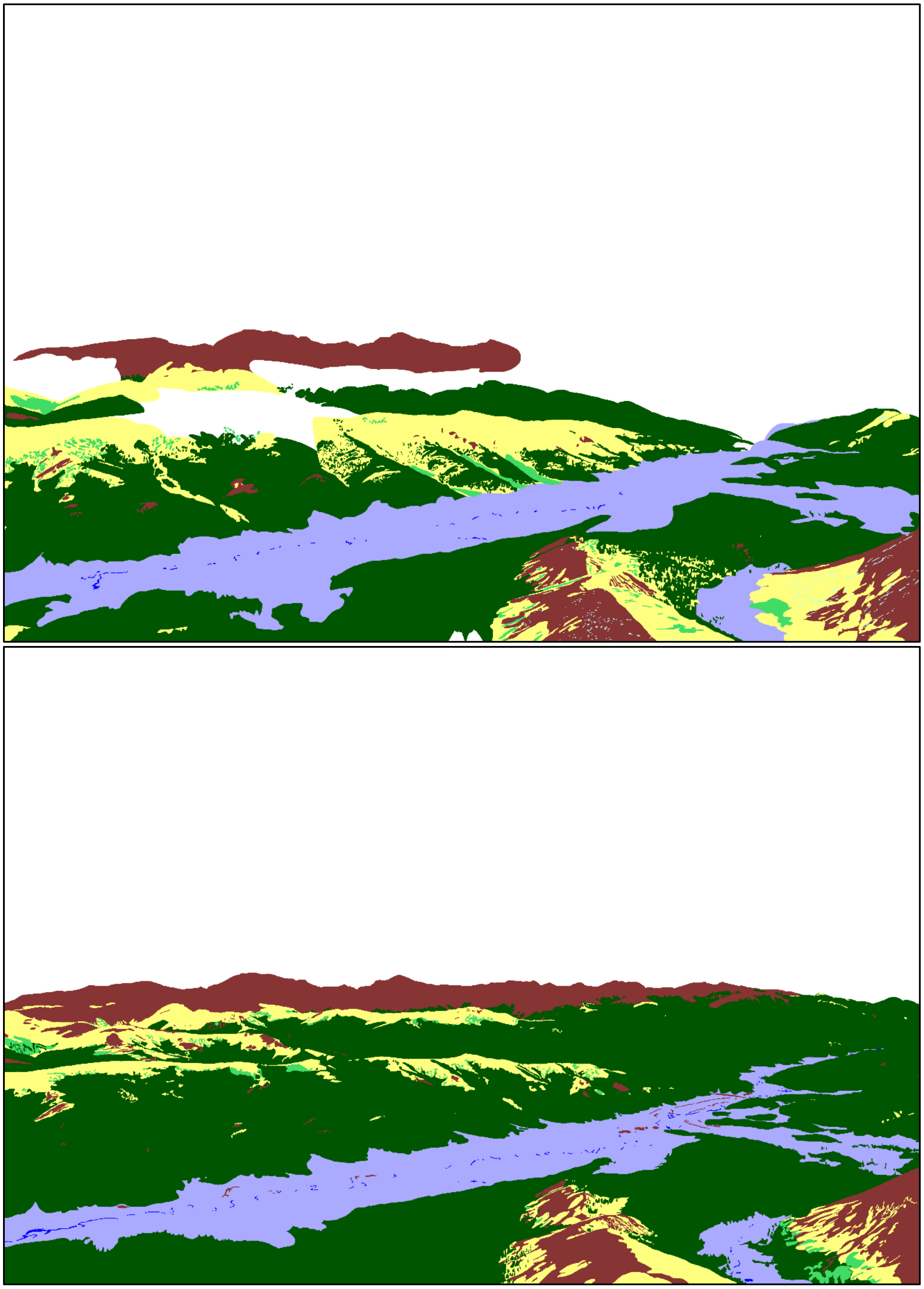

NID11

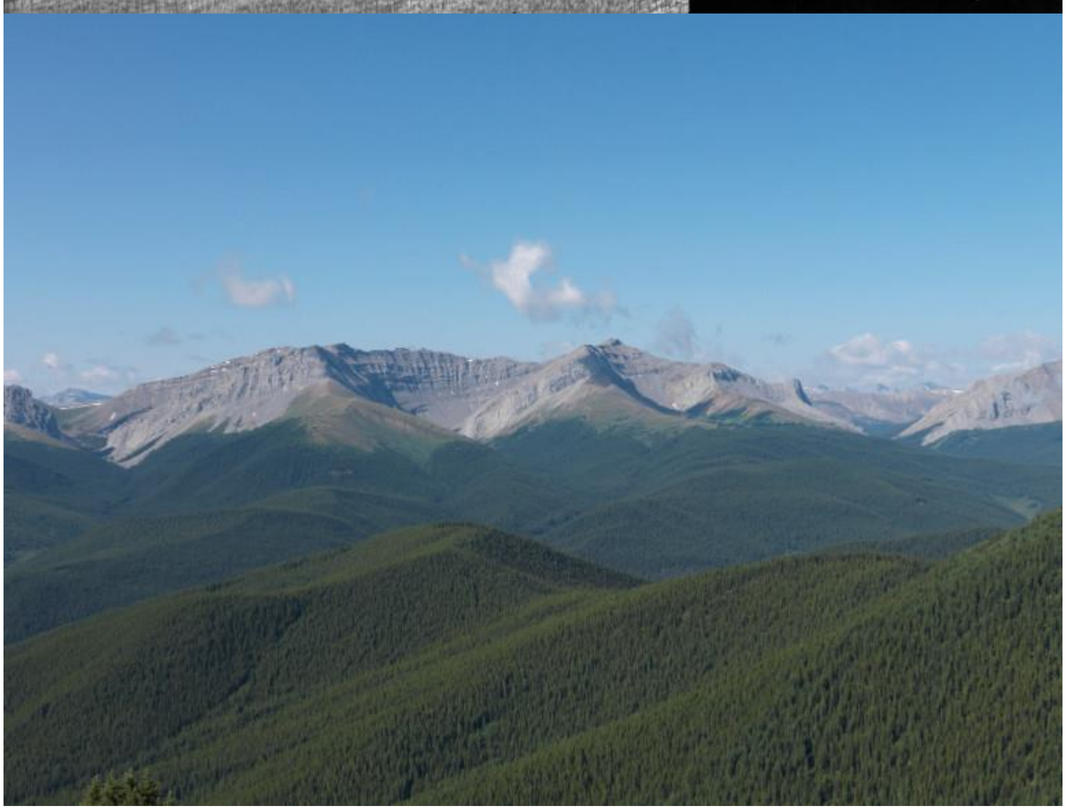

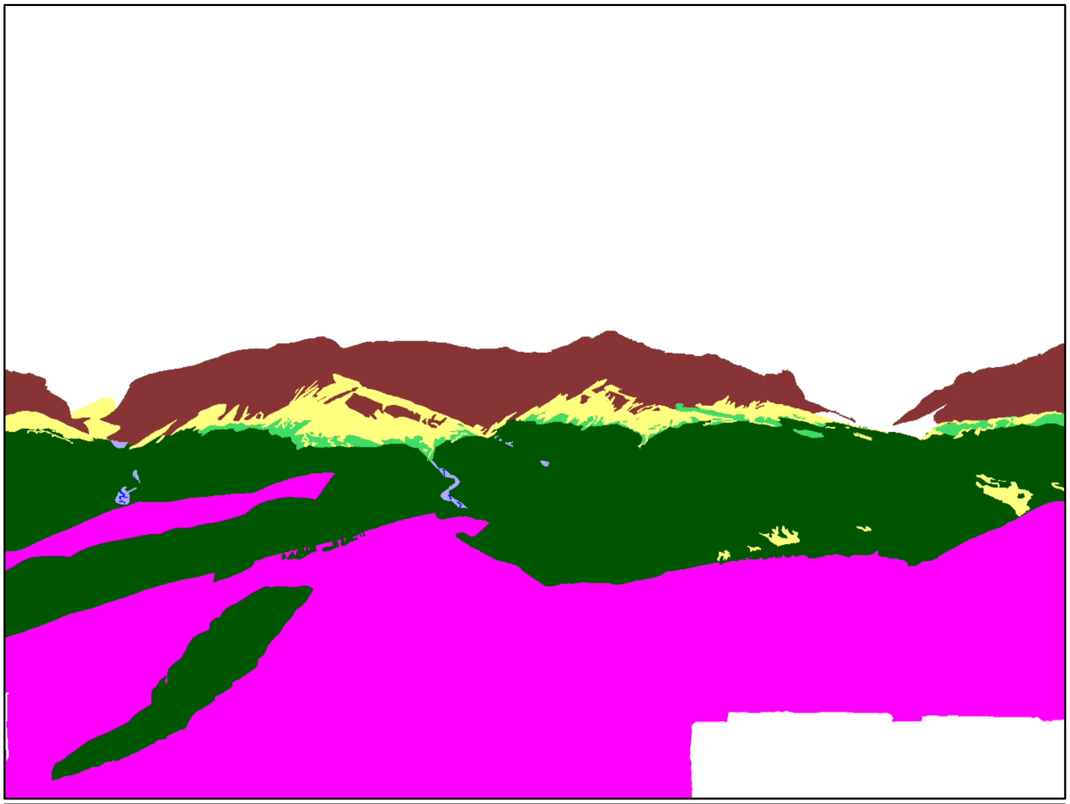

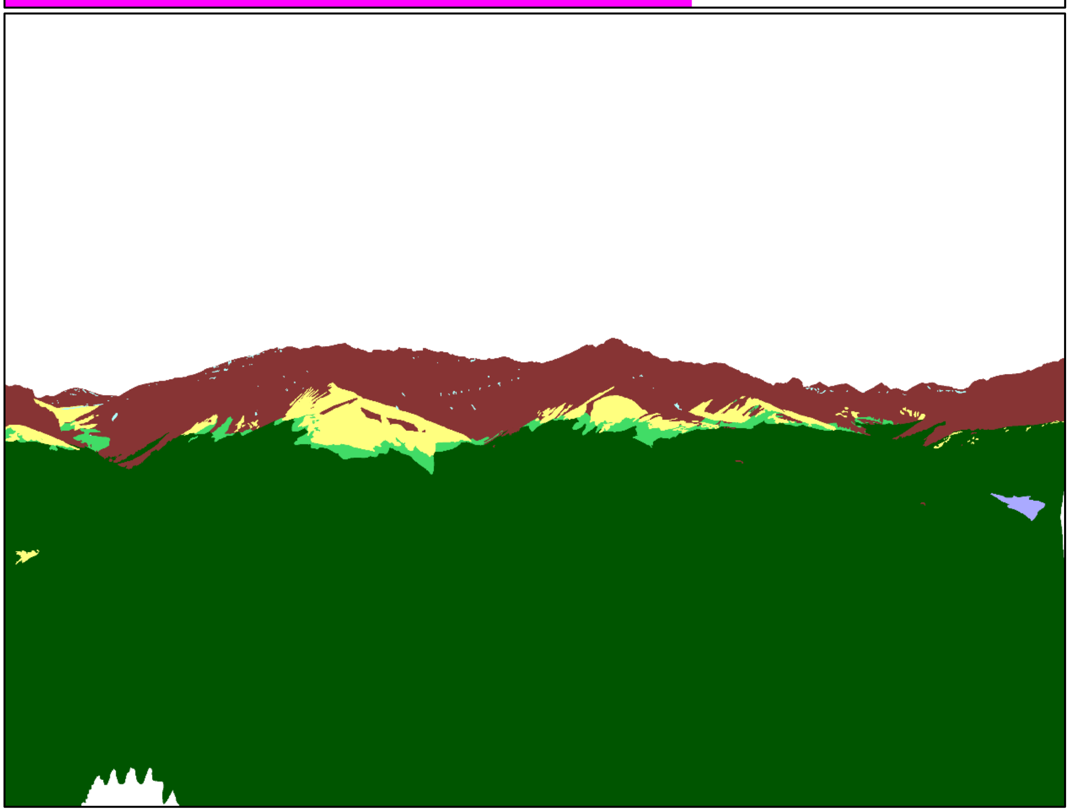

NID12

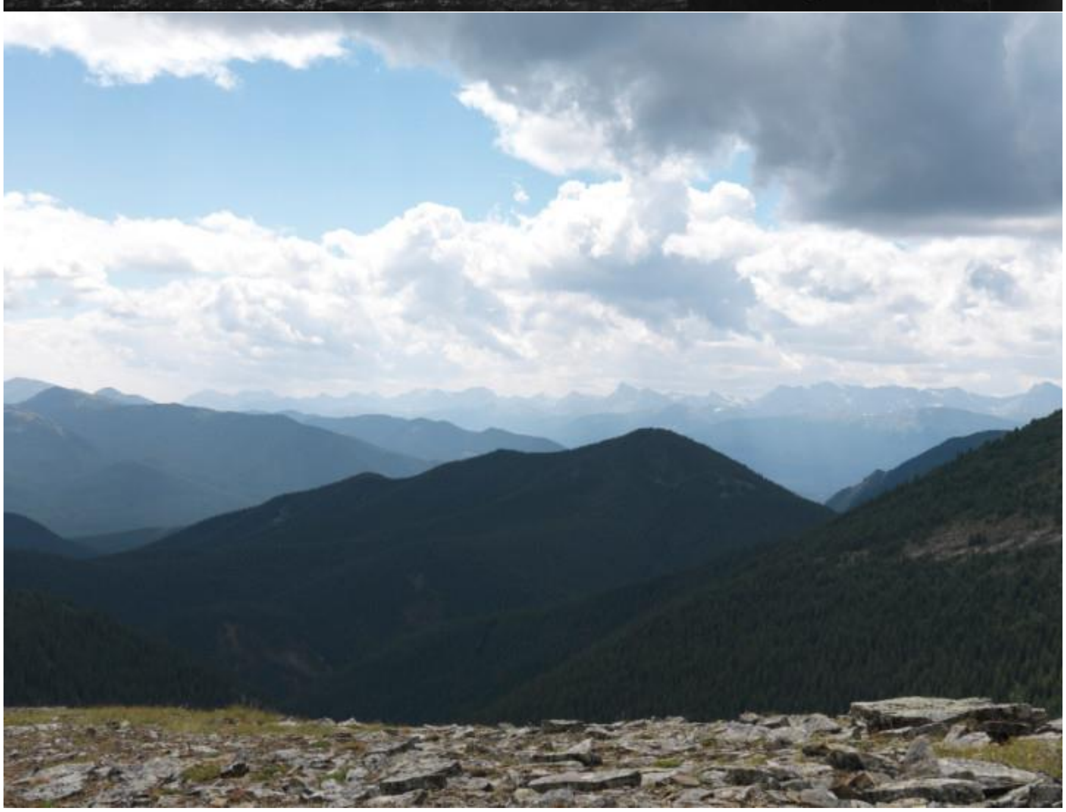

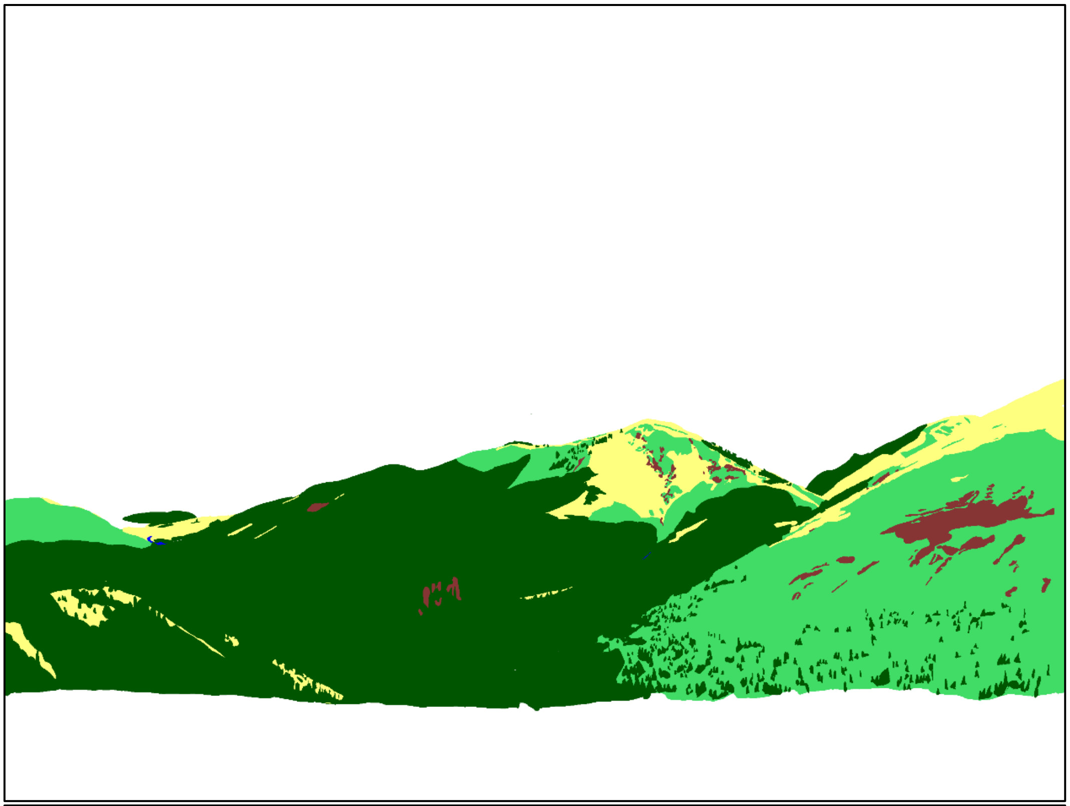

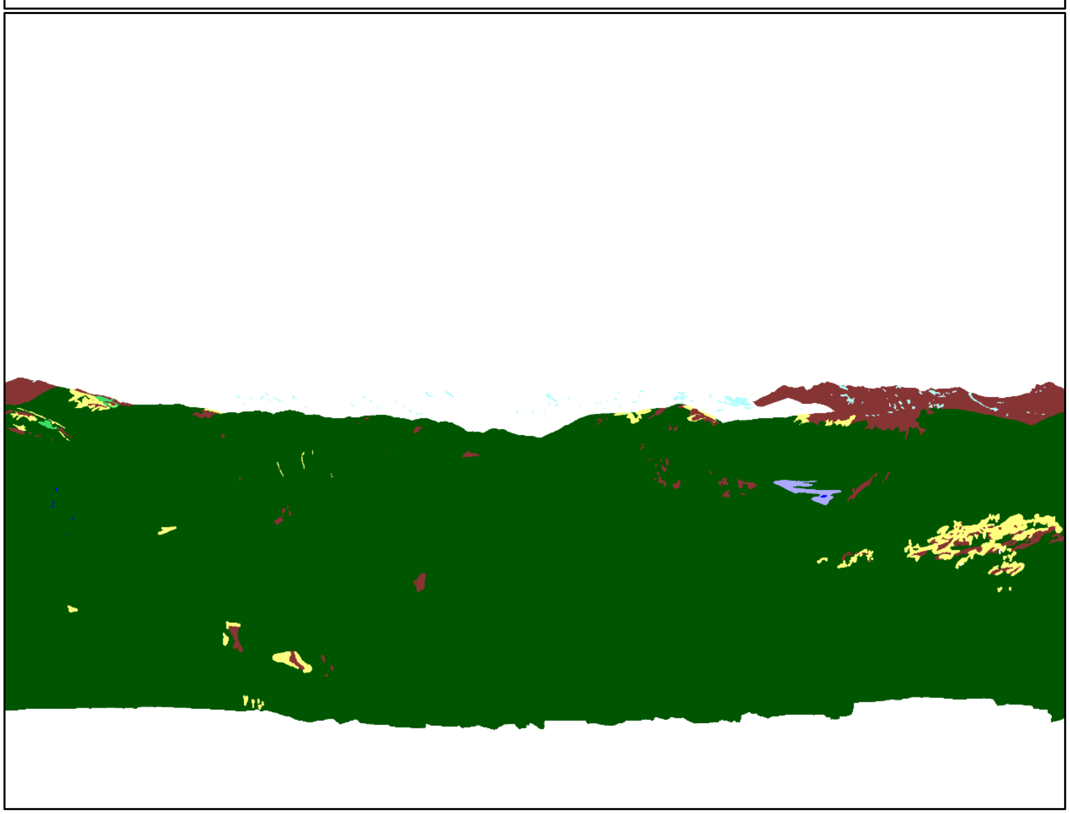

NID15

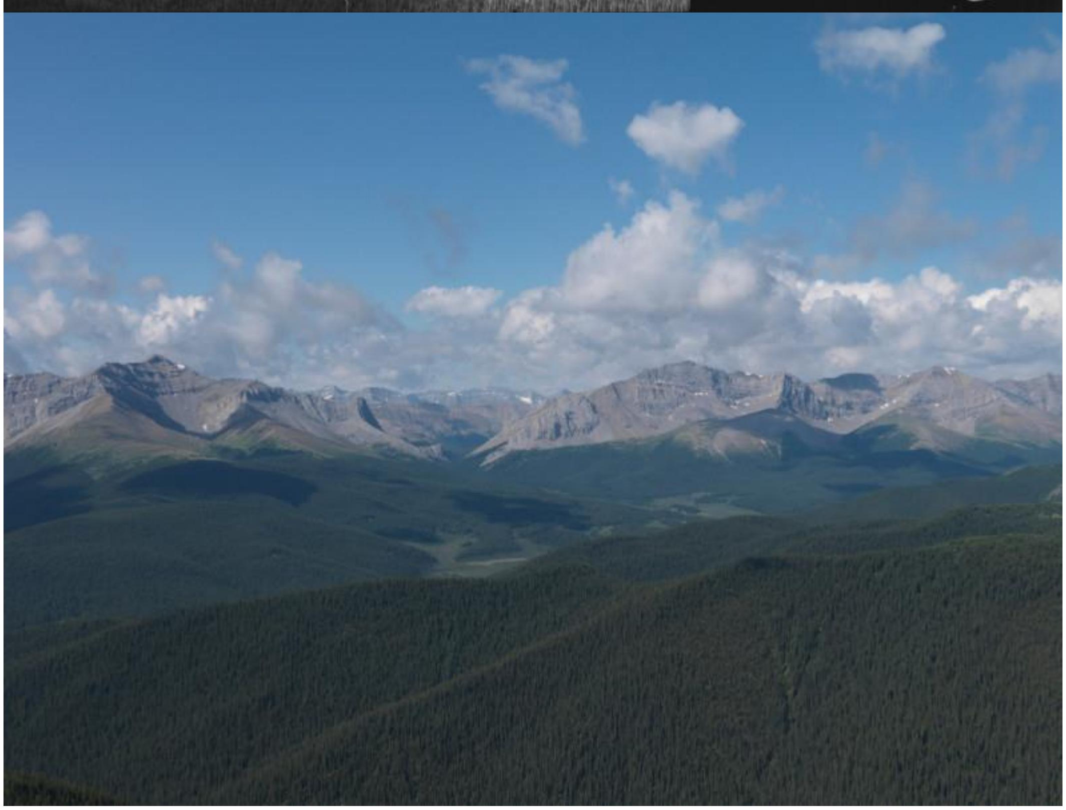

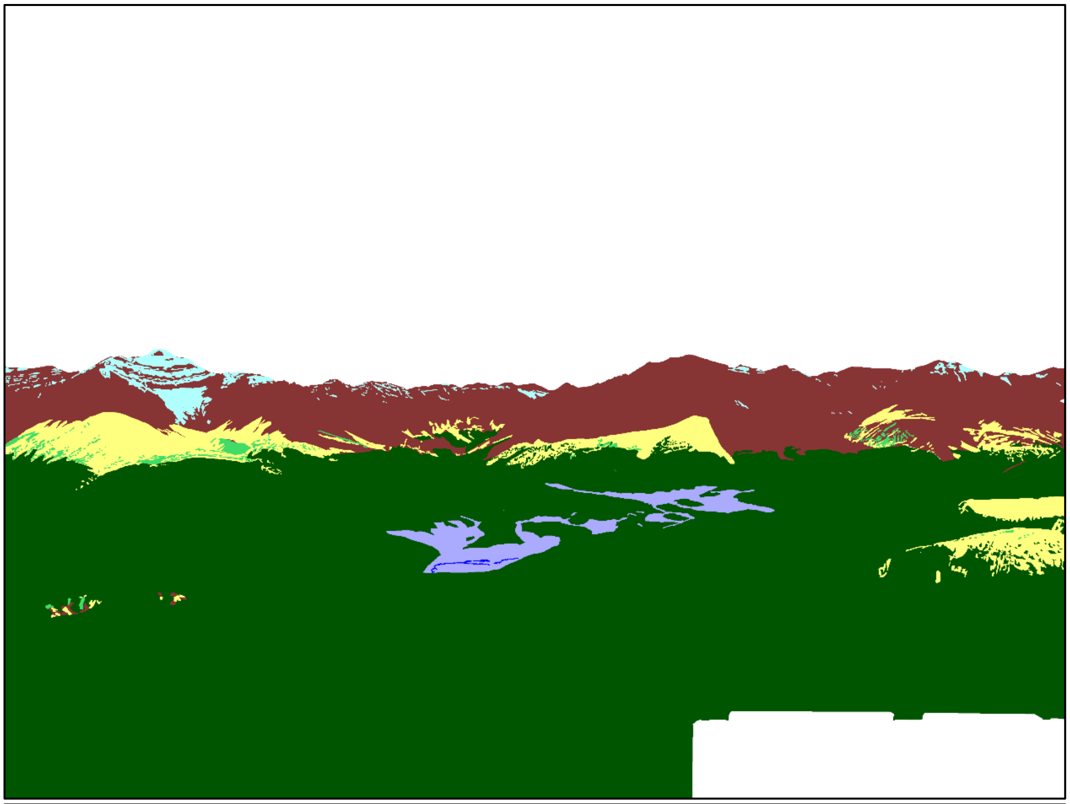

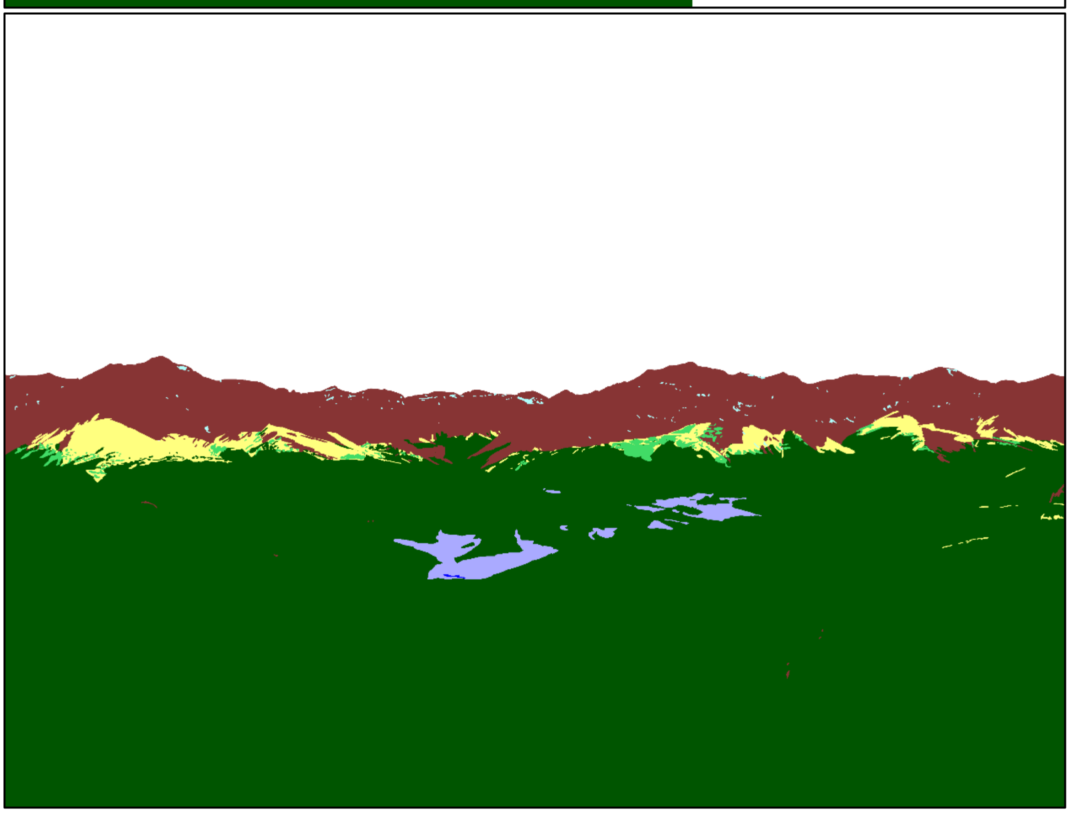

NID19

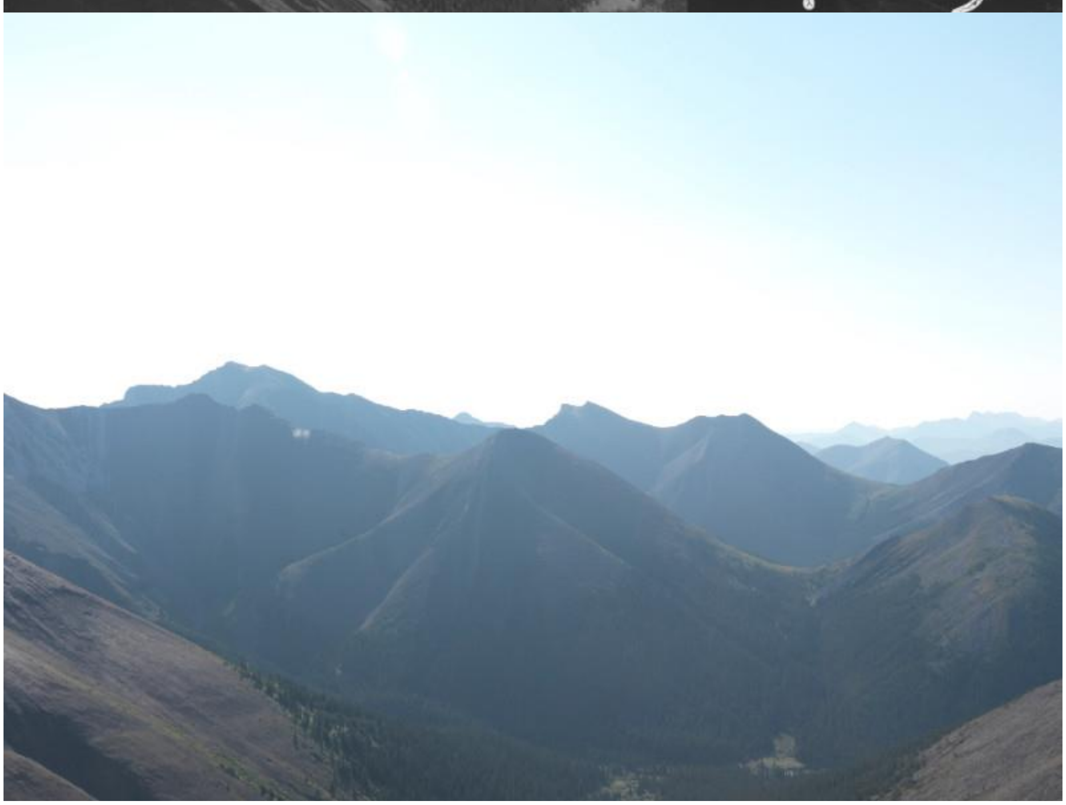

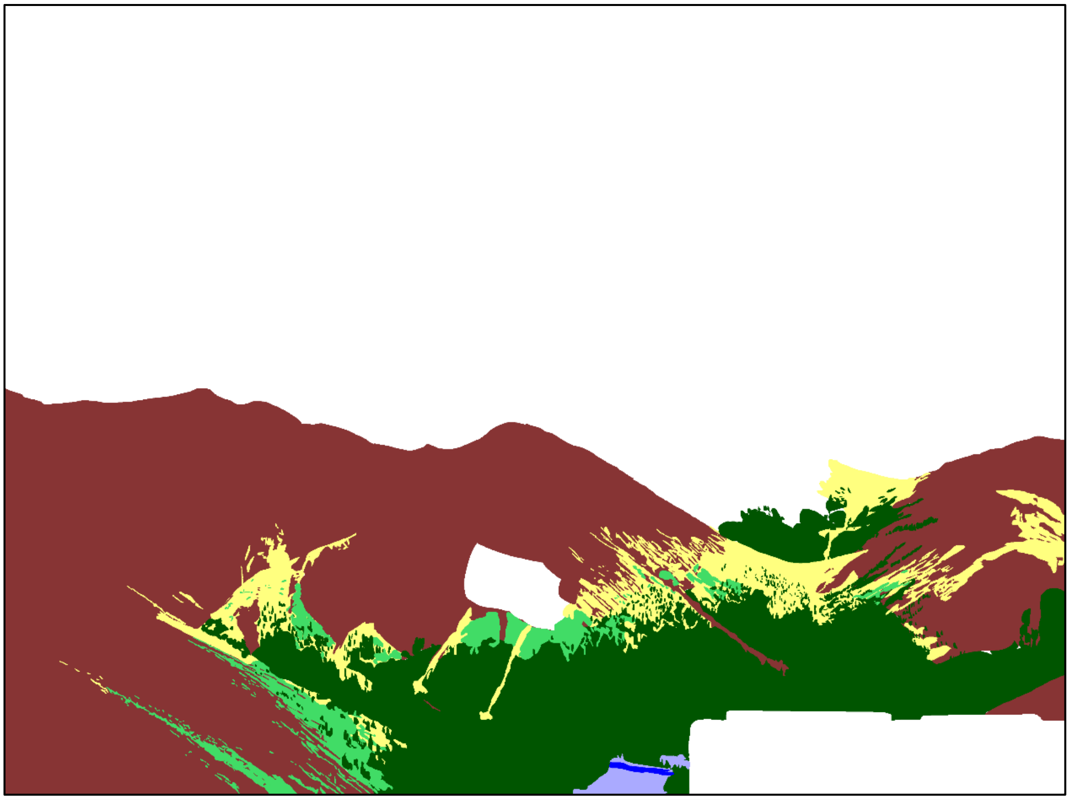

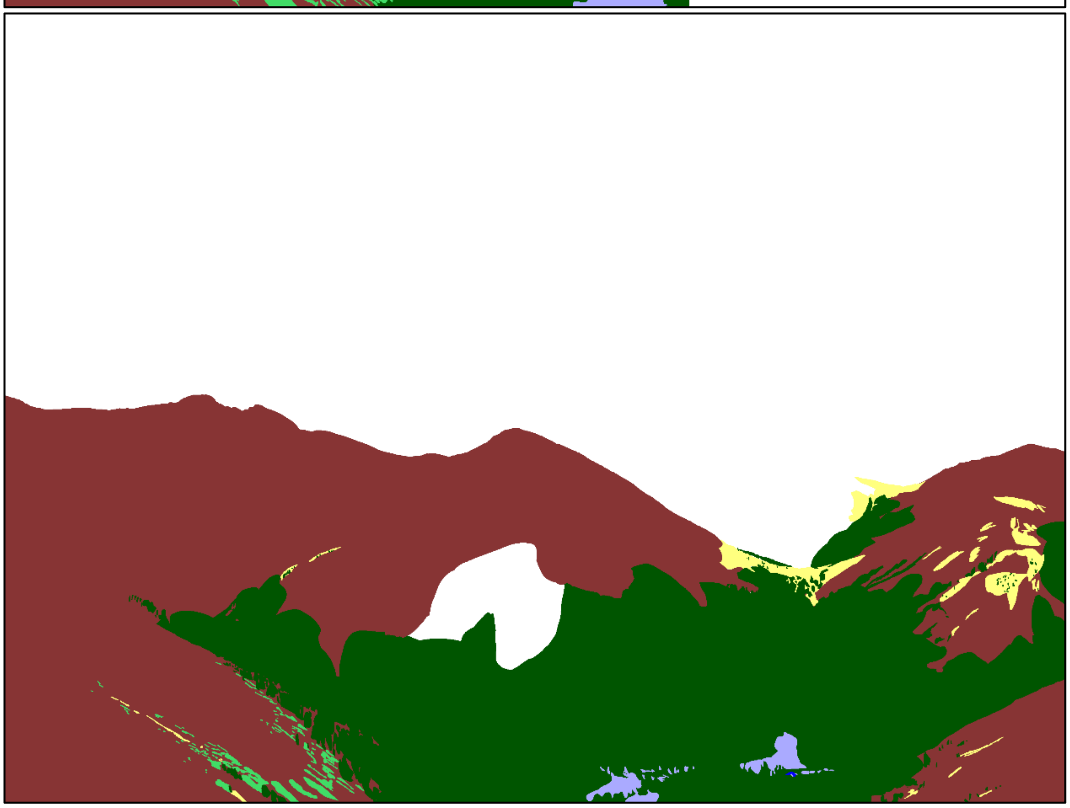

NID21

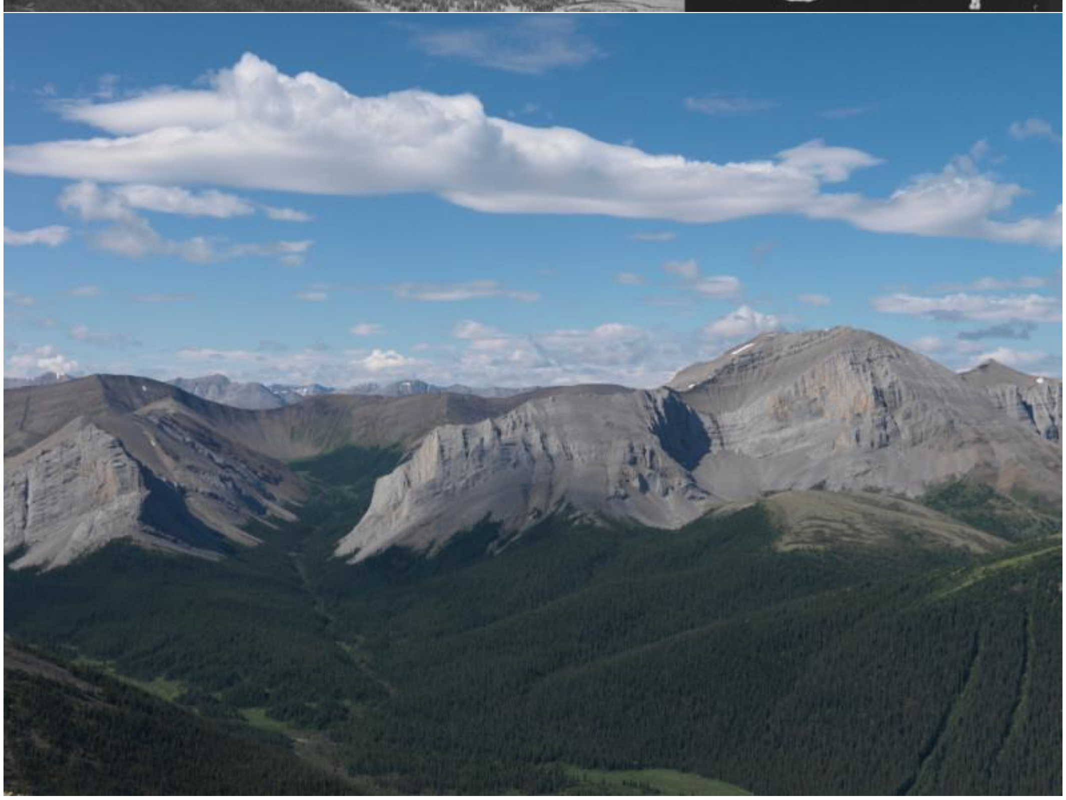

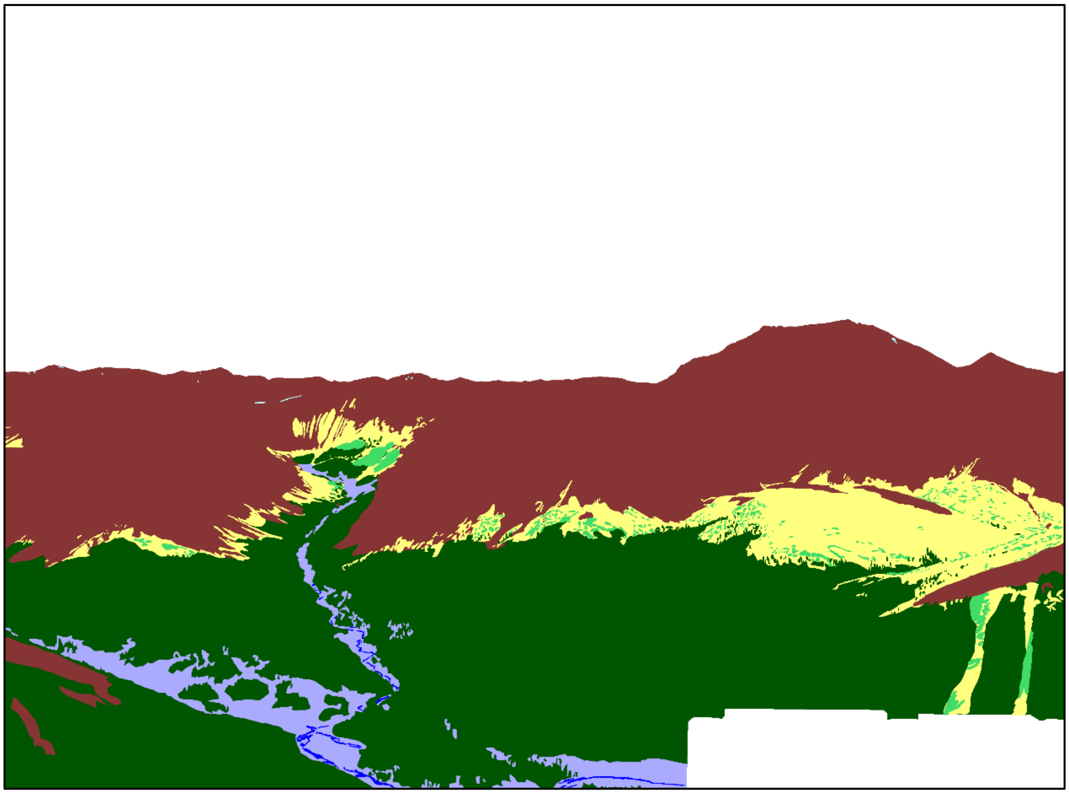

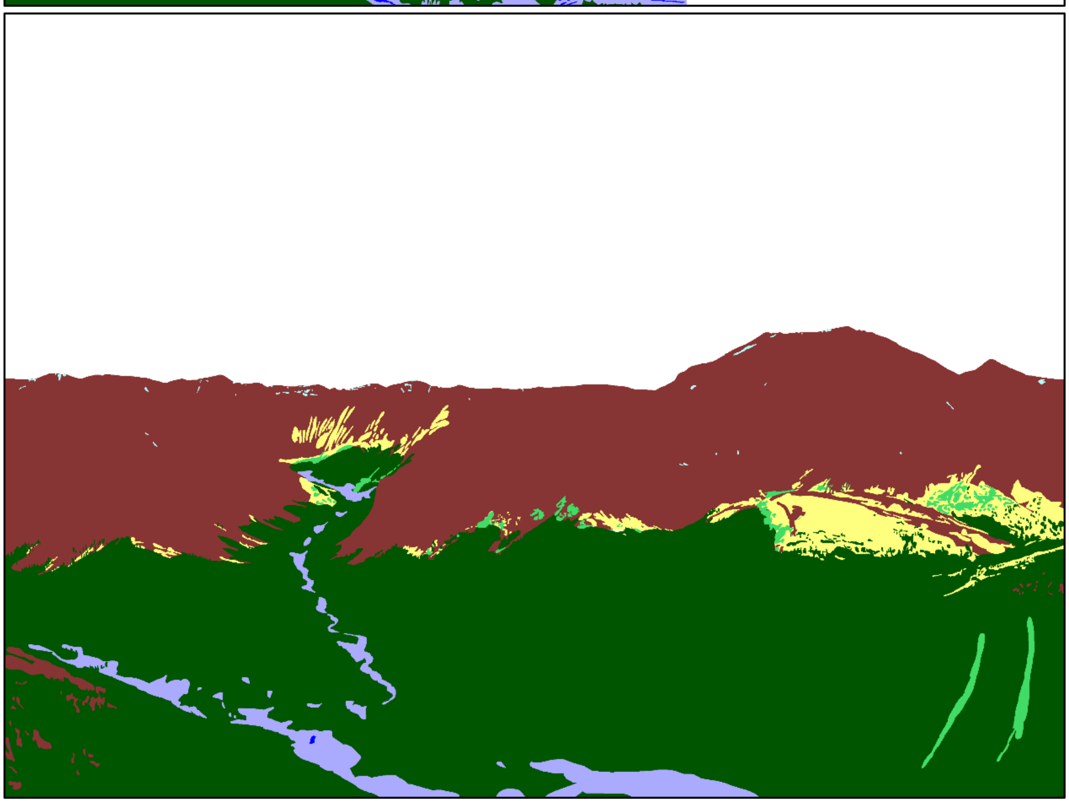

NID8

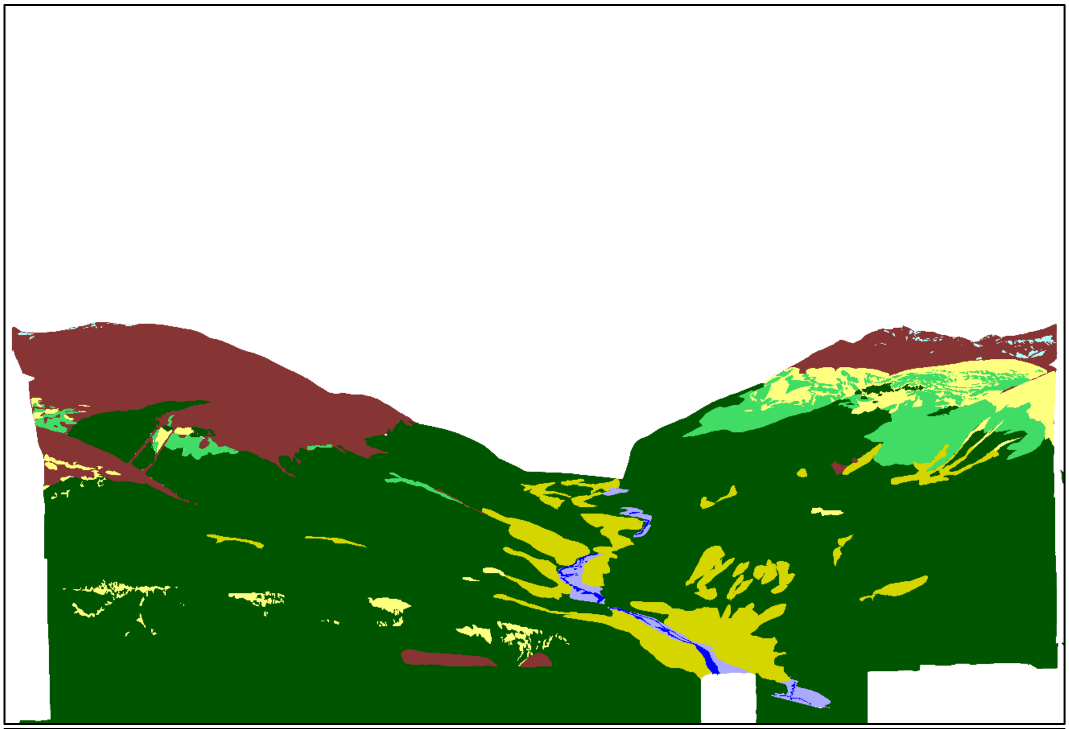

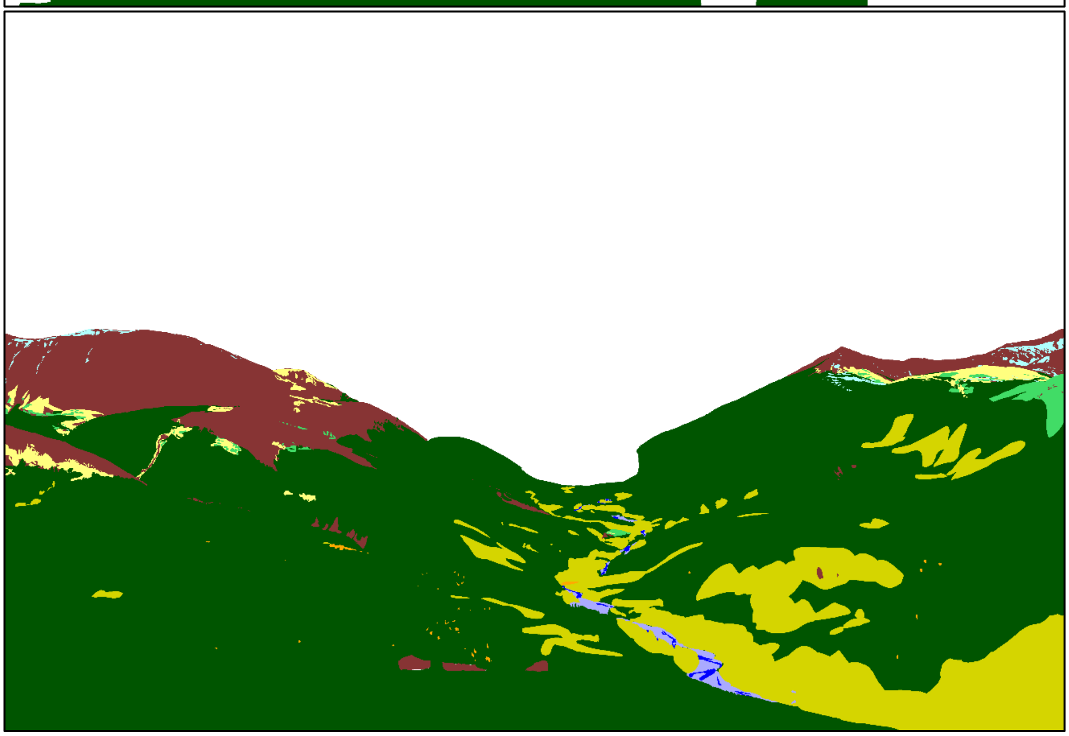

NID12B

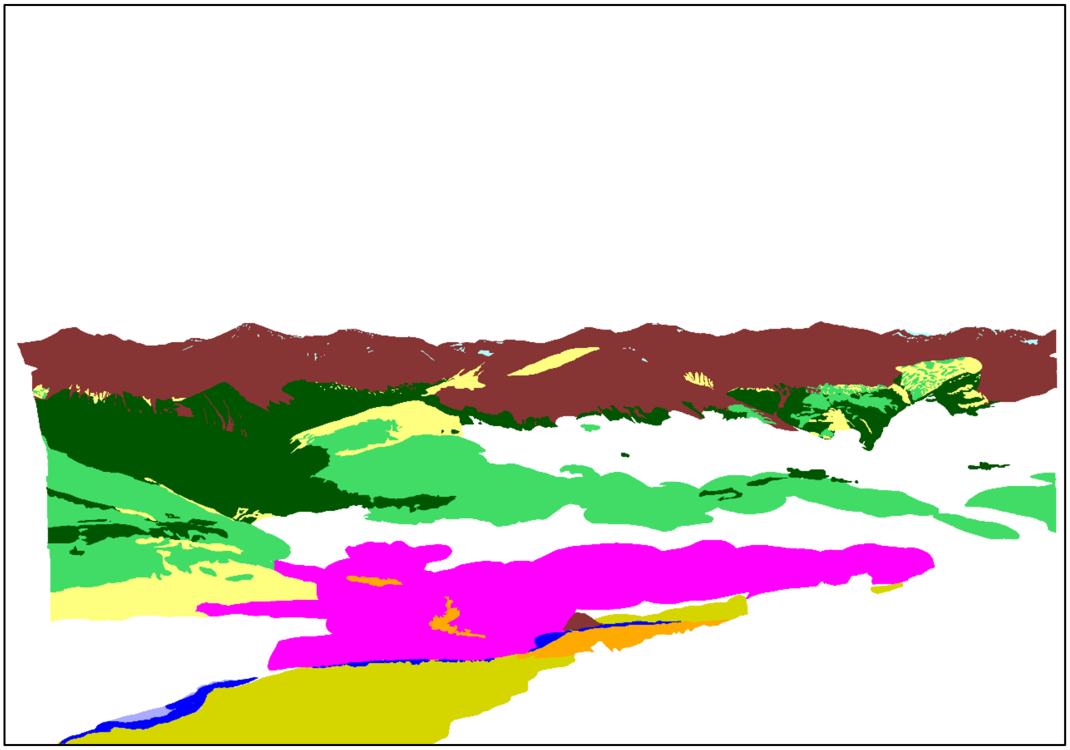

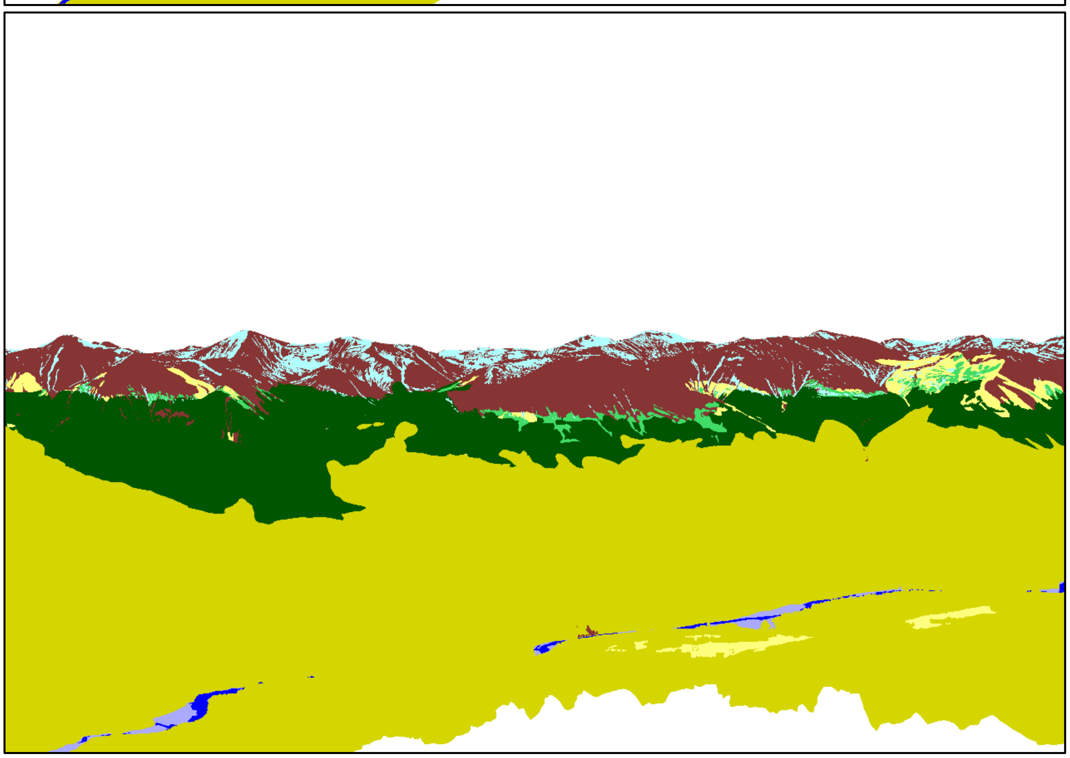

NID2

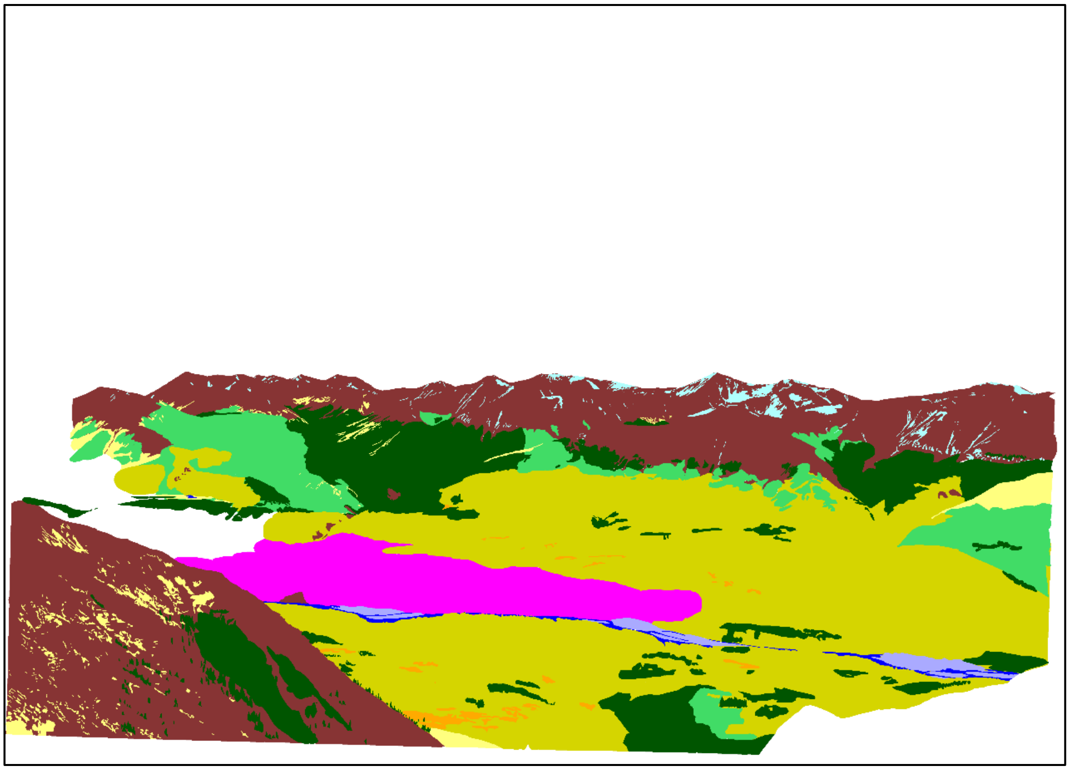

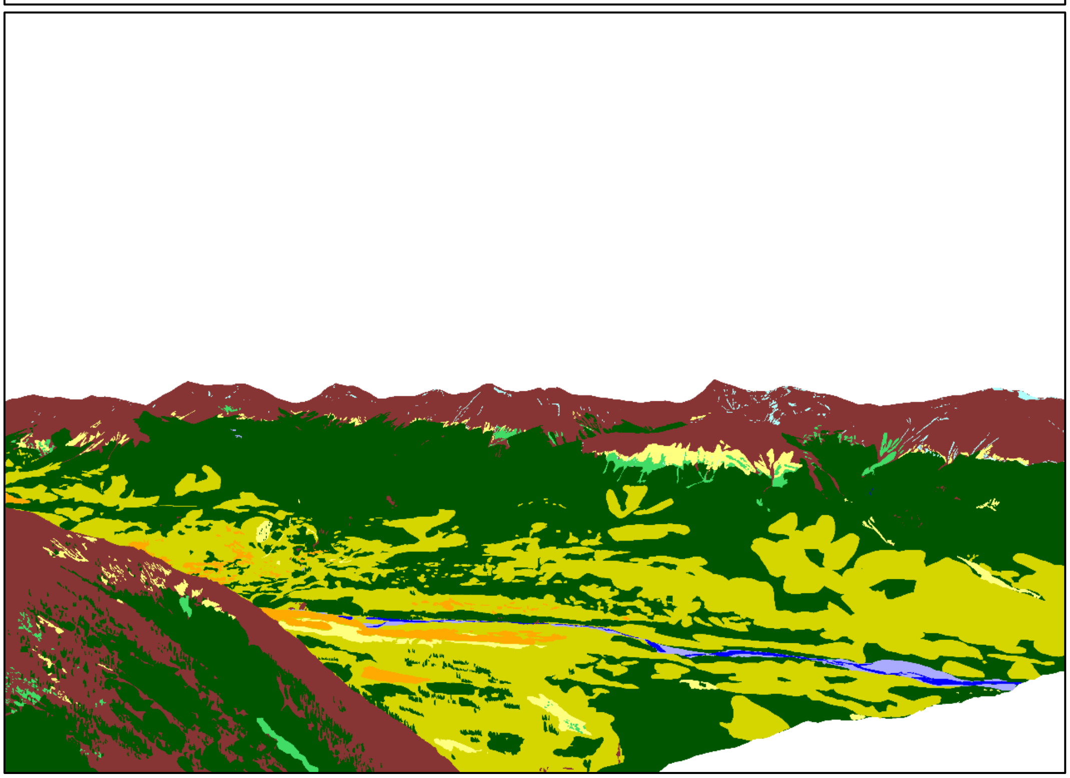

NID3

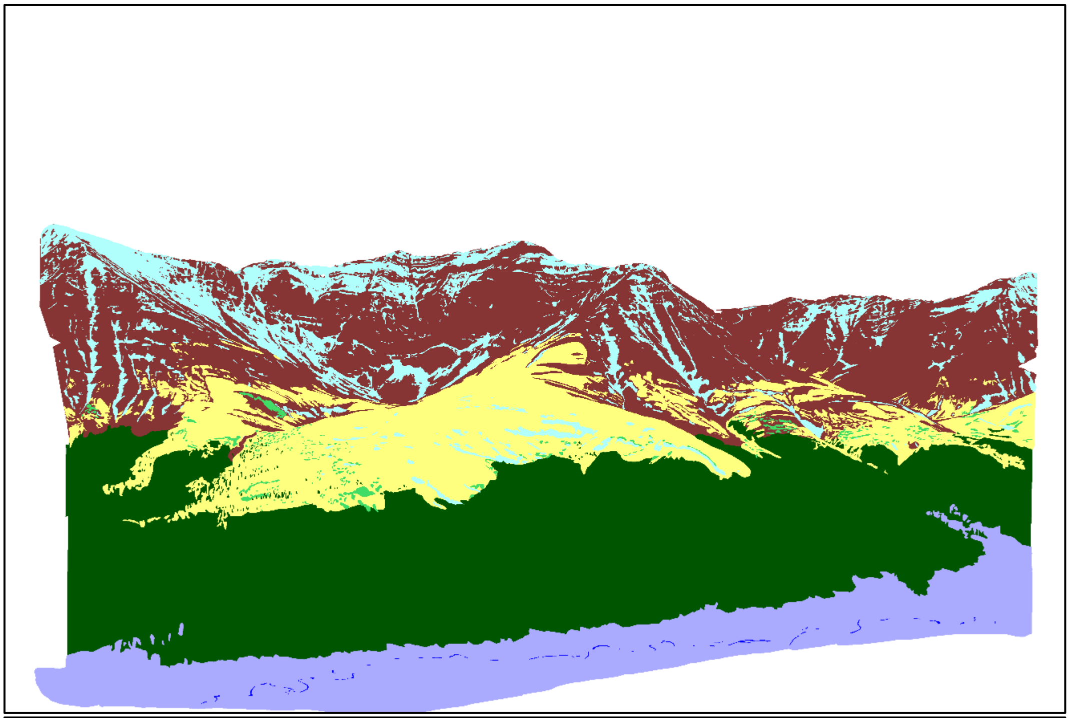

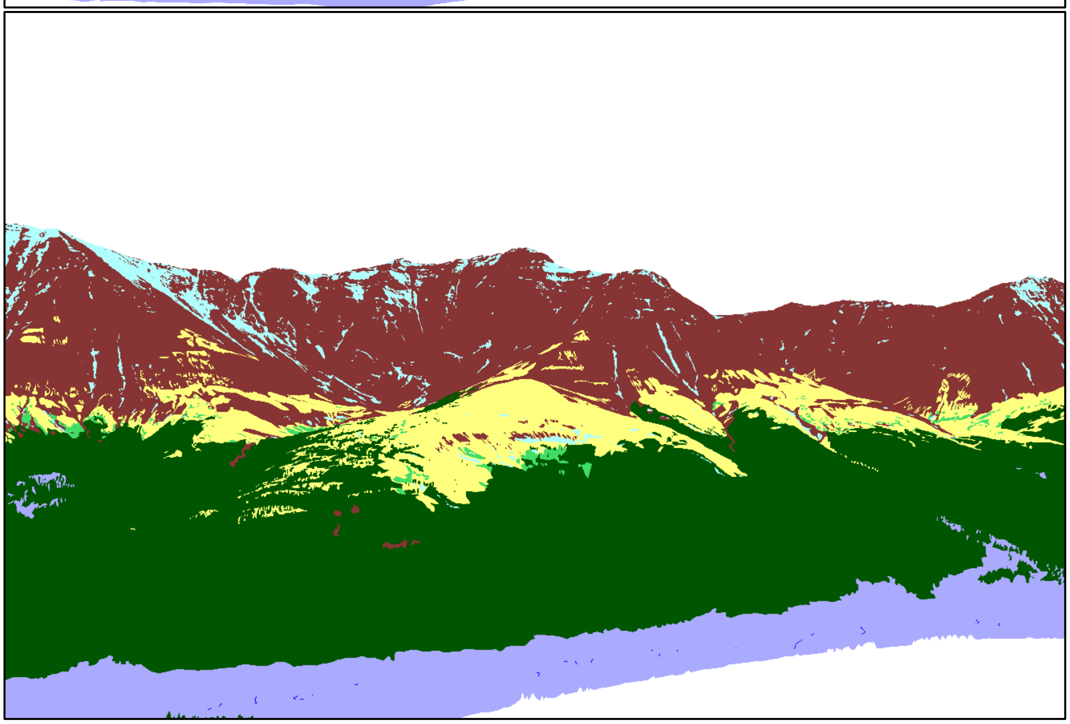

NID5

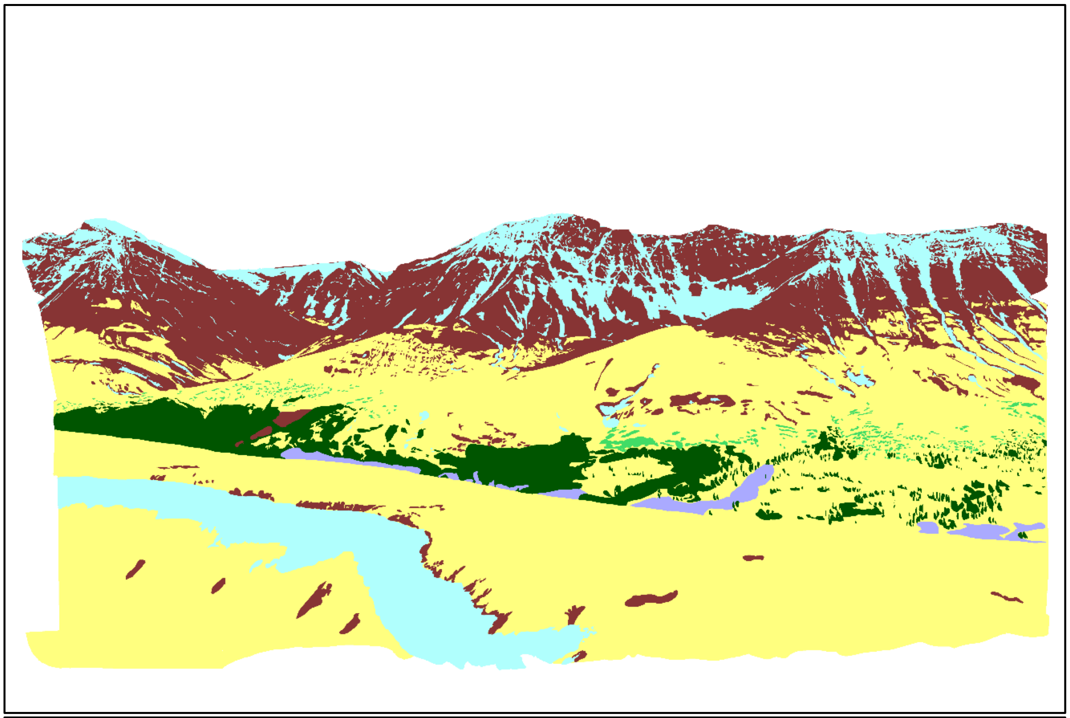

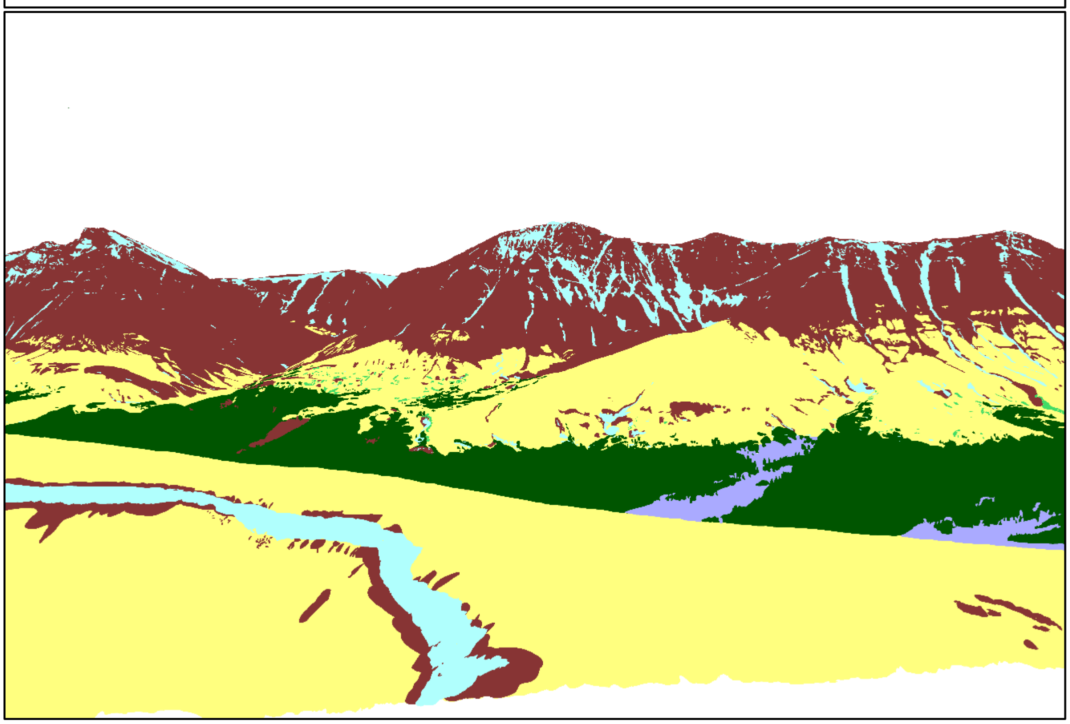

WHE245

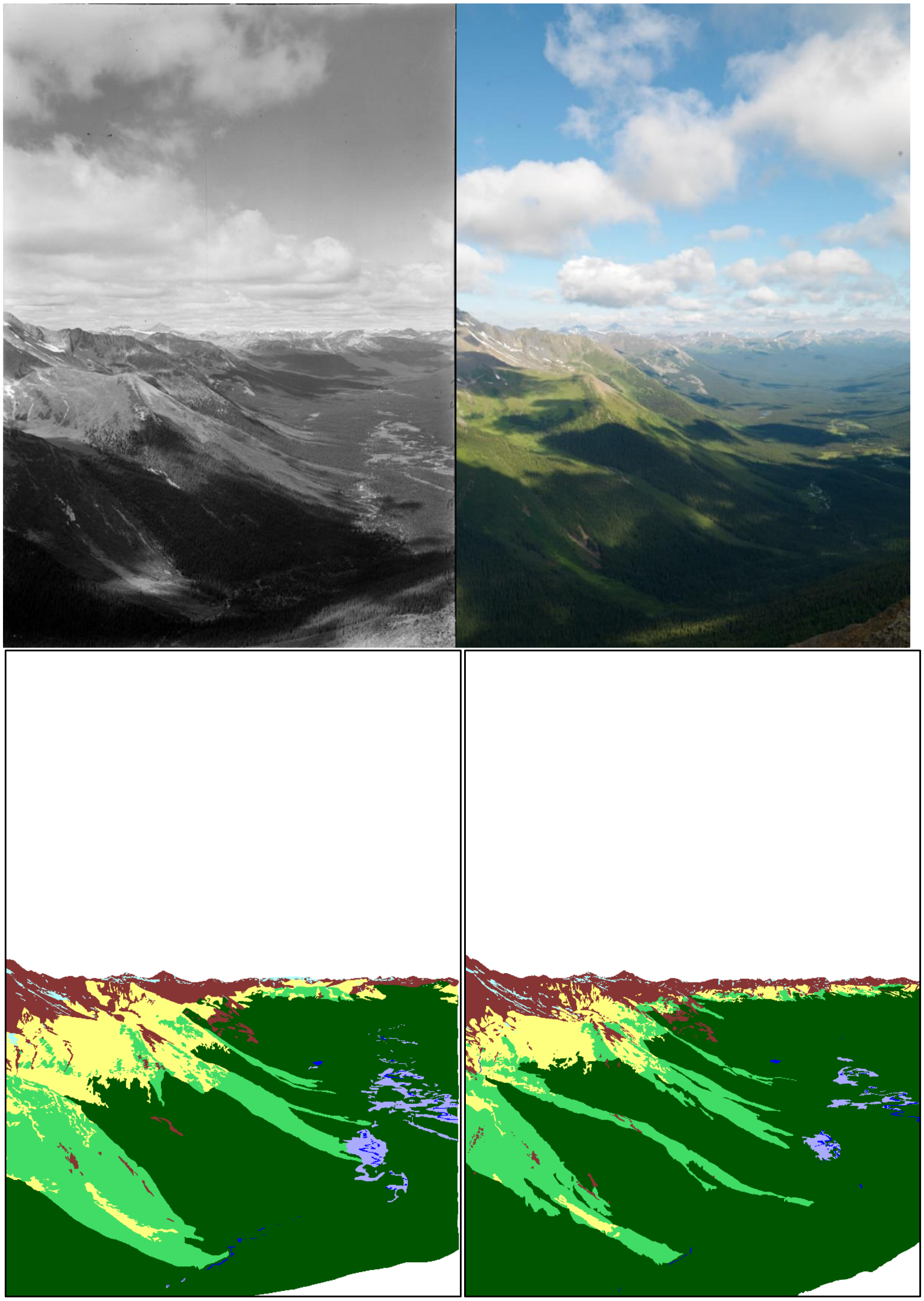

WHE247

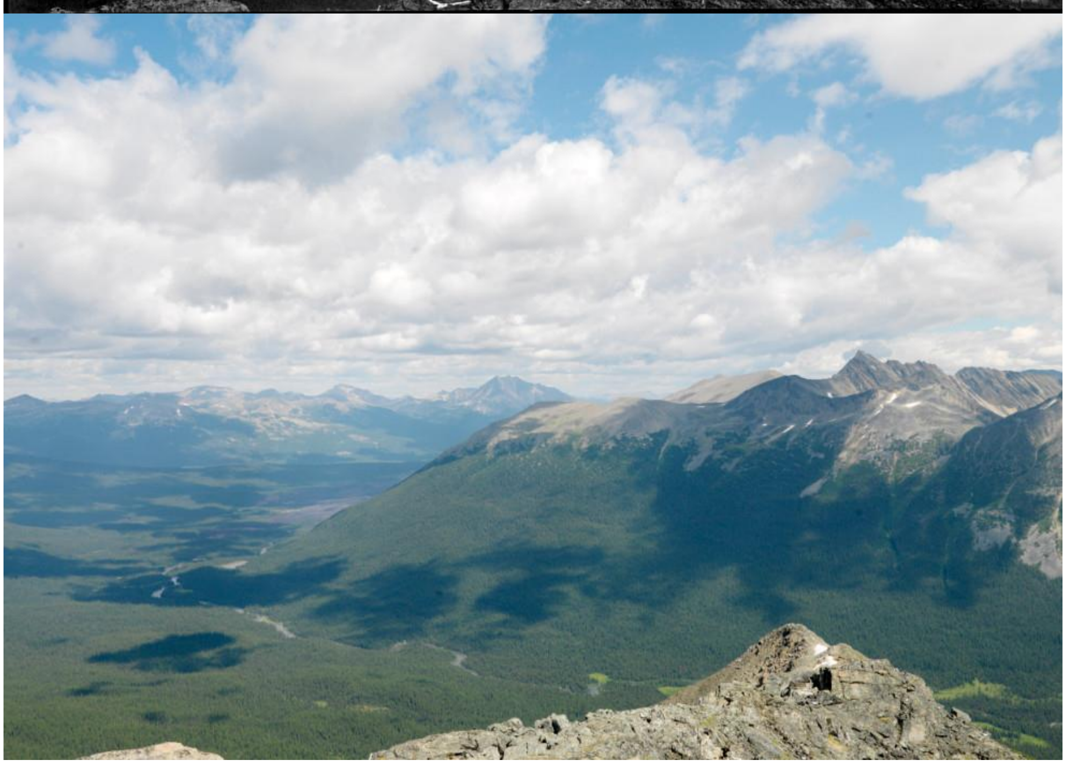

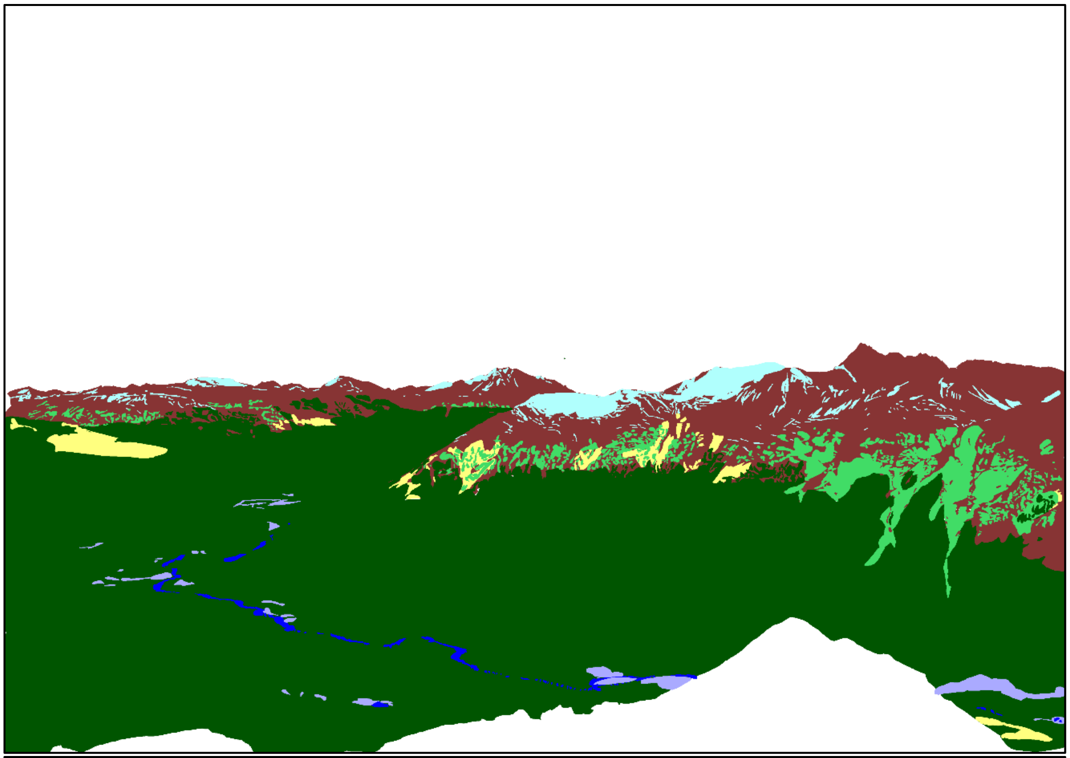

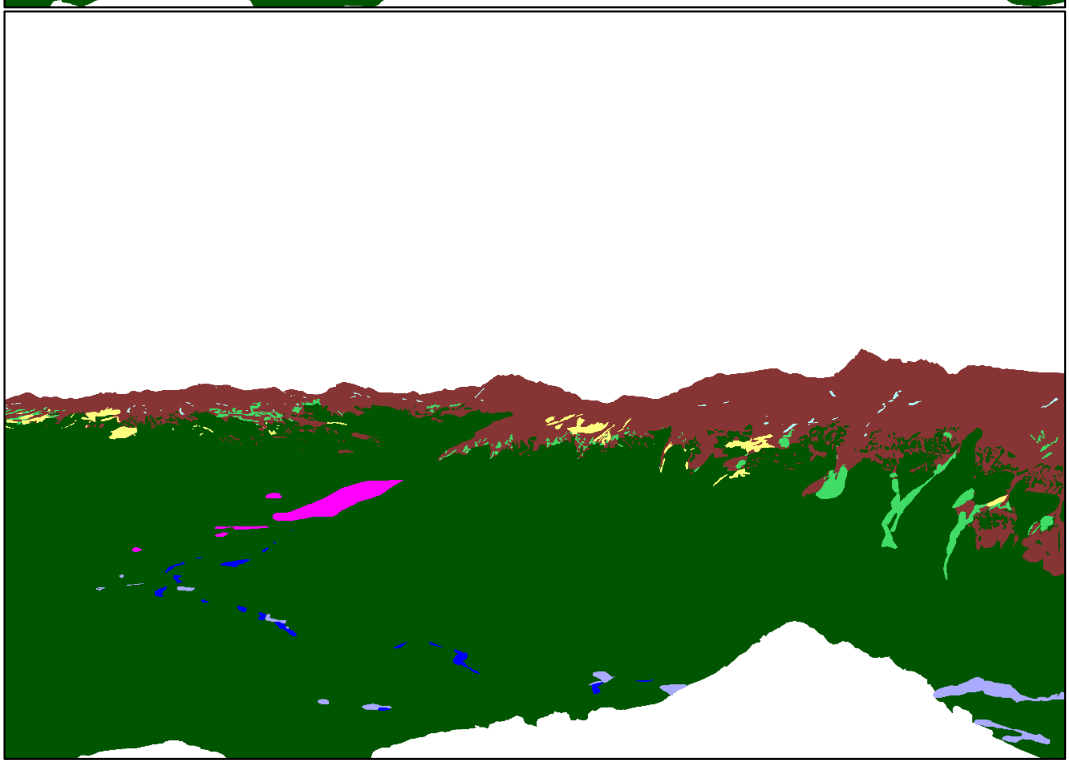

WHE248

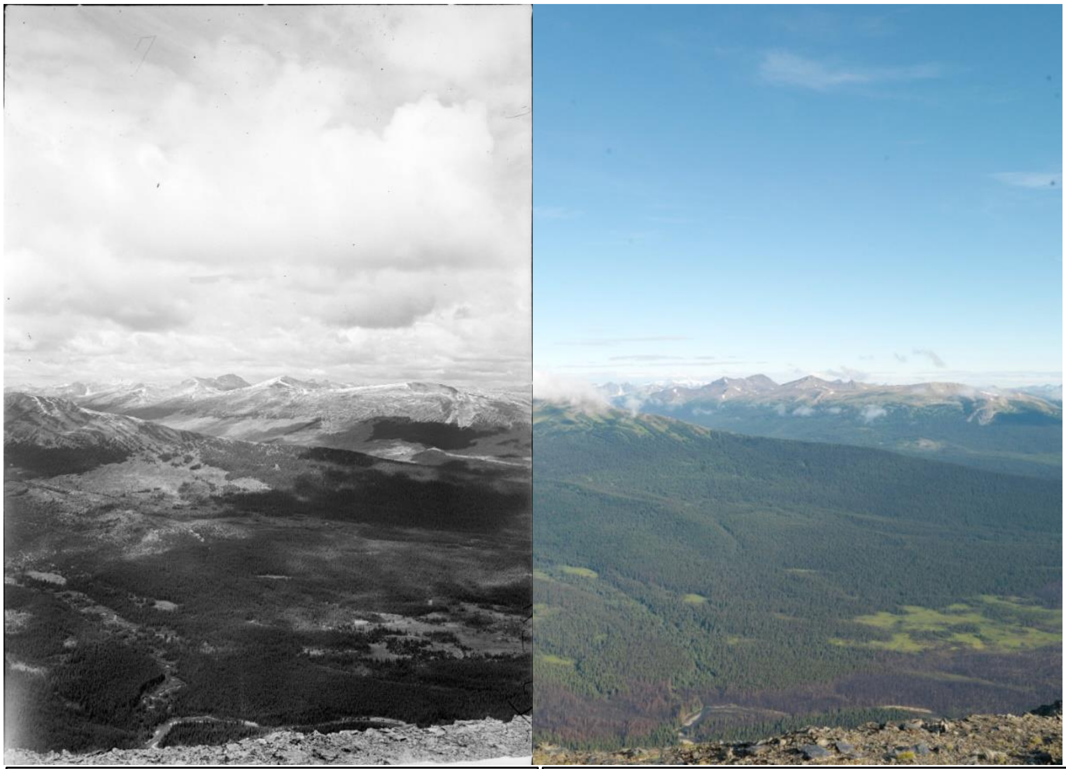

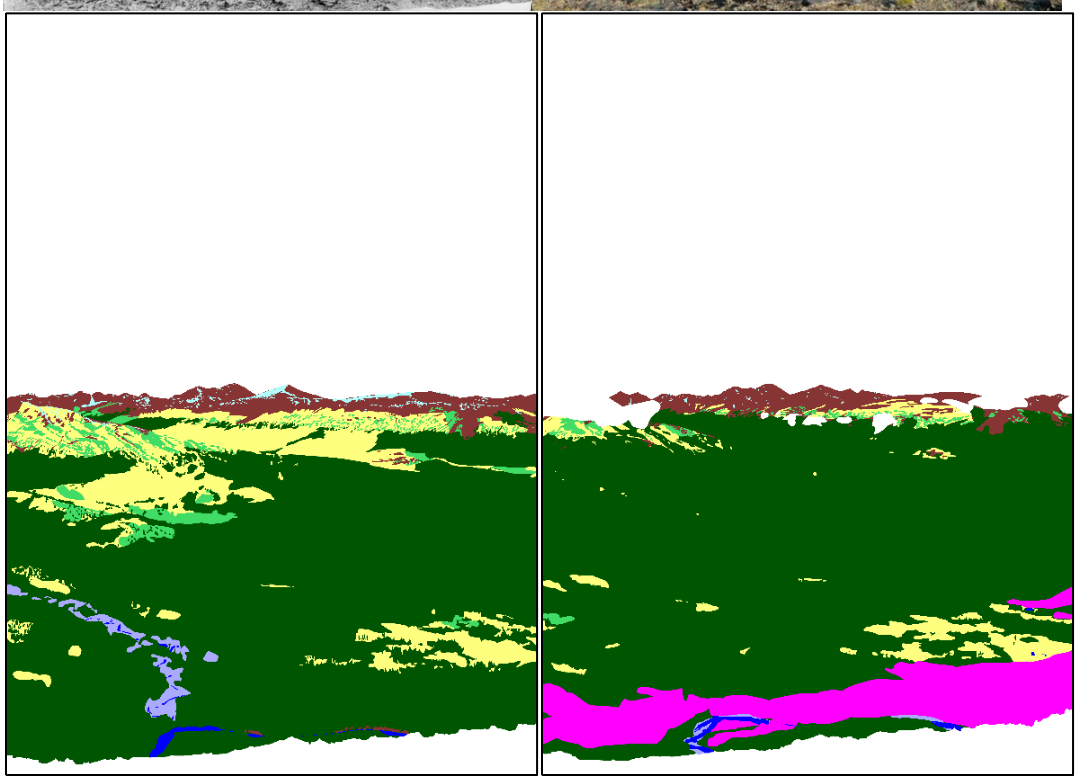

WHE249

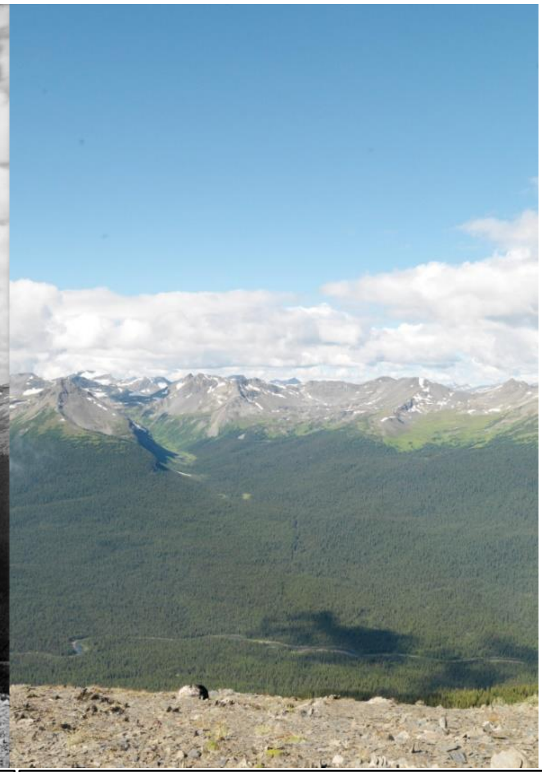

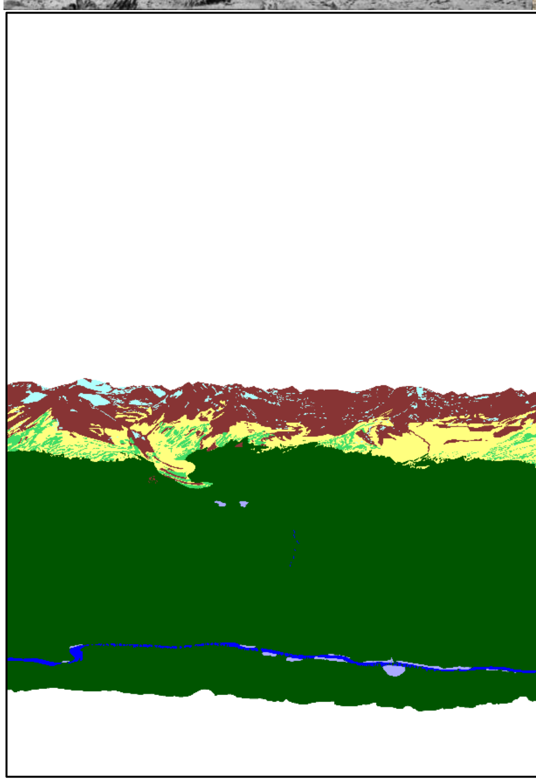

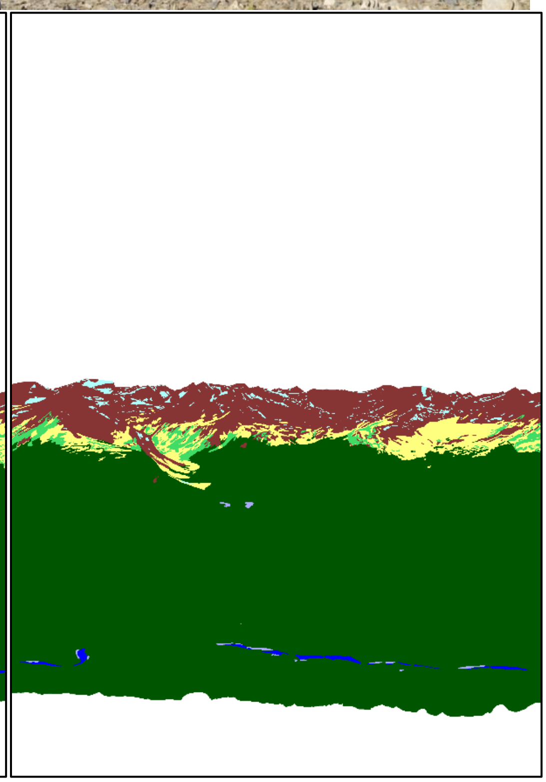

WHE250

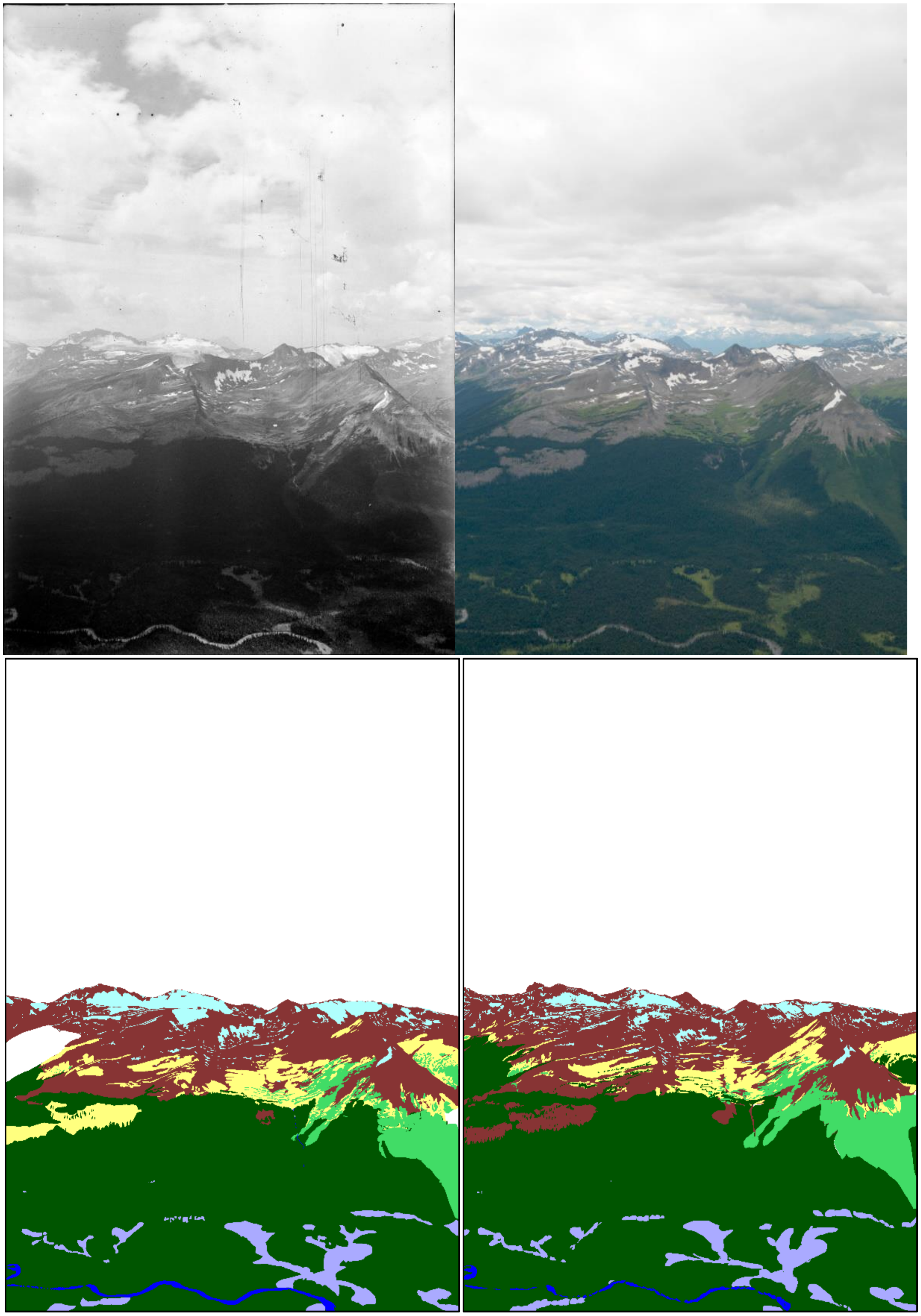

WHE251

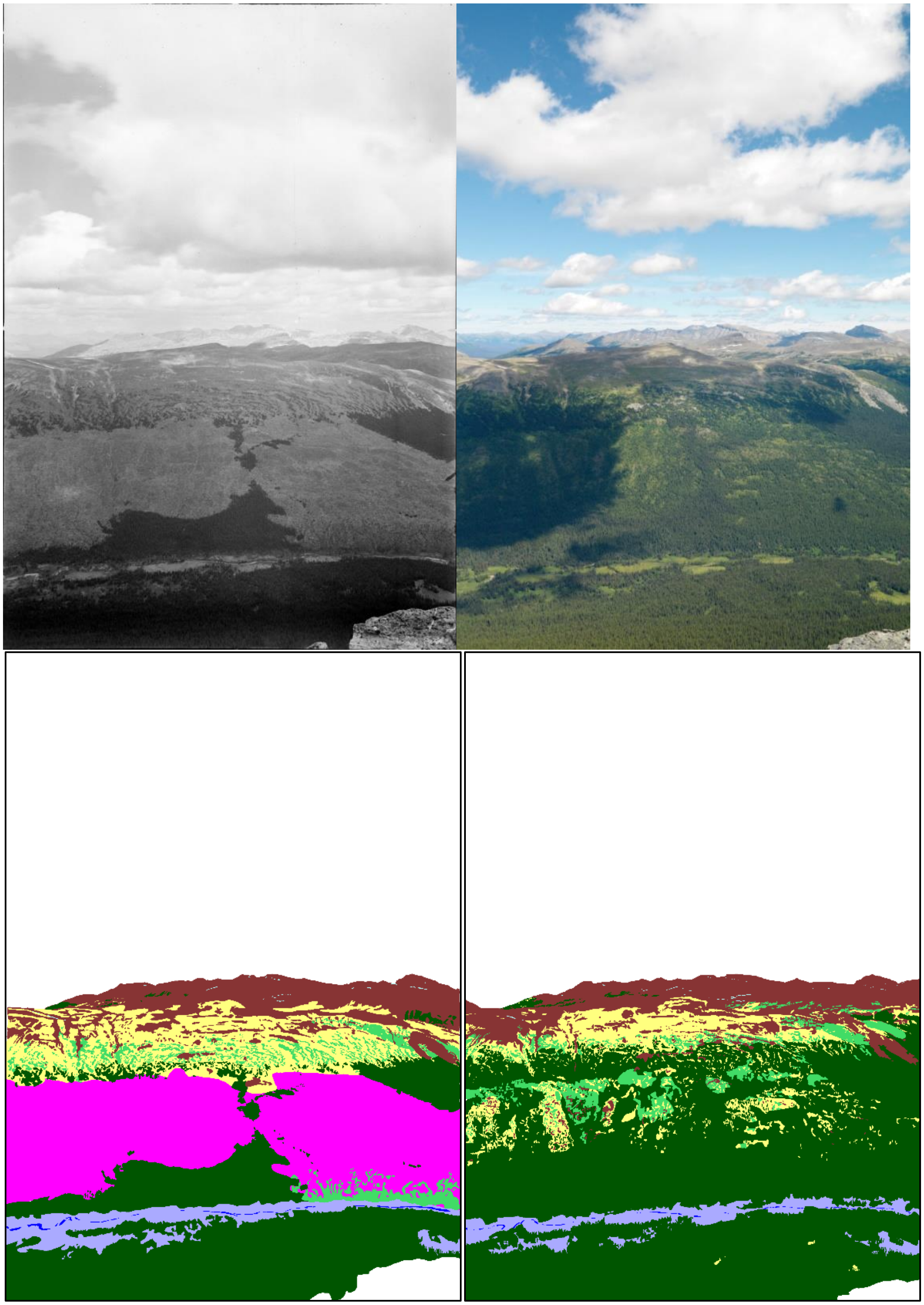

WHE254

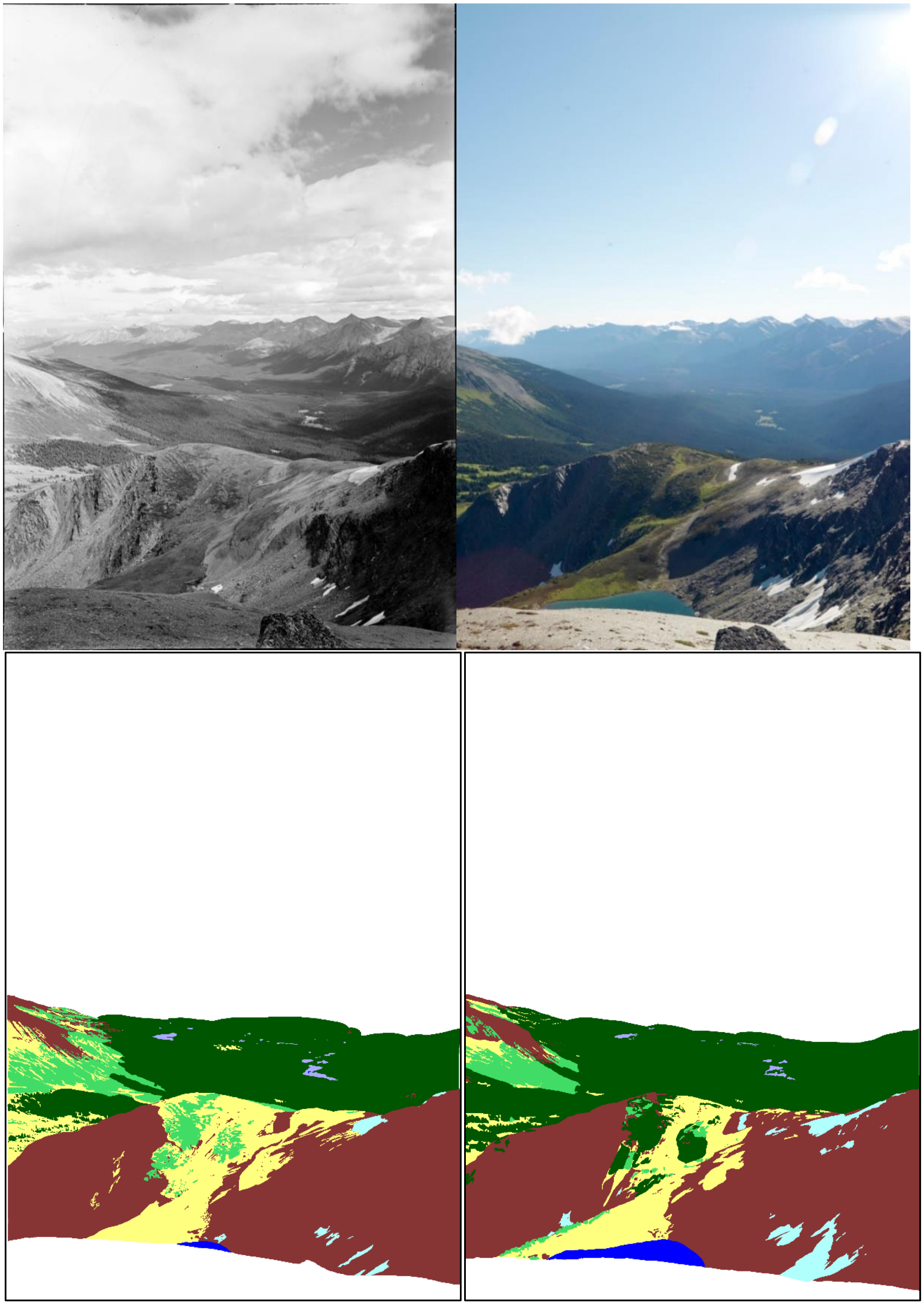

WHE289

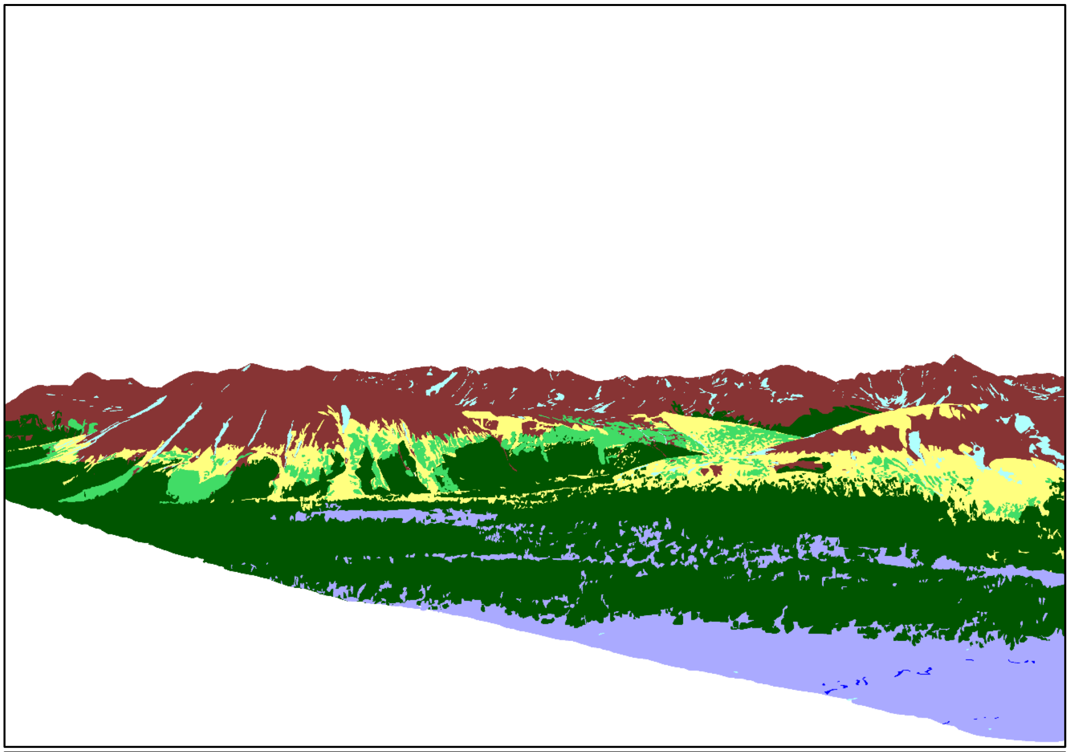

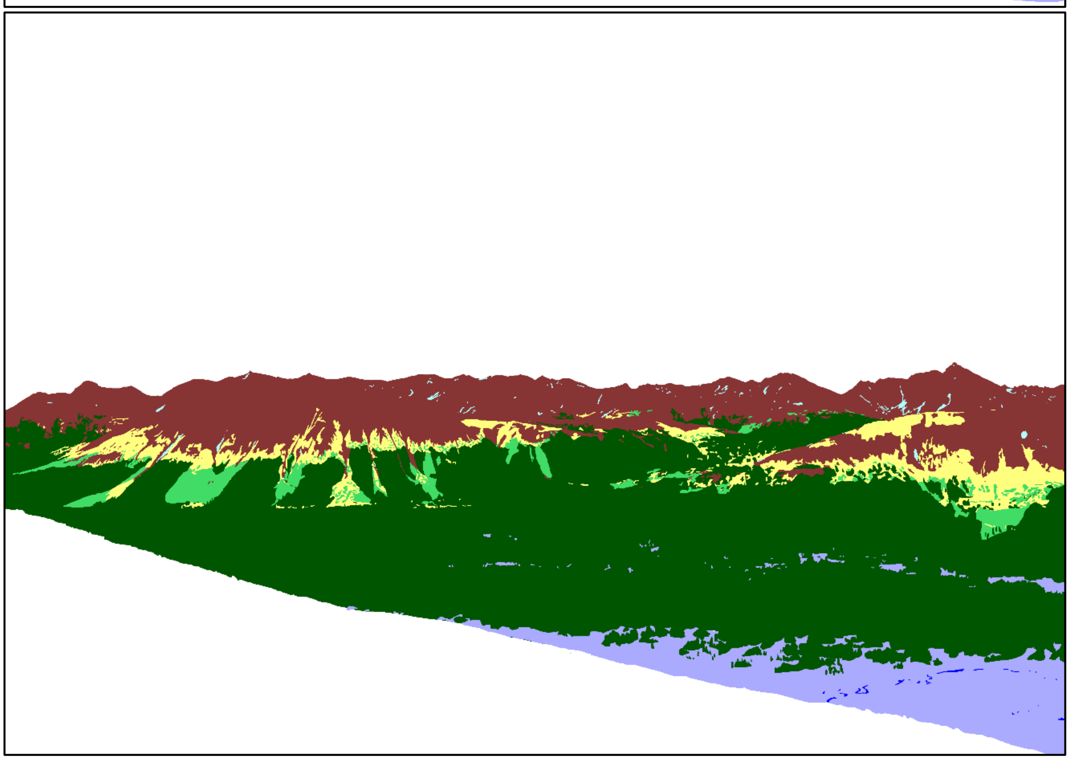

WHE292

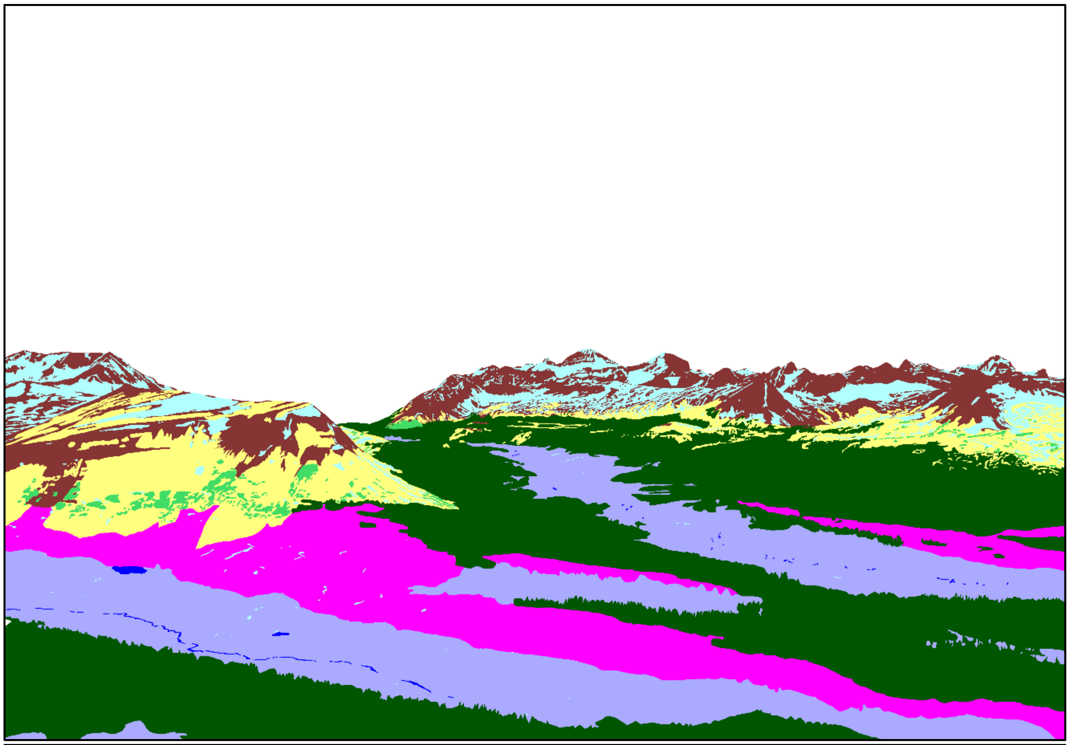

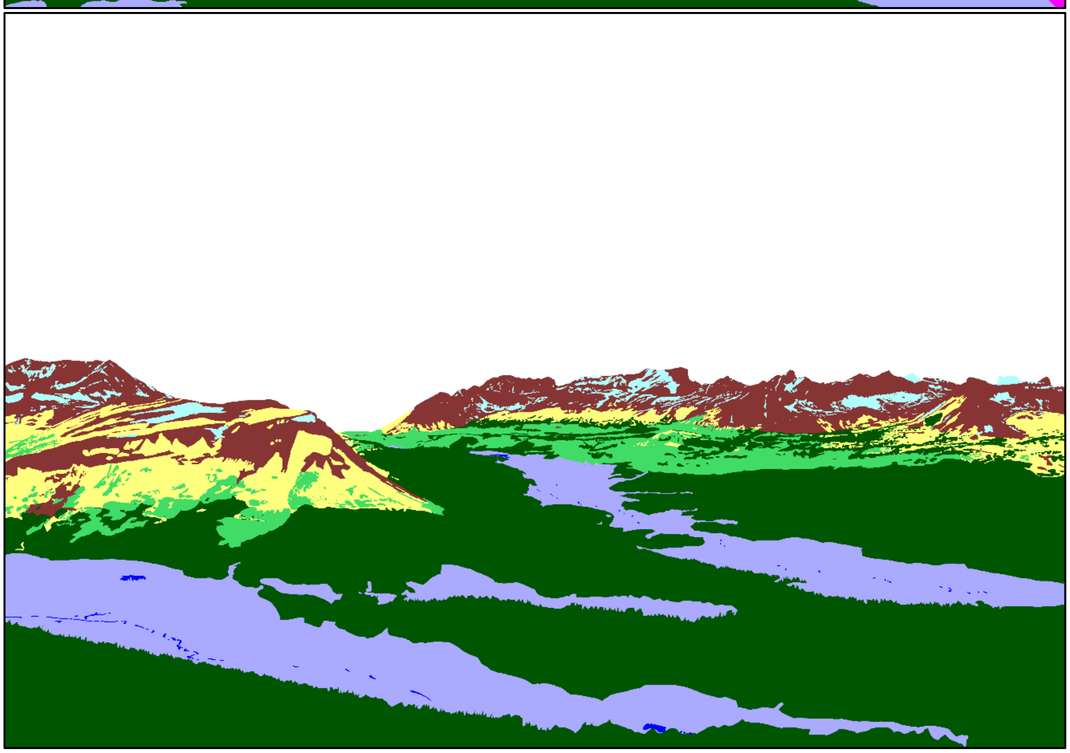

WHE297

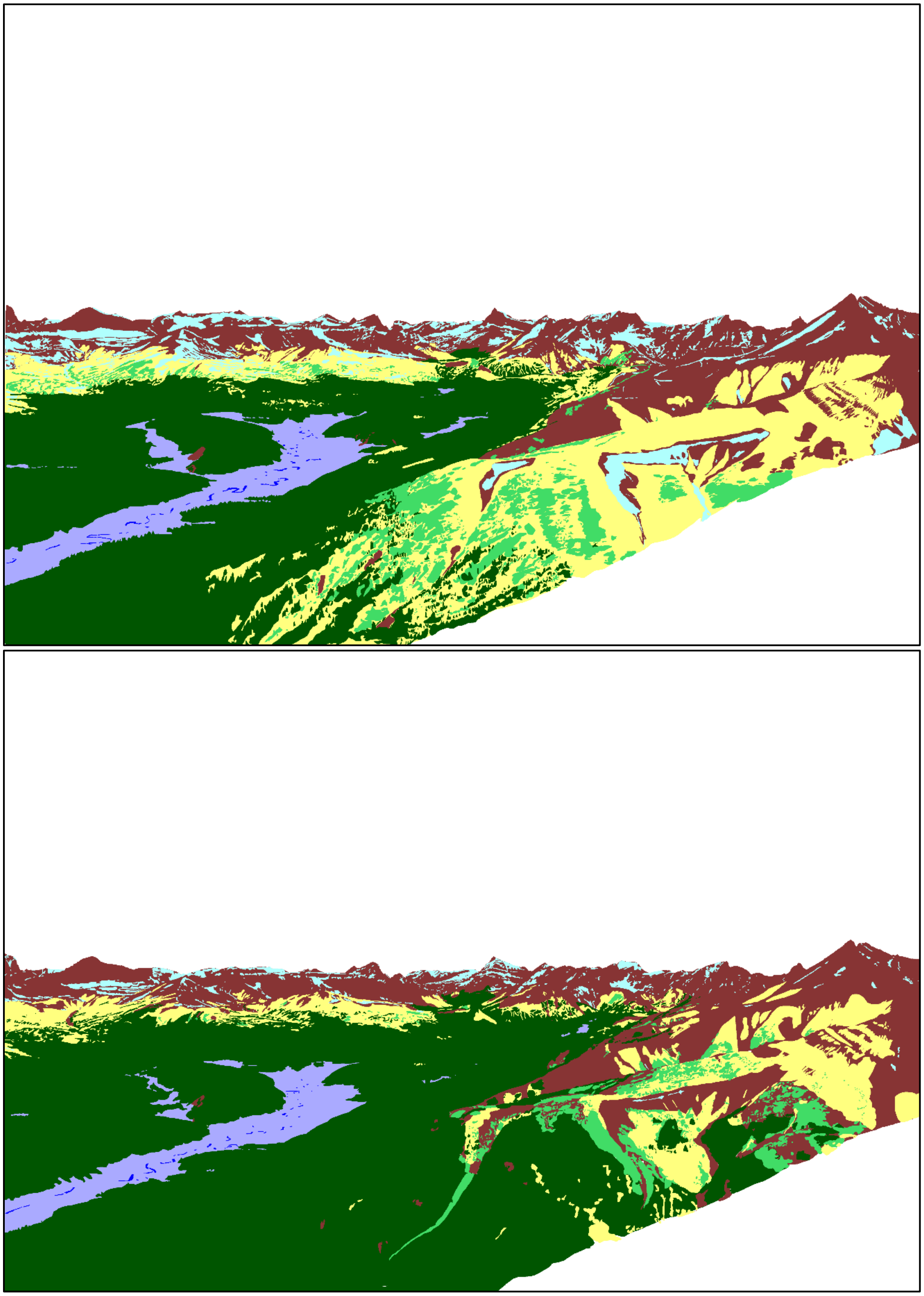

WHE309